

Pericardial Fat is a Nutritionally Regulated Depot of Brown Adipose Tissue

Shalini Ojha

MB BS, MRCPCH

Thesis submitted to the University of Nottingham for the
degree of Doctor of Philosophy

(November 2015)

Abstract

Introduction: Obesity and related cardio-metabolic complications have acquired global epidemic proportions. Suboptimal nutritional environment in early life induces adaptations in energy homeostasis, metabolism and adipose tissue development that may confer short-term survival advantages but are detrimental in later life, particularly if nutrient supply is restored.

Brown adipose tissue (BAT) has a unique role in energy homeostasis because it can provide a potential compensatory mechanism against excess weight gain via cold or diet-induced adaptive thermogenesis. Brown adipocytes also have a potential role in lipid and glucose metabolism and BAT activation can increase clearance of lipids and glucose from the circulation. Pericardial fat, particularly epicardial adipose tissue (fat present between the myocardium and the visceral layer of the pericardium), is anatomically and clinically related to cardiac morphology and function and is believed to be a metabolically active organ that affects cardiac function and the evolution of cardiac pathologies. High expression of mRNA for uncoupling protein (UCP) 1 in adult human epicardial adipose tissue suggests that this may be a depot of BAT.

Hypotheses: In my thesis, I hypothesised that pericardial adipose tissue is a depot of brown fat in humans and sheep. I also hypothesised

that suboptimal nutrition in early life will affect adiposity and development of BAT in this depot.

Methods: UCP1 mRNA expression and protein abundance and other BAT and white adipose tissue related genes were studied in pericardial adipose tissue. In the first study, pericardial fat was sampled from newborn and 30 day old sheep born to mothers fed with 100% or 60% of their total metabolisable energy (ME) requirement from 110 day gestation to term. In the second study, pericardial fat was sampled from near-term (140 day gestation) fetuses delivered to mothers fed 100% or 60% of total ME requirement from 28 to 80 days and then fed ad libitum. Gene expression was measured by reverse transcription-polymerase chain reaction and protein abundance by Western blotting and immunohistochemistry.

To confirm the presence of BAT in the human epicardial fat depot, relative abundance of UCP1 was measured by Western Blotting in epicardial, paracardial, and subcutaneous fat samples taken from adults. In the final study, epicardial fat samples were collected from 63 children (0-18 years of age) undergoing cardiac surgery and gene expression of UCP1 and other BAT and WAT related genes identified by microarray. The presence of UCP1 was confirmed by immunohistochemistry.

Results: Pericardial adipose tissue is a depot of BAT in fetal and newborn sheep. Suboptimal maternal nutrition in late gestation reduces the abundance of UCP1 and downregulates other BAT related genes whilst suboptimal maternal nutrition in early-to-mid gestation followed by *ad libitum* feeding to term, increases adiposity, enhances UCP1 abundance and upregulates genes involved in brown and white adipogenesis.

Epicardial fat from newborn infants, children, adolescents and older adults contains UCP1 confirming that it is a BAT depot in humans. UCP1 gene expression in infancy and early childhood in humans is downregulated in children with poor nutritional states.

Conclusions: I have shown that adipose tissue depots present around the heart are a repository of brown fat, at least in humans and sheep. In view of the potential role of BAT in regulation of lipid and glucose metabolism, this may have therapeutic implications for treatment of cardiovascular complications of obesity. Suboptimal nutrition in utero and during early life compromises BAT development. Although the exact mechanism of how these changes affect the propensity towards obesity and metabolic dysregulation remains to be elucidated, a reduction in thermogenesis presents a plausible mechanism for the increased metabolic efficiency associated with nutritional deprivation in early life. BAT persists beyond the neonatal period in to adult life and,

therefore, presents a potential target for long lasting nutritional manipulations to promote better health.

Acknowledgements

I would like to express sincerest gratitude to my project supervisors, Professor Michael Symonds and Professor Helen Budge, for their generous support, unwavering encouragement and steadfast confidence in my abilities that enabled me to complete this thesis.

I am grateful to the University of Nottingham and the Higher Education Funding Council for England for the Clinical Lectureship that allowed me adequate time and funds to perform this work.

My sincerest thanks also go to Mr Attilio Lotto, Consultant Paediatric Cardiothoracic Surgeon at the Glenfield Hospital, whose unconditional support allowed me to perform the a-PAC study. Without the exceptional input from Mr Lotto and the Paediatric Cardiothoracic team at the Glenfield Hospital, particularly, help from the excellent Mr Giuseppe Pelella, this study would have been impossible.

I owe boundless gratitude to Mrs. Victoria Wilson for her indefatigable contribution in co-ordinating the a-PAC study, for teaching me laboratory techniques, providing technical support and most of all, for being a friend throughout the last few years.

In these years, I have learnt to use a number of scientific techniques and am deeply indebted to the laboratory experts who taught these to me. The foremost is Mr Mark Pope, who was untiringly tolerant and

supportive. I would like to specially thank Mrs. Catherin Pincott-Allen and express my appreciation for Mr Christopher Nolan and Dr Chitra Joseph of the Academic Unit of Clinical Oncology at the University of Nottingham for taking time to train me to perform histochemistry. I would like to offer a special thank you to the team at Plant Sciences in the University of Nottingham: Mr. Iqbal Khan, Mr. Naofel Aljafer and Mr. Marcos Castellanos, for performing the microarray analyses and teaching me how to analyse the data, and to Professor Sean May, Professor of Plant Cyberinfrastructure at the University of Nottingham for his advice in this work. I am grateful to Dr Lisa Szatkowski for helping me find the correct tools for anthropometric assessments. I also thank Professor Harold Sacks of the Baptist Memorial Hospital, Memphis, U.S.A, for providing the samples for the study of brown adipose tissue in adult epicardial fat.

I would like to show my appreciation for the works of Dr Sarah Pearce and Dr Lindsay Heasman, who performed the animal experiments and created the rich repository of sheep tissue for me to work on.

I appreciate the support and camaraderie of all my colleagues at Academic Division of Child Health, especially Dr Lindsay Robinson for her solidarity and friendship through all times. I am thankful to Dr Vivek Saroha, Dr Andrew Prayle, Dr Matthew Hurley, Miss Rachel Woods, Mr. Stuart Astbury, Mr Graeme Davies, Dr James Law, Dr Caroline Henry,

and Mr Mark Birtwistle who were my co-conspirators on this journey and to Dr Ian Bloor, Dr Neele Dellschaft and Dr Hernan Fainberg for sharing their experience from the other side of the PhD divide.

Finally, it leaves me to thank my family, especially my son, who spent a large part of his school holidays in my office so that I could complete this work.

Declaration

The work in this thesis was performed within the Academic Child Health Division, School of Clinical Sciences, University of Nottingham between February 2011 and February 2015.

This thesis illustrates my own work, completed under the supervision of Professor Michael Symonds and Professor Helen Budge, except where specified in this report. This report is an accurate representation of the work performed and no other study reproducing this work, to my knowledge, has been carried out within the University of Nottingham.

Shalini Ojha

March 2015

Publications and presentations

Some of the studies presented in this thesis have been published in peer reviewed journals and presented at scientific meetings.

Publications:

1. Ojha, S., L. Robinson, M. Yazdani, M. E. Symonds and H. Budge (2013). Brown adipose tissue genes in pericardial adipose tissue of newborn sheep are downregulated by maternal nutrient restriction in late gestation. *Pediatr Res* 74(3): 246-251.
2. Ojha, S., M. E. Symonds and H. Budge (2014). Suboptimal maternal nutrition during early-to-mid gestation in the sheep enhances pericardial adiposity in the near-term fetus. *Reprod Fertil Dev*.
3. Sacks, H. S., J. N. Fain, S. W. Bahouth, S. Ojha, A. Frontini, H. Budge, S. Cinti and M. E. Symonds (2013). Adult epicardial fat exhibits beige features. *J Clin Endocrinol Metab* 98(9): E1448-1455.

Presentations:

1. Changes in ovine adipose tissue in early postnatal life postnatal life (2014) Power of Programming Conference, Munich
2. Effect of suboptimal maternal nutrition on adipose tissue development in sheep fetus (2013) Neonatal Society Summer Meeting, Edinburgh
3. Presence of brown adipose tissue in epicardial fat of adult humans (2012) The Physiological Society, London.
4. Maternal nutrient restriction affects neonatal brown adipose tissue development (2012) Neonatal Society Summer Meeting, Canterbury
5. Ontogeny of Brown Adipose Tissue (2012) Adipose Tissue Discussion Group, Cambridge
6. Ontogeny of brown adipocyte markers in the pericardial adipose tissue in newborn sheep (2011) Neonatal Society Autumn Meeting, London

Abbreviations

ADP	adenosine diphosphate
ADR	adrenergic receptor
ADRP	adipose Differentiation Related Protein
AMP	adenosine monophosphate
ATP	adenosine triphosphate
BAT	brown adipose tissue
BLAST	Basic Local Alignment Search Tool
BCA	bicinchoninic acid
BMI	body mass index
BMP	bone morphogenetic protein
CABG	coronary artery bypass grafting
CCD	charged coupled device
C/EBP	CCAAT-enhancer binding protein
CHD	coronary heart disease
CMO	Chief Medical Officer
CRE	cAMP response element
CRP	C reactive protein

CT	computer tomography
CtBP	C-terminal-binding-protein
DIO2	type 2 iodothronine deiodinase
e-	electron
EAT	epicardial adipose tissue
ETC	electron transport chain
En-1	engrailed -1
¹⁸ F-FDG	2-[18F]- fluoro-2-desoxy-glucose (FDG)
FFA	free fatty acids
GDP	guanosine diphosphate
GLUT	glucose transporter
GR	glucocorticoid receptor
GTP	guanosine triphosphate
H+	hydrogen ion
HAZ	height for age z-score
HoX	homobox
HPA	Hypothalamo-pituitary-adrenal
HSL	hormone sensitive lipase
HTA	Human Tissue Authority

IGF	insulin like growth factor
IGFBP	insulin like growth factor binding protein
IHC	immunohistochemistry
IR	insulin receptor
IL	interleukin
KCNK3	potassium channel, subfamily K, membrane 3
IMM	inner mitochondrial membrane
MCP1	monocyte chemotactic protein 1
MRI	Magnetic Resonance Imaging
<i>Myf5</i>	myogenic factor 5
NCBI	National Centre for Biotechnology Information
NE	norepinephrine
NHS	National Health Service
NOO	National Obesity Observatory
NRF	nuclear respiratory factor
NRES	National Research Ethics Service Committee
NST	nonshivering thermogenesis
OD	optical density
PAI1	plasminogen activator inhibitor 1

PAT	pericardial adipose tissue
PAGE	polyacrylamide gel electrophoresis
PET	Positron Emission Tomography
PGC	peroxisome proliferator-activated receptor- γ coactivator
PPAR	peroxisome proliferator-activated receptor
pRb	retinoblastoma protein
PRDM	PR (PRD1-BF1-RIZ1 homologous)-domain-containing protein
PRLR	prolactin receptor
REC	Research Ethics Committee
REE	resting energy expenditure
RIN	RNA integrity number
RIP	receptor interacting protein
SaO ₂	oxygen saturation
SDS	sodium dodecyl sulphate
SEM	standard error of mean
SRC	steroid receptor co-activator
TEE	total energy expenditure
TGM	transglutaminase

TNF α	tumour necrosis factor alpha
UAR	UCP1 gene activating region
UCP1	uncoupling protein 1
UV	ultraviolet
VAT	visceral adipose tissue
VDAC	voltage dependent anion channel
VGEF	vascular endothelial growth factor
VLDL	very low density lipoprotein
WAT	white adipose tissue
WAZ	weight for age z-score
WHZ	weight for height z-score
WHO	World Health Organisation

Table of contents

Abstract iii

Acknowledgements vii

Declaration x

Publications and presentations xi

Abbreviations..... xii

Table of contents..... xvii

Table of Figures..... xxix

Table of Tablesxxxii

1 Introduction..... 1

1.1 Obesity 1

1.1.1 Obesity is a global epidemic 1

1.1.2 Childhood obesity tracks into adulthood..... 2

1.1.3 Obesity is a burden on physical and mental health of individuals and the society 4

1.1.4 Obesity is a socio-economic burden 5

1.1.4.1 The metabolic syndrome..... 5

1.1.5 Causes of obesity 6

1.2 Influences of early life nutrition on obesity, metabolic syndrome and cardiovascular diseases in adult life..... 7

1.2.1 Consequences of undernutrition in early life 7

1.2.2 Consequences of overnutrition in early life..... 9

1.3 Adipose tissue 11

1.3.1	Classification of adipose tissue	11
1.4	Adipogenesis	13
1.4.1	Commitment of stem cells to adipose lineage	13
1.4.2	Terminal differentiation of adipocytes.....	13
1.4.3	Brown and white adipogenesis occurs via two distinct pathways	15
1.4.4	Development of adipose tissue in fetal life	18
1.5	White adipose tissue	19
1.5.1	Endocrine functions of white adipose tissue.....	19
1.5.1.1	Leptin	20
1.5.1.2	Adiponectin	21
1.6	Brown adipose tissue.....	22
1.6.1	Uncoupling protein 1 – the unique BAT protein.....	23
1.6.1.1	Mode of action of UCP1.....	23
1.6.1.2	Activation of UCP1	26
1.6.1.3	Regulation of UCP1 biosynthesis	26
1.6.2	Brown fat development	28
1.6.2.1	Brown adipose tissue develop from myogenic precursors	28
1.6.3	Adrenergic control of brown adipose tissue.....	29
1.6.3.1	UCP1 gene expression is regulated by adrenergic stimulation	30
1.6.3.2	Adrenergic systems control brown adipose tissue metabolism.....	30
1.6.4	Role of thyroid hormones in BAT thermogenesis	33
1.6.5	Other metabolic actions of BAT	35
1.6.5.1	Lipid metabolism and BAT	35
1.6.5.2	Glucose metabolism and BAT	37

1.7	Brite adipocytes - a different type of adipocytes are present in white adipose depots	38
1.7.1	Origin of brite adipocytes	39
1.8	Energy balance and its role in obesity	41
1.8.1.1	Energy expenditure in humans	42
1.8.2	Role of BAT in energy balance in humans	44
1.8.2.1	Cold induced non-shivering thermogenesis in humans	44
1.8.2.2	Diet induced thermogenesis in humans.....	45
1.8.3	Role of BAT in obesity in humans	47
1.9	Distribution of adipose tissue	49
1.10	Pericardial adipose tissue	51
1.10.1	Anatomy of adipose tissue in and around the heart	51
1.10.2	Normal physiological functions of pericardial adipose tissue	55
1.10.3	Role of pericardial adipose tissue in cardiovascular pathologies	56
1.10.3.1	Evidence of association of pericardial adiposity with cardiovascular disease in humans.....	57
1.10.4	Pericardial adipose tissue is a BAT depot in adult humans.....	60
1.11	Use of animal models	61
1.11.1	Sheep as a model of developmental programming in humans.....	62
1.12	Hypotheses and aims	64
1.12.1	Chapter 3.....	64
1.12.2	Chapter 4.....	64
1.12.3	Chapter 5.....	65
1.12.4	Chapter 6.....	65

2	Materials and methods	66
2.1	Procedural and legislative declaration and ethical approvals	66
2.1.1	Approvals for the animal experiments	66
2.1.2	Approvals for the human studies.....	66
2.1.2.1	Study of brown adipose tissue in epicardial fat of adult humans	66
2.1.2.2	Study of brown adipose tissue in pericardial fat of newborns, infants and children	67
2.2	Animal experiments	68
2.2.1	Experimental procedure: Effect of maternal nutrient restriction on UCP1 and other BAT associated genes in pericardial adipose tissue of newborn sheep.....	68
2.2.2	Experimental procedure: Suboptimal maternal nutrition during early-to-mid gestation in the sheep enhances pericardial adiposity in the near-term fetus	70
2.3	Human Studies	71
2.3.1	Epicardial fat is a depot of brown adipose tissue in adult humans	71
2.3.2	Brown adipose tissue is present epicardial fat of newborn infants, children and adolescents	72
2.4	Laboratory procedures	74
2.4.1	Tissue analysis	75
2.4.1.1	Total ribonucleic acid extraction from tissue samples	75
2.4.1.1.1	Principle	75
2.4.1.1.2	RNA extraction procedure.....	76
2.4.1.1.3	Determination of RNA concentration purity and integrity.....	79
2.4.1.2	Reverse Transcription polymerase chain reaction (RT-PCR)	82
2.4.1.2.1	Principle of Reverse transcription polymerase chain reaction	82

2.4.1.2.2	Procedure for Reverse transcription polymerase chain reaction	84
2.4.1.3	Quantitative Polymerase Chain Reaction	84
2.4.1.3.1	Principle of Quantitative Polymerase Chain Reaction	84
2.4.1.3.2	Selection of the reference gene	92
2.4.1.3.3	Development of oligonucleotide primers for Q-PCR.....	93
2.4.1.4	Quantitative Polymerase Chain Reaction - procedure	96
2.4.1.4.1	Hot start PCR procedure.....	96
2.4.1.5	Microarray analysis	102
2.4.1.5.1	Principles of microarray analysis	102
2.4.1.5.2	Procedure: microarray analysis using GeneChip®	103
2.4.2	Protein analysis	105
2.4.3	Preparation of mitochondrial extracts.....	105
2.4.3.1	Assessment of protein concentration.....	106
2.4.3.1.1	Bicinchoninic acid total protein determination.....	106
2.4.3.1.2	Bradford assay	108
2.4.3.2	Western Blotting.....	111
2.4.3.2.1	Principle of Western Blotting.....	111
2.4.3.2.2	Western Blotting procedure	113
2.4.3.3	Immunohistochemistry	122
2.4.3.3.1	Sample preparation for IHC	122
2.4.3.3.2	IHC staining	124
2.4.3.3.3	Antibodies used for immunohistochemistry	127
2.4.4	Statistical analysis	128
3	Effect of maternal nutrient restriction on UCP1 and other BAT associated genes in pericardial adipose tissue of newborn sheep	130
3.1	Introduction.....	130

3.1.1	Hypothesis and aim	132
3.2	Methods.....	133
3.2.1	Experimental design	133
3.2.2	Laboratory procedures.....	135
3.2.2.1	mRNA detection.....	135
3.2.2.2	Protein Analysis	137
3.2.3	Statistical Analysis	138
3.3	Results.....	139
3.3.1	Whole body, heart and adipose tissue weights and adipose tissue composition.....	139
3.3.2	Mitochondrial proteins in the newborn and effect of maternal nutrient restriction	141
3.3.3	Effect of maternal nutrient restriction on BAT related genes.....	143
3.3.4	Effect of maternal nutrient restriction on BAT related transcription factors	145
3.3.5	Effect of maternal nutrient restriction on WAT related genes and adipokines.....	147
3.3.6	Effect of maternal nutrient restriction on β adrenergic receptors and type 2 iodothyronine deiodenase gene.....	150
3.3.7	Effect of maternal nutrient restriction on genes involved in glucose metabolism	152
3.3.8	Relationship between UCP1 gene expression and protein abundance.....	154
3.4	Discussion.....	155
3.4.1	Pericardial adipose tissue changes from BAT to WAT in infancy	155
3.4.2	BAT development is modulated by maternal nutrient restriction in late gestation	156
3.4.3	Total amount of UCP1 in the pericardial depot.....	157

3.4.4	Correlation between UCP1 abundance and gene expression	158
3.4.5	Maternal nutrient restriction affects genes controlling non-shivering thermogenesis	158
3.4.6	BAT in the pericardial depot.....	160
3.5	Conclusion	161
4	Suboptimal maternal nutrition during early-to-mid gestation followed by <i>ad libitum</i> feeding in the sheep enhances pericardial adiposity in the near-term fetus	162
4.1	Introduction.....	162
4.1.1	Hypothesis and aim	163
4.2	Methods	164
4.2.1	Animal and diet.....	164
4.2.2	Laboratory procedures.....	166
4.2.2.1	Histology	166
4.2.2.2	Gene expression.....	166
4.2.2.3	Mitochondrial protein analysis	167
4.2.3	Statistical analysis	167
4.3	Results.....	168
4.3.1	Whole body and adipose tissue weights and pericardial adipose tissue composition.....	168
4.3.2	Presence of UCP1 in pericardial adipose tissue of sheep at 140 d gestation.....	170
4.3.3	Effect of maternal nutrient restriction on genes involved in adipogenesis.....	174
4.4	Discussion.....	177
4.4.1	Suboptimal maternal nutrition in early-to-mid gestation followed by <i>ad libitum</i> feeding enhances fetal adiposity.....	177

4.4.2	Suboptimal maternal nutrition in early-to-mid gestation followed by ad libitum feeding enhances adipogenic potential in the fetal pericardial depot.....	178
4.4.3	Suboptimal maternal nutrition in early-to-mid gestation followed by ad libitum feeding increases thermogenic potential of the fetal pericardial depot	180
4.5	Conclusion	184
5	Epicardial fat is a depot of brown adipose tissue in adult humans	185
5.1	Introduction.....	185
5.1.1	Hypothesis and aim	186
5.2	Methods	186
5.2.1	Ethical approval	186
5.2.2	Adipose tissue samples	186
5.2.3	Preparation of mitochondrial extract.....	187
5.2.3.1	Assessment of protein concentration.....	187
5.2.3.2	Western Blotting Procedure	187
5.2.4	Statistical analysis	188
5.3	Results.....	189
5.3.1.1	Mitochondrial protein in adult human adipose tissue.....	189
5.3.2	UCP1 in epicardial, visceral paracardial, and subcutaneous fat	189
5.3.3	Correlation between relative protein abundance and fold change in gene expression	190
5.3.4	Correlation between relative UCP1 abundance and age and body mass index	190
5.4	Discussion.....	196
5.4.1	UCP1 gene expression does not correlate with protein abundance in human EAT	197
5.4.2	UCP abundance in human EAT does not correlate with BMI or age of the subjects	198

5.4.3	The limitations	200
5.4.4	Significance of UCP1 in human EAT.....	200
5.5	Conclusion	202
6	Brown adipose tissue is present in epicardial fat of newborn infants, children and adolescents.....	203
6.1	Introduction.....	203
6.1.1	Hypothesis.....	205
6.2	Methods.....	206
6.2.1	Ethical and Regulatory Approvals	206
6.2.2	Adipose tissue samples	206
6.2.3	Laboratory analysis.....	208
6.2.3.1	Analysis of gene expression	208
6.2.3.2	Immunohistochemistry	209
6.2.4	Data collection	210
6.2.5	Statistical analysis	211
6.3	Results.....	212
6.3.1	Anthropometric assessment of participants.....	214
6.3.1.1	Anthropometric measures of children 0-2 years of age.....	216
6.3.1.1.1	Newborn infant anthropometric measures were normal but Asian infants were significantly lighter and shorter than Caucasian infants.	218
6.3.1.1.2	Wasting was present in one-third of children undergoing cardiac surgery between 29 days and 2 years of age	220
6.3.2	Analysis of gene expression	222
6.3.2.1	UCP1 gene is expressed in epicardial fat in children	222
6.3.2.2	UCP1 in children 0-2 years of age.....	224
6.3.2.2.1	Effect of gender on expression of UCP1 gene in epicardial adipose tissue of children 0-2 years of age	225

6.3.2.2.2	Effect of use of propranolol on expression of UCP1 gene in epicardial adipose tissue of children 0-2 years of age.....	225
6.3.2.2.3	Effect of ethnic origin on expression of UCP1 gene in epicardial adipose tissue of children 0-2 years of age.....	225
6.3.2.2.4	There is no correlation between UCP1 gene expression in epicardial adipose tissue and age in children 0-2 years of age	227
6.3.2.2.5	UCP1 gene expression in epicardial adipose tissue is associated with weight for age z-score in children 0-2 years of age	228
6.3.2.2.6	The correlation between UCP1 gene expression in epicardial adipose tissue and weight for age z-score is independent of age, gender, baseline oxygen saturations and use of propranolol	230
6.3.2.3	UCP1 in epicardial adipose tissue of newborn infants	231
6.3.2.3.1	UCP1 gene expression in epicardial adipose tissue of newborn infants (0-28 days) is independent of age, gender, ethnic origin, weight for age z-score or baseline oxygen saturations.....	231
6.3.2.4	Epicardial fat mRNA expression of other genes involved in brown and white adipose tissue development and metabolism.....	233
6.3.2.4.1	Effect of gender on gene expression	233
6.3.2.4.2	Effect of ethnic origin on gene expression in epicardial fat	233
6.3.2.5	Expression of leptin gene in epicardial fat is associated with weight for age z-score in 0-2 year old children	236
6.3.2.6	Expression of leptin gene in epicardial fat is not associated with age in children 0-2 years of age	236
6.3.3	Gene expression in children with high vs. low UCP1 gene expression	238
6.3.4	Uncoupling Protein 1 is present in epicardial adipose tissue	241
6.3.4.1	Epicardial adipose tissue of newborn infants is predominantly brown fat.....	241
6.3.4.2	Islands of brown adipose tissue are present in epicardial fat of older infants and adolescents.	243
6.4	Discussion.....	247

6.4.1	Human epicardial adipose tissue is a depot of brown fat in newborn infants and children.....	247
6.4.2	Caucasian children have a higher expression of UCP1 gene when compared to children of South Asian and mixed ethnicity	249
6.4.3	There was no difference in UCP1 gene expression between boys and girls in early childhood.....	251
6.4.4	UCP1 gene expression was not affected by treatment with propranolol	253
6.4.5	In early childhood (0-2 years), gene expression of UCP1 in epicardial fat is downregulated in children with lower weight for age z-scores	256
6.4.6	In early childhood (0-2 years), gene expression of leptin in epicardial fat is downregulated in children with lower weight for age z-scores	259
6.4.7	Children with high UCP1 gene expression have a different mRNA expression pattern as compared to children with low UCP1 gene expression	260
6.4.8	Epicardial fat in children.....	263
6.4.9	Strengths of the study	266
6.4.10	Limitations of the study	267
6.5	Conclusion	269
7	Summary and conclusions	270
7.1	Pericardial fat is a depot of brown adipose tissue	270
7.2	Pericardial fat is a nutritionally regulated depot of brown adipose tissue	271
8	Future research.....	274
8.1	Implications for future research	275
8.2	Implications for public health	276
9	References	278

10	Appendices	310
10.1	Ethical approvals for human studies	310
10.1.1	Study of brown adipose tissue in epicardial fat of adult humans	310
10.1.2	Study of brown adipose tissue in pericardial fat of newborns, infants and children	313
10.2	Data collection proforma for the Study of brown adipose tissue in pericardial fat of newborns, infants and children.....	318
10.3	Clinical characteristics of participants	320
10.4	Abstracts of original peer reviewed publications and papers.....	330
10.4.1	Brown adipose tissue genes in pericardial adipose tissue of newborn sheep are downregulated by maternal nutrient restriction in late gestation.....	330
10.4.2	Adult Epicardial Fat Exhibits Beige Features	332
10.4.3	Suboptimal maternal nutrition during early-to-mid gestation in the sheep enhances pericardial adiposity in the near-term fetus.....	334
10.5	Details of suppliers.....	336

Table of Figures

Figure 1.1. Prevalence of obesity in school age children in England by year of measurement, school year and gender.....	3
Figure 1.2 The three types of adipocytes	12
Figure 1.3. Genes involved in brown and white adipogenesis.....	17
Figure 1.4. Mechanism of action of uncoupling protein 1	25
Figure 1.5. Activation of UCP1 by adrenergic stimulation	32
Figure 1.6 Regulation of brown adipose tissue (BAT) by thyroid hormones ...	34
Figure 1.7. Lipid uptake by brown adipocytes	36
Figure 1.8 Components of energy balance in adult humans	43
Figure 1.9 Adipose tissue in and around the heart.....	54
Figure 2.1 Chromatograms of micro-capillary electrophoresis from two RNA samples showing different degrees of degradation	81
Figure 2.2. Reverse Transcription.....	83
Figure 2.3. Polymerase chain reaction with Taq polymerase	87
Figure 2.4. Standard Curve.....	89
Figure 2.5 Melt Curve	91
Figure 2.6. Standard curve for estimation of protein content in mitochondrial extract.....	110
Figure 2.7. Representative of All blue prestained Precision Plus Protein standards on a 4-20% Tris-HCl Criterion™ Gel	116
Figure 2.8. Configuration of the polyacrylamide gel and nitrocellulose membrane in relation to the electrodes during electroblotting	118
Figure 2.9. Ponceau S staining of nitrocellulose membrane showing the electroblotting of protein on to the membrane and molecular weight markers on either side.....	119
Figure 3.1. Experimental study design for Chapter 3	134

Figure 3.2 A: UCP1, B: cytochrome c and C: VDAC protein abundance in pericardial adipose tissue of sheep in early postnatal life and the effect of maternal nutrient restriction in late gestation.....	142
Figure 3.3. Gene expression of A: UCP1, B: KCNK3, C: TGM2 and D: prolactin receptor (PRLR) in pericardial adipose tissue of sheep in early postnatal life and the effect of maternal nutrient restriction in late gestation.	144
Figure 3.4. Gene expression of A: BMP7, B: PPAR γ , C: PGC1 α and D: PRDM16 receptor in pericardial adipose tissue of sheep in early postnatal life and the effect of maternal nutrient restriction in late gestation	146
Figure 3.5. Gene expression of A: HOXc9, B: RIP140, C: leptin and D: adiponectin in pericardial adipose tissue of sheep in early postnatal life and the effect of maternal nutrient restriction in late gestation	149
Figure 3.6. Gene expression of A: β 1ADR, B: β 2ADR, C: β 3ADR and D: DIO2 in pericardial adipose tissue of sheep in early postnatal life and the effect of maternal nutrient restriction in late gestation.....	151
Figure 3.7 Gene expression of A: Insulin receptor, B: Glucose transporter type 4 (GLUT4), C: Glucocorticoid receptor (GR) in pericardial adipose tissue of sheep in early postnatal life and the effect of maternal nutrient restriction in late gestation	153
Figure 3.8 UCP1 gene expression is not correlated to protein abundance in pericardial adipose tissue of newborn lambs.....	154
Figure 4.1 Experimental study design for Chapter 4	165
Figure 4.2 Representative images of pericardial adipose tissue structure at 140 day gestation in fetal sheep	171
Figure 4.3 Effect of suboptimal maternal nutrition in early-to-mid gestation on (A) uncoupling protein 1 (UCP1) mRNA expression and (B) UCP1 protein abundance in pericardial adipose tissue of 140 day gestation sheep fetus ..	172
Figure 4.4. Effect of suboptimal maternal nutrition in early-to-mid gestation on adipogenesis	183
Figure 5.1. Relative protein abundance of UCP1 in fat samples	193

Figure 5.2 Correlation between relative protein abundance and fold change in gene expression of UCP1 in human epicardial adipose tissue.....	194
Figure 5.3. Correlation between relative protein abundance of uncoupling protein 1 (UCP1) in epicardial adipose tissue and age and body mass index (BMI) of adult humans	195
Figure 6.1. Uncoupling protein 1 (UCP1) gene expression in epicardial fat in children.....	223
Figure 6.2 Uncoupling protein 1 (UCP1) gene expression in epicardial adipose tissue of children 0-2 years of age.....	226
Figure 6.3 Uncoupling protein 1 (UCP1) gene expression in epicardial adipose tissue of children 0-2 years of age does not correlate with age.....	227
Figure 6.4 Uncoupling protein 1 (UCP1) gene expression in epicardial adipose tissue of children 0-2 years of age correlates with weight for age z-score....	229
Figure 6.5 Leptin gene expression in epicardial adipose tissue of children 0-2 year old correlates with weight for age z-score	237
Figure 6.6 Representative images of epicardial adipose tissue from a 6 day old male infant	242
Figure 6.7 Representative images of epicardial adipose tissue from an 18 month old male child.....	244
Figure 6.8 Representative images of epicardial adipose tissue from a 3 year old male child.....	245
Figure 6.9 Representative images of epicardial adipose tissue from a 17 year old male.....	246

Table of Tables

Table 2.1 PCR Primer Sequences for Sheep Studies	95
Table 2.2. Reaction mixture for classical PCR	96
Table 2.3. Hot Start PCR programme.	97
Table 2.4. Q-PCR reaction mixture	101
Table 2.5. Q-PCR programme conditions	101
Table 3.1. Mean total body weight, pericardial adipose tissue and heart weights and total protein and total mitochondrial protein contents of pericardial adipose tissue (relative to protein content of control group) in offspring of control and nutrient restricted mothers at Day 0 and Day 30 life.	140
Table 4.1. Mean total body weight, visceral and pericardial adipose tissue weights, and total protein and total mitochondrial protein contents of pericardial adipose tissue in near term fetuses born to control and nutrient-restricted mothers at 140 days of gestation.	169
Table 4.2. Multiple regression analyses for uncoupling protein 1 (UCP1) gene expression and relative protein content as dependent variable and mother's nutrition group, mother's weight, fetal weight and pericardial adipose tissue weight as independent variables (n=12)	173
Table 4.3. Effect of suboptimal maternal nutrition in early-to-mid gestation on genes expression of adipogenic transcription factors in pericardial adipose tissue of fetus at 140 days of gestation	175
Table 4.4. Effect of suboptimal maternal nutrition in early-to-mid gestation on genes expression of β -adrenergic receptors, genes involved in adipocyte metabolism and adipokines in pericardial adipose tissue of fetus at 140 days of gestation.....	176
Table 5.1. Characteristics of patients.....	191
Table 5.2. Total mitochondrial protein content of adipose tissue in different depots.....	192
Table 6.1 Basic characteristic of the participants	213

Table 6.2 Anthropometric assessment of all participants and those included in gene analyses	215
Table 6.3. Weight for age, height for age and body mass index z-scores of 0-2 year old children	217
Table 6.4. Weight for age, height for age and body mass index z-scores of 0-2 year old children classified according to ethnic origin.....	217
Table 6.5. Weight for age, height for age and body mass index z-scores of newborn infants classified according to gender.....	219
Table 6.6 Weight for age, height for age and body mass index z-scores of newborn infants classified according to ethnic origin.....	219
Table 6.7. Weight for age and height for age z-scores of 29 days to 2 year old children classified according to ethnic origin	221
Table 6.8 Multiple regression analysis of UCP1 gene expression in epicardial adipose tissue of 0-2 year old children.....	230
Table 6.9 Multiple regression analysis of UCP1 gene expression in epicardial adipose tissue of newborn infants.....	232
Table 6.10 Comparison between gene expression in males vs. females in epicardial adipose tissue of 0-2 year old children.....	234
Table 6.11 Comparison between gene expression in Caucasian vs. Asians subjects in epicardial adipose tissue of 0-2 year old children.....	235
Table 6.12 Comparison between gene expression in children with high vs. low UCP1 gene expression.....	240
Table 9.1 Characteristics of participants: diagnosis and medications.....	320

1 Introduction

1.1 Obesity

Obesity and overweight are defined by abnormal or excessive fat accumulation which may impair health. Although there is no universal definition of “healthy weight”, the World Health Organisation (WHO) expert committee has proposed a classification of overweight and obesity using body mass index (BMI) (WHO 1995). According to this widely accepted definition, an individual with a BMI of equal to or more than 30kg/m^2 is classified as obese, whilst a BMI in the range 25kg/m^2 to 29.9kg/m^2 is defined as overweight.

1.1.1 Obesity is a global epidemic

Using the above definition, just over a quarter (26%) of adults in England are classified as obese (NHSIC 2012). Similar trends are seen in other Western countries and the WHO have reported that, in Europe, the prevalence of obesity has risen up to three-fold in the last two decades and that the epidemic of obesity poses one of the most serious public health challenges (WHO 2006). With the adoption of the “Western lifestyle” involving decreased physical activity and overconsumption of energy-dense food, the obesity epidemic has spread to the developing world where it is estimated that rates of obesity have tripled in the past two decades (Hossain et al. 2007).

Similar to the trend amongst adults, childhood obesity is also increasing to epidemic proportions. Forty-three million children were estimated to be overweight or obese in 2010 and the worldwide prevalence of childhood obesity and overweight has increased from 4.2% in 1990 to 6.7% in 2010 with an expected rise to over 9% by 2020 (de Onis et al. 2010). In the U.K., although, year on year, children are entering reception class weighing less, they are leaving primary school weighing more (Figure 1.1); in 2012, at the end of school Year 6 (11-12 year of age), 20.7% of boys and 17.7% of girls were classified as obese (BMI \geq 95th centile of the British 1990 (UK90) growth reference) (CMO 2012).

1.1.2 Childhood obesity tracks into adulthood

Overweight and obese children are at a significantly high risk of growing into overweight and obese adults (Singh et al. 2008) and have an increased risk of premature mortality and obesity related adult morbidities, particularly due to cardio-metabolic conditions such as type 2 diabetes, coronary heart disease, hypertension, and stroke (Reilly and Kelly 2011). Childhood obesity also has an adverse impact on social and economic outcomes in adulthood; obesity at a young age increases the risk of economic productivity losses (Neovius et al. 2008) and increases the risk of receiving disability allowance in later life (Karnehed et al. 2007).

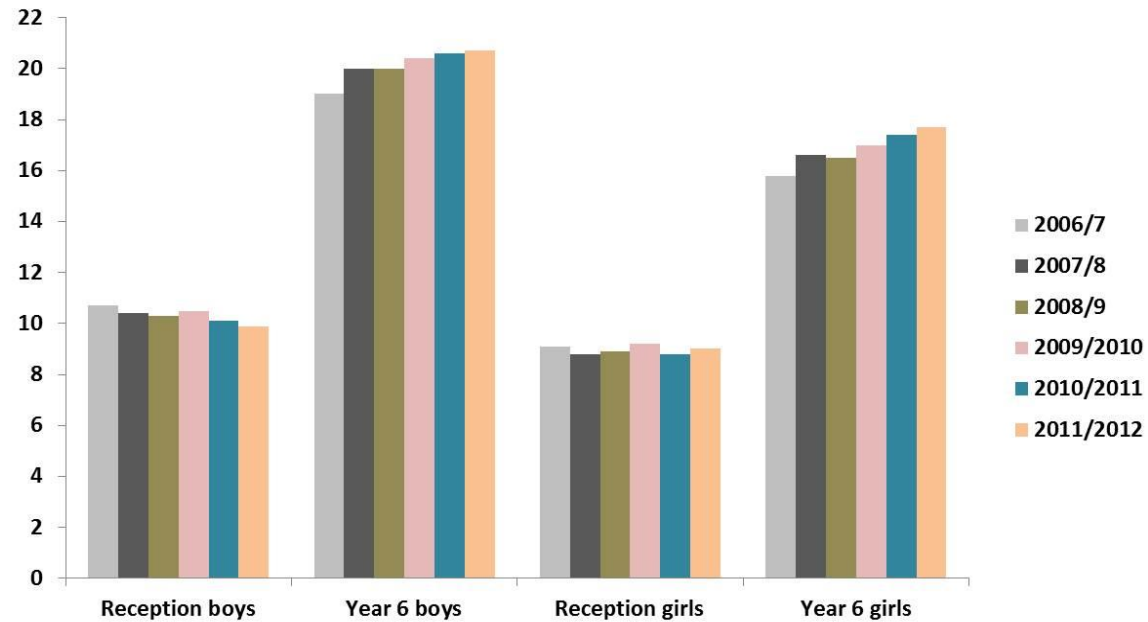


Figure 1.1. Prevalence of obesity in school age children in England by year of measurement, school year and gender

Children were classified as obese where their BMI \geq 95th centile of the British 1990 (UK90) growth reference. Adapted from Chief Medical Officer's Report 2012 (data source Public Health England) (CMO 2012).

1.1.3 Obesity is a burden on physical and mental health of individuals and the society

Obesity is associated with a significant increase in morbidity and mortality and is a major public health problem. It causes, or exacerbates, many health problems both independently and in association with other conditions such as Type 2 diabetes (Kopelman 2000).

Obesity is associated with a significantly higher risk of several conditions such as the metabolic syndrome, hypertension, coronary heart disease (CHD), insulin resistance, Type 2 diabetes, dyslipidaemias, obstructive sleep apnoea, certain types of cancers and musculoskeletal disorders such as osteoarthritis (Kopelman 2000, Visscher and Seidell 2001). Being overweight or obese can decrease life expectancy. In the Framingham Heart Study, the risk of death within 26 years of entering the study increased by 1% for each extra pound (0.45kg) increase in weight between the ages of 30 and 42 years, and by 2% between the ages of 50 and 62 years (Hubert 1986).

In addition to the direct physical consequences, obesity also has a major impact on the psychological wellbeing and quality of life of adults (Jia and Lubetkin 2005) and in children (Friedlander et al. 2003).

Systematic reviews of the relationship between mental health problems and overweight and obesity reveal that increase in the risk of

depression (Luppino et al. 2010), anxiety (Garipey et al. 2010) and general emotional disorders (Scott et al. 2008).

1.1.4 Obesity is a socio-economic burden

The consequences of obesity are not limited to its direct impact on health. Overweight and obesity can also have adverse social consequences for the individual, for example leading to social discrimination, personal loss of earnings and effects on the wider economy through loss of productivity and increased use of benefit payments from government (NOO 2010). Estimates of the direct costs of treating obesity and its related morbidities to the National Health Service (NHS) in England were over four billion pounds in 2008 (NOO 2010). The long-term cost of childhood obesity is estimated to be £588-686 million per year (CMO 2012) whilst the indirect costs associated with obesity are estimated to be even higher and could be between £2.6 to £15.8 billion (NOO 2010).

1.1.4.1 The metabolic syndrome

A cluster of interrelated risk factors for cardiovascular disease and diabetes including elevated fasting blood glucose, raised blood pressure, dyslipidaemia, high cholesterol and obesity (particularly central obesity, measured as elevated waist circumference) have become known as the metabolic syndrome (Alberti et al. 2009).

Individuals with the metabolic syndrome have an elevated risk of CHD,

stroke, myocardial infarction and cardiovascular mortality (Isomaa et al. 2001, Bonora et al. 2004). With or without obesity (as measured by BMI), metabolic syndrome is a major health problem and is a vital contributor to the ill health caused by increasing adiposity.

1.1.5 Causes of obesity

Obesity develops when energy intake exceeds energy expenditure over a significant period of time. Body weight is ultimately determined by complex interactions between genetic, environmental and physiological mediators of food intake and energy expenditure and the debate whether obesity is caused by over-eating, lack of physical activity or genetic predisposition is unresolved (Visscher and Seidell 2001). Epidemiological trends indicate that changes in dietary and physical activity patterns are a cause of increasing obesity on a global scale. However, epidemiological, genetic and metabolic studies reveal that some individuals appear to have a greater predisposition to become obese and acquire obesity-related co-morbidities than others. An increasing body of epidemiological and experimental evidence suggests that factors in the periconceptual period, in utero and early childhood may determine this susceptibility to obesity and its associated illnesses in later life (Gillman 2005).

1.2 Influences of early life nutrition on obesity, metabolic syndrome and cardiovascular diseases in adult life

It is now accepted that the origins of childhood and adult obesity may lie in the early years including the time in utero and even the pre-conception period. The recent demographic shift of populations in most parts of the world and of varied genetic backgrounds towards a more obese phenotype suggests the influence of factors other than solely genetics (Finucane et al. 2011). The idea that maternal wellbeing is crucial for the future health of the baby is well recognised and, gradually, the concept of developmental origins of health and diseases has become well established (Gillman 2005).

1.2.1 Consequences of undernutrition in early life

In 1977, Forsdahl linked mortality from arteriosclerotic heart disease in a Swedish cohort with infant mortality in the same cohort and suggested that poverty in childhood and adolescence followed by prosperity, is a risk factor of cardiovascular diseases (Forsdahl 1977). Later, Barker and colleagues demonstrated a similar relationship in the population of England and Wales (Barker and Osmond 1986). Barker et al. also investigated how periods of undernutrition at different stages of fetal life were associated with birth phenotypes and with later metabolic abnormalities in adulthood (Barker et al. 1993). Barker and Hales

proposed the “thrifty phenotype hypothesis” proposing that the epidemiological associations between poor fetal and infant growth and the subsequent development of type 2 diabetes and the metabolic syndrome result from the effects of poor nutrition in early life, which produces permanent changes in metabolism that later manifest as disorders of metabolic homeostasis (Hales and Barker 2001).

This link between early life environment and health in later life is described as “developmental programming” (Lucas 1991). The term defines a process by which a stimulus or an insult during a critical period of development has lasting effects on the structure or function of tissues and body systems. Tissues and systems of the body go through critical periods of growth and development while in utero and during early childhood. Adverse environmental influences, such as inadequate nutrition, during these critical periods can permanently alter the structure and function of tissues and organs and these early life changes can subsequently render affected individuals more susceptible to disease in later life. For example, the metabolic, functional or structural changes that occur in response to suboptimal nutrition in utero and in early life in order to enable the individual to survive the adversity experienced in the fetal period become detrimental later in life if the environment changes to one of nutrient excess, leading to increased risk of metabolic syndrome, obesity and cardiovascular diseases.

Nutrition in fetal life is a central stimulus of programming for susceptibility to diseases in later childhood and adulthood. Long term follow up of the offspring of pregnant women who suffered undernutrition during the Dutch famine of 1944-45 provides epidemiological evidence of the effects of prenatal exposure to maternal undernutrition on adult health such as those who were exposed to famine in early gestation had a more atherogenic lipid profile (Roseboom et al. 2001), higher risk of CHD (Roseboom et al. 2000) and higher BMI (Ravelli et al. 1999).

Adipose tissue is present from very early in fetal development and changes in maternal nutrition during various stages of pregnancy can alter fetal adiposity and programme later obesity (Symonds et al. 2007). Various mechanisms such as alterations in glucocorticoid metabolism (Budge et al. 2005), insulin and glucose homeostasis (Gardner et al. 2005), alterations in the hypothalamo-pituitary-adrenal (HPA) axis (Vieau et al. 2007) and increase in fetal adiposity (Budge et al. 2005) contribute to the programming of adipose tissue.

1.2.2 Consequences of overnutrition in early life

Risk of obesity and metabolic syndrome in adult life can be influenced by both extremes of nutrition in early life and the relationship between birth weight and adult obesity is actually J- or U-shaped with increases in adult BMI seen both in those born small and in those born large for

gestation age in comparison to those who were of appropriate birth weight (Curhan et al. 1996). This association between early overnutrition and later obesity and metabolic syndrome has been described as the “developmental overnutrition hypothesis.” This hypothesis advocates that high glucose, fatty acid and amino acid concentrations during critical periods of development result in permanent changes in appetite control, neuroendocrine functioning and/or energy metabolism which increase the risk of obesity and metabolic syndrome in later life (Armitage et al. 2008).

Both animal experimental data and human epidemiological evidence converge to suggest that the nutritional environment during fetal development impact upon specific physiological control systems and induce permanent changes that produce a lifelong susceptibility to obesity and the metabolic syndrome. Preventative strategies to reduce the burden of obesity and the metabolic syndrome should, therefore, be targeted to children and started in early life or even before birth.

1.3 Adipose tissue

In mammals, adipose tissue is the only tissue that has an unlimited potential to grow. It varies in amount and distribution between individuals and is generally considered to exist in two compartments – subcutaneous adipose tissue, located beneath the skin, and visceral adipose tissue, located around the internal organs.

1.3.1 Classification of adipose tissue

Mammalian adipose tissue is classified into white adipose tissue (WAT) and brown adipose tissue (BAT). In addition, a novel type of adipocyte, “brown-in-white” or “brite” or “beige” adipocyte has now been recognised. All the three types of adipocytes are characterised by large intracellular stores of fat but are otherwise dissimilar in embryological origin, structure and/or function (Figure 1.2).

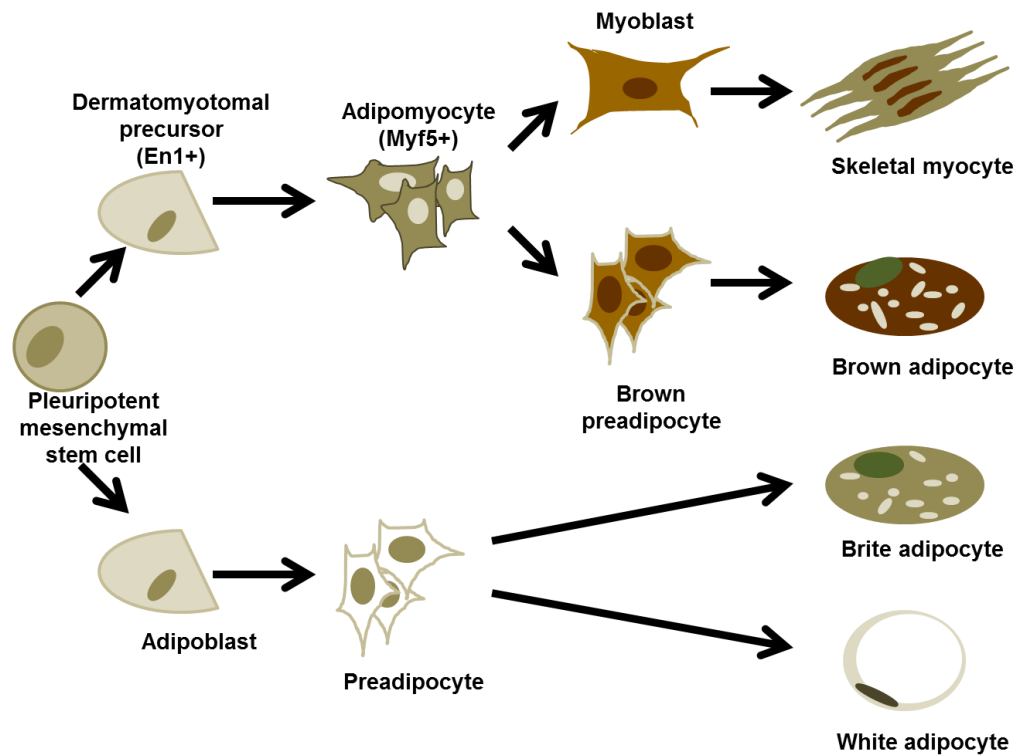


Figure 1.2 The three types of adipocytes

Three different types of adipocytes arise from the pleuripotent mesenchymal stems cells: Classic brown adipocytes that arise from the dermatomyotome, via Myf5+ precursors, express classic BAT markers such as UCP1 and PCG1 α as well as novel markers Zic1 and Lhx8. These cells reside in classic BAT depots, “brite” adipocytes that are brown adipocytes within WAT depots that possess the total machinery for adaptive thermogenesis but have a different gene expression pattern (absence of myogenic markers, Zic1 and Lhx8) and arise from preadipocytes, and white adipocytes that express leptin and S-100 surface markers.

UCP: uncoupling protein; Myf5: myogenic factor 5; En1: engrailed 1;

Figure adapted from Kajimura et al. 2010 (Kajimura et al. 2010).

1.4 Adipogenesis

The biogenesis of adipocytes comprises the differentiation of mesenchymal stem cells to committed precursor cells called preadipocytes, followed by terminal differentiation into mature adipocytes (Rosen and Spiegelman 2000) (Figure 1.2).

1.4.1 Commitment of stem cells to adipose lineage

When appropriately stimulated, pluripotent mesenchymal stem cells undergo commitment to the adipocyte lineage. The exact mechanisms behind this commitment remain unresolved but several drivers have been identified. Bone morphogenetic protein (BMP) signalling is implicated in the commitment of stem cells to the adipocyte lineage and BMP4 and BMP2 both induce mouse stem cells to form preadipocyte-like cells which can differentiate into cells with adipocyte phenotype (Tang and Lane 2012). Other signalling pathways, such as Wnt signalling, activate this lineage commitment of mouse stem cells while Hedgehog (Hh) signalling has an inhibitory effect.

1.4.2 Terminal differentiation of adipocytes

The next step of adipogenesis is the terminal differentiation of committed precursors to adipocytes. In this process the adipocytes acquire characteristics such as the machinery for lipid transport and synthesis, insulin action and secretion of adipocyte specific proteins.

Several transcriptional regulators and extranuclear factors come together to orchestrate adipocyte differentiation. Induction of differentiation is marked by the activation of C/EBP- β and C/EBP- δ which directly induce the expression of PPAR- γ and C/EBP- α . These are key regulators of adipocyte differentiation (Tang et al. 2005). In addition, several other transcription factors such as the Kruppel-like factors, steroid regulatory element binding transcription factors and cyclic AMP response element-binding protein (CREB) promote differentiation of preadipocytes into adipocytes whilst others, such as members of the forkhead and GATA families, repress adipogenesis (Moreno-Navarrete and Fernandez-Real 2012).

Extranuclear regulation of adipogenesis is controlled by hormones, cytokines and growth factors. Insulin and insulin-like growth factor-1 (IGF-1) promote adipogenesis via multiple pathways including the phosphorylation of CREB (Klemm et al. 2001). Thyroid hormones induce adipogenesis via thyroid receptor alpha 1 which are highly expressed in subcutaneous fat of obese subjects while another type of thyroid receptor, type alpha 2, antagonises this action (Ortega et al. 2009). Over excretion of cortisol (hypercortisolism) promotes adipogenesis and adipose tissue redistribution. Adipose tissue sensitivity to glucocorticoids is regulated by 11 β -hydroxydehydrogenase (11 β HSD) 1 which promotes adiposity and is mediated by the glucocorticoid receptors (Budge et al. 2005). Fibroblast growth factors

also show adipogenic activity in human preadipocytes (Hutley et al. 2004). Recent advances in this field have highlighted the role of epigenetic factors and microRNAs in adipocyte differentiation and these remain an area of intense research interest and activity (Hilton et al. 2013).

1.4.3 Brown and white adipogenesis occurs via two distinct pathways

Despite differences in morphology and physiological functions, brown, white and brite adipocytes share several similar transcriptional cascades such as C/EBPs and PPAR γ which control their terminal differentiation. However, there are key differences that specifically promote one genetic programme over the other and white and brown adipogenesis occur along two parallel pathways with distinct sets of transcription factors governing each process (Kajimura et al. 2010) (Figure 1.3). Genes such as BMP 7 (Tseng et al. 2008), PR (PRD1-BF1-RIZ1 homologous)-domain-containing protein (PRDM16) (Seale et al. 2007), CCAAT-enhancer binding protein (C/EBP) β (Kajimura et al. 2009), peroxisome proliferator-activated receptor γ (PPAR γ) and PPAR γ co-activator (PGC) 1 α (Fruhbeck et al. 2009) are expressed along the brown adipogenic pathway whilst another set of transcription factors including BMP4 (Schulz and Tseng 2009), adipose differentiation related protein (ADRP) and homobox (Hox) C9 (Cantile et al. 2003) is

specific to white adipogenesis. The extent to which these separate processes can be reset in utero has not yet been established.

Brown adipocytes arise from the dermomyotomal precursors that are positive for the myogenic factor 5 (Myf5) gene, an early marker of myocyte development. The induction of the brown fat programme requires several transcription factors including PRDM16 which increases the transcriptional activity of PGC1 α which itself is a master regulator of mitochondrial biogenesis and oxidative metabolism in most cell types, including brown adipocytes and muscle cells (Kajimura et al. 2010).

The third type of adipocyte, described as brown-in-white (brite or beige) cells and present in WAT depots, has a distinctive pattern of gene expression and is believed to differentiate via a discrete developmental pathway from mesodermal stem cells that are not positive for Myf5. Thus, through the differentiation process, mesenchymal precursors transform into three distinctive types of adipocytes – white, brown and brite cells (Figure 1.2).

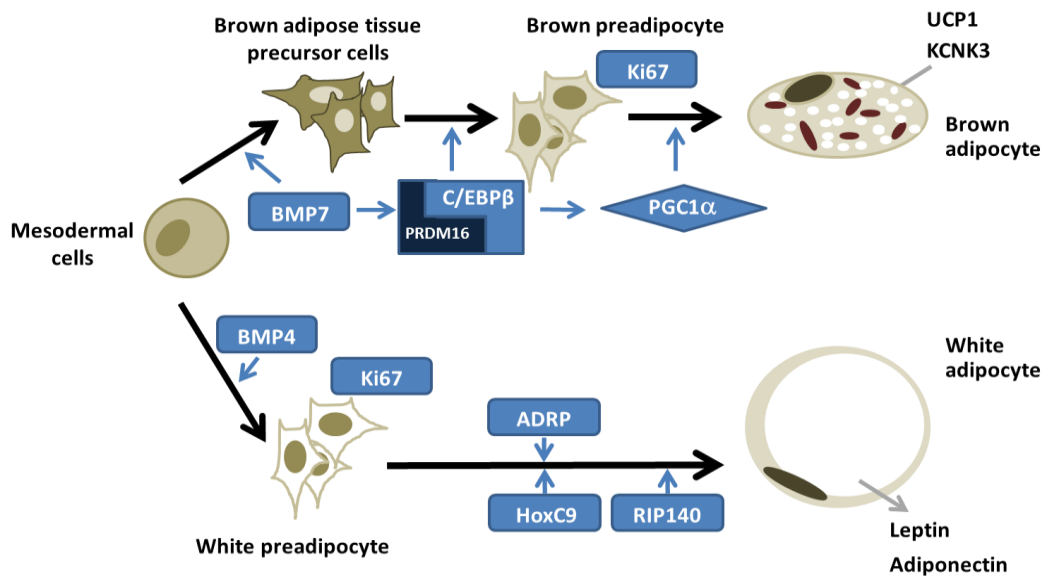


Figure 1.3. Genes involved in brown and white adipogenesis

White and brown adipogenesis occur along two parallel pathways with distinct sets of transcription factors governing each process. UCP: uncoupling protein; KCNK: potassium channel, subfamily K, member 3; BMP: bone morphogenetic protein; ADRP: adipose differentiation related protein; Hox: homobox; RIP: receptor interacting protein; PRDM: PR (PRD1-BF1-Riz1 homologous)-domain-containing protein; PGC1 α : peroxisome proliferator-activated receptor- γ coactivator; C/EBP: CCAAT enhancer binding protein.

1.4.4 Development of adipose tissue in fetal life

Fetal adipose depots possess the dual characteristics of brown and white adipose tissue (Merklin 1974). Although WAT cannot be macroscopically detected during embryogenesis in rodents, in humans WAT development begins well before birth and distinct WAT deposits can be detected around the head by 14 weeks (Poissonnet et al. 1984). In a study of 488 human abortuses of both sexes, Poissonnet et al. identified that early to mid-gestation was the crucial period for adipose tissue development (Poissonnet et al. 1984). Thus, macroscopic evidence of adipose tissue development in the human fetus is first seen in early to mid-gestation with demonstrable aggregations of mesenchymal cells and adjacent proliferation of blood vessels present by 14 weeks of gestation. WAT progressively appears in the trunk, then the limbs and by 28 weeks adipose deposits are present in all potential visceral and subcutaneous sites. Further development in the third trimester occurs mostly as a result of increase in size of the pre-existing fat lobules (Poissonnet et al. 1984). In human fetus, BAT appears before WAT and is present in several locations in the human fetus and newborn infant (Aherne and Hull 1966).

The development of adipose tissue in the ovine fetus follows a similar pattern with an early proliferative phase marked by high expression of Ki-67 (Pope et al. 2013), a gene expressed in all active phases of the

cell cycle but absent in the resting cells (Scholzen and Gerdes 2000), followed by a preparative phase during which adipose depots continue to grow and accumulate lipid (Pope et al. 2013).

1.5 White adipose tissue

WAT forms the major bulk of adipose tissue in adult humans and has the primary function of lipid synthesis and storage. White adipocytes are leptin and S100-B immunoreactive spherical cells, with most of their volume taken up by a single cytoplasmic lipid droplet, and a small nucleus that appears to be squeezed in a corner. In addition, WAT has vital roles in intermediary metabolism of glucose and fatty acids, regulation of insulin sensitivity, appetite control, and energy metabolism and endocrine functions (Gesta and Ronald Kahn 2012).

1.5.1 Endocrine functions of white adipose tissue

White adipose tissue expresses numerous receptors that allow it to respond to afferent signals from circulating hormones and the central nervous system and also secrete a variety of bioactive peptides, known as adipokines (or due to their role in inflammation, adipocytokines), which act at both local (autocrine and paracrine) and systemic (endocrine) levels. The importance of the endocrine role of adipose tissue is demonstrated by the myriad metabolic consequences of excess adiposity, as in obesity, and adipose tissue deficiency such as

lipodystrophy, both of which are associated with the metabolic syndrome (Kershaw and Flier 2004).

1.5.1.1 Leptin

Leptin is a 16 kDa hormone secreted by adipocytes which acts at the hypothalamus to control appetite and energy expenditure (Gesta and Ronald Kahn 2012). The circulating concentration of leptin is directly proportional to adipose tissue mass, particularly subcutaneous adipose tissue, and increases in the postprandial state (Poppitt et al. 2006).

Leptin expression is also increased by a variety of other factors such as insulin, glucocorticoids and tumour necrosis factor (TNF) α and is decreased by growth hormone, FFAs and β 3-adrenergic stimulation (Margetic et al. 2002).

Leptin acts on the arcuate nucleus in the hypothalamus to inhibit orexigenic neuropeptides and activate anorexigenic pathways and thus serves as a metabolic signal of energy sufficiency (Gesta and Ronald Kahn 2012). It also has a role in regulation of immune functions and plays a critical role in regulating proliferation of T lymphocytes (Lord et al. 1998).

Subcutaneous adipocytes express and secrete leptin more than visceral adipocytes (Van Harmelen et al. 1998). The plasma concentration of leptin correlates with size of body fat mass. In infants born to mothers with diabetes, cord blood leptin concentrations are elevated in parallel

with infant adiposity (Edwards et al. 2005). Obese individuals have increased plasma concentrations of leptin whilst subjects with some of the lipodystrophies may have undetectable levels (Maffei et al. 1995). Plasma concentrations of leptin are elevated after high-fat meals and reduced by fasting (Poppitt et al. 2006).

In humans, leptin regulates appetite, body weight and fat mass. Plasma concentrations increase after several days of overeating and with increased fat mass. This signals satiety and appetite regulators in the hypothalamus in order to suppress appetite. This resultant anorexic response attempts to decrease food intake. Fasting causes a sharp decrease in leptin concentrations and the resulting hypothalamic effects stimulate appetite. However, individual responses to leptin are variable. In obesity, circulating leptin concentrations are high and may not produce appropriate anorexic responses as leptin resistance often accompanies obesity. In obese individuals therefore, exogenous leptin fails to reduce appetite or increase energy expenditure (Klingenspor et al. 1996).

1.5.1.2 Adiponectin

Adiponectin is a 30 kDa adipokine with potential anti-inflammatory and anti-atherogenic properties and a strong inverse association with insulin resistance (Diez and Iglesias 2003). Although the exact role of adiponectin is not known, its concentrations are reduced in obese

individuals, decline before the onset of obesity and insulin resistance (Hotta et al. 2001).(Arita et al. 2012) and increase when insulin sensitivity improves after weigh loss (Diez 2003).

1.6 Brown adipose tissue

Homeothermic species maintain body temperature by a variety of regulatory mechanisms which enable heat generation or heat loss in order to survive exposure to environmental temperatures outside the thermoneutral range of the organism (Lean 1989). Heat is produced in response to cold exposure by an increase in body metabolism, i.e. thermogenesis. In addition to the basal metabolic rate and increased muscular activity i.e. shivering, mammals possess an additional mechanism for generating heat in which a unique organ, BAT, produces heat by a process known as non-shivering thermogenesis.

Although known for more than 500 years (Gessner 1551), BAT has been recognised as a heat producing organ only in the last 60 years and its varied metabolic roles in mammalian physiology have not yet been unravelled. Traditionally, BAT has been viewed as the thermogenic organ for maintaining core body temperature in small mammals and its role in humans was thought to be restricted to the newborn period. However, its recent rediscovery in adult humans (Cypess et al. 2009, Saito et al. 2009, van Marken Lichtenbelt et al. 2009, Virtanen et al. 2009) has re-stimulated interest in this organ.

Brown adipocytes are polygonal cells with several smaller lipid droplets and numerous large mitochondria. These cells stain for the unique BAT protein called uncoupling protein (UCP)1.

1.6.1 Uncoupling protein 1 – the unique BAT protein

The identification of UCP1, the unique BAT protein which drives non-shivering thermogenesis (Aquila et al. 1985) has increased our understanding of BAT function. It was discovered following the observation that the inner mitochondrial membrane of isolated brown adipocytes has high ion permeability (Nicholls and Bernson 1977).

UCP1 is expressed exclusively in the inner mitochondrial membrane in brown adipocytes and is the only protein which can mediate adaptive non-shivering thermogenesis (Nedergaard et al. 2001).

1.6.1.1 Mode of action of UCP1

Mitchell's chemiosmotic hypothesis suggests that oxidation of nutritional substrates is coupled to adenosine triphosphate (ATP) generation by the movement of electrons through a series of electron transporters embedded in the inner mitochondrial membrane (Mitchell 1961). This movement establishes a proton electrochemical gradient which is dispelled when hydrogen ions (H^+) move back into the mitochondrial matrix via the F_0/F_1 ATP synthase. As the H^+ ions pass, the ATP synthase complex rotates and the rotational forces catalyse the generation of ATP from adenosine diphosphate (ADP). UCP1 acts by

uncoupling the process of substrate oxidisation and ATP synthesis by allowing the protons to pass passively from the intermembrane space to the mitochondrial matrix through an alternative channel, thus dissipating the proton-motive force without generation of ATP (Figure 1.4). Instead, the oxidised energy is released as heat.

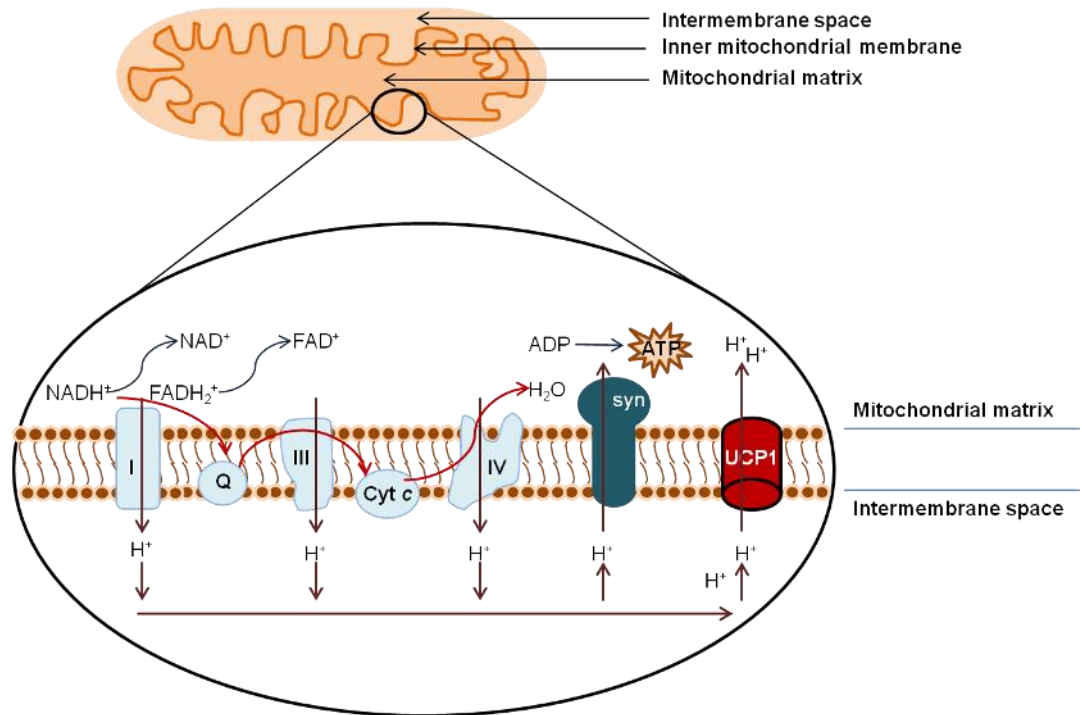


Figure 1.4. Mechanism of action of uncoupling protein 1

NAD: nicotinamide adenine dinucleotide; NADH: nicotinamide adenine dinucleotide dehydrogenase; ADP: adenosine diphosphate; ATP: adenosine triphosphate; FAD: Flavin adenine dinucleotide; FADH: Flavin adenine dinucleotide dehydrogenase; H₂O: water; H⁺: hydrogen ion; Cyt c: cytochrome c; syn: ATP synthase; I: electron transport chain (ETC) complex I; Q: cofactor Q; III: ETC complex III; IV: ETC complex IV.

1.6.1.2 Activation of UCP1

Whilst in its active state, UCP1 is a potent proton translocator; in the resting state it does not have any residual proton conductance due to the presence of inhibitory nucleotides and normal oxidative phosphorylation continues undisturbed (Shabalina et al. 2010). Hence, for non-shivering thermogenesis to occur, UCP1 activation is required. Despite extensive research, a comprehensive understanding of the process of activation of UCP1 has not been achieved, although it is accepted that the presence of free fatty acids (FFA) is mandatory for UCP1 induced thermogenesis (Cannon and Nedergaard 2004).

1.6.1.3 Regulation of UCP1 biosynthesis

The human UCP1 gene is located on chromosome 4q31 spanning 13Kb consisting of 9Kb of transcribed region and is 79% homologous to the rat UCP1 gene (Cassard et al. 1990). The molecular mechanisms regulating the expression of rodent UCP1 gene have been described recently. The gene has a proximal promoter region that contains several cAMP response elements (CREs), a silencer region and a complex enhancer which can override the action of the silencer (Kozak et al. 1994). In addition, this region also contains CCAAT enhancer binding protein (C/EBP) responsive elements, where C/EBP α and β appear to have similar actions in increasing gene expression (Yubero et al. 1994). The upstream region of the gene has a complex enhancer region, with

several response elements within a short sequence which regulate the specificity of UCP1 expression (Del Mar Gonzalez-Barroso et al. 2000). The response elements include the UCP1-gene activating region, CREs, brown fat regulatory elements and retinoic acid response elements. The region also contains the peroxisome proliferator-activated receptor (PPAR) response element as well as the thyroid hormone responsive element (TRE). TRE functions as a repressor in the unliganded state and amplifies the effect of adrenergic stimulation in the presence of thyroid hormones (Cannon and Nedergaard 2004).

The elevation of intracellular cAMP concentration via β -adrenergic stimulation is the most well recognised pathway of UCP1 gene regulation (Collins et al. 2010). cAMP activates cAMP-dependent protein kinase A (PKA) which increases the expression of the gene encoding UCP1. A vital mediator of this action is the transcription co-activator PGC1 α . PGC1 α is a key regulator of thermogenesis in brown adipocytes and in its absence the cAMP regulated activation of UCP1 is severely blunted (Uldry et al. 2006).

The expression of PGC1 α gene is in turn enhanced by a 140 kDa transcription factor called PRDM16 which is expressed selectively in brown adipocyte. It functions as a co-regulator to activate PGC1 α and can also directly increase expression of UCP1 and several other key BAT specific genes (Seale et al. 2007).

1.6.2 Brown fat development

Brown adipocytes are derived from mesenchymal stem cells (as discussed in Section 1.4) but the differentiation pathway by which they develop is not completely clear.

1.6.2.1 Brown adipose tissue develop from myogenic precursors

BAT and WAT have several common characteristics; both differentiate via a PPAR γ -driven transcription pathway and it was assumed that both types of adipose tissue have a common progenitor. The discovery that brown fat and skeletal muscle, but not white fat, develop from *Myf5* expressing progenitors (*Myf5*⁺) revealed that BAT and skeletal muscles share a common lineage (Seale et al. 2008). This was coupled with the finding that knockout of PRDM16 in brown fat induces skeletal myogenesis including a large increase in expression of myogenic genes. Conversely, the ectopic expression of PRDM16 in myoblasts suppresses myogenesis and induces expression of BAT genes such as UCP1, cell death inducing DFFA-like receptor A (CIDEA) and PGC1 α (Seale et al. 2008). These findings have revealed a close relationship between the developmental origins of skeletal muscles and BAT. Other studies also support this relationship. Atit et al. found that Engrailed-1 (En-1) expressing cells of the central dermomyotome give rise to dorsal dermis, epaxial muscles and interscapular BAT in mice (Atit et al. 2006) suggestive of a common embryological origin for muscles and BAT. The

transcriptional similarities of brown preadipocytes and myogenic cells have also been demonstrated in microarray analysis where interlinkage between brown preadipocytes and myocytes reflect their common origin whilst demonstrating their difference from WAT (Timmons et al. 2007).

Other similarities between BAT and skeletal muscles are demonstrated by studies of mitochondrial proteomic signatures. At transcript and proteome levels, BAT mitochondria are similar to mitochondria in skeletal muscles and differ from those in WAT (Forner et al. 2009). These similarities between BAT and skeletal muscle reflect that both tissues are adrenergically regulated organs which control adaptive thermogenesis and may explain why, like skeletal muscle, BAT primarily functions as an organ of lipid catabolism rather than storage (Seale et al. 2008). It also explains the presence of UCP1 expressing brown adipocytes interspersed between muscle bundles in obesity resistant mice (Almind et al. 2007).

1.6.3 Adrenergic control of brown adipose tissue

BAT depots are richly innervated with adrenergic nerves and these sympathetic innervations are the major regulator of proliferation, differentiation and apoptosis as well as metabolic functions such as lipolysis and thermogenesis in brown adipocytes.

Several different types of adrenergic receptors are present in BAT cells. Cells in BAT have all the three types of beta (β) adrenergic receptors

(ADR); $\beta 1$ ($\beta 1\text{ADR}$), $\beta 2$ ($\beta 2\text{ADR}$) and $\beta 3$ ($\beta 3\text{ADR}$) (Rohlfis et al. 1995) but in mature brown adipocytes $\beta 3\text{ADRs}$ are predominant (Bronnikov et al. 1999) and the most thoroughly investigated.

1.6.3.1 UCP1 gene expression is regulated by adrenergic stimulation

Cold exposure increases UCP1 in BAT mitochondria due to NE release at $\beta 3\text{ADR}$ nerve endings on brown adipocytes (Ricquier et al. 1984). Adrenergic stimulation increases intracellular cAMP concentration which activates the CREs on the UCP1 gene increasing protein production (Cannon and Nedergaard 2004). Beta-adrenergic stimulation also increases the expression of PGC1 α and PPAR γ further optimising induction of the UCP1 gene.

1.6.3.2 Adrenergic systems control brown adipose tissue metabolism

The thermogenic response to NE stimulation is also predominantly mediated via $\beta 3\text{ADRs}$ (Zhao et al. 1994). Activation of these receptors promotes lipolysis of stored triglycerides (Collins 2011). Beta adrenergic stimulation activates the GTP-binding protein G which, in turn, activates adenylyl cyclase to increase cyclic adenylyl monophosphate (cAMP) concentration within the cells. Cyclic-AMP turns on PKA which then phosphorylates hormone sensitive lipase (HSL) and lipid droplet binding proteins such as perilipin. Phosphorylation of perilipin releases triglycerides from the lipid droplets enabling the lipases to hydrolyse

them into FFA and glycerol. The FFAs are transported to the mitochondria by fatty acid transporting protein known as fatty acid binding protein 4 (FAB4). The FFAs activate UCP1 and also become the thermogenic substrate for the action of UCP1 (Figure 1.5).

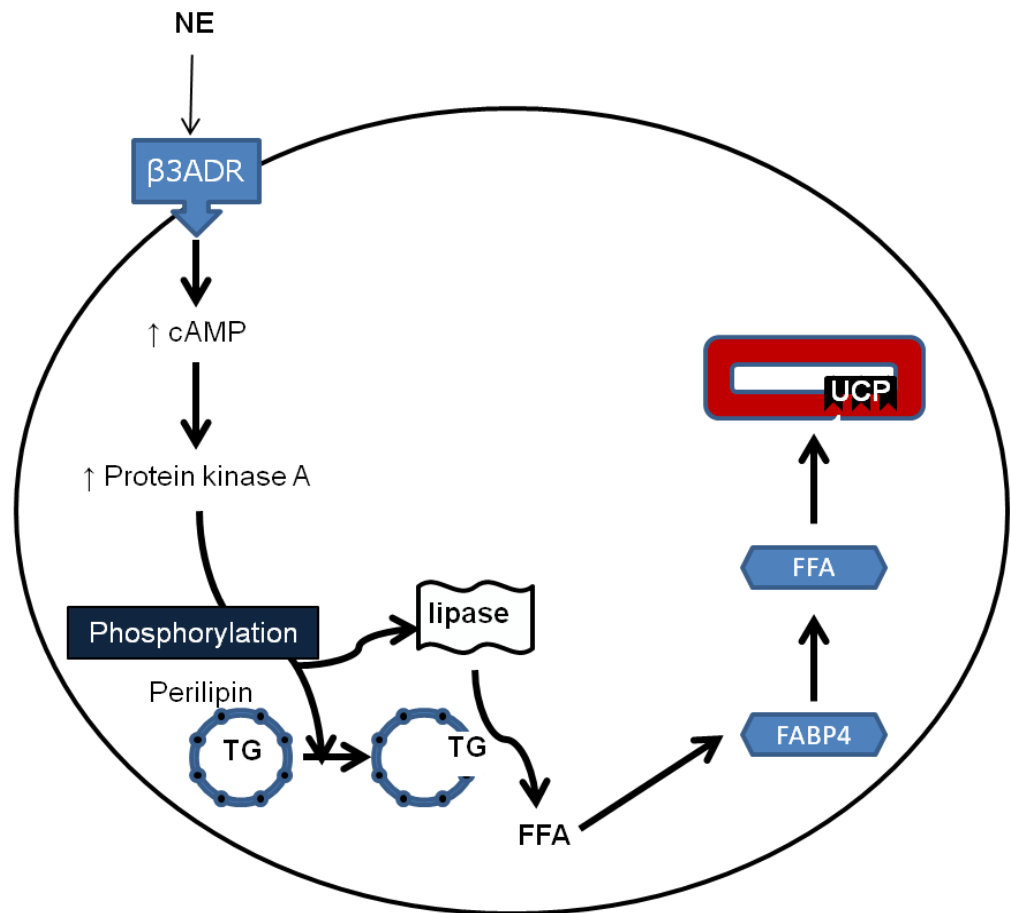


Figure 1.5. Activation of UCP1 by adrenergic stimulation

Adrenergic stimuli such as norepinephrine (NE) stimulate β_3 adrenergic receptors (β_3 ADRR) which activate adenylyl cyclase to increase intracellular concentration of cyclic adenosine monophosphate (cAMP). cAMP stimulates protein kinase A which phosphorylates perilipin and lipases. Perilipin breaks the triglyceride (TG) globule while the lipases hydrolyse the triglycerides to release free fatty acids (FFA). The FFAs are carried by fatty acid binding protein 4 (FABP4) to the mitochondria where they activate uncoupling protein 1 (UCP1) and act as the substrate for non-shivering thermogenesis.

1.6.4 Role of thyroid hormones in BAT thermogenesis

Thyroid hormones are an important determinant of overall energy expenditure (Kim 2008) and are important regulators of BAT function (Figure 1.6). NE or cold stress causes a rapid increase in type 2 iodothyronine deiodinase (DIO2) in BAT (Silva and Larsen 1983). DIO2 catalyses the conversion of thyroxine (T4) into triiodothyronine (T3). T3 is a form of thyroid hormone that is 10 times as potent as T4. This intracellular conversion of T4 into T3 within brown adipocytes produces high intracellular T3 concentration which saturates thyroid hormone receptors and induces a rapid increase in UCP1 gene expression and protein synthesis (Bianco and Silva 1987).

Thyroid hormones may also activate BAT by a central mechanism involving decreased activity of hypothalamic AMP-activated protein kinase (AMPK) and increased sympathetic nervous system activity with upregulation of thermogenesis in brown adipocytes (Lopez et al. 2010) (Figure 1.6).

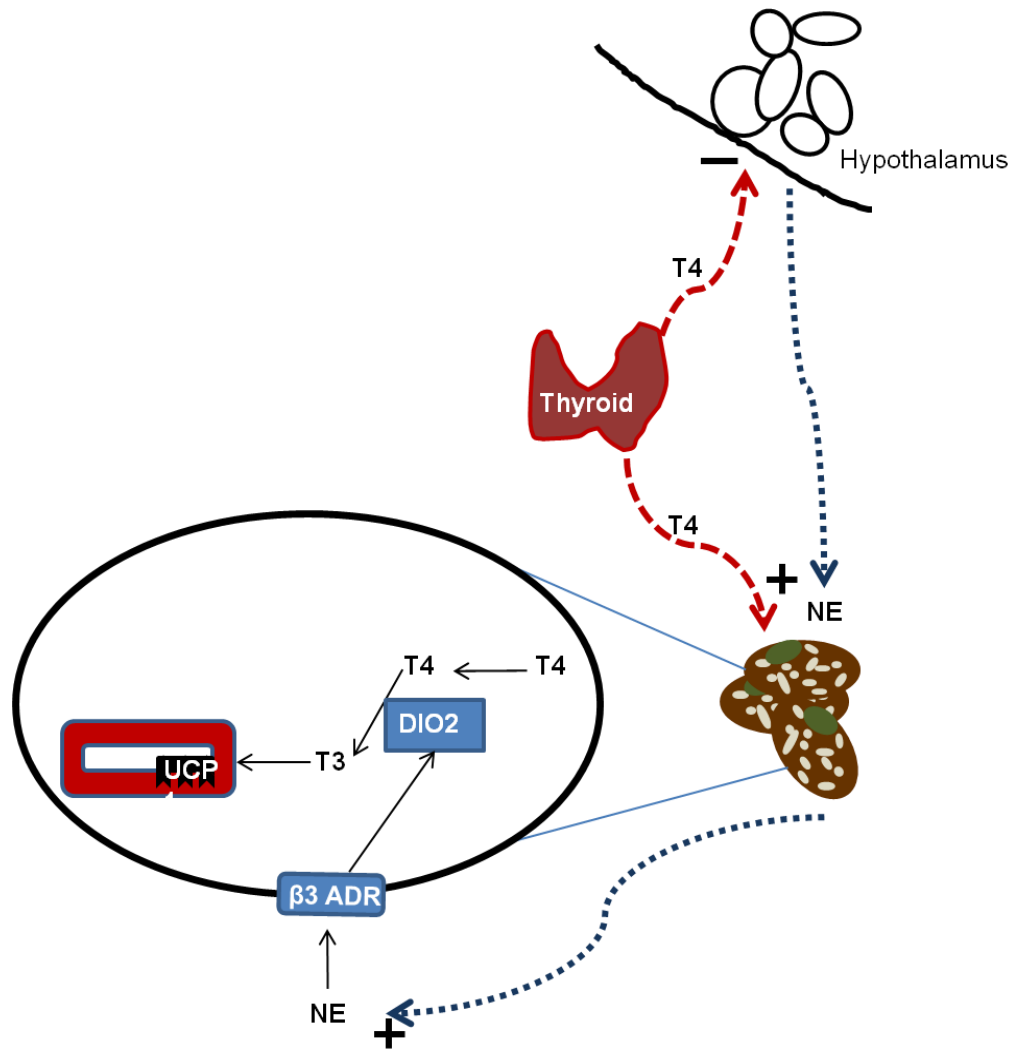


Figure 1.6 Regulation of brown adipose tissue (BAT) by thyroid hormones

Beta adrenergic stimulants such as norepinephrine (NE) act via β -3 adrenergic receptors (β 3ADR) to increase the action of type II iodothyronine deiodinase (DIO2). Circulating thyroxine (T4) is converted to tri-iodothyronine (T3) by the action of DIO2 within the brown adipocyte. T3 activates UCP1 gene expression. Thyroid hormones also act on the hypothalamus to decrease cyclic-AMP activated protein kinase (PKA) levels and increase adrenergic drive to BAT.

1.6.5 Other metabolic actions of BAT

The primary role of BAT in metabolism and energy homeostasis is adaptive thermogenesis. Additionally, in the course of this action, it has other effects on body metabolism.

1.6.5.1 Lipid metabolism and BAT

Lipids derived from circulating chylomicrons are a major thermogenic substrate in BAT (Cannon and Nedergaard 2004). Brown adipocytes produce and secrete lipoprotein lipase into the surrounding blood vessels. Triglyceride laden chylomicrons and very low density lipoproteins (VLDL) are hydrolysed by lipoprotein lipase to produce FFA and monoacylglycerols. The FFA are taken up by the brown adipocytes (Festuccia et al. 2011) . This mechanism enables BAT to function as a lipid clearing organ purging the local circulation of excess lipids (Bartelt et al. 2011) (Figure 1.7). The production of lipoprotein lipase in brown adipocytes and the subsequent clearance of circulating lipids by BAT is enhanced by NE (Carneheim et al. 1984), cold exposure (Bartelt et al. 2011) and exposure to PPAR γ agonist rosiglitazone (Festuccia et al. 2009). The FFAs taken up by the brown adipocytes are channelled towards intracellular stores of triglycerides for use as thermogenic substrates later or are used up in thermogenesis by being directly transported to the mitochondria (Festuccia et al. 2011).

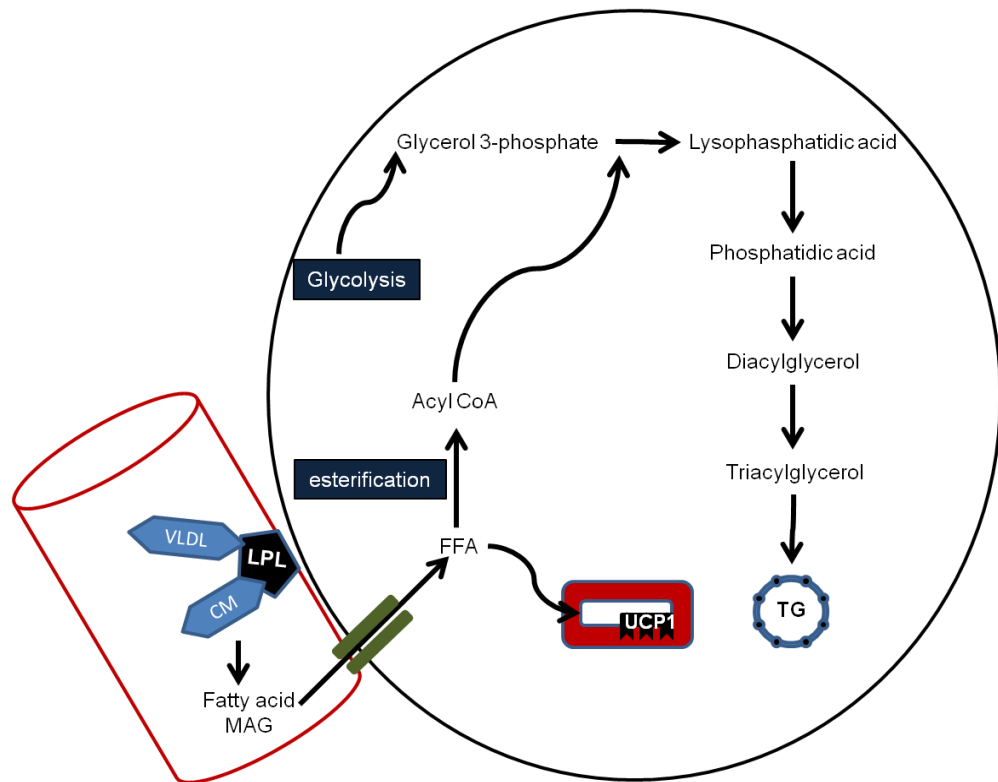


Figure 1.7. Lipid uptake by brown adipocytes

Brown adipocytes secrete lipoprotein lipase (LPL) that breaks down circulating very low density lipoproteins (VLDL) and chylomicrons (CM) to release monoacyl glycerol (MAG) and free fatty acids (FFA) which are taken up by the adipocytes. Within the cell, the FFAs are esterified to acyl co-enzyme A (acyl CoA) and further metabolised to synthesise triglycerides (TG) by the process of lipogenesis or directly transferred to the mitochondria where they activate uncoupling protein 1 (UCP1) and provide the substrate for non-shivering thermogenesis.

1.6.5.2 Glucose metabolism and BAT

Brown adipocytes display a very high rate of glucose uptake per unit weight of tissue (Cannon and Nedergaard 2004). This high uptake has been amply demonstrated in humans during the identification of BAT in adult humans by the uptake of the ^{18}F -labeled glucose analogue known as 2-fluoro-2-deoxy-glucose (^{18}F -FDG) during positron emission tomography (PET) computerised tomography (CT) scans (Cypess et al. 2009, Saito et al. 2009, van Marken Lichtenbelt et al. 2009, Virtanen et al. 2009).

Glucose uptake by BAT is enhanced by cold exposure in both rats (Greco-Perotto et al. 1987) and in humans (Orava et al. 2011). This response is mediated by β -adrenergic stimulation via cAMP (Chernogubova et al. 2004) which increases de novo synthesis of glucose transporter (GLUT) 1 and increases the abundance of GLUT1 in the brown adipocyte plasma membrane (Dallner et al. 2006).

The alternative regulation of glucose uptake by brown adipocytes is through the insulin stimulated translocation of GLUT4 to the plasma membrane of the brown adipocytes (Teruel et al. 1996). This pathway is similar to that seen in white adipocytes and is probably more active under conditions of decreased thermogenesis (Cannon and Nedergaard 2004). Circulating insulin binds to insulin receptors (IR) on brown adipocytes and activates tyrosine kinase and downstream signalling

with pleiotropic effects including increased production and translocation of GLUT4 on to the plasma membranes and increased glucose uptake in the brown adipocytes (Sugden and Holness 1993). The glucose taken up under the influence of insulin is used for de novo fatty acid synthesis or may be stored as glycogen. BAT is one of the most insulin responsive tissues with respect to stimulation of glucose uptake and even in small amounts, it is a potentially significant glucose clearing organ (Cannon and Nedergaard 2004).

1.7 Brite adipocytes - a different type of adipocytes are present in white adipose depots

In addition to the discreet depots of BAT, brown adipocyte like cells are also present in WAT depots in adult animals. These cells have been variously named brite, brown-in white, brown-like, or beige adipocyte (Klingenspor et al. 2012). Brite adipocytes are inducible i.e. islands of brown-like adipocytes appear within white fat depots of rodents following chronic exposure to β_3 adrenergic stimulation or cold (Pisani et al. 2011).

This discovery that adipocytes within WAT depots can be stimulated to acquire brown-like characteristics has generated interest in brite adipocytes. Adult humans typically have low amounts of BAT; increased BAT volume and activity correlates with lower BMI (van Marken Lichtenbelt et al. 2009, Virtanen et al. 2009), increased energy

expenditure (Cypess et al. 2015), reduced WAT accumulation (Chalfant et al. 2012) and improved glucose and lipid metabolism (Ouellet et al. 2012). UCP1 ablated mice are lean when reared at room temperature (Enerback et al. 1997) but rapidly develop obesity when kept at thermoneutral conditions (Feldmann et al. 2009) while transgenic expression of UCP1 prevents obesity in mice (Kopecky et al. 1995). These findings suggest that stimulation of activity of brite cells in WAT of humans could potentially improve metabolic health and prevent obesity.

1.7.1 Origin of brite adipocytes

Precursors of UCP1 positive cells that are present within WAT depots are negative for Myf5 indicating that brite adipocytes have origins distinct from that of classical brown adipocytes (Petrovic et al. 2010). A population of platelet derived growth factor α positive adipocyte progenitors can differentiate into brite or white adipocytes; they acquire brite characteristics under β 3ADR stimulation and develop into white adipocytes when the animal is fed a high fat diet (Lee et al. 2012). Other studies have also demonstrated that it is possible to convert adipocyte precursors found in WAT into mature adipocytes which display the full characteristics of brown adipocytes including adaptive thermogenesis and respond to various brown adipocyte stimulating signals such as β -adrenergic agonists, fatty acids, prostaglandins, thyroid hormones and natriuretic peptides (Pisani et al. 2011). Chronic

treatment with rosiglitazone, a PPAR γ agonist, induces the expression of UCP1 and PGC1 α and mitochondriogenesis in precursor cells from WAT depots in mice (Petrovic et al. 2010) and in human multipotent adipose derived stem cells (Pisani et al. 2011) and the effect is PPAR γ dependent as exposure to specific PPAR γ antagonist abolishes UCP1 mRNA expression. These findings suggest that cellular plasticity exists between white and brite adipocytes at the precursor stage and WAT depots can be induced to develop brite cells and acquire brown fat-like characteristics (Bartelt and Heeren 2014).

These distinctive brown-in-white (“brite”) or “beige” adipocytes are not classic brown adipocytes as they have a different pattern of gene expression (these cells express UCP1 but do not express *Zic1* and *Lhx8*, two brown adipocyte specific genes (Walden et al. 2012)) and do not express *Myf5* in mice (Petrovic et al. 2010) or in human cells (Pisani et al. 2011). This also indicates that these distinctive cells do not arise from classic brown adipocyte precursors but have a developmental origin and molecular characteristics which make them a separate class of adipocytes, distinct from both classical WAT and BAT.

1.8 Energy balance and its role in obesity

As discussed earlier in Chapter 1.1.5, obesity and excess adiposity are consequences of intake of energy in excess of expenditure over a prolonged period. However, this simple mathematical relationship does not completely explain differences in the extent of weight gain in different individuals within the same obesogenic environment. Body weight regulation appears to defy the first law of thermodynamics (energy can neither be created nor destroyed, only converted from one form to another) until this straightforward physical law is applied in conjunction with an understanding of the dynamic physiological adaptations to altered body weight that lead to changes in both the resting metabolic rate as well as the energy cost of physical activity (Leibel et al. 1995).

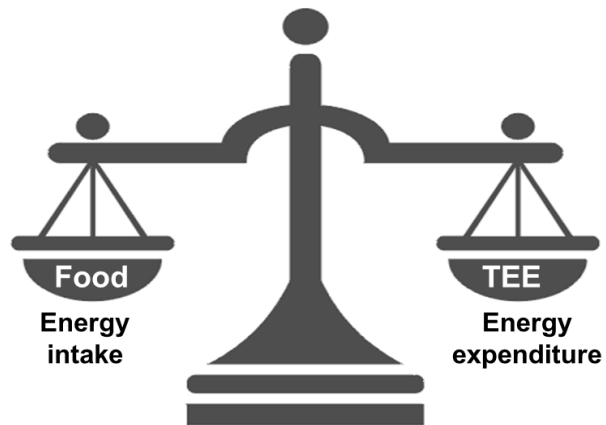
Leibel and colleagues measured energy expenditure and the thermic effect of feeding in obese and normal weight subjects at their usual body weights and after losing or gaining 10 to 20% of their body weight to demonstrate that maintenance of a reduced or elevated body weight is associated with compensatory changes in energy expenditure. These compensations oppose the maintenance of a body weight that is different from the individual's usual weight and may account for the poor long-term efficacy of treatments for obesity (Leibel et al. 1995).

The complexity of the homeostatic mechanisms that regulate body weight presents a challenge to understanding the causes of obesity.

The concept of energy balance and an understanding of how the body achieves and maintains this balance may be a useful framework for designing the strategies for prevention or treatment of the condition.

1.8.1.1 Energy expenditure in humans

Energy intake in humans occurs as food while energy expenditure is composed of several components (Figure 1.8) (Rosenbaum and Leibel 2010, van Marken Lichtenbelt and Schrauwen 2011). Of the total energy expenditure (TEE), 5-10% is spent in digestion and metabolism of the ingested nutrients. The body's obligatory cardio-respiratory work such as the works of breathing and maintaining circulation and the energy spent in maintaining the ionic gradients across cell membranes constitute up to 60% of TEE. This component of TEE is termed as the resting energy expenditure (REE). The remaining energy expenditure is largely variable. Approximately 30% of TEE can be spent in voluntary muscular activity (exercise) whilst a highly variable proportion (estimated to be 5-30%) can be spent in non-exercise activity thermogenesis such as involuntary muscular activities (other than shivering). In addition to these, there is an additional component of TEE comprised of non-shivering thermogenesis that can be induced either by cold or diet.



Components of total energy expenditure (TEE)

Obligatory		Facultative			
Resting energy expenditure (cardiorespiratory work, maintenance of transmembrane ion gradient)	Diet induced thermogenesis (digestion and metabolism)	Voluntary activity (exercise)	Non-exercise activity thermogenesis	Cold induced non- shivering thermogenesis	Diet induced thermogenesis
60%	5-10%	variable	5-30%	variable ?inducible	variable ?inducible

Figure 1.8 Components of energy balance in adult humans

1.8.2 Role of BAT in energy balance in humans

It is now accepted that BAT plays a role in energy balance in humans through the life span.

1.8.2.1 Cold induced non-shivering thermogenesis in humans

Thermogenesis mediated by uncoupling of substrate oxidation and ATP synthesis by UCP1 in BAT has long been accepted as the mode of thermoregulation in the human newborn infant (Bruck 1967). The evidence of existence of this mechanism in adults has been available for some time (Davis 1961) but it has only become widely accepted since the rediscovery of BAT in adult humans (Saito et al. 2009, van Marken Lichtenbelt et al. 2009, Virtanen et al. 2009).

Virtanen et al. showed that, in response to cold exposure, radio-labelled glucose (^{18}F -FDG) uptake in the supraclavicular area is higher than that in the adjacent WAT suggesting that activation of BAT by cold exposure may substantially contribute to energy expenditure (Virtanen et al. 2009). Adults exposed to intermittent periods of cold over a 10 day period reported less shivering and improved tolerance to lower temperature (van der Lans et al. 2013). This process of cold acclimation was shown to induce BAT recruitment (both volume and activity of BAT was increased on ^{18}F -FDG PET-CT scanning) accompanied by an increase in non-shivering thermogenesis in the participants.

The inverse relationship between cold-activated radio-labelled glucose uptake into supraclavicular adipose tissue and adiposity further suggests that BAT contributes to energy balance in humans (Saito et al. 2009). A further role of BAT in metabolism is evidenced by increased uptake of non-esterified FFAs during cold exposure suggesting that triglycerides are the main source of BAT thermogenesis (Ouellet et al. 2012). This study showed that in conditions designed to minimise shivering, cold resulted in a significant increase in oxidative metabolism in BAT. Although the response elicited was variable, enhanced BAT activation was associated with 1.8-fold increase in whole-body energy expenditure.

1.8.2.2 Diet induced thermogenesis in humans

Intake of food induces a thermogenic response known as diet-induced thermogenesis (DIT) (Figure 1.8). This increased expenditure of energy has two components: an obligatory component including the energy required for digestion and assimilation of the ingested nutrients and a facultative component which dissipates energy as heat (van Baak 2008).

BAT has a role in DIT in rodents (Rothwell and Stock 1979, Glick et al. 1985). BAT may also play a role in the facultative component of DIT in humans. Changes in TEE in response to overfeeding correlate with changes seen with mild cold exposure and both correlate with fasting

plasma NE concentrations, suggesting a common regulatory mechanism which may be BAT activation via sympathetic stimulation (Wijers et al. 2007).

However, currently there is very little evidence of BAT regulated DIT being a significant contributor to energy balance in humans and the suggestion that BAT maintains energy balance by burning calories in response to excess intake has been questioned as being incompatible with evolutionary biology (Kozak 2010). Williams and Kolodny found that patients who had a high fat, very low carbohydrate meal prior to the investigation, had a significantly lower frequency of uptake ^{18}F -FDG on PET-CT scan compared to those who fasted suggesting that BAT activity was reduced in the postprandial state (Williams and Kolodny 2008). Similarly, Vrieze and colleagues demonstrated that cold-stimulated ^{18}F -FDG uptake was significantly more prominent in the fasting state when compared to postprandial scan from the same individual (Vrieze et al. 2012). The standardised diet ingested by the participants in this study contained 34 g of fat, 37 g of carbohydrates, and 23 g of protein (respectively, 56%, 27%, and 17% of the energy). Both these studies demonstrated reduction in BAT activity as indicated by uptake of ^{18}F -FDG, a glucose analogue, following intake of fat-rich, carbohydrate-poor meals. The lower glucose uptake in the postprandial state in these studies may be due to the higher contribution of lipid oxidation in BAT expenditure following intake of a fat-rich meal. This is

particularly plausible as fatty acids are the primary substrate for BAT metabolism (Cannon and Nedergaard 2004). Vosselman et al. studied the effect of a high carbohydrate, low fat meal (78% carbohydrate, 10% fat, and 12% protein) and demonstrated the increased postprandial uptake of glucose in BAT (Vosselman et al. 2013). These findings suggest that BAT may have a role in postprandial metabolism however it is as yet unclear if activation of BAT makes a significant contribution to energy balance after food intake.

1.8.3 Role of BAT in obesity in humans

As described in Section 1.6, the recent rediscovery of BAT in adult humans has reignited the debate on the role of BAT in adult humans. Following the evidence that BAT plays a part in energy balance in adult humans, it is postulated that BAT may play a vital role in obesity (Cypess et al. 2009, van Marken Lichtenbelt et al. 2009).

Early evidence to support the hypothesis that increased BAT can induce weight loss came from patients with pheochromocytomas. Pheochromocytomas are rare neuroendocrine tumours which secrete large amounts of NE. In the presence of high circulating NE, brown adipocytes may be reactivated and contribute to the weight loss seen in this condition (Hadi et al. 2007, Wang et al. 2011). This suggests that adequate stimulation can reactivate BAT in adult humans to such an extent that it can have a significant impact on energy balance.

Rodent studies show that BAT can produce up to 300W/kg of energy when maximally stimulated (Power et al. 1989) and previous estimates, made from extrapolation from animal studies, suggested that in humans, 40 to 50 g of BAT, if maximally stimulated, would increase daily energy expenditure by 20% (Rothwell and Stock 1983). Such estimates are considered to be overoptimistic and have been challenged in more recent literature (van Marken Lichtenbelt and Schrauwen 2011). Cypess et al. compared unstimulated oxygen consumption rate in mouse BAT with that in human BAT and found that human BAT has an oxygen consumption rate which is nearly 50% of the value in mouse BAT, even in the unstimulated state (Cypess et al. 2013).

Noticeable amounts of BAT have now been discovered in adult humans and the inverse correlation of volume and activation of BAT with BMI and adiposity suggests that BAT has a role to play in obesity (Cypess et al. 2009, van Marken Lichtenbelt et al. 2009). However, for BAT to have its maximal impact on weight control, it needs to be stimulated such as by cold exposure as seen in people who work outdoors in cold environments (Huttunen et al. 1981). As most individuals in the current milieu live in thermoneutral conditions (or compensate for cold temperatures by dressing adequately and prevent exposure to cold), BAT, even if present in considerable amounts, is unlikely to be fully activated.

In view of these arguments, it appears that 50g of active BAT would amount to only ~2.5-5% of total energy expenditure in human adults. This value is conservative when compared to older estimates (Power et al. 1989), but is still sufficient to have a substantial impact on energy balance and, therefore, on body weight control in adult humans (van Marken Lichtenbelt and Schrauwen 2011). In the management of overweight or obesity, any measure which can create a consistent negative balance over a prolonged period of time is likely to produce weight loss. It has been calculated that even as little as negative balance of 100 kcal/day can produce weight loss with considerable beneficial effects on health of the individual (Fruhbeck et al. 2009). It is entirely plausible that this degree of negative energy balance could be achieved by activating the relatively small amounts of BAT present in adult humans.

Currently, very little is known about the physiology of BAT in humans. Research is needed to study the presence of BAT in various adipose tissue depots in humans and investigate the methods by which BAT may be activated to promote a negative energy balance which can combat excess weight gain.

1.9 Distribution of adipose tissue

In 1947, Vague proposed that the regional distribution of adipose tissue is an important determinant of the relationship between obesity and the

metabolic problems that accompany it (Vague 1947). Several studies have shown that excess adiposity in the upper body is better correlated with increased mortality and higher risks for metabolic syndrome than excess fat in the lower body, gluteofemoral distribution, and further investigations have demonstrated that the detrimental influence of abdominal obesity on the metabolic process is mediated by visceral adiposity (Wajchenberg 2000). The visceral fat depot is contained within the body cavity and surrounds the internal organs. The largest accumulation is intraabdominal but smaller depots are present around other organs such as the heart.

Visceral fat is uniquely deleterious because of its anatomical site and close vascular connections with vital organs, exposing the nearby organs to the full and undiluted repertoire of metabolites and adipocytokines produced by the visceral adipocytes (Montague and O'Rahilly 2000). In addition, visceral adipocytes have a different metabolic profile which is more actively lipolytic as compared to subcutaneous adipocytes (Hellmer et al. 1992). Visceral adipocytes are more responsive to glucocorticoids (Fried et al. 1993), produce less leptin (Lefebvre et al. 1998) and secrete more inflammatory adipokines (Eriksson et al. 1998).

1.10 Pericardial adipose tissue

Most research in visceral adipose tissue is concentrated around visceral abdominal adiposity but there are other areas of visceral fat accumulation which can have significant impacts on local organ function. The heart and great vessels are surrounded by layers of adipose tissue. These layers constitute a complex organ, composed of adipocytes, stromal and inflammatory cells, nerves and blood vessels, which has a myriad of paracrine influences on the function and structure of the heart (Iozzo 2011). Growing recognition of the importance of these ectopic adipose tissue depots in the pathophysiology of cardiovascular diseases (Shimabukuro 2009) has generated interest in cardiac adiposity.

1.10.1 Anatomy of adipose tissue in and around the heart

The various compartments of fat in, and around, the heart have been previously described using different terminologies and there appears to be a degree of ambiguity in their definitions (Iacobellis 2009, Kaushik and Reddy 2011). The term myocardial fat refers to the triglyceride droplets within the cardiac myocytes. Outside of this, the heart and the great vessels are surrounded by the pericardium. The pericardium has two layers – the inner visceral pericardium, or epicardium, and the outer parietal pericardium (Figure 1.9). The adipose tissue present between the heart and the visceral layer of the pericardium i.e. in direct contact

with the myocardium is called epicardial adipose tissue (Sacks and Fain 2007) and is mainly located in the atrioventricular and intervertricular grooves and along the branches of the coronary arteries, and, to a lesser extent, on the ventricular surfaces (Iacobellis et al. 2005). The adipose tissue present outside of the visceral pericardium, either within the two layers of the pericardium or outside the parietal pericardium has been referred to as paracardial fat (Sacks and Fain 2007).

The distinction between epicardial and paracardial adipose tissue is highlighted by the fact that they have different embryological origins. Epicardial adipose tissue originates from the splanchnopleuric mesoderm (Ho and Shimada 1978), whilst paracardial adipose tissue originates from the primitive thoracic mesenchyme (Moore and Persaud 2003). In parallel to their different embryological origins, the two depots derive their blood supply from different sources. The epicardial adipose tissue is supplied by the coronary circulation and the paracardial adipose tissue is supplied by the mediastinal vasculature including the branches of the internal thoracic artery (Taguchi et al. 2001). However, several authors opt to use the term 'pericardial adipose tissue' to refer to the fat present around the heart. This is because of the difficulties in consistently separating the epicardial and paracardial adipose tissue layers at dissection during surgery and on ultrasound and other imaging studies (Greif et al. 2009, McAuley et al. 2011, Wong et al. 2011). Pericardial adipose tissue is, thus, defined as the adipose tissue

present within, and immediately outside, the pericardium and includes both epicardial and paracardial adipose tissue (Figure 1.9).

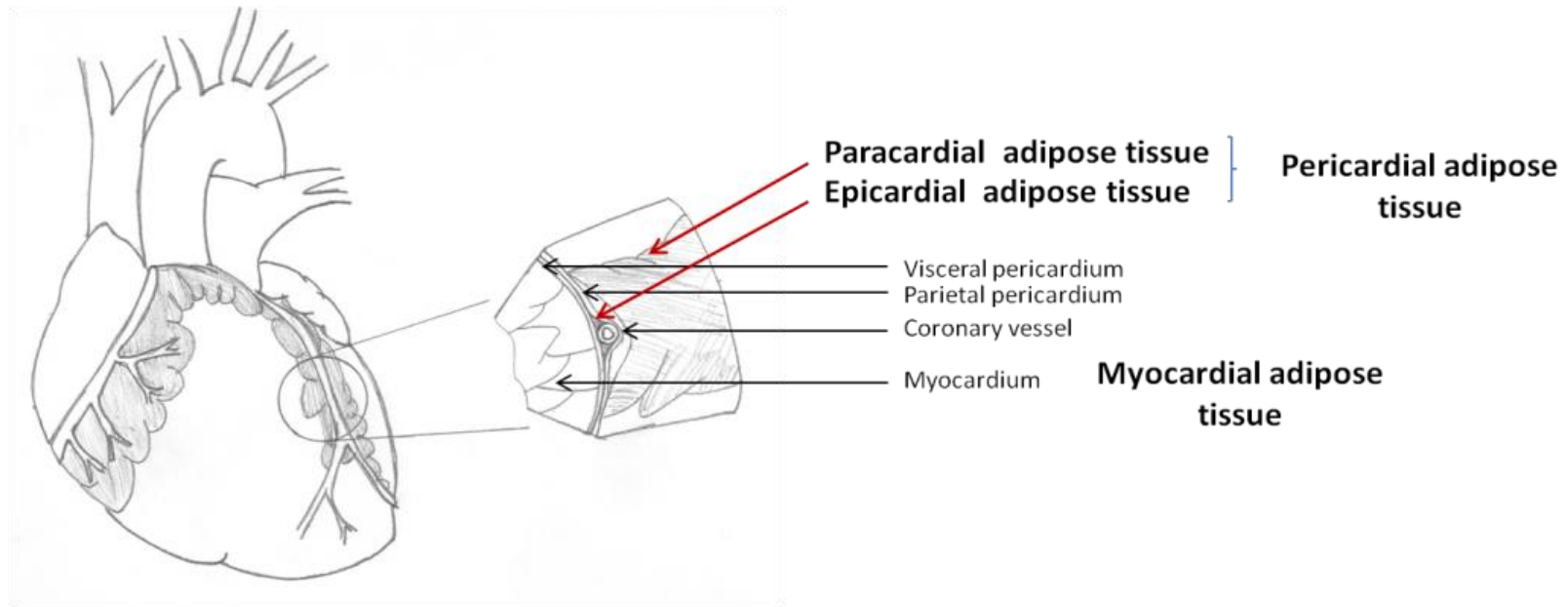


Figure 1.9 Adipose tissue in and around the heart

Pericardial adipose tissue is the fat present in the immediate vicinity of the heart: the fat present between the myocardium and the visceral layer of the pericardium (epicardial adipose tissue) and the fat present between the two layers of the pericardium and immediately outside the parietal pericardium (paracardial adipose tissue).

1.10.2 Normal physiological functions of pericardial adipose tissue

Several putative physiological functions of adipose tissue present in, and around, the heart have been proposed (Rabkin 2007). Like all visceral adipose tissue depots, it was traditionally thought to be a protective layer of padding around the vital organ (Keegan et al. 2004). Anatomically pericardial fat provides mechanical protection of the heart and the coronary arteries, buffering them against the torsion induced by the arterial pulse wave and cardiac contraction.

In the recent years, other roles for the tissue have been proposed (Iacobellis et al. 2005). Epicardial adipose tissue depot is a site of lipid and energy metabolism. Compared to other visceral fat depots, epicardial fat has a greater capacity to take up and incorporate, as well as, breakdown and release FFAs (Marchington et al. 1989). The myocardium takes up FFAs from the coronary circulation and 50-70% of the energy consumed by the heart muscles is derived from oxidation of FFAs. Epicardial fat, due to its high lipolytic activity and ability to release FFA, may be a ready local source of energy for the myocytes during periods of high metabolic demand (Marchington et al. 1989). It is also proposed that epicardial adipose tissue acts as a buffer to protect the myocardium against exposure to excessive levels of FFAs in the coronary circulation (Iacobellis and Bianco 2011). By scavenging excess FFAs from the coronary circulation and the myocardium itself,

and incorporating them in to the intracellular compartment, epicardial adipocytes may act a barrier against toxic levels of FFA in the myocardium and local coronary circulation (Iozzo 2011).

Additionally, fat around the heart may have endocrine and/or paracrine functions. Adipokines produced by epicardial adipocytes in close contact with the coronary vascular adventitia could directly enter the coronary circulation by diffusion across the vessel wall and be transported downstream. These molecules could also diffuse in to the interstitial fluid of the vessel wall and interact with the vasa vasorum, endothelial and vascular smooth muscle cells of the coronary arteries or travel further via the vasa vasorum to influence other parts of the coronary circulation. In lean individuals and in rodents, epicardial fat produces protective adipokines such as adiponectin (discussed in Section 1.5.1.2), nitric oxide (a potent vasodilator) and prostaglandin I₂, an inhibitor of endothelial dysfunction (Fitzgibbons and Czech 2014).

1.10.3 Role of pericardial adipose tissue in cardiovascular pathologies

Under physiological conditions, epicardial adipose tissue is a mechanical and possibly biochemical cardio-protective organ, as discussed above. However in pathological circumstances, particularly when present in excess as in obese individuals, epicardial fat can affect the heart and coronary arteries through vasocrine or paracrine secretion

of proinflammatory cytokines (Sacks and Fain 2007, Clement et al. 2009). Atherosclerotic plaques do not develop in myocardial bridges where the vessel walls are free of adipose tissue (Ishii et al. 1998) suggesting that the local influence of epicardial adipocytes may be required for genesis of atherosclerotic plaques.

Increase accumulation of fat in the pericardial depot in obesity is accompanied by structural and functional changes in the adipocytes such as cellular hypertrophy, increased lipolysis and a reduction in ability to incorporate triglycerides. (Fitzgibbons and Czech 2014). The adipose tissue is invaded by increased numbers of inflammatory cells such as macrophages with a resultant increase in secretion of pro-inflammatory cytokines (Mazurek et al. 2003) and reduction in production of anti-atherosclerotic adipokines such as adiponectin (Greif et al. 2009). In this setting, the beneficial paracrine effects of epicardial adipose tissue are lost and the adipocytokines released from epicardial adipocytes can readily reach cardiac myocytes and coronary vessels (as described in Section 1.10.2) to produce a pro-inflammatory effect which may contribute to the pathophysiology of coronary vascular diseases (Clement et al. 2009).

1.10.3.1 Evidence of association of pericardial adiposity with cardiovascular disease in humans

Adipose tissue around the heart has been of interest to physicians for quite some time with reports of “fatty heart” as the cause of sudden

death in the Victorian era (Bedford 1972). More recent epidemiological data provide evidence for association between pericardial adipose tissue volume and several cardio-metabolic pathological conditions (Ding et al. 2008, Ding et al. 2009, Greif et al. 2009). Pericardial adipose tissue volumes correlate with several cardiovascular metabolic risk factors such as hypertension, blood glucose and lipid profile and with the presence of coronary artery calcification (Rosito et al. 2008). They are more closely associated with coronary artery disease than other adipose tissue depots (Taguchi et al. 2001). The prevalence of cardiovascular and coronary heart diseases are associated with pericardial fat despite adjustment for age, sex, body mass index, waist circumference (Ding et al. 2009, Mahabadi et al. 2009). Associations have been reported with coronary artery calcification (Liu et al. 2010) and severity of coronary artery disease (Taguchi et al. 2001). Additionally, this depot of fat appears to affect cardiac function as there is evidence that in obese subjects, as pericardial adiposity increases, cardiac function decreases (Ruberg et al. 2010).

A meta-analysis of 15 case control studies (total number of participants = 2872) investigating the relationship between epicardial adiposity and coronary artery disease found that epicardial fat thickness was higher in the patients than in controls and those with coronary plaques had significantly higher epicardial fat volumes as compared to those without plaques (Xu et al. 2012). Similarly, meta-analysis of studies that

measured epicardial fat in patients with or without the metabolic syndrome demonstrated that those with the metabolic syndrome have significantly higher volumes of epicardial fat (Pierdomenico et al. 2013).

Pericardial adipose tissue is highly correlated with abdominal and other visceral adipose tissue depots (Mahabadi et al. 2009). Some authors have suggested that it is possible that pericardial adiposity is a marker of general visceral adiposity and its correlation with cardiometabolic risk factors could merely be a reflection of general adiposity rather than an independent marker of obesity or cardiovascular diseases (Liu et al. 2010). However, evidence from multifactorial analyses suggests that pericardial fat is associated with incident cardiac events independent of traditional risk factors and anthropometric measures of obesity (waist circumference and BMI) and visceral abdominal adiposity (Ding et al. 2009, Mahabadi et al. 2009, Thanassoulis et al. 2010). Despite this controversy, pericardial adipose tissue remains an important visceral fat depot whose proximity to coronary vasculature suggests that it may have a paracrine role in the pathogenesis of cardiovascular disease and, therefore, may be important in evolution of metabolic syndrome. The exact relationship between pericardial adipose tissue and cardiovascular pathologies and the metabolic syndrome remains to be unravelled. Further research is required to investigate the potential role of fat around the heart in the pathophysiology of cardiovascular illness.

1.10.4 Pericardial adipose tissue is a BAT depot in adult humans

Although pericardial fat has the gross appearance of white fat in human adults, some of its components, particularly epicardial fat, evolves from BAT and has recently been shown to express high levels of UCP1 mRNA (Sacks et al. 2009).

In adipose tissue samples collected from 28 patients undergoing coronary artery bypass grafting (CABG) for critical coronary atherosclerosis, Sacks and colleagues found that UCP1 gene expression was 5-fold higher in EAT when compared to substernal fat. UCP1 gene expression was even lower (barely detectable) in samples taken from subcutaneous adipose tissue from the sternum, abdomen and leg (Sacks et al. 2009). The gene expression of other BAT related genes, PRDM16 and PGC1 α were also higher in EAT when compared to subcutaneous fat (Sacks et al. 2009). These findings raised the possibility that epicardial fat may be a depot of BAT. However, demonstration of gene expression of UCP1 is not conclusive evidence of presence of BAT as gene expression does not necessarily equate to presence of functional protein (Nedergaard and Cannon 2013). Further research to demonstrate the BAT specific protein, UCP1, in pericardial adipose tissue is required to confirm that brown fat is present in the fat depot around the heart.

1.11 Use of animal models

Epidemiological data from human populations have provided ample evidence of the links between early life nutrition and later cardiovascular illness and obesity. Prospective investigations into human cohorts would be of enormous value to further elucidate this relationship and to obtain insight into the underlying mechanisms. However, such prospective studies would be complex, expensive and confounded by the influences of uncontrollable variables of genetic and environmental origin (Taylor and Poston 2007). Randomised trials of nutritional or behavioural modifications in pregnant women and young children are often unfeasible or ethically impossible and observational studies are fraught with confounding variables and the absence of appropriate controls (Symonds et al. 2000). It is, therefore, imperative to use animal models to explore the impact of in utero nutrition and post weaning environments on the development of adipose tissue.

Nearly 50 years ago, Widdowson and McCance conducted some of the first experiments on rat models of altered early nutrition (Widdowson and McCance 1963) and since then several investigators have induced developmental programming of diseases and health in many animal species with use of diverse interventions ranging from alterations in maternal nutrition, placental function and modifications of postnatal diet and growth (Gillman 2005). Animal studies allow more comprehensive

elucidation of cellular changes which occur during the evolution of obesity and the mechanisms behind these changes can be studied in greater detail.

1.11.1 Sheep as a model of developmental programming in humans

Like humans, the sheep is a precocial species carrying one or two fetuses born, at term, after a long gestation (Symonds et al. 2007).

Responses to changes in maternal nutrition at different periods of fetal and early neonatal development can be better clarified in a sheep model as the diet can be manipulated to coincide with precise periods of fetal organogenesis which are comparable with those during human fetal development (Festing 2006).

The similarities between sheep and humans also include a variety of metabolic functions, particularly in BAT development and function. Both species are precocial thermoregulators, BAT is most abundant at the time of birth and nonshivering thermogenesis is activated immediately after birth in both the species (Symonds et al. 2003).

In addition, both humans and sheep have mature HPA axes (Fowden et al. 1998) and the central neural network of regulation of appetite and energy balance (Muhlhausler et al. 2004) is already developed at time of birth. Other factors such as organ growth rates, fetal metabolic rate and protein turnover are also similar between the two species.

In contrast, rodents are small, litter bearing, altricial species with shorter gestation and an HPA axis which develops in the postnatal period (Bouret et al. 2004). The neural pathways and endocrine mechanisms that modulate energy balance and adipose tissue development are largely developed in late gestation in both sheep and humans, whilst a large part of this development occurs during the postnatal period in rodents. Therefore, sheep provide a model for studying the developmental programming effects of nutritional variations in early life which is more closely aligned to humans.

1.12 Hypotheses and aims

1.12.1 Chapter 3

Given that UCP1 gene is expressed in epicardial depot of adult humans (Sacks et al. 2009), I hypothesised that BAT is present in pericardial adipose tissue in newborn sheep.

Maternal nutrition during different phases of gestation affects expression of UCP1 gene and UCP1 abundance in perirenal BAT in the fetus (Clarke et al. 1997, Budge et al. 2004). I hypothesised that maternal nutrient restriction during late gestation, coincident with maximal growth of the fetus, would compromise the abundance and development of BAT in the newborn over the first month of life.

1.12.2 Chapter 4

Suboptimal nutrition of the fetus during active period of adipogenesis may programme later adipose tissue dysfunction such that, in adulthood, these adipocytes have an enhanced lipogenic and proliferative potential which ultimately leads to obesity (Symonds et al. 2012). Excess accumulation of fat in the pericardial depot has been associated with a number of cardiovascular risk factors (Taguchi et al. 2001, Ding et al. 2008).

In the study described in Chapter 4, I hypothesised that, in fetal sheep, suboptimal maternal nutrition between early-to-mid gestation followed

by ad libitum feeding until term will increase fetal adiposity and upregulate the expression of genes which control adipogenesis.

1.12.3 Chapter 5

Given that in adult humans, relatively high levels of UCP1 gene expression is present in EAT, I hypothesised that UCP1 is significantly more abundant in EAT when compared to other adipose tissue depots thus confirming that epicardial fat is a depot of BAT in adult humans.

1.12.4 Chapter 6

I hypothesised that BAT is present in epicardial depot in infants and children and, given that gene expression of UCP1 in human adults is inversely proportional to BMI and is higher in women than in men (Cypess et al. 2009), that the gene expression of UCP1 is correlated with age and weight for age and is higher in girls than in boys. I also hypothesised that UCP1 gene expression will be higher in children of Caucasian origin when compared to children of Asian (Indian sub-continent) origin.

Propranolol is a non-selective β -adrenergic antagonist. As discussed in Section 1.6.3, development and metabolism of brown fat as well as regulation of UCP1 gene is mainly regulated by β -adrenergic receptors (ADR) (Cannon and Nedergaard 2004). Therefore, I hypothesised that gene expression of UCP1 is downregulated in children receiving regular propranolol therapy.

2 Materials and methods

2.1 Procedural and legislative declaration and ethical approvals

2.1.1 Approvals for the animal experiments

All animal experiments performed in the studies included in this thesis were conducted in accordance with the UK Home Office and UK Animals (Scientific Procedures) Act (1986) by Professor M.E Symonds under Home Office Project Licence Numbers 40/2925, 40/3346 and PPL 40/3560. In addition, all experimental procedures were completed with ethical approval from the University of Nottingham.

2.1.2 Approvals for the human studies

2.1.2.1 Study of brown adipose tissue in epicardial fat of adult humans

Samples included in the study of brown adipose tissue in epicardial fat of human adults (Chapter 5) were obtained from participants in the Human Epicardial Fat Adipokines and Coronary Atherosclerosis study. Ethical approval for this study was obtained from the Baptist Memorial Health Care Corporation Institutional Review Board (Appendix 10.1.1) and samples were collected after taking written informed consent from participants. Adipose tissue samples preserved in dry ice were transferred from the Baptist Memorial Health Care Corporation, Memphis, Tennessee, to the University of Nottingham. The transfer was

conducted with an appropriate tissue transfer agreement between the two institutions and all procedures including the storage and transfer of the tissue samples were performed in keeping with the Human Tissue Act (HTA) 2004.

2.1.2.2 Study of brown adipose tissue in pericardial fat of newborns, infants and children

The sample collection for the study of pericardial adipose tissue in children was conducted with ethical approval from National Research Ethics Service Committee (NRES) East Midlands – Nottingham 2 (REC reference number: 12/EM/0214) (Appendix 10.1.2). Further to this, the study had institutional approval from the University Hospitals of Leicester. The samples were collected only after obtaining informed consent from the parents/guardians of the participating children and from any young person themselves, if they were deemed by their clinical team to possess the capacity to give informed consent. After collection, the samples were temporarily stored at the Biomedical Research Unit, Glenfield Hospital and transferred by myself or Mrs. Victoria Wilson to Academic Child Health, University of Nottingham within seven days of sample collection. A tissue transfer agreement, under the Human Tissue Act (HTA), was in place to allow the transfer of samples from the Glenfield Hospital, University Hospitals of Leicester to the University of Nottingham. All procedures including the storage and transfer of the tissue samples were performed under the Human Tissue

Act (HTA) 2004 and both the Biomedical Research Unit, Glenfield Hospital and Academic Child Health, University of Nottingham are HTA approved facilities. Data on participant's age, weight, height, medications and other medical conditions were collected as detailed in the protocol agreed by the National Research Ethics Service Committee (NRES) East Midlands – Nottingham 2 (REC reference number: 12/EM/0214).

2.2 Animal experiments

2.2.1 Experimental procedure: Effect of maternal nutrient restriction on UCP1 and other BAT associated genes in pericardial adipose tissue of newborn sheep

This study (Chapter 3) was undertaken at the University of Nottingham, United Kingdom. Animal procedures were performed by Dr Sarah Pearce and Professor Michael Symonds.

Seventeen twin-bearing Border Leicester cross Swaledale sheep of similar age, body weight, and fat distribution, and with a known mating date were group housed and fed to fully meet their total metabolic requirements. At 110 day of gestation, each was individually housed and randomly assigned to a nutrition group. Eight mothers were fed and consumed 100% of total metabolisable energy requirements for maternal body weight and stage of pregnancy, whereas the remaining nine were nutrient restricted and fed with 60% of total metabolisable

energy requirements until term. The diet comprised chopped hay and concentrates and was provided in a 3:1 ratio. All animals had continual access to minerals, thus ensuring adequate intake of all vitamins and minerals regardless of nutrition group. All mothers delivered twins naturally at term. Colonic temperatures were recorded from each lamb around the time of birth and all remained normothermic (i.e. between 39 and 40 °C)

One offspring was randomly selected for tissue sampling within 12 hours of birth (day 0) and underwent humane euthanasia by intravenous injection of barbiturate (200 mg/kg pentobarbital sodium; Euthatal; RMB, Animal Health, U.K.). Subsequently, each mother reared a single lamb until it was 30 days old, during which time mothers were fed hay *ad libitum* and up to 1 kg of concentrate throughout lactation. This procedure had no differential effect on the growth of the remaining twin or maternal milk production and the second lamb was humanely euthanased (as above) and tissue samples at 30 days postnatal age. At tissue sampling, pericardial adipose tissue was immediately dissected, placed in liquid nitrogen, and stored at -80 °C until further analysis. All operative procedures and experimental protocols had the required Home Office approval as designated by the U.K. Animals (Scientific Procedures) Act (1986) and detailed in Section 2.1.1.

2.2.2 Experimental procedure: Suboptimal maternal nutrition during early-to-mid gestation in the sheep enhances pericardial adiposity in the near-term fetus

The animal procedures for this study (Chapter 4) were performed by Dr Lindsay Heaseman and Professor Michael Symonds. Animal protocols were designed in accordance with the Animals (Scientific Procedure) Act, 1986 under Home Office supervision as described in Section 2.1.1.

With U.K. Home Office regulatory approval, twelve pregnant Welsh Mountain sheep of similar age (median, 3 years), body weight, and fat distribution were mated with one of two Texel rams on a known mating date and then group housed and fed 100g concentrate/day with access to hay ad libitum. All 12 sheep were carrying one fetus each and at 28 days of gestation, each sheep was individually housed. The animals' metabolisable energy (ME) requirement was calculated according to body weight, taking into account the requirements for both maternal maintenance and growth of the conceptus on the basis of producing a 4.5kg lamb at term (147 days of gestation) (AFRC 1993). Five mothers were randomly assigned to the control group (C) and were fed, and consumed, 100% of their total ME requirements, whereas the remaining seven were nutrient restricted (NR) and fed with 60% of total ME requirement (i.e. a 40% global reduction in macronutrient content) until 80 days of gestation. Sheep in both groups were then fed to appetite for the remaining period of gestation.

After 80 days, animals in both groups consumed 8-10.9 MJ/d i.e. 150% of their total ME requirement for that stage of gestation. The diets contained hay to concentrate in approximately a 3:1 ratio with respect to dry weight and had adequate minerals and vitamins. At 140 d gestation, each sheep was humanely euthanased by intravascular administration of 100mg/kg Phenobarbital sodium (Euthathal (200mg/g Phenobarbital sodium), RMB Animal Health, UK). The entire uterus was removed, and the fetus was similarly euthanased. Pericardial, and all other, adipose tissues were completely dissected, weighed, placed in liquid nitrogen, and stored at -80°C until processed and analysed as detailed below. All operative procedures and experimental protocols had the required U.K. Home Office approvals designated by the Animals (Scientific Procedures) Act (1986).

2.3 Human Studies

2.3.1 Epicardial fat is a depot of brown adipose tissue in adult humans

The adipose tissue samples for this study (Chapter 5) were provided by Professor Harold Sacks and were collected from patients undergoing cardiac surgery at The Baptist Heart, Baptist Memorial Hospital, Memphis, Tennessee.

Samples of adipose tissue were taken from EAT (from near the region of the right coronary artery), paracardial fat (from the anterior

mediastinum), substernal fat, upper abdominal and lower extremity subcutaneous adipose depots from individuals undergoing CABG. The samples were the remaining tissue from previous studies (Sacks et al. 2009, Fain et al. 2010, Sacks et al. 2011) and had been preserved (frozen at -80°C). With appropriate ethical approval and in keeping with the Human Tissue Act 2004, the samples were transferred to the Academic Division of Child Health, University of Nottingham on dry ice and stored at -80°C until further analysis.

2.3.2 Brown adipose tissue is present epicardial fat of newborn infants, children and adolescents

Adipose tissue samples for this study (Chapter 6) were provided by Mr Attilio Lotto (Paediatric Cardiothoracic Surgeon) and his team. The samples were collected from children undergoing cardiac surgery at the East Midlands Congenital Heart Centre at the Glenfield Hospital. All participants had congenital heart disease.

Although, due to small volumes, it is difficult to consistently separate the fat present around the heart in infants and children in to epicardial adipose tissue (i.e. fat present between the myocardium and visceral pericardium) and paracardial adipose tissue (i.e. fat present between the visceral and parietal layers of the pericardium) at dissection (Greif et al. 2009, McAuley et al. 2011, Wong et al. 2011), the fat samples for this study were taken from as close to the myocardium as possible and

are therefore considered to be primarily epicardial adipose tissue samples.

A sample of epicardial adipose tissue (approximately 5 grams) was collected during the dissection of the pericardium as a part of the standard process undertaken during cardiac surgery. Cardiac surgery is mostly performed through a median sternotomy. The pericardial sac is opened to reach the heart and great vessels and pericardiotomy is performed as an inverted 'T'. This opens the pericardium longitudinally with an extension transversally at the level of the diaphragm. Adipose tissue is present in this area. A small sample from this fat depot, was removed taking care to obtain the sample from as close to the myocardium as possible. Approximately 3 grams of tissue were placed in a collection tube containing 20 ml of Allprotect Tissue Reagent[®] (Qiagen, West Sussex, UK) for RNA extraction and lipid analysis and another 2 grams were placed in a tube containing 3% formalin for immunohistochemistry.

With appropriate ethical approval and in keeping with the Human Tissue Act 2004, the samples were transferred to the Academic Division of Child Health, University of Nottingham. The samples preserved in Allprotect Tissue Reagent[®] were transferred at room temperature. In the laboratory at Academic Child Health, University of Nottingham, the samples were removed from the solution, snap frozen in liquid nitrogen

and then stored at -80°C until further analysis. The formalin-fixed samples were transferred and stored at room temperature until further analysis.

2.4 Laboratory procedures

All chemicals, reagents and laboratory procedures were assessed and implemented in compliance with the UK Health and Safety Executive's Control of Substances Hazardous to Health (COSHH, SI NO. 1657, 1988) and Risk Assessment guidelines. Laboratory procedures were carried out at the Academic Child Health Department, School of Medicine, University of Nottingham. The procedures used in the study were either as recommended by the manufacturers and suppliers or optimised within Academic Child Health by myself, Mr M Pope and Mrs. V Wilson. All materials were purchased from Sigma-Aldrich (Poole, Dorset, UK) unless otherwise specified. Details of suppliers are given in Appendix 10.5.

To maintain the integrity of the tissue, all sheep pericardial adipose tissue samples were 'snap' frozen in liquid nitrogen and stored at -80°C until further analysis. Human adipose tissue samples obtained during cardiac surgery were immediately emerged in Allprotect Tissue Reagent[®] (Qiagen, West Sussex, UK) and stored at room temperature. Within one month of collection, the samples were snap frozen and stored at -80°C until further analysis. Each individual tissue sample was

stored in labelled double bags and stored in the -80°C freezers in the laboratories of Academic Child Health, University of Nottingham.

2.4.1 Tissue analysis

All experiments were performed with precautions to minimise contamination of samples and reagents. All equipment used was either taken from sterile packs or autoclaved. Filter tips used were sterile and all work was carried out wearing gloves. The work space and equipment were cleaned with 70% denatured ethanol (Ecolabs, Surrey, U.K) and RNAase ZAP[®] (Ambion, California, USA). Sterile nuclease free water (Ambion, Inc, UK) was used for all dilutions and experimental preparations. Tissue samples were removed from -80°C freezers and transferred on dry ice prior to processing. The desired amount of the sample was dissected and placed in labelled containers for later use. Remaining samples, if any, were returned to -80°C for storage until needed. All experimental work was performed on ice.

2.4.1.1 Total ribonucleic acid extraction from tissue samples

2.4.1.1.1 Principle

To extract total ribonucleic acid (RNA) from tissue, samples are lysed and homogenised in a buffer solution that contains guanidine-isothiocyanate and phenol in a monophasic. This causes the denaturing and dissolution of all proteins and inhibition of any RNAase activity, ensuring that intact RNA will be obtained at the end of the process. This

method is adapted from the published and widely used single step acidified phenol-chloroform homogenisation method (Cox and Arnstein 1963). Addition of chloroform and brief incubation followed by centrifugation separates the mixture into three layers - the top clear aqueous phase has RNA dissolved in it, the intermediate phase has the DNA and the lower phase has the dissolved proteins. The upper aqueous phase, the aqueous RNA solution, is treated with ethanol to provide appropriate binding conditions and then purified by RNA centrifuge column where total RNA (>100µg) binds to the membrane. Further washing with ethanol and guanidium salt-based buffers removes any contamination and final elution of RNA can be performed using nuclease-free water.

2.4.1.1.2 RNA extraction procedure

For analysis, each sample of adipose tissue was identified by the animal/participant number and transferred into a dry ice box. Adequate amount of tissue (1000mg) was chopped from each sample and placed into Dispomix tubes (Medic Tools, Zurich, Switzerland) on dry ice. For the animal studies, approximately 500mg of each tissue sample was processed for RNA extraction and for the human studies 100mg was processed due to the limited amount of samples available. The Dispomix tubes were labelled with randomly allocated numbers to avoid any bias during the experiments.

Two millilitres of TRI[®] reagent (Sigma Chemical Co. Poole, UK) was added to each sample and the samples were then allowed to thaw on ice. Each sample was homogenised in the Dispomix homogeniser (Medic Tools, Zurich, Switzerland) at 3000rpm for 40 seconds. The homogenate was centrifuged at 3000g for 1 minute and incubated in a water bath at 37°C for 2 minutes. The homogenate was mixed by vortexing five times over 30 seconds and centrifuged at 2500g for 5 minutes at room temperature. The lower aqueous phase was transferred into a 2ml eppendorf tube and 400µl of chloroform was added to it. The solution was mixed by vortexing and allowed to incubate at room temperature for 10 minutes. The mixture was further centrifuged at 12000g for 15 minutes at 4°C. This centrifugation separated the mixture into 3 phases such that the upper aqueous phase contained the RNA. This was carefully aspirated and placed in a 1.5ml eppendorf tube. An equal volume of 70% chloroform (analytical-grade chloroform (Fisher Scientific, Leicestershire, UK)) was added and mixed by vortexing.

The following steps of RNA purification were carried out using the RNeasy Plus[®] kit (Qiagen, West Sussex, UK). The RNeasy Plus[®] Universal kit was used for the animal studies while the RNeasy Plus[®] Mini kit was used for RNA extraction from the human adipose tissue samples. RNeasy spin columns were prepared for each sample and 700µl of the sample added to the column. The column was centrifuged

at 8000g for 15 seconds and the flow through discarded. This step was repeated until the total sample volume (in 700µl aliquots) passed through the column. The membrane in the RNeasy spin column bound all the RNA and the contaminants were washed away in the flow through. Next, 700µl of Buffer RW1 was added to each RNeasy spin column and the column centrifuged at 8000g for 15 seconds to wash the spin column membrane. The flow-through was discarded. In the next step, 500µl of RPE buffer was added to the RNeasy spin column which was then centrifuged at 8000g for 15sec and the flow through discarded. Another 500µl of RPE buffer was added to the RNeasy spin column which was centrifuged at 8000g for 2 minutes and the flow through discarded. The RNeasy spin column was centrifuged at 8000g for 1 minute in a fresh collection tube to eliminate any possible carryover of buffer RPE and to remove any residual flow-through which might remain on the outside of the RNeasy spin column. In all these steps, the RNeasy spin column was always removed carefully so that the column did not come in contact with the flow through and the collection tube was always emptied completely. The collection tubes were discarded and RNeasy spin column placed in a new 1.5ml eppendorf tube. To elute the RNA from the RNeasy spin column, 50µl of RNase-free water was added to the centre of the column membrane and the column centrifuged for 1 minute at 8000g. This step was repeated by adding the solvent back to the spin column and repeating

the centrifugation to increase the RNA yield. The spin column was then discarded.

2.4.1.1.3 Determination of RNA concentration purity and integrity

RNA concentration and purity measurements were determined using a Nanodrop[®]ND-1000 (Nanodrop Technologies, Wilmington, USA) spectrophotometer. The ratio of the optical density (OD) at 260 and 280 nm were measured by spectrophotometry and a ratio of 1.8-2.2 was considered an acceptable indicator of good RNA quality (Manchester 1996).

RNA obtained from human adipose tissue were further analysed for RNA integrity by the Agilent 2100 Bioanalyzer (Agilent Technologies, USA). RNA samples were electrophoretically separated on a micro-fabricated chip and subsequently detected via laser induced fluorescence detection. The use of a RNA ladder as a mass and size standard during electrophoresis allowed the estimation of RNA band sizes and integrity of the RNA was assessed by visualisation of the 18S and 28S ribosomal RNA bands (Figure 2.1). The Bioanalyzer 2100 software calculated the RNA integrity number (RIN) based on the shape of the curve in the electropherogram and samples were selected for microarray if the RIN was >7 and intact 18S and 28S bands were processed.

The extracted RNA was diluted to 1 µg/µl to normalise samples for quantitative reverse transcription (RT) and stored in appropriately labelled tubes at -20°C until further analysis.

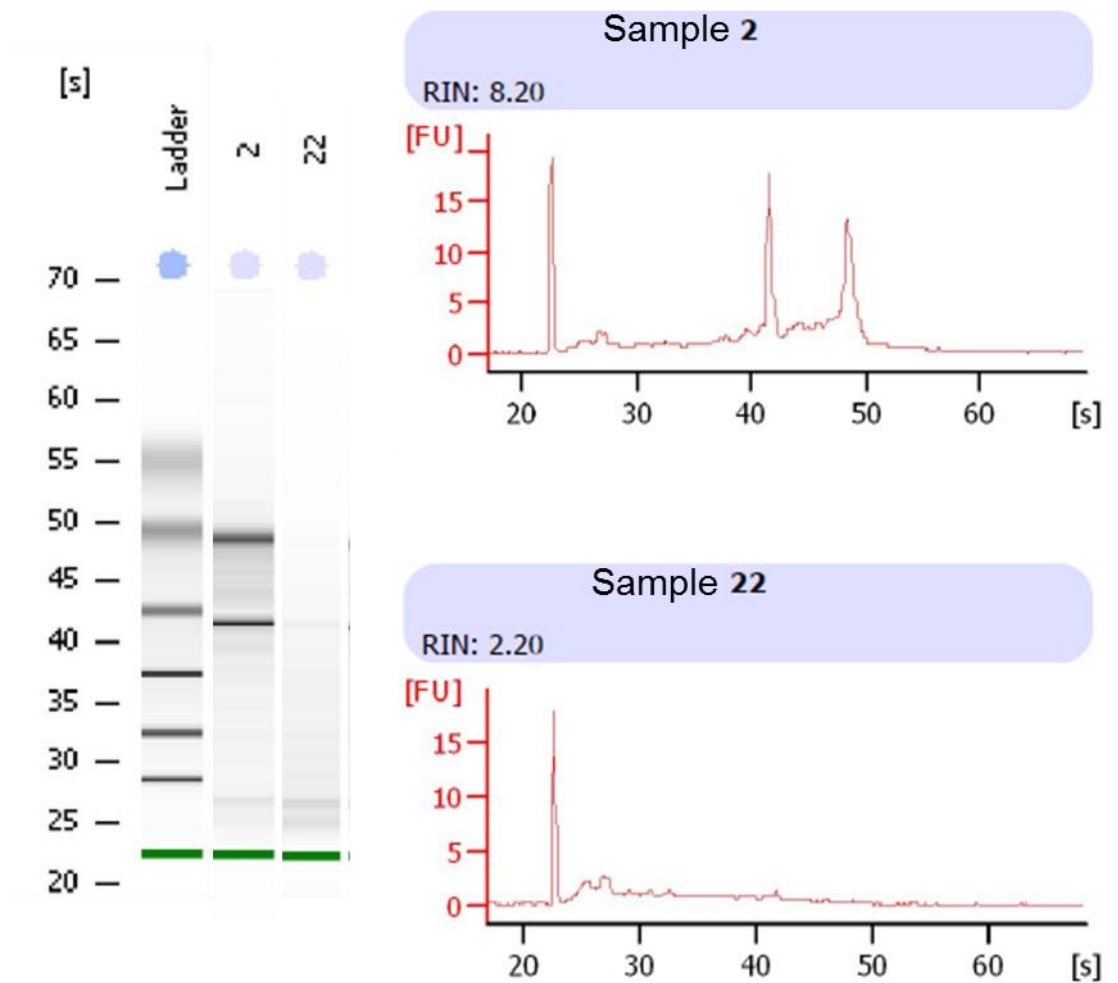


Figure 2.1 Chromatograms of micro-capillary electrophoresis from two RNA samples showing different degrees of degradation

Sample 2 had a RNA integrity number (RIN) of 8.2 and the electropherogram is typical of high-quality RNA showing a clearly visible 28/18S ribosomal RNA peak ratio and a small 5S RNA. Sample 22 is degraded (RIN = 2.2) as indicated by a shift in the electropherogram to shorter fragment sizes and decrease in fluorescent signal as dye intercalation sites are destroyed.

2.4.1.2 Reverse Transcription polymerase chain reaction (RT-PCR)

2.4.1.2.1 Principle of Reverse transcription polymerase chain reaction

By utilising proper reverse transcription reagents, RNA can be transcribed into single-stranded complementary deoxyribonucleic acid (cDNA). Following this, DNA polymerisation can amplify this result to form multiple copies of the cDNA.

The extracted purified mRNA is mixed with primers, deoxynucleotide triphosphatase (dNTP) mix, Reverse Transcriptase, DNA polymerase and RNAase inhibitors. All mRNAs have a poly-A terminal end. The reaction is initiated by annealing the oligo-dT primer to its complimentary sequence on the mRNA strand where further elongation and transcription of the first cDNA strand occurs by the enzymatic action of Reverse Transcriptase. The template strand of mRNA is then removed by RNAase and the cDNA strand is free for amplification by PCR (Figure 2.2). This produces cDNA strands that can be utilised for quantitative polymerase chain reactions (Q-PCR).

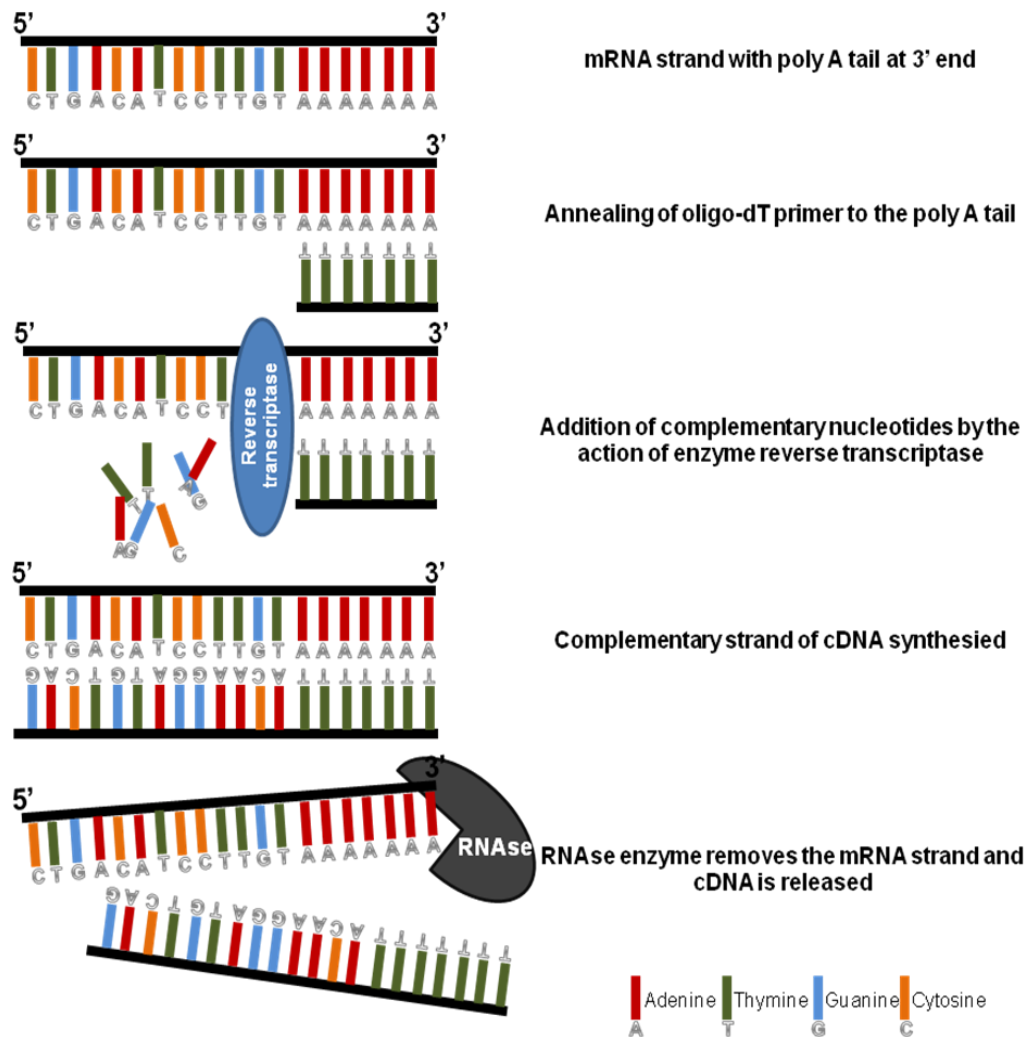


Figure 2.2. Reverse Transcription

Messenger RNA (mRNA) strands have a poly A tail to which the oligo-dT primer anneal. Reverse transcriptase enzyme then adds the complementary nucleotides to synthesise the complementary DNA (cDNA) strand. Action of RNAse removes the mRNA and releases the cDNA for further amplification by polymerase chain reaction.

2.4.1.2.2 Procedure for Reverse transcription polymerase chain reaction

RT-PCR was performed using the High Capacity RNA-to-cDNA kit (Applied Biosystems, Warrington, UK). The kit components were stored at -20°C and allowed to thaw on ice prior to the reactions. Two sterile 0.2ml eppendorf tubes were labelled for each sample, one for the reverse transcription (RT+) reaction and one for a no-reverse transcription enzyme control (RT-) to ensure transcription efficiency. In each tube, 2µg of total mRNA was mixed with 10µl of 2X RT Buffer. One microlitre of 20X enzyme mix was added to the RT+ tube and volume in both the tubes made up to 20µl by adding nuclease-free water. The reaction mixture was centrifuged for 1 minute at 5000g and incubated for 60 minutes at 37°C followed by heating to 95°C for 5 minutes and holding at 4°C in the Techne Touchgene Gradient thermal cycler (Techne Incorporate, New Jersey, USA). The cDNA prepared by this process was stored at -20°C.

2.4.1.3 Quantitative Polymerase Chain Reaction

2.4.1.3.1 Principle of Quantitative Polymerase Chain Reaction

Polymerase chain reaction (PCR) was developed by Kary Mullis in 1983 as a revolutionary technique that can amplify a single segment of DNA and create billions of copies within few hours. The reaction is initiated by annealing of an oligonucleotide sequence, called the primer, to

single stranded DNA. Primers are short pieces of custom built oligonucleotides which are a complementary match of the segment of the DNA that is being copied. Enzymes called DNA polymerase attach near the end of the annealed primer and elongate the chain by adding more nucleotides. Naturally occurring DNA polymerases are denatured at higher temperatures. The DNA polymerase used in laboratories, Taq polymerase, is derived from *Thermus aquaticus*, a thermophilic bacteria, and works at 72°C. Amplification of the target sequence occurs by repeated cycles of heat denaturation of the double stranded DNA, annealing of primers to the complimentary sequence and extension of the annealed primer by the action of Taq polymerase. After each cycle the amount of DNA is doubled leading to an exponential increase. Thus, 2^n , where n = the number of thermal cycles, strands of DNA are produced at the end of the PCR process (Figure 2.3).

Quantitative PCR (Q-PCR), also called real-time PCR, allows the detection and quantification of a sequence of DNA or mRNA simultaneously, without the need for additional steps such as Northern blotting. This reduces the time, expenditure, and probability of contamination and removes the use of hazardous reagents such as ethidium bromide (Kochanowski and Jilg 1999). The simplest method involves a DNA binding fluorescent dye, SYBR Green which adheres to minor grooves on the DNA and fluoresces at a much higher intensity when bound to DNA, compared with the dye in free solution (Denman

and McSweeney 2005). As the amplification occurs, more copies of the DNA are produced and bind to the dye and the resulting intensity of the fluorescent signal is proportional to the amount of DNA. The detector unit within the Q-PCR instrument will only detect the signal when a certain threshold of fluorescence is crossed. The instrument is programmed to calculate the baseline, defined as the PCR cycles in which a reporter fluorescent signal is accumulating but is beneath the limits of detection of the instrument (this is generally from cycles three to 15). The computer then determines an arbitrary threshold calculated as ten-times the standard deviation of the average signal of the baseline fluorescent signal between cycles three to 15. This threshold of fluorescence is then used to determine the cycle threshold (C_t) or crossing point (C_p) that is the fractional PCR cycle number at which the reporter fluorescence is greater than the minimal detection level determined by the programme i.e. the threshold fluorescence (Arya et al. 2005). The more the number of templates at the start of the reaction, the fewer number of cycles needed to cross the threshold and hence C_t can be used as the parameter for quantification of initial amount of the target template.

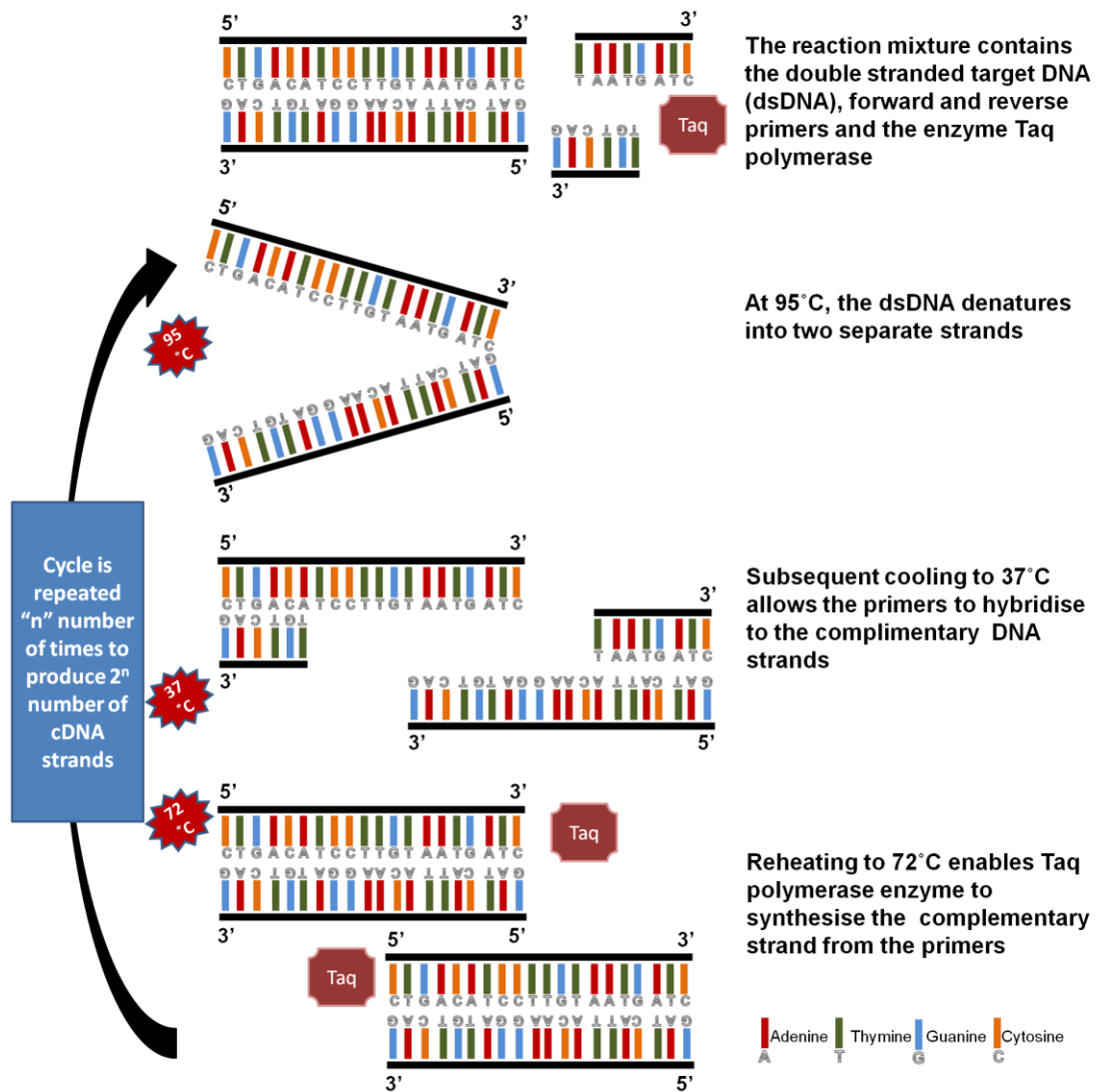


Figure 2.3. Polymerase chain reaction with Taq polymerase

At 95°C, the dsDNA (double stranded DNA) denatures into two separate strands. Subsequent cooling to 37°C allows the primers to hybridise to the complimentary DNA strands. The sample mixture is then reheated to 72°C to allow Taq polymerase to synthesise the complementary strands from the primer. The cycle is repeated starting with heating the mixture to 95°C again.

2.4.1.3.1.1 The standard curve

The plot of the log of initial target copy number for a set of known standard serial dilutions versus C_t is a straight line (Higuchi et al. 1993). This curve, called the standard curve (Figure 2.4) is used to determine the quantity of amount of the target in the “unknown” samples of interest. The instrument measures the C_t of the unknown samples and uses the C_t of the known dilutions on the standard curve to quantify the amount of target in the unknown sample (Arya et al. 2005). Generation of the standard curve also enables the calculation of efficiency of the reaction (E) and correlation coefficients (R^2) of the duplicate samples and acts as a positive control for verification of the experiment.

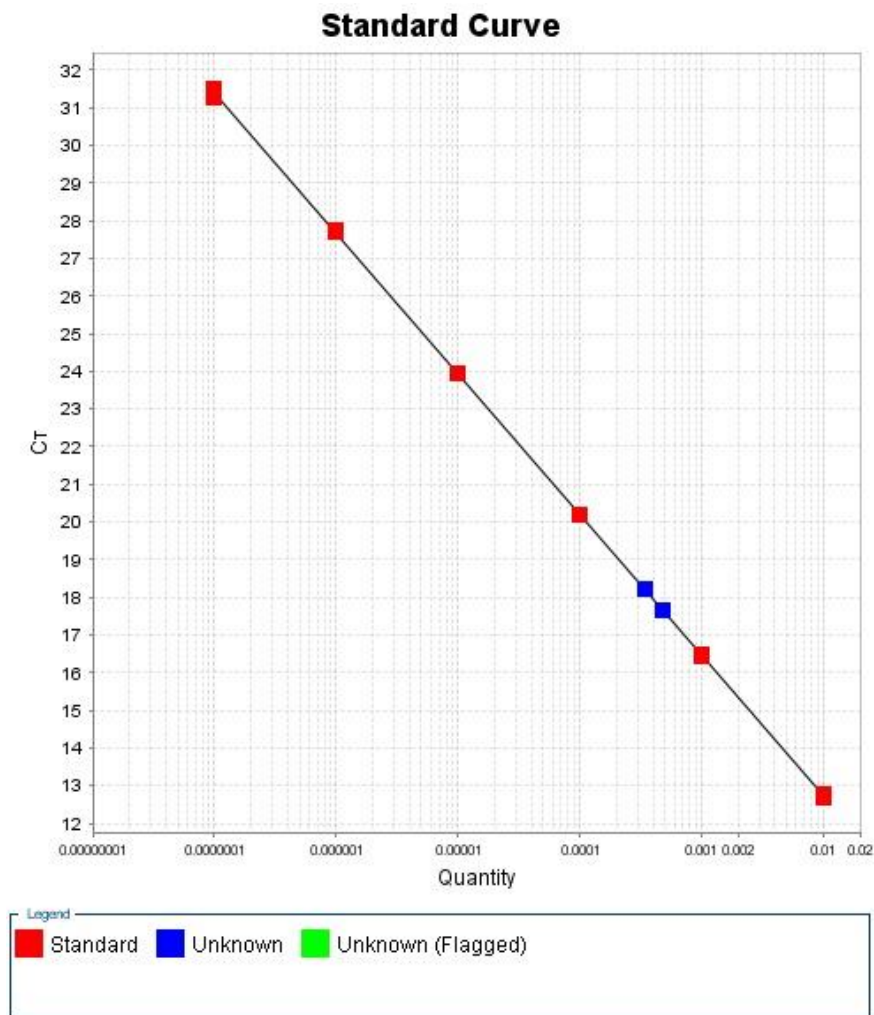


Figure 2.4. Standard Curve

A linear graph of the exponential polymerase chain reaction is created by plotting the cycle number at cycle threshold against logarithm of the known dilution series. The standard dilutions are generated by using duplicated ten-fold serial dilutions of purified template of the target cDNA. The assays have a six log linear dynamic range from 10^{-2} to 10^{-7} copies of the template cDNA.

2.4.1.3.1.2 Excluding non-specific products of PCR

It is important to note that SYBR green will indiscriminately bind to any strand of DNA and the assay must be optimised so that only the specific target of interest is amplified and that non-specific products such as primer dimers are excluded. The Q-PCR instrument performs a dissociation curve (also called the “Melt Curve”) analysis after the completion of the cycles by monitoring the loss of fluorescence signal, as the temperature is slowly raised from 60°C to 95°C causing the double-stranded amplicon to dissociate at a given melting temperature to release the SYBR green (Denman and McSweeney 2005). A single specific amplicon will dissociate at a single specific temperature, producing a single sharp dissociation curve (Figure 2.5). Presence of non-specific products can be discovered during this analysis by the presence of multiple or broader dissociation peaks.

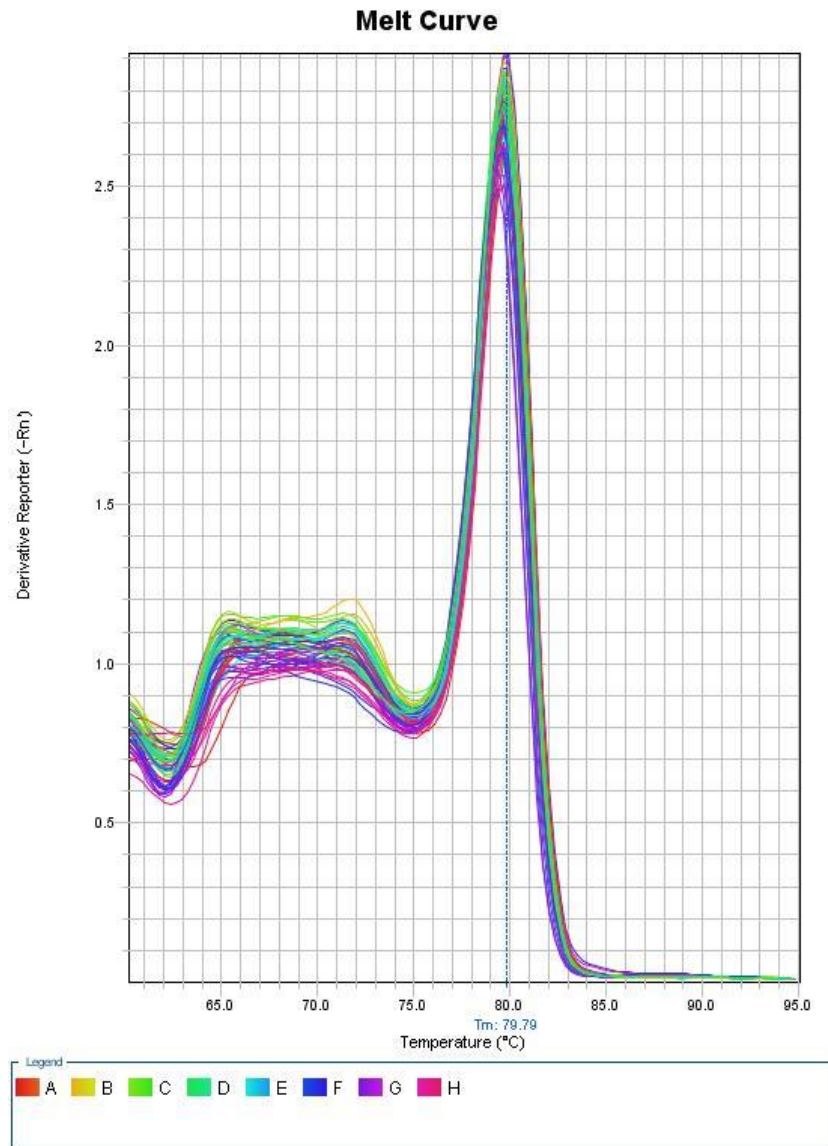


Figure 2.5 Melt Curve

A single peak of melting temperature of all the samples (A-H) indicates specificity of the product amplified. In this example, it is apparent that the melting temperature of all the amplicons occurs at the same temperature (80 °C). No contaminating products are present in this reaction as contaminant DNA or primer dimers would show up as an additional peak separate from the desired amplicon peak

2.4.1.3.1.3 Quantification of gene expression

To quantify gene expression in any experimental sample, it is important to correct the variation in starting RNA abundance. This can be achieved by analysing the expression of a gene, called the reference gene that is expressed at relatively constant high levels across all cells. Relative quantification of gene expression can then be determined using a mathematical model called the comparative threshold ($2^{-\Delta\Delta C_t}$) method (Livak and Schmittgen 2001). $2^{-\Delta\Delta C_t}$ gives the amount of the target gene in the sample, normalised to an endogenous reference gene and relative to the normalised-calibrator. To obtain valid and reliable results from this calculation, the amplification efficiencies of the reference and target gene must be approximately equal to each other and above 90% (Arya et al. 2005).

2.4.1.3.2 Selection of the reference gene

Errors can happen in Q-PCR reactions due to minor differences in the starting amount of RNA, quality of RNA or differences in efficiency of cDNA synthesis and PCR amplification. These can be minimised by using a reference gene, a cellular RNA that is amplified with the target and serves as an internal reference against which the target RNA values can be normalised. Genes such as 18S, GAPDH, IPO8 and YWAZ have been commonly used for this purpose. Theoretically, all these genes have a constant level of expression across all cells.

However, in practice, none of the genes are ideal references. Thus, multiple reference genes are analysed for each set and the crossing threshold values for each reference gene processed through the geNorm software v3.5 (Primer Design, Ltd, Southampton, UK). This software uses an algorithm of the geometric mean and pair wise variation of each gene compared to all other genes analysed, to calculate a stability value for each gene and selects the most suitable gene for use as reference gene (Vandesompele et al. 2002).

2.4.1.3.3 Development of oligonucleotide primers for Q-PCR

Primer sequences used in this study were either taken from previously published studies or designed in house using the Beacon Designer 4.0 software (Premier Biosoft, Palo Alto, USA) by Mr Mark Pope and myself using sequences from the appropriate species from the National Centre for Biotechnology Information (NCBI) online database by Mr Mark Pope and myself. Primers were selected such that they flank exon boundaries in the intron sequence and have optimum annealing temperatures; guanine-cytosine base pair content and length were chosen to achieve the most favourable reaction conditions. The NCBI nucleotide Basic Local Alignment Search Tool (BLAST) database was used to further ensure selection of the correct sequence. DNA standards were prepared from the final products of a PCR run on 2% agarose gel electrophoresis and extracted using the QIA quick gel extraction kit (28704; Quigen, Crawley, UK). A standard curve was generated for

each gene to ensure uniformity, efficiency and accuracy for each 96-well plate. Product validation for each primer was also confirmed by product size on gel electrophoresis and, when necessary, gene sequencing was performed with the results checked against known sequences on the GenBank Database (Benson et al. 2011). Primers were manufactured by and acquired from Sigma Aldrich as lyophilised powder and stored in nuclease free water at a stock concentration of 100µmol/l.

All primer sequences used in this study are detailed in Table 2.1.

Table 2.1 PCR Primer Sequences for Sheep Studies

Gene	Primer sequence	Reference
UCP1	Forward 5'-AGAGGTGGTCAAGGT CAG	(Budge et al. 2004)
	Reverse 5'-ATTCTGTAAGCATTGTAAGTC C	
PGC1 α	5'-GTG TGT GTT TGC CTG GTT TG	Primer design (UK)
BMP7	Forward 5'-GTCCAAG CGC CCAAGAAC	(Pope et al. 2013)
	Reverse 5'-TGCCTCTGGTCGCTG CTG	
BMP4	Forward 5'- AGTCTGGGGAGGAGGAAGAG	(Pope et al. 2013)
	Reverse 5'- GGGATGCTGCTGAGGTTAAA	
Leptin	Forward 5'-CCA GGA TGA CAC CAA AAC C	(Bispham et al. 2003)
	Reverse 5'-TGG ACA AAC TCA GGA GAG G	
Adiponectin	Forward 5'- ATCAAACCTCTGGAACCTCCTATCTAC	(Pope et al. 2013)
	Reverse 5'- TTGCATTGCAGGCTCAAG	
Ki67	Forward 5'-TCAGTGAGCAGGAGGCAGTA	(Pope et al. 2013)
	Reverse 5'- GGAAATCCAGGTGACTTGCT	
RIP 140	Forward 5'- CGAGGACTTGAAACCAGAGC	(Pope et al. 2013)
	Reverse 5'- TCTTAGGGACCATGCAAAGG	
PPAR γ	Forward 5'- GACCCGATGGTTGCAGATTA	(Pope et al. 2013)
	Reverse 5'- TGAGGGAGTTGGAAGGCTCT	
C/EBP β	Forward 5'- ACGACTTCCTCTCCGACCTC	(Pope et al. 2013)
	Reverse 5'- CCCAGACTCACGTAGCCGTA	
IPO8	Forward 5'- GCCCTTGCTCTTCAGTCATT	(Pope et al. 2013)
	Reverse 5'- GTGCAACAGCTCCTGCATAA	
HOXc9	Forward 5'- GACCTGGACCCCAGCAAC	(Pope et al. 2013)
	Reverse 5'- GCTCGGTGAGGTTGAGAAC	
β 1ADR	Forward 5'-CGCTCACCAACCTCTTCATC	Developed in house
	Reverse 5'-CAC ACA GGC TCT CAA TGC TG	
β 2ADR	Forward 5'-ATTGCCTCCTCCATT GTG TC	Developed in house
	Reverse 5'-CATCCTGCTCCACTTGACTG	
β 3ADR	Forward 5'-CGCCTCCAACATGCCCTAC	Developed in house
	Reverse 5'-GCGTAGACGAAGAGCATCAC	
C/EBP α	Forward 5'-CTGGAGCTGACCAGTGACA	(Pope et al. 2013)
	Reverse 5'-GGGCAGCTGACGGAAGAT	
GR	Forward 5'-ACTGCCCCCAAGTGAAAACAGA	(Pope et al. 2013)
	Reverse 5'-ATGAACAGAAATGGCAGACATT	
PRLR1	Forward 5'-CTCCACCCACCATGACTGAT	Developed in house
	Reverse 5'-CAGCGAATCTGCACAAGGTA	
DIO2	Forward AGCCGCTCCAAGTCCACTC	Developed in house
	Reverse TTCCACTGGTGTCACCTCCT	
PRDM16	Forward GACGACCAGAACCTCACCAT	Developed in house
	Reverse TCTTTCACATGGACCAGCAG	
KCNK3	Forward CCTTCTACTTCGCCATCACC	Developed in house
	Reverse GTGCAGCAGGTACTIONCACGA	
TGM2	Forward TTTTCATGCTGGGTGAGTTCA	Developed in house
	Reverse AACTTGGGGTTGACATCCAG	

Abbreviations: UCP, Uncoupling protein; BMP, Bone Morphogenetic Protein; PPAR, peroxisome proliferator-activated receptor; PGC, PPAR γ co-activator; TGM, Transglutaminase; KCNK3, potassium channel, subfamily K, membrane 3; PRDM16, PR (PRD1-BF1-RIZ1 homologous)-domain-containing protein; HoX, Homobox; C/EBP, CCAAT-enhancer binding protein; DIO2, type 2 iodothyronine deiodinase; ADRP, Adipose Differentiation Related Protein; ADR, adrenergic receptor; GR, glucocorticoid receptor; PRLR, prolactin receptor; RIP, Receptor interacting protein

2.4.1.4 Quantitative Polymerase Chain Reaction - procedure

2.4.1.4.1 Hot start PCR procedure

Conventional or classical PCR (cPCR) was performed for primer optimisation and creation of cDNA Q-PCR standards. Eppendorf tubes (200µl) were appropriately labelled and the reaction mixture was added per tube as given in Table 2.2.

Table 2.2. Reaction mixture for classical PCR

Step	Volume per tube
Random cDNA template or Nuclease-free water for negative control	2 µl
1:40 dilution of forward primer	4 µl
1:40 dilution of reverse primer	4 µl
PCR master mix (One Taq™ Hot Start Quick Load® 2X Master Mix with standard buffer (New England BioLabs inc. USA))	10 µl

Tubes were centrifuged for one minute at 10,000g and loaded in to the Techne thermal cycler and run at a 60°C hot start PCR programme (Table 2.3). The second phase repeats for 35 cycles.

Table 2.3. Hot Start PCR programme.

Process	Temperature (°C)	Duration (minutes)
Initiation	105	4
Enzyme activation	96	15
<i>Repeated for 35 cycles:</i>		
Denaturing of cDNA strands	94	0.5
Primer annealing	60	0.5
Primer extension	72	1
Final extension	72	7
Hold	4	

The second phase of cDNA denaturation, primer annealing and extension is repeated for 35 cycles.

2.4.1.4.1.1 Agarose gel electrophoresis and DNA extraction

Products of PCR can be analysed by separating them on an agarose matrix. The phosphate backbone of the DNA molecules makes them negatively charged. The fragments can thus be separated according to their size by the application of an electric field. Addition of an intercalating DNA dye such as ethidium bromide, which fluoresces when exposed to ultra-violet light, enables visualisation of the DNA bands within the matrix. Positive control DNA, called “DNA ladder”, is run simultaneously to identify the size of the unknown bands.

The gel matrix was prepared by dissolving 2% w/v of agarose (electrophoresis grade) (Invitrogen Life Technologies) in TAE buffer (made from a stock solution of tris (hydroxymethyl aminomethane base (tris), glacial acetic acid (Fischer Scientific), EDTA buffer), heated and mixed with 7µl of 10mg/ml ethidium bromide for visualisation, and cooled to form a gel. PCR products and DNA marker (ladder) (100bp Blue eXtendec Bioron, Ludwigshafen, Germany) were passed through the gel at 100V for 60 minutes. Ladder and PCR products were visualised under an ultraviolet (UV) trans-illuminator charged coupled device (CCD) camera (Fuji film luminescent image analyser LAS-1000 v1.01).

The fluorescent bands were cut out and cPCR products extracted and purified using the QIAquick Gel Extraction Kit (Qiagen, West Sussex,

UK). The gel bands were weighed and dissolved in Buffer QG by heating at 50°C for 10 minutes. Three volumes of Buffer QG were used for one volume of gel (assuming 100mg of gel ~ 100µl). One gel volume of isopropanol was added to the dissolved gel and mixed by vortex. The sample was then applied to the QIAquick column placed in a 2ml collection tube and centrifuged at 10,000g for 1 minute. The flow through was discarded and 0.5ml of Buffer QG was added to the spin column, centrifuged at 10,000g for 1 min and flow through discarded again. Following this, 0.75ml of Buffer PE was added to the spin column which was again centrifuged for 1 minute and the flow through discarded. The spin column was again centrifuged and any remaining flow through was discarded to remove any residual ethanol. To elute the PCR product, the QIAquick column was then placed in a clean 1.5ml eppendorf tube and 30µl of Buffer EB was directly added on to the membrane. The column was allowed to rest for 1 minute and then centrifuged for 1 minute at 10,000g.

Integrity and concentration of the PCR product was analysed using the Nanodrop®ND-1000 (Nanodrop Technologies, Wilmington, USA) spectrophotometer. All the extracted cDNA samples were diluted to 1ng/µl and stores at -20°C until needed.

Samples from newly designed primer products were sent for DNA sequencing within the University of Nottingham's Centre for Genetics

and Genomics (Queen's Medical Centre, Nottingham, UK) and cross-referenced against the NCBI online database.

2.4.1.4.1.2 Q-PCR procedure

2.4.1.4.1.2.1 Standard curve

For each gene analysed, serial 1:10 dilutions were prepared from the 1ng/μl template cDNA obtained from cPCR and gel electrophoresis. Dilutions up to and including 1×10^{-8} were prepared. These were run, in duplicate, with a negative (nuclease-free water) and positive control (random c-DNA sample) on a Q-PCR plate to verify the efficiency of the experiment.

2.4.1.4.1.2.2 Q-PCR of unknown samples

Samples and standards with a negative control were run in duplicate on a 96-well Q-PCR plate (Abgene, Thermo Fisher Scientific Inc. UK) in 10μl aliquots. The reaction mixture was as given in Table 2.4.

The PCR plates were sealed with an Abgene plate sealer and thermal seals (Alpha Laboratories, Hampshire, UK) and placed in the StepOne Plus Real Time PCR System (Applied Biosystems, Warrington, UK) and the Q-PCR run as per the protocol in Table 2.5.

Table 2.4. Q-PCR reaction mixture

Reagent	Volume per reaction
SYBR [®] Green (Applied Biosystems, Warrington, UK)	5 µl
1:40 dilution of forward primer	1 µl
1:40 dilution of reverse primer	1 µl
cDNA	3 µl

Table 2.5. Q-PCR programme conditions

Process	Temperature	Duration
Initial denaturing of the cDNA strand	95 °C	15 minutes
Denaturing of cDNA strands	95 °C	15 seconds
Annealing of the primers	58-62 °C	30 seconds
<i>(Above steps repeated for 45 cycles)</i>		
Melt curve analysis	65 to 95 °C in 1 °C increments	15 minutes
<i>(Above step repeated for 31 cycles)</i>		
Hold	95 °C	10 minutes

2.4.1.5 Microarray analysis

2.4.1.5.1 Principles of microarray analysis

Microarray is an orderly arrangement of thousands of identified sequenced genes printed on an impermeable solid support, usually glass or silicon chip. Each sequenced gene corresponds to a fragment of genomic DNA, cDNA, PCR products or chemically synthesised oligonucleotides that represents a single gene. It is then used to run a high-throughput and versatile technology used for parallel gene expression analysis for thousands of genes of known and unknown function.

RNA extracted from biological sample of interest is labelled to generate the target for the microarray. The mRNA extracted from the biological sample of interest and the reference is separately converted into cDNA using a reverse-transcriptase enzyme. This step also requires a short primer to initiate cDNA synthesis. Next, each cDNA is labelled with a different tracking molecule, often fluorescent cyanine dyes. The product is then purified to remove contaminants such as extra primers, proteins and unincorporated nucleotides.

The microarray slides are incubated at high temperature with solutions of saline-sodium buffer, sodium dodecyl sulphate and bovine serum albumin to reduce non-specific binding. The labelled and purified cDNA is then competitively hybridised against the oligonucleotides on the

immobilised array and ideally, each molecule in the labelled cDNA will bind only to its appropriate complementary target sequence on the microarray chip.

Un-hybridised cDNA fragments are removed by washing; slide is dried and placed in a scanner to determine how much labelled cDNA is bound to each target spot. The photo-excitation of each spot is then measured using a fluorescent microscope. This information is captured digitally and subjected to various analyses to extract the relevant biological information. Thus microarrays provide a powerful tool with which to screen biological specimens for alteration in the expression of mRNAs that accompany and may regulate physiological and pathological changes.

2.4.1.5.2 Procedure: microarray analysis using GeneChip®

mRNA extracted from epicardial adipose tissue samples were tested for integrity using the Agilent 2100 bioanalyzer (Agilent Technologies, Santa Clara, USA) and subsequent mRNA processing was completed using the GeneChip® 3' IVT Express kit (Affymetrix, High Wycombe, UK).

Poly-A RNA controls were diluted and spiked into mRNA samples prior to cDNA synthesis as positive controls to assess the labelling. First and second strand cDNA synthesis was performed using the first and second strand master mixes provided in the kit. cDNA was then

transcribed *in vitro* to synthesise biotin labelled array RNA (aRNA) using the IVT kit with incubation for 16 hours at 40°C. aRNA purification was completed with RNA binding beads followed by elution with aRNA elution solution for each sample. After elution, the yield of purified aRNA was determined through a Nanodrop spectrophotometer at 260 nm wavelength absorbance. The aRNA samples were then fragmented using fragmentation buffer provided in the kit with incubation at 94 °C for 35 min. To assess fragmentation, samples were run on an Agilent 2100 bioanalyzer and demonstrated peak sizes of approximately 100-120 nt.

Samples were hybridised to an Affymetrix® Human Genome U133 plus 2.0 array (Affymetrix, High Wycombe, UK) with one cartridge per sample in a hybridisation oven for 16 hours at 45 °C. Following hybridisation, the samples were washed using a 450/250 Fluidics Station. Streptavidin Phycoerythrin was used for staining; this binds to biotinylated aRNA. Each GeneChip® was loaded into Affymetrix® Genechip® Scanner 3000 for analysis of fluorescence.

Quality control of labelling and hybridisation, as well as data analysis was conducted using Partek (Partek Inc., St. Louis, USA).

2.4.2 Protein analysis

2.4.3 Preparation of mitochondrial extracts

Mitochondrial preparations were made from the tissue samples using the method described by Symonds et al. (Symonds et al. 1992). Ten millilitres of [hydroxymethyl] amino methane (tris) – sucrose homogenisation buffer (10mM tris, 250mM sucrose and 1mM ethylenediaminetetraacetic acid (EDTA)) were added to approximately 1 g of frozen pericardial adipose tissue which was then allowed to thaw on ice. The thawed tissue was homogenised using an Ultra Turrax homogeniser for 2X 30 seconds until no clumps of tissue were visible. The homogenate was transferred to a glass homogenisation tube and further homogenised with 10 strokes in the Potter-Elvehjem homogeniser. This homogenate was transferred into a centrifuge tube and volume made up to 20ml with the tris-sucrose homogenisation buffer. A 500µl aliquot was collected from each sample for total protein concentration analysis. The remainder was centrifuged at 1000rpm for 10 minutes at 4°C. The supernatant was passed through 2 layers of gauze to remove the excess lipid tissue. The filtered supernatant was centrifuged at 10,000rpm for 30 minutes at 4°C. A 1ml aliquot of the supernatant was collected for cytochrome c analysis and the rest discarded. The remaining mitochondrial pellet was re-suspended in the tris-sucrose buffer by adding 100µl at a time. The volume of the

resulting sample was noted and the mitochondrial preparations stored at -20°C until further analysis.

In the human studies, due to limited sample size, the above method was modified to prepare mitochondria from 100-200mg of sample. The second homogenisation was performed by a hand-held mini-Potter-Elvehjem homogeniser and only one layer of gauze used to remove excess lipids.

2.4.3.1 Assessment of protein concentration

Total protein concentrations and protein concentrations of the mitochondrial homogenates were measured using Bicinchoninic acid (BCA) assay or the Bradford assay.

2.4.3.1.1 Bicinchoninic acid total protein determination

2.4.3.1.1.1 Principle of BCA assay

This assay depends on two reactions. In the first reaction, the protein peptide bonds from a tetradentate- Cu^+ complex with copper (II) ions (Cu^{++}) followed by this complex combining with BCA to form a BCA- Cu^+ complex (purple in colour) in the second reaction. The interaction of Cu^{++} with peptide bonds occurs in an alkaline environment and thus Cu^{++} is reduced to Cu^+ . BCA acts as a detection agent for this reduced copper ion. In this reaction, two molecules of BCA chelate with one cuprous ion (Cu^+). The resulting complex absorbs light at 562nm

making the solution purple in colour. As the amount of this complex formed depends on the concentration of the protein in the solution, the intensity of light absorption at 570nm wavelength is proportional to the concentration of protein in the sample.

2.4.3.1.1.2 BCA assay procedure

BCA reagent was prepared by mixing two reagents – Reagent A (1% bicinchoninic acid + 2% sodium carbonate + 0.16% sodium tartarate + 0.4% sodium hydroxide made to a volume of 500ml with distilled water and pH corrected to 11.25) and Reagent B (containing 4% cupric sulphate made to a volume of 25ml in distilled water). Protein samples were first diluted to 1:20 and made up to a total volume of 50µl with normal saline. Normal saline was used as control and standard dilutions of Bovine Serum Albumin (BSA) were used to prepare the standard curve. For the reaction, 10µl of sample, control or standard was pipetted in duplicate to each well of a 96 well plate (PS-Microplates-flat bottom, Greiner Bio-One GmbH, Frickenhausen, Germany) and 200µL of the BCA reagent added to each. The plate was incubated while shaking at 37°C for 30 minutes, then placed into a plate reader (Bio-Teck uQuant, ReTiSoft Inc. Ontario, Canada) and absorbance measured at 562nm. Results that were within 10% of each other are considered suitable for analysis.

The standard curve (Figure 2.6) was generated by plotting the concentration of BSA with the measured absorbance at 562nm. Protein concentrations in the samples were calculated by linear regression analysis of the standard curve and corrected for initial dilution.

2.4.3.1.2 Bradford assay

2.4.3.1.2.1 Principle of the Bradford assay

The Bradford Reagent (Sigma-Aldrich, Saint-Louise, Missouri, USA) consists of Brilliant Blue G in phosphoric acid and methanol. The procedure is based on the binding of Coomassie Brilliant Blue G-250 to protein in the sample. The binding of the dye to protein causes a shift in the absorption maximum of the dye from 465 to 595 nm, and it is the increase in absorption at 595 nm. The magnitude of the shift in absorption is proportional to the quantity of protein present and can be measured by a Spectrophotometer capable of measuring absorbance in the 595 nm range.

2.4.3.1.2.2 Bradford assay procedure

The Bradford assay was performed at room temperature by mixing 1 part of the protein sample to 30 parts of the Bradford Reagent. A serial dilution of protein standards and blank samples (no protein) were included in the assay to produce a standard curve. Colour development begins almost immediately and protein concentration was determined

by measuring the absorbance at 595 nm and comparison to the standard curve.

The assay was performed in a 96 well plate. The Bradford Reagent was gently mixed and allowed to reach room temperature. Protein standards were prepared with serial dilutions of known concentration of bovine serum albumin to produce a series of standards ranging from 0.1- 1.4 mg/ml.

Five microliters of protein standard, sample or blank solution (nuclease free water) was pipetted in to each well of the 96 well plate and 250 μ l of Bradford Reagent was added to each well. The 96 well plate was put on a shaker for 30 seconds to allow for the samples and reagent to mix and incubated at room temperature for 5 minutes. The absorbance was measured at 595 nm using a plate reader (Bio-Teck uQuant, RETiSoft Inc. Ontario, Canada). Three repeat measurements were taken at 5, 10 and 20 minutes.

The net absorbance vs. protein concentration of each standard was plotted to generate a standard curve and protein concentration of the unknown samples were calculated by comparing the net absorbance at 595 nm of the sample against the standard curve (Figure 2.6).

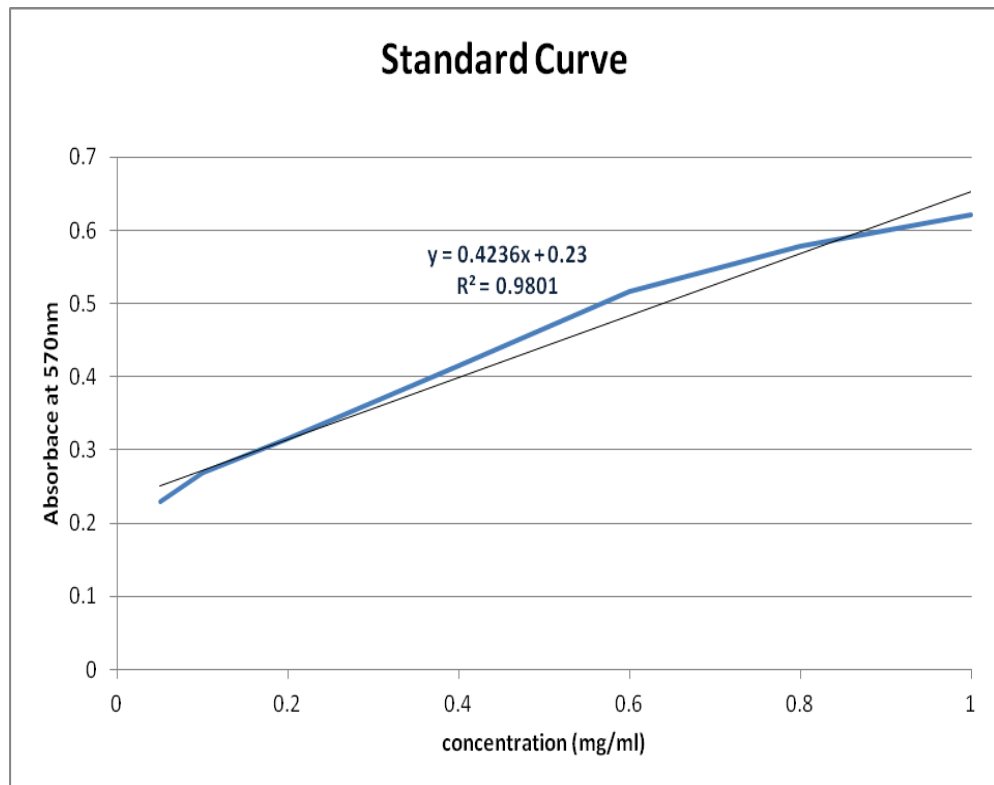


Figure 2.6. Standard curve for estimation of protein content in mitochondrial extract

The absorbance at 570 nm is plotted against the concentration of standard dilutions of bovine serum albumin to generate a linear graph that is then used to calculate the protein content of the experimental samples.

2.4.3.2 Western Blotting

Western Blotting, as described by Burnette (Burnette 1981), is used to measure the abundance of selected proteins. This is achieved by sodium dodecyl sulphate-polyacrylamide gel electrophoresis (SDS-PAGE) and each Western blot is performed in duplicate.

2.4.3.2.1 Principle of Western Blotting

Sodium dodecyl sulphate (SDS) is an anionic compound that can wrap around the polypeptide backbone of proteins. It binds in a specific mass ratio of 1.4g SDS to 1g protein and confers a negative charge to the resultant SDS-protein complex. This negative charge is proportional to the peptide length i.e. each denatured polypeptide strand from a particular protein has equal charge or charge density per unit length and the amount of charge on the polypeptide is proportional to its size. Thus, the SDS-protein complexes can be separated depending on their size by electrophoresis through a polyacrylamide gel. During electrophoresis, the negatively charged SDS-protein complexes move towards the anode at a rate that is inversely proportional to their size.

To enable the separation by size, the polypeptide chains have to adopt a random coil configuration. The disulphide bridges in proteins have to be broken before this can happen. This is done during preparation of the protein sample by adding 2-mercaptoethanol or dithiothreitol (DTT) and incubating at 100°C for 10 minutes.

The size of the pores in the polyacrylamide gel depends on the concentration of the acrylamide and the bis-acrylamide that is used for cross-linking. This produces a sieving effect so that the migration of the polypeptide during SDS-PAGE is determined by its molecular weight and not the electrical charge it is carrying.

After the polypeptides have been separated on the gel by SDS-PAGE, they are transferred on to nitrocellulose membrane for immunoblot analysis. This is done by applying an electric current to the gel and the nitrocellulose membrane so that the negatively charged polypeptides move from the gel on to the membrane in exactly the same configuration as they separated by SDS-PAGE.

The areas on the nitrocellulose membrane that are not occupied by the polypeptides blotted from the gel are “blocked” by incubating with non-specific proteins so that the primary antibody does not bind to them.

The nitrocellulose membrane is then incubated in an appropriate dilution of the primary antibody. If the membrane contains the antigen (i.e. appropriate polypeptide) corresponding to the primary antibody, it will bind to it and the excess primary antibody is washed at the end of the incubation.

To enable visualisation of the bound primary antibody, the membrane is incubated with a “secondary antibody” which is an anti-immunoglobulin antibody coupled to a reporter group such as horseradish peroxidase

(HRP) enzyme. After incubation, the excess secondary antibody is washed off and the nitrocellulose membrane is incubated with a substrate which emits light upon reaction with the polypeptide-primary antibody- secondary antibody complex. The membrane is visualised in a Charge Coupled Device (CCD) camera where the complex shows as a visible band. The concentration of the band is then measured by densitometry which gives a semi-quantitative estimate of the protein concentration.

2.4.3.2.2 Western Blotting procedure

2.4.3.2.2.1 Gel preparation and electrophoresis assembly

Glass plates and combs supplied in the Mini-PROTEAN 3 cell (Bio-Rad, Ontario, Canada) were used to cast polyacrylamide gels. The resolving gel (12%) was prepared (4ml 30% acrylamide/8% bisacrylamide (37:5:1) solution, 3.3ml distilled water, 2.5ml 1.5M Tris (pH 8.8), 100µl 10% sodium dodecyl sulphate, 100µl 10% ammonium persulphate, 4µl N,N,N',N' tetramethyl ethylenediamine) and poured between the spacer and short glass plates (a thickness of 1.5mm) and allowed to set for 1 hour. A small amount of water saturated butanol was poured on top of the gel to prevent desiccation during polymerisation.

Stacking gel was prepared (1.7ml 30% acrylamide/8% bisacrylamide (37:5:1) solution, 6.8ml distilled water, 1.25ml 1.5M Tris (pH 8.8), 100µl 10% sodium dodecyl sulphate, 100µl 10% ammonium persulphate, 10µl

N,N,N',N' tetramethyl ethylenediamine) and poured on top of the resolving gel and combs inserted to create wells. The gel was allowed to polymerise for 30 minutes and the combs then removed.

The gels (within the glass sandwich) were transferred into the Electrode assembly and placed into the inner chamber of the vertical slab electrophoresis unit (part of the Mini-PROTEAN cell 3 systems). The inner chamber was placed into the Mini Tank (outer chamber). The inner chamber was filled with diluted (5X) Tris-Glycine Electrophoresis buffer (25mM Tris Base (151.0g), 250mM Glycine (940g) 10% sodium dodecyl sulphate (500ml) and made up to 10L with distilled water) such that the wells were filled with it and its level was between the tops of the two glass plates of the gel sandwich. The lower chamber was also filled with the same solution.

2.4.3.2.2.2 Protein sample preparation for loading

The protein samples (mitochondrial extract) were prepared on ice by diluting the mitochondrial extracts with [hydroxymethyl] amino methane (tris) – sucrose homogenisation buffer (the buffer that was initially used for preparation of mitochondria) to a protein concentration of 4.2µg/l. This was performed so that the final preparation contained 1µg/µl of protein. The diluted mitochondrial extract was mixed with 50µl of protein dissociation buffer (100 ml 50mM Tris (pH 6.8) containing 5ml β-mercaptoethanol (5%), 20ml 10% sodium dodecyl sulphate (2%) and

10ml glucerol (10%)) and 14µl of glycerol-bromophenol blue (0.01g bromophenol blue, 14.9ml 0.01M sodium hydroxide, 23.5ml distilled water). The samples were denatured at 100°C for 10 minutes and immediately placed on ice.

2.4.3.2.2.3 Gel loading

Each well was loaded with 10µl (containing 10µg of protein) of the prepared protein sample. Precision Plus Protein™ standards (All Blue) (Bio-Rad, Ontario, Canada) was used as the protein molecular weight marker (Figure 2.7). Ten microlitres of this was loaded into at least one well in each gel. Any potentially empty wells were filled with bromophenol blue to ensure even electrophoresis. One sample known to contain the protein of interest and one which did not (i.e. positive and one negative control samples) were run on each gel to allow comparison of abundance.

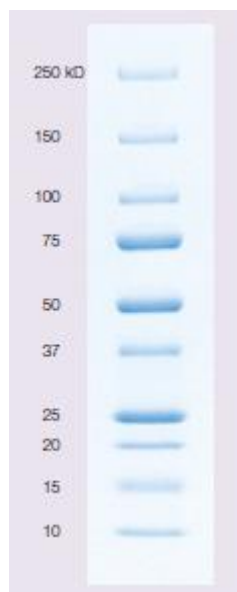


Figure 2.7. Representative of All blue prestained Precision Plus Protein standards on a 4-20% Tris-HCl Criterion™ Gel

(From Instruction Manual, Precision Plus Protein™ Standards, Catalog #161-0373, (Bio-Rad, Ontario, Canada))

2.4.3.2.2.4 Electrophoresis

The proteins were separated by electrophoresis at a constant voltage of 200V for approximately 35 minutes (until the colour in the protein preparation reached the bottom of the resolving gel).

2.4.3.2.2.5 Electroblotting

The gel was extracted from between the glass plates and the separated protein transferred on to a nitrocellulose membrane (AmershamTM HybondTM-ECL membrane, GE Healthcare, Little Chalfont, U.K.) by electroblotting in the Bio-Rad Mini-PROTEAN 3 electroblotting apparatus (Bio-Rad, Ontario, Canada). The gel and nitrocellulose membrane were placed between 2 Scotch-BriteTM (3M Company, U.S.A) in to a cassette and inserted in to the electroblotter in the configuration shown in Figure 2.8. The proteins were blotted at a constant voltage of 60V for 1 hour.

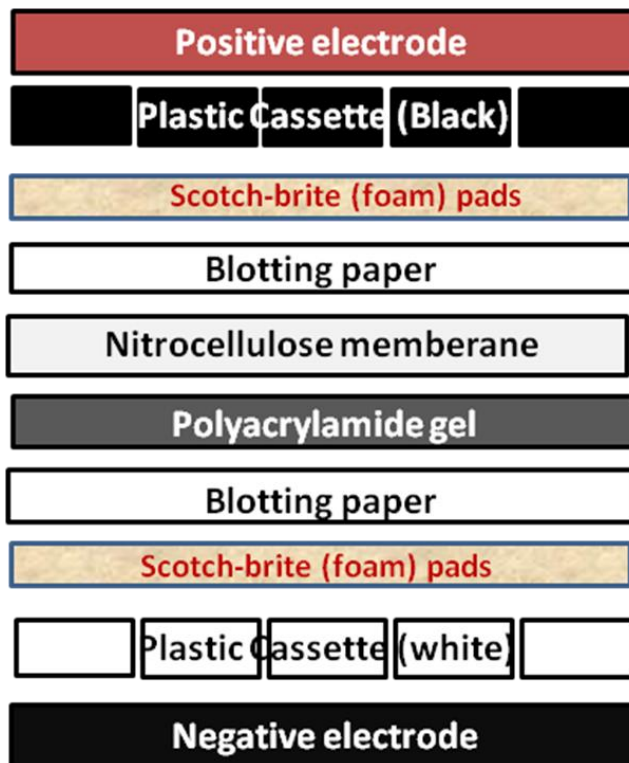


Figure 2.8. Configuration of the polyacrylamide gel and nitrocellulose membrane in relation to the electrodes during electroblotting

The nitrocellulose membrane was stained by Ponceau S stain ((2g (2%(w/v)) Ponceau S, 30g (30%(w/v)) trichloroacetic acid, 30g (30%(w/v)) sulphosalicylic acid in 100ml of distilled water; diluted 1:10 with distilled water prior to use) for visualisation of the proteins on the membrane and verification of even blotting. An example of a membrane stained with Ponceau S is given in Figure 2.9. At this point, the positions of the molecular weight markers were noted and marked with PEN-R1 (Antigen-Antibody pen for Rabbit Primary Antibody, Alpha Diagnostics, San Antonio. U.S.A).

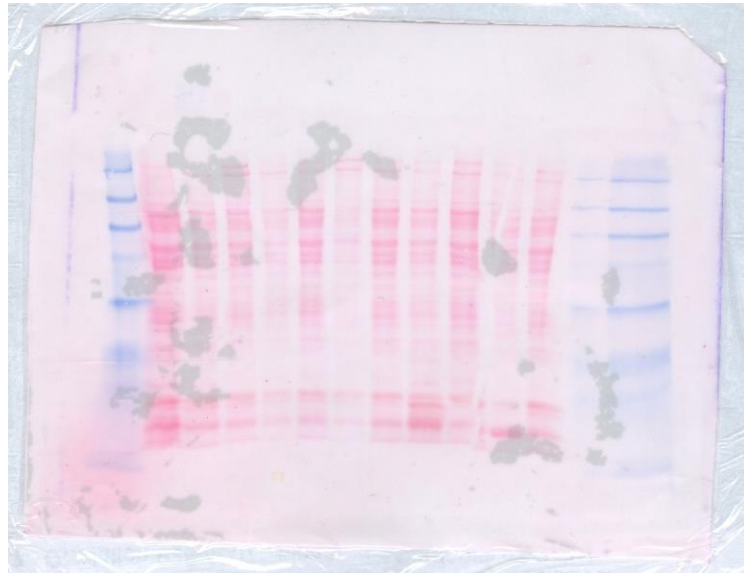


Figure 2.9. Ponceau S staining of nitrocellulose membrane showing the electroblotting of protein on to the membrane and molecular weight markers on either side

The grey areas visible on the membrane represent air bubbles between membrane and plastic wrapper trapped in the process of encasing the membrane in plastic. They are not integral to the membrane.

2.4.3.2.2.6 Immunodetection

The nitrocellulose membrane was incubated overnight at 4°C in a blocking solution (10% (w/v) non-fat milk (Marvel, Premier Bands UK Ltd.) in TTBS (Tris-sodium chloride (20mM (24.22g) Tris Base and 500mM (292.2g) sodium chloride in distilled water) with pH corrected to 7.5 with concentrated HCl made up to 10l volume with distilled water) mixed with 0.2% Tween 20) in order to block any remaining binding sites on the membrane. The membrane was further incubated in this solution for 30min, with shaking at room temperature, to ensure even blocking before the blocking solution was discarded and the membrane washed twice with TTBS. The membrane was then incubated whilst shaking at room temperature, with the primary antibody in appropriate dilution in normal rabbit serum to establish non-specific binding. The primary antibody was diluted in 3% (w/v) dried non-fat milk solution made with Marvel and TTBS. The membrane was then washed again in TTBS for 3X10 minutes, whilst shaking before adding the secondary antibody (HRP conjugated swine anti-rabbit immunoglobulin (PO217; Dako Ltd.) diluted 1:1000 in 3% (w/v) Marvel in TTBS). The incubation with the secondary antibody was performed for 1 hour, whilst shaking at room temperature. The secondary antibody solution was discarded, the membrane washed whilst shaking at room temperature for 4X 15 minutes and then with TBS for 30min whilst shaking at room

temperature. The final step was incubation in TBS for 45min, at room temperature without shaking.

2.4.3.2.2.7 Detection of Chemiluminescence

The membrane was incubated in working HRP substrate prepared by mixing equal volumes of Luminol reagents and Peroxide solution (Reagents A and B of Chemiluminescent HRP substrate Immunobilon™ Western (Millipore Corporation, Billerica, U.S.A)). The HRP substrate was left to reach room temperature for 10min and then the membrane was incubated with it for 5 minutes. The excess substrate was drained off and the membrane covered in clean plastic wrap.

The membrane was exposed in a CCD camera (Fuji, Luminescent Image Analyser LAS-1000) for 5minutes. Longer exposure time was used, if required to visualise the bands. Approximate sizes of the visualised bands were calculated using regression analysis of the molecular weight markers. Densitometry was performed on the visualised bands using Aida software (Aida Image Analyzer version 4.15.025 (Raytest Isotopenmessgeräte GmbH, Straubenhardt, Germany) to estimate the relative abundance of the proteins studied.

2.4.3.3 Immunohistochemistry

Histology is the study of structure of cells and their formation into tissues and organs. Immunohistochemistry (IHC) is a combination of anatomical, immunological and biochemical techniques for detection of specific antigens (e.g. proteins) in cells of a tissue section. It enables visualisation of the distribution of specific antigens in the proper tissue context.

2.4.3.3.1 Sample preparation for IHC

2.4.3.3.1.1 Principles of IHC sample preparation

2.4.3.3.1.1.1 Tissue fixation

Tissue samples for IHC must be rapidly preserved to prevent breakdown of the cellular proteins and tissue architecture. Neutral buffered formalin (10%) which contains 4% formaldehyde induces cross-links between proteins, or between proteins and nucleic acids, involving hydroxymethylene bridges. This enables the proteins to retain their secondary structures (Werner et al. 2000).

2.4.3.3.1.1.2 Tissue embedding

To maintain the natural shape and architecture of the tissue sample during long term storage and sectioning, the formalin fixed samples are embedded in paraffin. The tissue is first dehydrated by graded alcohol solutions, washed with a clearing agent such as xylene and then embedded in warm paraffin.

2.4.3.3.1.1.3 Sectioning and Mounting

Formalin fixed-paraffin embedded tissue samples need to be sectioned into 5-8µm and mounted onto glass slides. Pre-treatment of the slides with adhesives such as 3-aminopropyltriethoxysilane (APTS) or poly-L-lysine allows the tissue to couple and adhere to the slide surface especially dried in an oven.

2.4.3.3.1.1.2 Procedure of IHC sample preparation

Tissue samples from each human participant was removed during cardiac surgery and immediately immersed in 10% formalin (10% v/v formaldehyde in 0.9% w/v sodium chloride (Fischer Scientific) solution). Samples from sheep were also preserved similarly. The samples were allowed to remain immersed in this solution for at least 48 hours to enable appropriate tissue fixation. Samples were trimmed and loaded into a Histosette II (Simport, Quebec, Canada) 30mm X 20mm X 5mm cassettes and processed through six stages of ethanol dehydration followed by three stages of xylene for ethanol removal. The samples were then embedded in paraffin wax at 60°C by the Shandon Excelsior™ tissue wax processor (Thermo Scientific). The wax was allowed to set overnight.

Tissue sections of 5µm were cut from the formalin-fixed, paraffin embedded samples using a sledge microtome (Anglia Scientific, Cambridge, UK). The sections were rinsed in 70% ethanol, de-wrinkled

by floating in warm water (45°C) and mounted on to Superfrost™ Plus slides (Menzel-Gläser Inc, Braunschweig, Germany). The slides were dried on a heat rack for 15 minutes and incubated at 37°C in a drying oven for 24 hours.

2.4.3.3.2 IHC staining

2.4.3.3.2.1 Principles of IHC staining

2.4.3.3.2.1.1 Epitope (Antigen) recovery

The paraffin must be completely removed from the sections to allow the antibodies to reach the antigen. Organic solvents such as xylene can dissolve and remove the paraffin. Further to this, methylene bridges produced during formaldehyde fixation can also mask antigen presentation and interrupt antibody binding. These can be removed by heat treatment (heat-induced epitope retrieval (HEIR)).

2.4.3.3.2.1.2 Quenching

Staining procedures depend on biotin, peroxidises and/or phosphatases and hence these proteins have to be masked (or quenched) to prevent false positive or high background detection. This can be achieved by chemically inhibiting all enzymatic activity.

2.4.3.3.2.1.3 Blocking nonspecific sites

Nonspecific binding to antibody to random proteins in the sample causes high background staining and masks target antigen detection.

Blocking of reactive sites to which primary and secondary antibodies may otherwise bind by incubating the tissue sections in buffer solutions such as normal serum, non-fat dry milk or bovine serum albumen can prevent non-specific antibody binding.

2.4.3.3.2.1.4 Immunodetection

Antibody-mediated antigen detection can be direct or indirect. In the direct method, the antibody specific to the target antigen is conjugated with signalling markers such as fluorescent dyes or enzymes which then signal the binding of the labelled antibody to specific tissue sites. In the indirect method, the target antigen specific primary antibody first binds to the protein on the tissue section. The section is then washed and treated with a labelled secondary antibody such as one conjugated with horseradish peroxidase (HRP) enzyme which develops a brown precipitate in the presence of 3,3 diaminobenzidine (DAB), a chromogenic substance, through catalytic conversion.

2.4.3.3.2.1.5 Counterstaining

In the final step, the tissue section is counterstained to provide contrast to the primary stain and allow easier visualisation of the tissue architecture and antibody uptake.

2.4.3.3.2.2 Procedure for IHC staining

Two slides per participant and a negative control were labelled with a random identifier and loaded into the Leica BondMax™ IHC slide processor (Leica Microsystem, Wetzlar, Germany) and run on the automated software programme (Vision Biosystems Bond Version 3.4A) using bond polymer refine detection reagents (Leica Microsystem, Wetzlar, Germany).

In this protocol, slides were first treated with xylene for one minute followed by a one minute ethanol wash, incubation at 95°C with an epitope retrieval solution and treatment with peroxide block for 5 minutes at room temperature. All the samples (excluding the negative controls) were then treated with 150µl of pre-optimised primary rabbit polyclonal antibody to UCP1 (ab10983, Abcam, Cambridge, UK) diluted to 1:500 for 30 minutes. The sections were then exposed to 150µl of HRP conjugated secondary anti-mouse and anti-rabbit antibody for eight minutes followed by treatment with 3,3 DAB for 10 minutes to allow for brown precipitation to develop. The sections were then counterstained with Harris' haematoxylin for 5 minutes. Between each of the above mentioned steps, the sections were washed with Bondwash buffer and distilled water. Tissue sections were mounted with coverslips using DPX mounting medium and dried overnight.

Immunostaining was detected using the EnVision+ System (HRP-DAB-rabbit) (Dako, Ely, UK) with appropriate controls undertaken in the

absence of the primary antibody. Sections were imaged using a Nikon Eclipse 90i microscope with charge - coupled device high-speed colour camera (Micropublisher 3.3RTV; QImaging, Surrey, BC, Canada) using Velocity 5 software (Improvision, Coventy, UK). Sections were visualised at 10X, 20X and 40X magnifications and photographed at 20X and 40X magnifications for analysis of 10 random areas. A previously manually validated technique on Volocity imaging software was used to calculate the positive stained cell percentage, normalised against total cell number.

2.4.3.3.3 Antibodies used for immunohistochemistry

Immunohistochemistry for ovine tissue was performed using a UCP1 primary antibody raised against ovine UCP1 at a dilution of 1:750 as described by Pope et al. (Pope et al. 2014).

All human adipose tissue samples for immunohistochemistry (excluding the negative controls) were treated 1:500 dilution of pre-optimised primary rabbit polyclonal antibody to UCP1 (ab10983, Abcam, Cambridge, UK).

2.4.4 Statistical analysis

Each individual sample was run in duplicate and, before any statistical analysis, coefficient of variance between the duplicates was calculated using Microsoft Office Excel 2010 (Microsoft Corporation, Berkshire, UK). A coefficient of variation of <5% was accepted as supporting the reproducibility of the respective assay and data points that were within this limit of variability were accepted for further statistical analysis.

Statistical analysis was performed using IBM SPSS Statistics v.22.0 statistical software for Windows package (IBM Corporation, NY, USA). All data were subjected to the Kolmogorov-Smirnov normality test for determining if their distribution was parametric or non-parametric. In this test, a p value of ≥ 0.05 indicates that the data are normally distributed. Comparisons between comparable groups were made using the analysis of variance (ANOVA) for data that were normally distributed or Kruskal-Wallis one-way analysis of variance for non-parametric data, with multiple group post hoc Bonferroni or Dunn's correction tests applied respectively. Correlation between gene expression and protein concentration for UCP1 and gene expression, UCP1 abundance and other biological parameters were determined by calculating the correlation coefficients and linear regression analysis.

The software GraphPad Prism v 5.00 (GraphPad Software, California, USA) is used to produce all statistical graphs and data are presented as mean \pm standard error of mean (SEM).

The anthropometric assessments of participants was performed using the Emergency Nutrition Assessment Tool (Erhardt and Pollgorm 2011) and the World Health Organisation (WHO) Anthro (version 3.2.2, January 2011).

Statistical analysis for initial quality control of labelling and hybridisation, as well as data analysis of the microarray results were conducted using the Partek software (Partek Inc., St. Louis, USA).

Further details of statistical analysis will be included in the individual sections, where relevant.

3 Effect of maternal nutrient restriction on UCP1 and other BAT associated genes in pericardial adipose tissue of newborn sheep

The work described in this chapter has been published (Ojha et al. 2013). The article is included in Appendix 10.4.1.

3.1 Introduction

In the newborn, BAT is essential for thermoregulation and its function is critical for survival. In a post-mortem study of 20 infants with gestation age between 28 to 42 weeks, Aherne and Hull described the anatomical distribution of BAT in newborn infants. They found BAT depots on the back, between the scapulae, in the posterior triangle of the neck and around the neck muscles extending under the clavicle into the axillae, in islands around the trachea, oesophagus and the large vessels in the mediastinum and around the suprarenal glands and the kidneys in the abdomen (Aherne and Hull 1964). In addition to these classically described depots, it has recently been recognised that BAT is also present in other locations.

The presence of BAT around the heart of human adults has been suggested by the presence of BAT-specific UCP1 gene expression in epicardial fat (Sacks et al. 2009). Cardiac natriuretic peptides increase the expression of UCP1 and the transcription co-regulator PGC1 α and

induce mitochondriogenesis in adipocytes (Bordicchia et al. 2012). It has been postulated that brown adipocytes present in the vicinity of the heart may protect it from hypothermia (Sacks et al. 2009) and metabolic stresses (Festuccia et al. 2011). The exact role of BAT around the heart is unclear and there are currently no studies of BAT in pericardial depot of newborn infants or of BAT development in this depot in the perinatal period.

In the sheep, in perirenal adipose tissue, UCP1 appears around mid-gestation (Clarke et al. 1997) and, thereafter, its expression increases up to term gestation before rapidly declining after birth so that it is undetectable by the end of the first month of life (Finn et al. 1998). Maternal nutrition affects both gene expression and abundance of uncoupling protein in the offspring. Late gestation maternal nutrient restriction downregulates UCP1 gene expression but protein abundance in the perirenal depot is not affected (Budge et al. 2004). Increase in abundance of UCP1 in the near term fetus in response to increased maternal nutrition provides further evidence of nutritional regulation of UCP1 (Budge et al. 2003). Other mitochondrial membrane proteins such as voltage dependent anion channels (VDAC) and cytochrome *c*, important for energy metabolism within the adipocytes, are also altered in response to changes in maternal nutrition (Mostyn et al. 2003).

In addition to UCP1, BAT and WAT differ in expression of several other genes such as transglutaminase 2 (TGM2) and the potassium channel, subfamily K, membrane 3 (KCNK3) which are nearly 4 times higher in human BAT than in WAT (Svensson et al. 2011). Other transcription factors such as PGC1 α are specifically involved in brown adipogenesis (Puigserver et al. 1998) whilst others such as adipose differentiation related protein (ADRP) and leptin are predominantly expressed in WAT (Pope et al. 2013). Type 3 β adrenergic receptors (β 3ADR) are the predominant adrenergic receptor involved in the process of NST in brown adipocytes (Festuccia et al. 2009). In conjunction with sympathetic stimuli, thyroid hormones are a major regulator of brown adipocyte function. The enzyme type 2 iodothyronine deiodinase (DIO2) catalyses the conversion of T4 to T3; T3 is ten times more active than T4 and the intracellular conversion of T4 into T3 within brown adipocytes produces high intracellular T3 levels which saturate thyroid hormone receptors and induce a rapid increase in UCP1 gene expression and protein synthesis (Bianco and Silva 1987).

3.1.1 Hypothesis and aim

As described in Section 1.12.1, the hypothesis for this study is: given that UCP1 gene is expressed in epicardial depot of adult humans (Sacks et al. 2009), I hypothesised that BAT is present in pericardial adipose tissue in newborn sheep.

3.2 Methods

This study was undertaken at the University of Nottingham, United Kingdom. Animal procedures were performed by Dr Sarah Pearce. Animal study protocols were designed in accordance with the Animals (Scientific Procedures) Act, 1986 under Home Office supervision. Tissue analysis was performed in the laboratories of Academic Child Health, University of Nottingham.

3.2.1 Experimental design

The experimental design for this study (as described in Chapter 2, (Section 2.2.1)) is summarised in Figure 3.1.

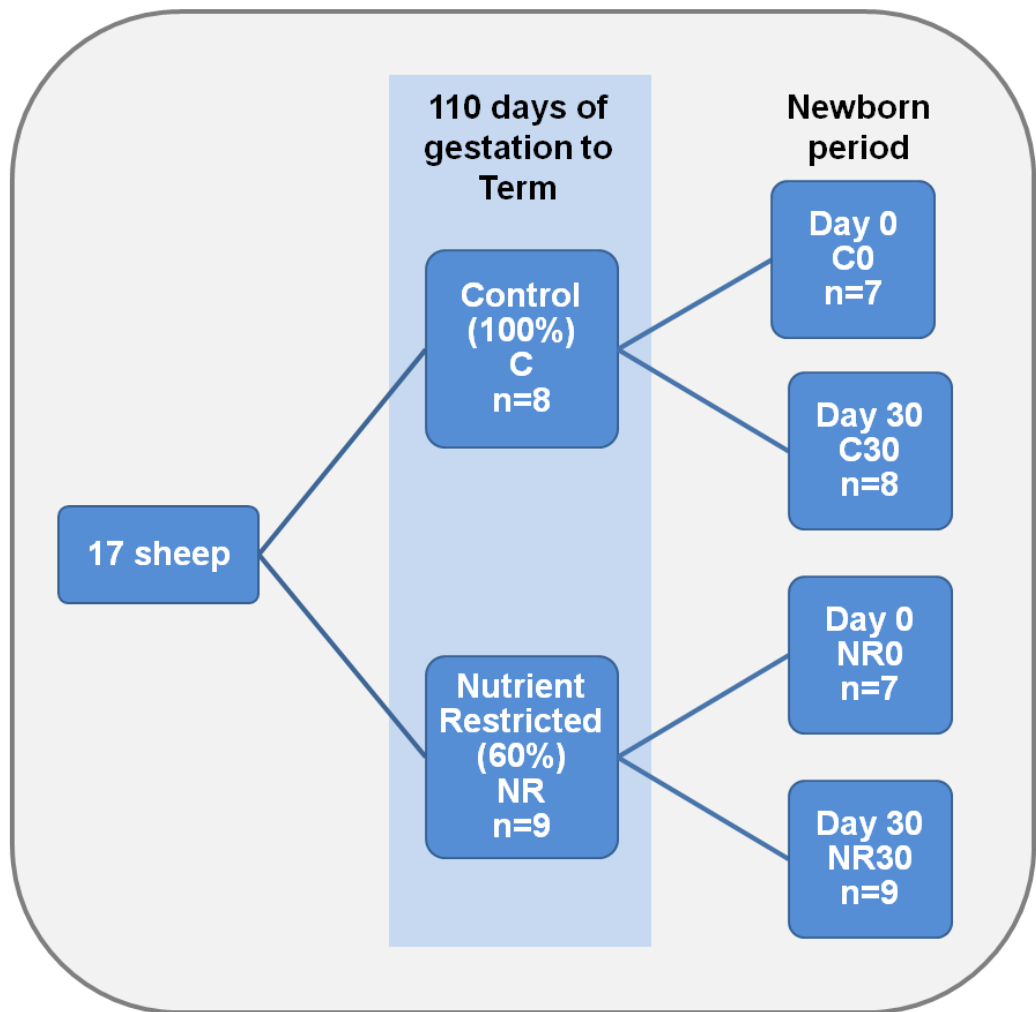


Figure 3.1. Experimental study design for Chapter 3

C: control (100% of normal energy requirements); NR: nutrient restricted (60% of normal energy requirements); Day 0: samples taken at 6 hours of age; Day 30: samples taken at 30 days of age. Three animals between C0 and NR0 groups expired during the experimental procedure.

3.2.2 Laboratory procedures

A complete description of the methods used in this study is located in Chapter 2 (Section 2.4).

The Q-PCR for PGC1 α and adiponectin were initially performed by Miss Momina Yazdani (Medical Student, University of Nottingham) under my supervision and were later repeated by myself, confirming Miss Yazdani's findings. The Q-PCR for PRDM16 and DIO2 was performed by Dr Lindsay Robinson.

3.2.2.1 mRNA detection

Total RNA was extracted from 500 mg of sheep pericardial adipose tissue using Tri-Reagent (Sigma Chemical Co, Poole, UK) followed by purification with an RNeasy Plus kit (Qiagen, West Sussex, UK). To verify the quantity and quality of total RNA extracted, spectrophotometric analysis (Nanodrop; Thermo Scientific, Wilmington, DE) was performed. For each sample, 2 μ g of RNA was reverse transcribed (RT) using reverse transcriptase and a Touchgene thermocycler (Techne; Barloworld Scientific, Stone UK). cDNA was synthesized from 2 μ g of RNA by reverse transcription in accordance with the manufacturer's protocol (High Capacity RNA to cDNA kit, Applied Biosystems, Warrington, UK). For each RT analysis, appropriate negative controls were included to ensure there was no

genomic DNA contamination. All cDNA was stored at -20°C until further analysis.

For each gene, a standard curve was generated to ensure uniformity, efficiency, and accuracy for each 96-well plate. DNA for the standard curve was made after DNA extraction (QIA quick gel extraction kit 28704; Quigen, Crawley, UK) of the final product of PCR and run with 2% agarose gel electrophoresis. In addition, correct product validation of all primers was confirmed by product size on gel electrophoresis and, when necessary, gene sequencing was performed with the results checked against known sequences on the GenBank Database.

To establish mRNA abundance, qPCR was performed using a 10- μl reaction consisting of 3 μl of cDNA, 5 μl of Fast SYBR Green Master Mix (Applied Biosystems), and 1 μl of forward and reverse ovine-specific oligonucleotide primers (Sigma–Aldrich, Gillingham, UK). The primer sequences are given in Table 2.1. The samples were run in duplicate and included a negative control and 10-fold dilution standard curve for standardization. qPCR was performed using the Step One Plus real-time PCR thermocycler (Applied Biosystems). Results were excluded and experimental analysis was repeated if the standard curve analysis demonstrated an efficiency of $<90\%$. Data were analysed using 18S mRNA as a housekeeping gene for the normalization of mRNA

expression and the $2^{-\Delta Ct}$ method and expressed as a ratio of the mean gene expression of day 0 control animals.

3.2.2.2 Protein Analysis

Mitochondria were prepared from 1 g of pericardial adipose tissue from each animal as described in Chapter 2, Section 2.4.3 and protein content was determined by bicinchoninic acid assay. The abundances of UCP1, VDAC, and cytochrome *c* were determined by western blotting using UCP1 and VDAC antibodies and cytochrome *c* antibody ((H-104); SC-7159 (Santa Cruz Biotechnology, Santa Cruz, CA)) at a dilution of 1 to 1,000. Specificity of the detection was confirmed using nonimmune rabbit serum and a range of molecular weight markers was included on all gels. Densitometry analysis was performed on all membranes following image detection using a Fujifilm LAS-1000 cooled CCD camera (Fuji Photo Film, Tokyo, Japan) and results were expressed in arbitrary units. All gels were run in duplicate and a reference sample and negative control (from either hepatic or adipose tissue of the same 6-h-old control lamb) was included on each gel to allow comparison between groups. The membrane was exposed in a CCD camera (Fuji Luminescent Image Analyser LAS-1000). Densitometry was performed on the visualized bands using Aida software (Aida Image Analyzer version 4.15.025 (Raytest Isotopenmessgerate GmbH, Straubenhardt, Germany) to determine the relative abundance of the proteins studied. Data were analyzed

following densitometry and expressed as a ratio of the mean gene expression of day 0 control animals.

3.2.3 Statistical Analysis

All data are presented as means \pm SEM and statistical significance was set at $p < 0.05$. Data were assessed for normality using the Kolmogorov–Smirnov test followed by appropriate parametric or nonparametric analyses. An independent Student’s test or Mann–Whitney test was used to assess both the effect of age and the maternal diet as appropriate. All data were analysed using PASW software (version 22; IBM, Chicago, IL).

3.3 Results

3.3.1 Whole body, heart and adipose tissue weights and adipose tissue composition

There was a significant increase in total body weight, heart weight and absolute and relative pericardial adipose tissue weights between day 0 and 30. However, there was no difference between offspring of control and nutrient restricted mothers at either age (Table 3.1). A significant reduction in total protein and mitochondrial protein content occurred between day 0 and 30 but there was no effect of maternal diet in late gestation at either age.

Table 3.1. Mean total body weight, pericardial adipose tissue and heart weights and total protein and total mitochondrial protein contents of pericardial adipose tissue (relative to protein content of control group) in offspring of control and nutrient restricted mothers at Day 0 and Day 30 life.

	C0 (n=7)	NR0 (n=7)	C30 (n=8)	NR30 (n=9)
Body Weight (kg)	4.46±0.34 ^a	4.26±0.16 ^b	15.59±0.77 ^c	14.84±0.55 ^d
Total pericardial adipose tissue weight (g)	4.61±0.43 ^e	4.01±0.33 ^f	97.28±11.93 ^g	98.56±3.17 ^h
Pericardial adipose tissue weight relative to total body weight (g/kg)	1.05±0.94 ⁱ	0.96±0.11 ^j	6.46±0.86 ^k	6.69±0.25 ^l
Heart weight (g)	33.37±2.16	30.60±1.06	62.88±1.19	60.69±2.09
Total protein (units)	1.00±0.08	0.8±0.14	0.23±0.04	0.28±0.04
Total mitochondrial protein (units)	1.00±0.20	0.79±0.09	0.11±0.02	0.13±0.01

Pericardial adipose tissue was sampled from 6 hour (0) and 30 day (30) old lambs born to sheep that consumed either 100% (C) or 60% (NR) of total metabolisable energy requirements to maintain maternal metabolism and fetal growth between 110 days of gestation and term. Values are means ± SEM. Comparisons a versus c, b versus d, e versus g, f versus h, i versus k and j versus l, p<0.05.

3.3.2 Mitochondrial proteins in the newborn and effect of maternal nutrient restriction

Both UCP1 and cytochrome *c* were significantly reduced in offspring born to nutrient restricted mothers at day 0, but not day 30, as the abundance of both these proteins declined with postnatal age to basal values irrespective of maternal diet in pregnancy. In contrast, the abundance of VDAC was unaffected by either postnatal age and/or maternal diet (Figure 3.2).

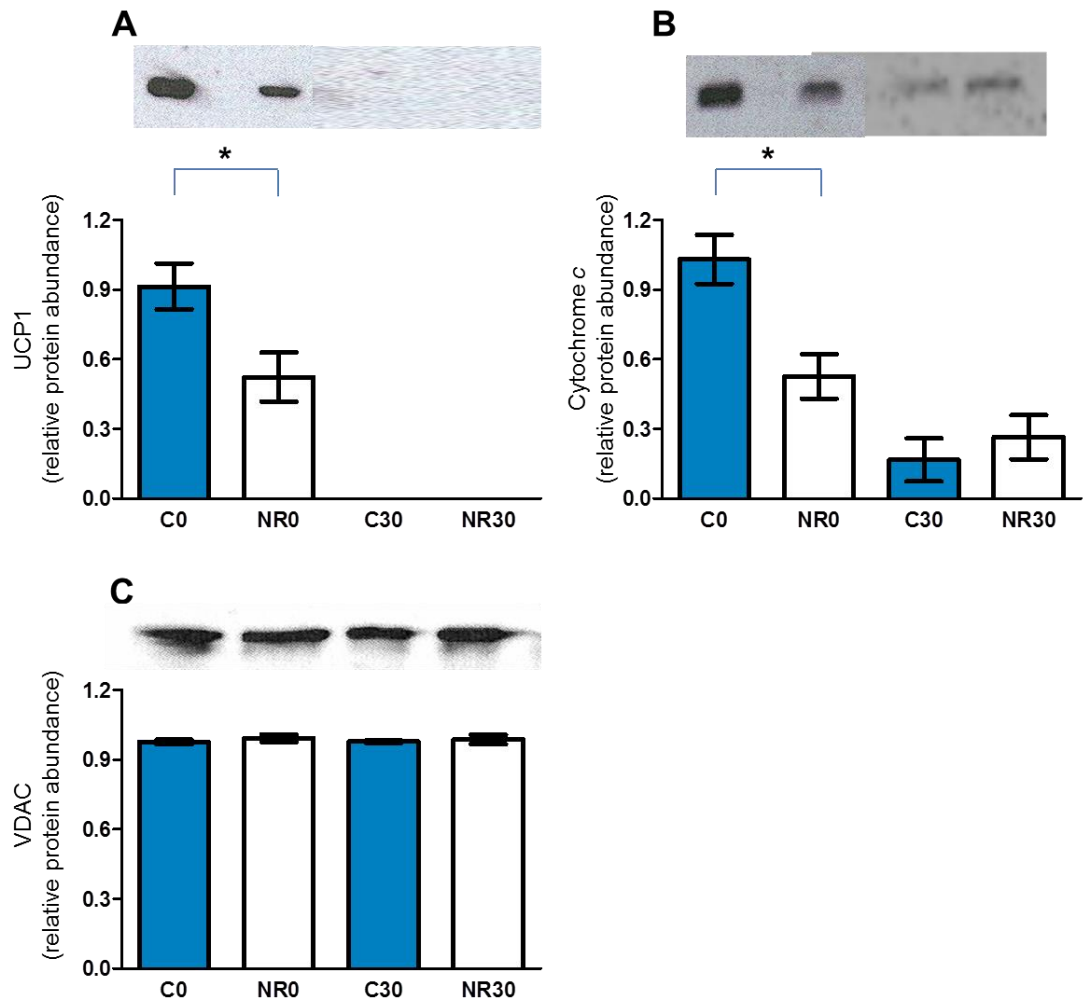


Figure 3.2 A: UCP1, B: cytochrome c and C: VDAC protein abundance in pericardial adipose tissue of sheep in early postnatal life and the effect of maternal nutrient restriction in late gestation

Pericardial adipose tissue was sampled from newborn, 0 (0) and 30 day old (30) lambs born to sheep that consumed either 100% (C) or 60% (NR) of total metabolisable energy requirements to maintain maternal metabolism and fetal growth between 110 days of gestation and term. UCP1 was not detected at 30 days in either nutritional group.

UCP1 was not detectable in the pericardial adipose tissue of offspring of control and nutrient restricted sheep at day 30 (C30 and NR30 in A).

Values are means \pm SEM; n=7-9 per group. * p <0.05

UCP1: uncoupling protein 1; VDAC: voltage dependent anion channel

3.3.3 Effect of maternal nutrient restriction on BAT related genes

Gene expression of UCP1 declined with age but was unaffected by maternal diet (Figure 3.3) Genes that are known to be highly expressed in human BAT, TGM2 and KCNK3, mRNA expression was significantly reduced in offspring born to nutrient restricted mothers on day 0 and was further reduced with age, irrespective of maternal diet (Figure 3.3). Gene expression for the prolactin receptor (PRLR) decreased with age but was also unaffected by maternal diet (Figure 3.3) similar to the expression of the UCP1 gene.

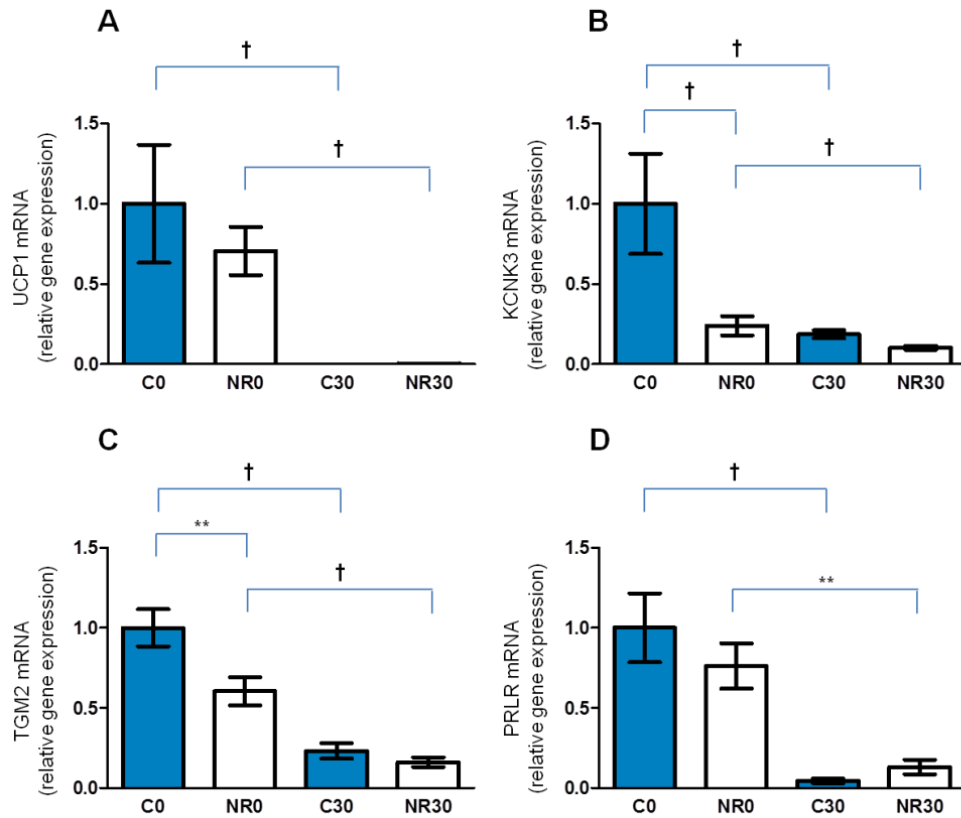


Figure 3.3. Gene expression of A: UCP1, B: KCNK3, C: TGM2 and D: prolactin receptor (PRLR) in pericardial adipose tissue of sheep in early postnatal life and the effect of maternal nutrient restriction in late gestation

Pericardial adipose tissue was sampled from 6 hours (0) and 30 day (30) old lambs born to sheep that consumed either 100% (C) or 60% (NR) of total metabolisable energy requirements to maintain maternal metabolism and fetal growth between 110 days of gestation and term. UCP1 gene expression was very low at 30 days in both nutritional groups.

UCP1 gene expression was detectable but extremely low in the pericardial adipose tissue of offspring of control and nutrient restricted sheep at day 30 (C30 and NR30 in A).

Values are means \pm SEM; n=7-9 per group. *p<0.05, **p<0.01, † p<0.001

UCP1: uncoupling protein 1; KCNK3: potassium channel, subfamily K, member 3; TGM2: transglutaminase 2; PRLR: prolactin receptor

3.3.4 Effect of maternal nutrient restriction on BAT related transcription factors

There was no change in the expression of bone morphogenetic protein (BMP)7, PRDM16 and PPAR γ while the transcription factor PGC1 α reduced with age but was unaffected by maternal nutrition (Figure 3.4).

The gene expression of BMP7 (Figure 3.4) showed a trend of being downregulated by maternal nutrient restriction, but the differences were not significant statistically as the Kruskal-Wallis one-way analysis of variance produced a p value of 0.35.

In the analysis of the results for the gene PGC1 α , one sample was excluded. The Q-PCR efficiency for this reaction was 98% and the R² was 0.99. The maximum coefficient of variation for any sample on the plate was 2.7%. Despite these, one sample appeared anomalous with C_t value much higher than two standard deviations over the mean for the group. This sample was, therefore, considered to be an outlier and not included in the statistical analysis.

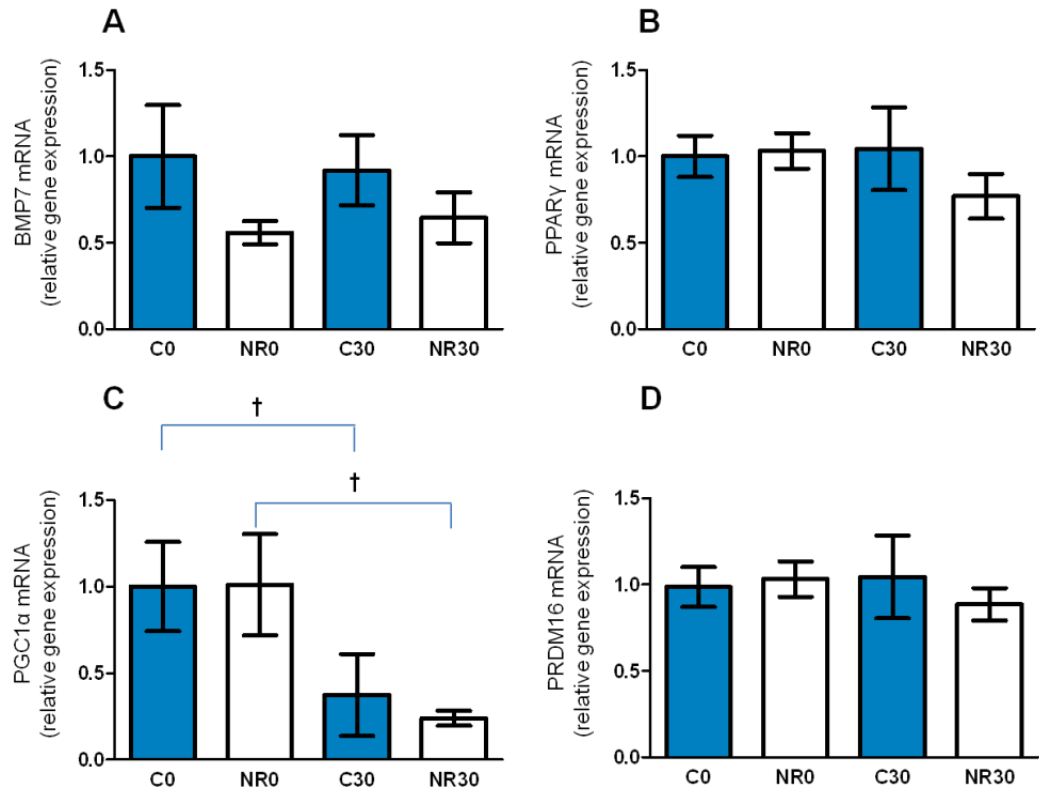


Figure 3.4. Gene expression of A: BMP7, B: PPAR γ , C: PGC1 α and D: PRDM16 receptor in pericardial adipose tissue of sheep in early postnatal life and the effect of maternal nutrient restriction in late gestation

Pericardial adipose tissue was sampled from 6 hours (0) and 30 day (30) old lambs born to sheep that consumed either 100% (C) or 60% (NR) of total metabolisable energy requirements to maintain maternal metabolism and fetal growth between 110 days of gestation and term. Values are means \pm SEM; n=7-9 per group. *p<0.05, **p<0.01, †p<0.001

BMP: bone morphogenetic protein; PPAR: peroxisome proliferator-activated receptor; PGC: PPAR co-activator; PRDM: PR (PRD1-BF1-RIZ1 homologous)-domain containing protein

3.3.5 Effect of maternal nutrient restriction on WAT related genes and adipokines

The gene expression of HOXc9 was not affected by maternal nutrient restriction and did not change with age (Figure 3.5). The expression demonstrated a tendency to be increased with maternal nutrient restriction at both Day 0 and Day 30 but the differences were not significant statistically (p value for Kruskal-Wallis one-way analysis of variance was 0.319). In this analysis, one sample was excluded. The Q-PCR efficiency for this reaction was 99% and the R^2 was 1. The maximum coefficient of variation for any sample on the plate was 4.4%. Despite these, the C_t value for one sample was higher than two standard deviations over the mean of its group. This sample was, therefore, considered to be an outlier and excluded from the analysis. The statistical analysis was repeated including this sample and this did not change the significance of the differences between the groups.

Gene expression of the co-repressor Receptor Interacting Protein (RIP) 140 was also unaffected by maternal nutrition. Further, the expression of this gene did not change significantly with age in the offspring of control mothers; however, in the offspring of nutrient restricted mothers, the expression of RIP140 was significantly higher at 30 days than at 6 hours of age (Figure 3.5).

Leptin expression increased with age in offspring of both control and nutrient restricted mothers but was not affected by nutrient restriction. Gene expression of adiponectin did not change with age. In offspring of nutrient restricted mothers, mRNA expression for adiponectin was significantly higher at Day 0 but at Day 30 this difference did not reach statistical significance among the offspring of control mothers.

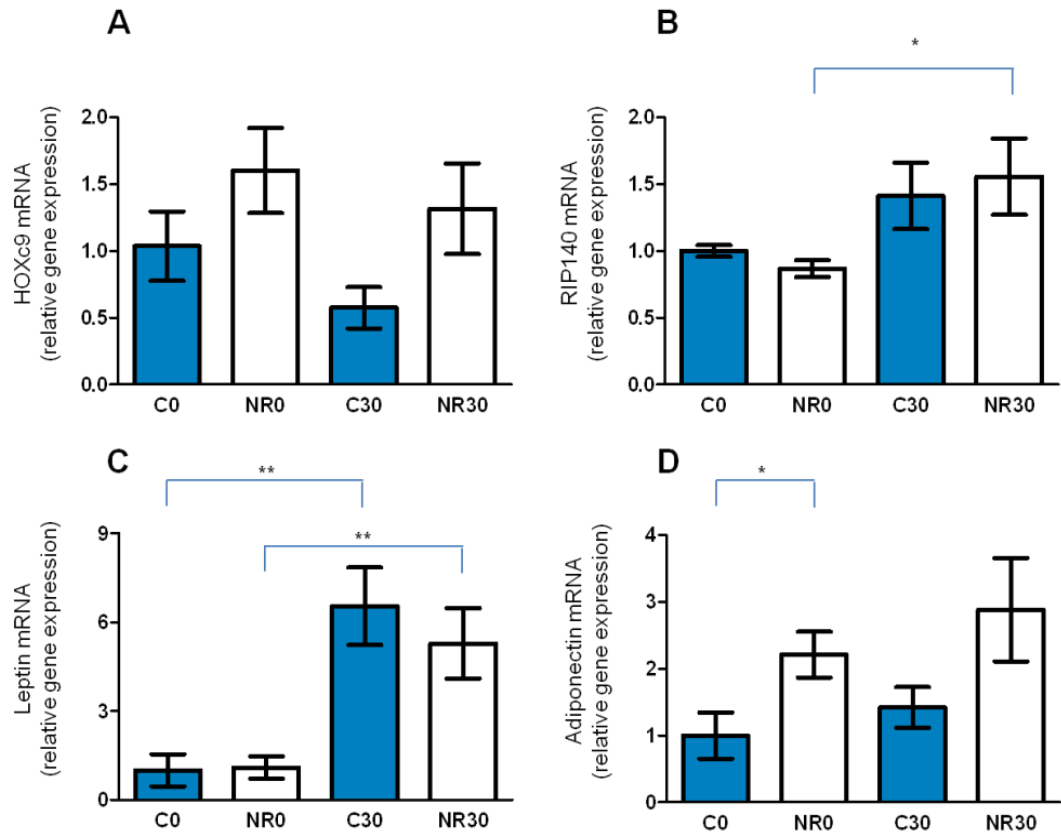


Figure 3.5. Gene expression of A: HOXc9, B: RIP140, C: leptin and D: adiponectin in pericardial adipose tissue of sheep in early postnatal life and the effect of maternal nutrient restriction in late gestation

Pericardial adipose tissue was sampled from 6 hours (0) and 30 day (30) old lambs born to sheep that consumed either 100% (C) or 60% (NR) of total metabolisable energy requirements to maintain maternal metabolism and fetal growth between 110 days of gestation and term. Values are means \pm SEM; n=7-9 per group. *p<0.05, **p<0.01, †p<0.001

HoX: homobox; RIP: receptor interacting protein

3.3.6 Effect of maternal nutrient restriction on β adrenergic receptors and type 2 iodothyronine deiodenase gene

Gene expression of type 1 β adrenergic receptors (β 1ADR) was not affected by age or maternal nutrient restriction (Figure 3.6). Gene expression of type 2 β adrenergic receptor (β 2ADR) increased significantly with age in offspring of both control and nutrient restricted mothers (Figure 3.6). In contrast, gene expression of β 3ADR was downregulated in offspring of nutrient restricted mothers both at Day 0 and at Day 30 (Figure 3.6).

The gene expression of type 2 iodothyronine deiodenase (DIO2) which converts T4 to T3 was also affected by maternal nutrition as it was lower in offspring of nutrient restricted mothers at Day 0 but not at Day 30 (Figure 3.6).

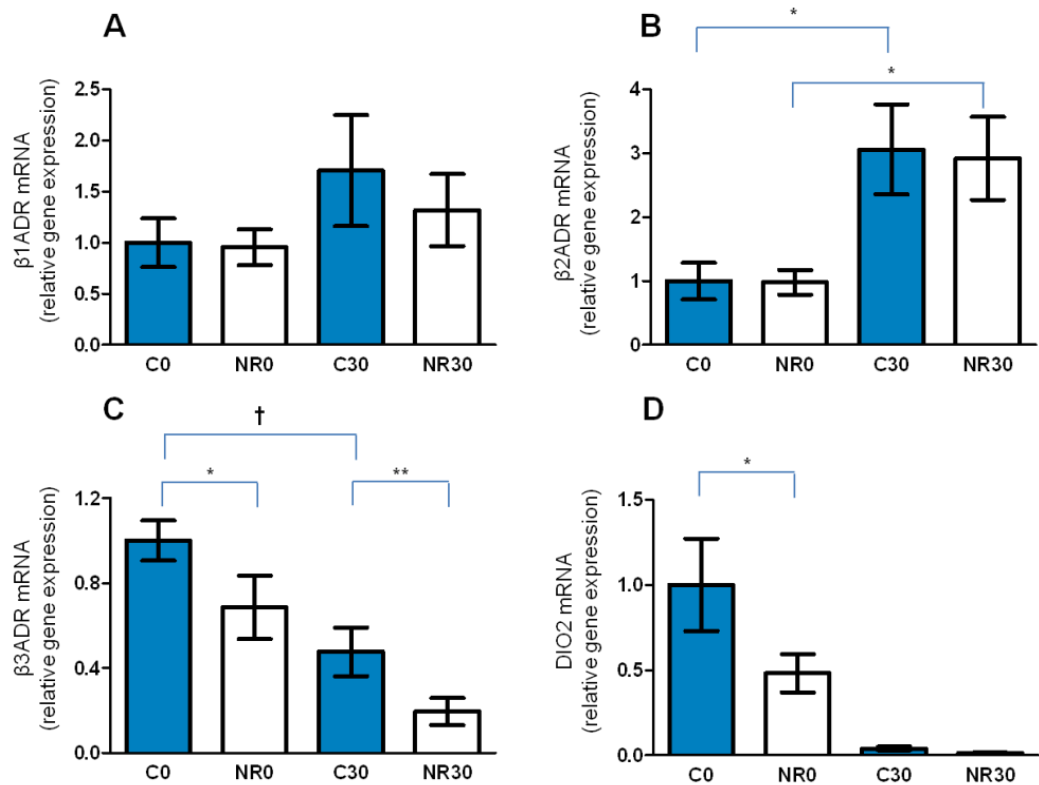


Figure 3.6. Gene expression of A: β1ADR, B: β2ADR, C: β3ADR and D: DIO2 in pericardial adipose tissue of sheep in early postnatal life and the effect of maternal nutrient restriction in late gestation

Pericardial adipose tissue was sampled from 6 hours (0) and 30 day (30) old lambs born to sheep that consumed either 100% (C) or 60% (NR) of total metabolisable energy requirements to maintain maternal metabolism and fetal growth between 110 days of gestation and term. Values are means ± SEM; n=7-9 per group. *p<0.05, **p<0.01, †p<0.001

β1ADR: type 1 β adrenergic receptor; β2ADR: type 2 β adrenergic receptor; β3ADR: type 3 β adrenergic receptor; DIO2: Type 2 iodothyronine deiodenase

3.3.7 Effect of maternal nutrient restriction on genes involved in glucose metabolism

The gene expression for insulin receptor (IR) was reduced in offspring of nutrient restricted mothers in the newborn offspring but not at 30 days of age (Figure 3.7). Neither the type 4 glucose transporter gene (GLUT4) nor the gene for glucocorticoid receptor (GR) was affected by maternal nutrition. In offspring of control mothers, the GR gene was increased significantly from Day 0 to Day 30 but this change did not reach statistical significance in offspring of nutrient restricted mothers (Figure 3.7).

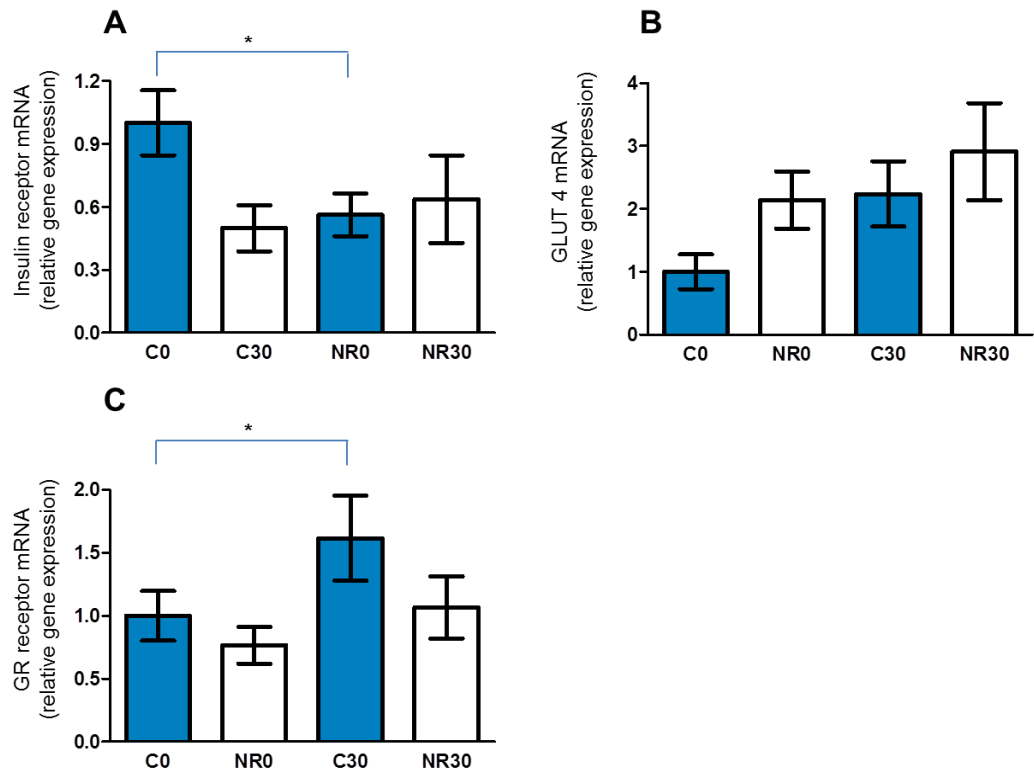


Figure 3.7 Gene expression of A: Insulin receptor, B: Glucose transporter type 4 (GLUT4), C: Glucocorticoid receptor (GR) in pericardial adipose tissue of sheep in early postnatal life and the effect of maternal nutrient restriction in late gestation

Pericardial adipose tissue was sampled from 6 hours (0) and 30 day (30) old lambs born to sheep that consumed either 100% (C) or 60% (NR) of total metabolisable energy requirements to maintain maternal metabolism and fetal growth between 110 days of gestation and term. Values are means \pm SEM; n=7-9 per group. *p<0.05, **p<0.01, †p<0.001

3.3.8 Relationship between UCP1 gene expression and protein abundance

There was no significant correlation between UCP1 gene expression and protein abundance at Day 0. The relationship was not tested at Day 30 due to absence of any detectable UCP1 in the older lambs (Figure 3.8).

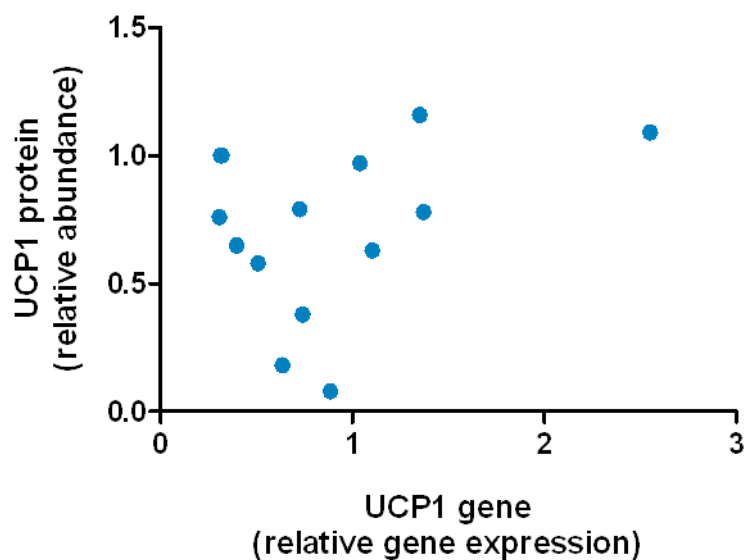


Figure 3.8 UCP1 gene expression is not correlated to protein abundance in pericardial adipose tissue of newborn lambs

Pericardial adipose tissue was sampled from 6 hour old lambs born to sheep that consumed either 100% or 60% of total metabolisable energy requirements to maintain maternal metabolism and fetal growth between 110 days of gestation and term.

UCP1: uncoupling protein1

3.4 Discussion

This study has shown, for the first time, that pericardial fat is a depot of BAT in postnatal sheep by determining the presence of mRNA and protein for the BAT-specific UCP1 (Ojha et al. 2013).

3.4.1 Pericardial adipose tissue changes from BAT to WAT in infancy

Similar to other adipose depots such as perirenal fat (Budge et al. 2004), pericardial adipose tissue changes from predominantly BAT to WAT in the early postnatal period. There is loss of UCP1 mRNA and protein and decrease in expression of BAT related genes with an increase in WAT related genes in this period.

Gene expression for UCP1 declines significantly from day 0 to day 30 and the protein is undetectable by Western blotting at 30 days. Genes such as TGM3 and KCNK3 which are known to have 4 times higher expression in human BAT than in WAT (Svensson et al. 2011) are highly expressed in sheep and their mRNA expression declines by 30 days of age, parallel to the decline in UCP1. PGC1 α also declines parallel to UCP1 but other transcription factors which regulate brown adipogenesis such as BMP7, PRDM16 and PPAR γ do not change over the first 30 days after birth. This suggests that, although brown adipocytes disappear, preadipocytes retain the potential to develop into brown adipocytes, a proposal supported by the discovery of BAT in

human adults (Cypess et al. 2009, van Marken Lichtenbelt et al. 2009, Virtanen et al. 2009) and the isolation of progenitor cells from human adult supraclavicular adipose tissue which can develop into mature brown adipocytes (Lee et al. 2011).

Gene expression of leptin, a marker of white adipocytes (Cinti et al. 1997), increases in the first 30 days of life. RIP140, a global regulator of energy balance, is highly expressed in WAT. It represses multiple metabolic pathways to reduce energy expenditure and functions as a coactivator of proinflammatory genes and macrophages (Rosell et al. 2011). In offspring of nutrient restricted mothers, RIP140 increases between day 0 and 30 while the gene expression of HOXC9 does not change in this period.

3.4.2 BAT development is modulated by maternal nutrient restriction in late gestation

In the newborn, UCP1 abundance decreases as a consequence of maternal nutrient restriction in late gestation. This is accompanied by a decline in cytochrome *c* but the abundance of VDAC remains stable. BAT has a high concentration of cytochrome *c*, a protein in the inner mitochondrial membrane which is part of the electron transport chain, and the cytochrome *c* content of BAT correlates with the high oxygen consumption in this tissue (Joel and Ball 1962). In perirenal adipose tissue and the lung, VDAC and cytochrome *c* are upregulated by

maternal nutrient restriction (Mostyn et al. 2003) and these current findings represent depot specific responses to alterations in the in utero environment.

3.4.3 Total amount of UCP1 in the pericardial depot

From a functional point of view, the truly relevant measure of the animal's thermogenic capacity is the total amount of UCP1 present in the whole animal or at least in one particular depot (Nedergaard and Cannon 2013). As changes in thermogenic capacity are not solely due to an increase or decrease in the amount of protein in the individual brown adipocyte or even per gram of BAT, but due to changes in the total amount of UCP1 in the whole BAT depot, the comparison between total UCP1 in the entire pericardial depot is the most relevant physiological parameter (Nedergaard and Cannon 2013). To calculate this, the entire depot has to be dissected and the total amount of UCP1 in it should be measured. Therefore, I have measured UCP1 in a small, randomly selected, sample taken from the dissected depot and calculated the total UCP1 by multiplying the measured value by the total amount of fat in the depot. In this study, we found that, at 6 hours of age, the total amount of UCP1 in the pericardial depot is significantly reduced in offspring of nutrient restricted mothers when compared to offspring of control mothers. This finding indicates that maternal nutrient restriction in late gestation reduces the thermogenic capacity of pericardial fat in the newborn sheep.

3.4.4 Correlation between UCP1 abundance and gene expression

As mRNA eventually translates into protein, it can be postulated that there should be some correlation between mRNA levels and protein abundance. However, in the newborn animals, UCP1 gene expression does not correlate with protein abundance. Lack of a correlation could be due to one or more reasons (Greenbaum et al. 2003). Several post-transcriptional mechanisms are involved in turning gene expression into protein abundance. These intermediary steps are not yet sufficiently understood to allow the simple computation of protein concentrations from mRNA expression. In addition, protein and mRNA have different half-lives and dramatic changes in UCP1 mRNA expression can be seen over short periods of time (Nedergaard and Cannon 2013). UCP1 mRNA has a half-life of a few hours whilst the half-life of the protein is 3-6 days (Puigserver et al. 1992). Therefore, lack of correlation between mRNA expression and protein abundance is biologically plausible even if perfect transcription to translation efficiency was present.

3.4.5 Maternal nutrient restriction affects genes controlling non-shivering thermogenesis

Importantly, this study has also demonstrated that maternal nutrient restriction in late gestation downregulates genes that control non-shivering thermogenesis, although the physiological significance of this change (i.e. the effect of altered gene expression on the thermogenic

capacity of the animal) remains to be confirmed in vivo. Offspring of nutrient restricted mothers have reduced expression of β 3ADR at birth and one month of age, whilst gene expression of DIO2 is significantly reduced in the newborn. The β 3ADR receptor promotes proliferation and differentiation of brown adipocytes, inhibits apoptosis and controls the process of non-shivering thermogenesis by upregulating fatty acid oxidation and activating DIO2 (de Jesus et al. 2001). The enzyme DIO2 is essential for optimal thermogenesis in brown adipocytes (Bianco and Silva 1987) and in its absence in mice basal UCP1 mRNA expression does not change, but the animals fail to increase their temperature on norepinephrine infusion when there is a 50% reduction in UCP1 expression (de Jesus et al. 2001). High local concentrations of T3 are essential for mitochondrial biogenesis (Klingenspor et al. 1996) and UCP1 gene expression and lipolysis are impaired in its absence (de Jesus et al. 2001). In this study, DIO2 and β 3ADR were downregulated with maternal nutrient restriction in late gestation. These, along with reduced UCP1, may be mechanisms which make the newborn less capable of modulating body temperature when challenged with cold stress, making the offspring of nutrient restricted mothers more susceptible to hypothermia.

Data from the Dutch “Hunger Winter” (the Famine of 1944-45) has shown that the timing of maternal nutrient restriction impacts upon the metabolic outcomes in the offspring (Roseboom et al. 2001). In guinea

pigs, maternal undernutrition increases the relative adiposity of the fetus and appears to preserve WAT at the expense of BAT in the interscapular depots (Kind et al. 2005). In sheep, maternal nutrient restriction in late gestation results in a 2.5 fold decrease in the abundance of UCP1 mRNA in near-term fetal adipose tissue but there is no effect on protein abundance at this stage (Budge et al. 2005). On the other hand, longer periods of nutrient restriction, extending throughout pregnancy, increase UCP1 expression in both sheep (Budge et al. 2005) and rats (Souza et al. 2012). Reduction in UCP1 when nutrition is restricted only in the late gestation may be an adaptation to conserve energy for the growth of other vital organs. This study has demonstrated that UCP1 and expression of BAT related genes are significantly reduced by maternal nutrition restriction in this period of maximal fetal growth. These changes occur in the absence of effect on birth weight, a finding that is in concordance with other studies using a similar degree of maternal nutrient restriction (Edwards and McMillen 2001). These changes in BAT related proteins and genes signify that subtle, but vital, changes in adipose tissue development can occur even when body weight is not obviously affected.

3.4.6 BAT in the pericardial depot

BAT has recently been shown to be present in pericardial adipose tissue of human adults (Sacks et al. 2009). The function of BAT around the heart in mammals is unclear, although it has been suggested that it

may serve to protect the myocardium from severe hypothermia which can precipitate potentially fatal arrhythmias (Sacks et al. 2009), have paracrine effects on cardiovascular function and act as a plasma lipid-clearing organ protecting the heart from hypertriglyceridemia (Festuccia et al. 2009). Although BAT development in pericardial adipose tissue of newborn animals is effected by maternal nutrition in late gestation, these changes do not persist as the animal grows and are not accompanied by alteration of genes predominantly expressed in WAT, indicating that the effect may be restricted to the newborn period. However, alteration of pericardial adipose tissue in older animals and humans and any long term outcomes remain to be investigated.

3.5 Conclusion

In summary, pericardial adipose tissue is a nutritionally regulated depot of BAT in newborn sheep. The depot changes from predominantly brown to white adipose tissue in the newborn period. Maternal nutrient restriction in late gestation reduces the abundance of UCP1 and downregulates other BAT related genes. Importantly, this nutritional intervention reduces the expression of β 3ADR and DIO2 which are key regulators of brown adipocyte development and non-shivering thermogenesis. BAT is present in the adipose tissue depots around the heart in human adults and I have shown that its development in early life is a target of nutritional programming.

4 Suboptimal maternal nutrition during early-to-mid gestation followed by *ad libitum* feeding in the sheep enhances pericardial adiposity in the near-term fetus

The work described in this chapter has been published (Ojha et al. 2014). The article is included in Appendix 10.4.3.

4.1 Introduction

Obesity, cardiovascular disease and type 2 diabetes are linked to inadequate fetal nutrition (Barker 1995). As discussed in Section 1.2, the link between early life environment and health in later life is described as “developmental programming” (Lucas 1991) which suggests that adverse environmental influences, such as inadequate nutrition, during these critical periods can permanently alter the structure and function of tissues and organs and these early life changes can subsequently render affected individuals more susceptible to disease in later life. Nutrition in fetal life is a central stimulus of programming for susceptibility to diseases in later life, a hypothesis that is supported by epidemiological evidence from long-term follow up of the offspring of pregnant women who suffered undernutrition during the Dutch famine of 1944-45.

The biogenesis of adipocytes comprises the differentiation of mesenchymal stem cells to committed precursor cells called preadipocytes, followed by terminal differentiation into mature adipocytes (Rosen and Spiegelman 2000). White and brown adipogenesis occur along two parallel pathways with distinct sets of transcription factors governing each process (Kajimura et al. 2010) (Figure 1.3). Genes such as bone morphogenetic protein (BMP) 7 (Tseng et al. 2008), PR (PRD1-BF1-RIZ1 homologous)-domain-containing protein (PRDM16) (Seale et al. 2007), CCAAT-enhancer binding protein (C/EBP) β (Kajimura et al. 2009), peroxisome proliferator-activated receptor γ (PPAR γ) and PPAR γ co-activator (PGC) 1 α (Fruhbeck et al. 2009) are expressed along the brown adipogenic pathway whilst another set of transcription factors including BMP4 (Schulz and Tseng 2009), adipose differentiation related protein (ADRP) and homobox (Hox) C9 (Cantile et al. 2003) are specific to white adipogenesis. The extent to which these separate processes can be reset in utero has not yet been established.

4.1.1 Hypothesis and aim

As described in Section 1.12.2, the hypothesis for this study is: in fetal sheep, suboptimal maternal nutrition between early-to-mid gestation followed by ad libitum feeding until term will increase fetal adiposity and upregulate the expression of genes which control adipogenesis.

4.2 Methods

4.2.1 Animal and diet

Animal procedures were performed by Dr Lindsay Heasman and Professor Michael Symonds. Animal protocols were designed in accordance with the Animals (Scientific Procedure) Act, 1986 under Home Office supervision as described in Chapter 2 (Section 2.1.1).

The details of the animal experiments and diet are given in Chapter 2 (Section 2.2.2) and summarised in Figure 4.1.

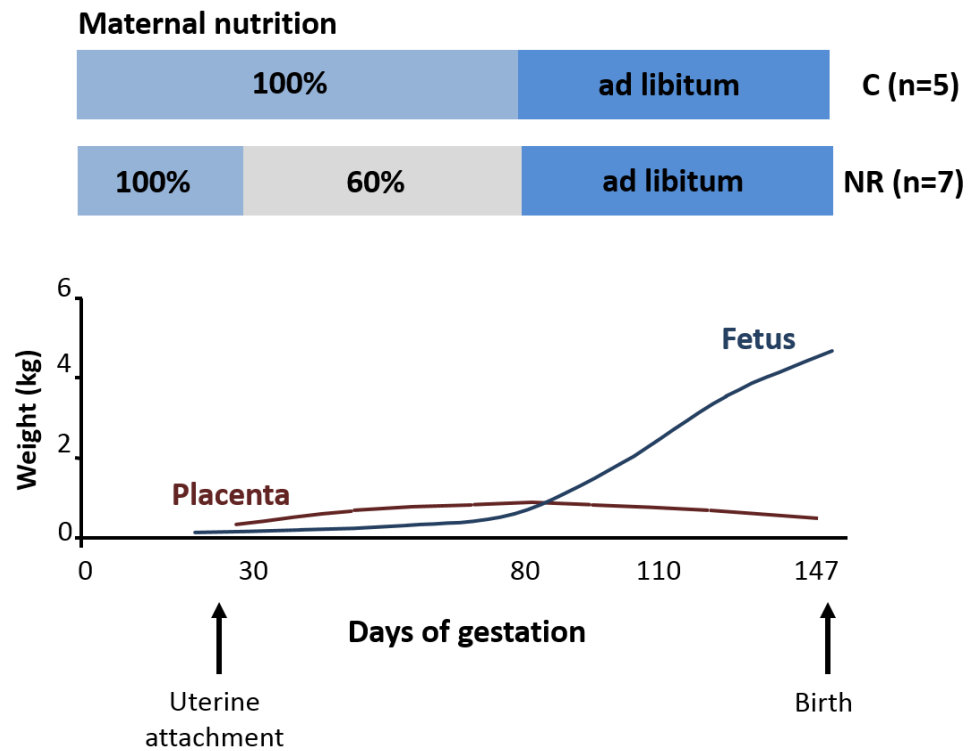


Figure 4.1 Experimental study design for Chapter 4

Filled bars represent the phases of nutritional intervention in control (C (fed 100% of total metabolisable energy requirement followed by ad libitum feeding after 80 d of gestation)) and nutrient restricted (NR (restricted to 60% of total metabolisable requirement between 28 and 80 days of gestation followed by ad libitum feeding until term gestation)). The graph depicts the growth of the fetus and the placenta from the point of placental attachment to term gestation.

4.2.2 Laboratory procedures

4.2.2.1 Histology

Adipose tissue samples were fixed in formalin and embedded in paraffin. Sections were cut at 5 μm and processed as described in Chapter 2 (Section 2.4.3.3).

4.2.2.2 Gene expression

Total RNA was extracted from 500mg of pericardial adipose tissue and processed as described in Chapter 2 (Section 2.4.1.1).

Primer sequences were designed as described in Chapter 2 (Section 2.4.1.3.3) and are given in Table 2.1.

mRNA abundance was determined by Q-PCR as described in Chapter 2 (Section 2.4.1.3). Multiple reference genes were analysed for each set and the crossing threshold values for each reference gene were processed through the geNorm software v3.5 (Primer Deisgn, Ltd, Southampton, UK). IPO8 had the most stable expression and data were analysed using IPO8 as a housekeeping gene for the normalisation of mRNA expression. The $2^{-\Delta\text{Ct}}$ method was used (Schmittgen and Livak 2008) and relative gene expression was calculated as a ratio of the mean gene expression of offspring of C mothers.

4.2.2.3 Mitochondrial protein analysis

Mitochondria were prepared from 1g of pericardial adipose tissue from each animal and processed as described in Chapter 2 (Section 2.4.1.5).

Total and mitochondrial protein content of the tissue was determined by the Bradford assay as given in Chapter 2 (Section 2.4.3.1.2). The abundance of UCP1, voltage dependent anion channel-1 (VDAC), and cytochrome c were determined by Western blotting using antibodies and procedures described in Chapter 2 (Section 2.4.3.2). Data were analysed following densitometry and expressed as a ratio of the mean protein abundance of offspring born to C animals.

4.2.3 Statistical analysis

All data are presented as means \pm standard error of mean (SEM) and statistical significance was set at $p < 0.05$. Data were assessed for normality using the Kolmogorov-Smirnov test followed by appropriate parametric or nonparametric analyses. An independent Student's T-test or Mann-Whitney test was used to assess the effect of the maternal diet as appropriate. Multiple linear regression analyses were performed to assess the associations of UCP1 gene expression and relative protein content with mother's weight, fetal weight and weight of pericardial adipose tissue. All data were analysed using PASW software (version 21; IBM, Chicago, IL).

4.3 Results

4.3.1 Whole body and adipose tissue weights and pericardial adipose tissue composition

There was no effect of the maternal dietary regime on her body weight near to term (control (C): 43.40 ± 1.24 kg; nutrient-restricted (NR): 43.37 ± 1.02 kg) or on the body weight of the fetus, although NR mothers weighed less at 80 days gestation, immediately after the period of nutritional intervention (C: 40.1 ± 1.03 ; NR: 36.4 ± 0.81 kg ($P < 0.01$)). However, the nutritionally manipulated fetuses possessed more total and pericardial fat, in both absolute and relative terms (Table 4.1).

Table 4.1. Mean total body weight, visceral and pericardial adipose tissue weights, and total protein and total mitochondrial protein contents of pericardial adipose tissue in near term fetuses born to control and nutrient-restricted mothers at 140 days of gestation.

	C (n=5)	NR (n=7)	Effect of suboptimal maternal nutrition (p-value)
Body weight (kg)	4.85 ± 0.28	4.80 ± 0.28	NS
Total visceral adipose tissue weight (g)	18 ± 0.51	22 ± 0.32	0.038
Total pericardial adipose tissue weight (g)	3.86 ± 0.38	4.95 ± 0.46	0.041
Pericardial adipose tissue weight relative to total body weight (g/kg)	0.79 ± 0.06	1.04 ± 0.10	0.040
Total protein in pericardial adipose tissue (mg/g)	3.46 ± 0.26	5.46 ± 0.80	0.067
Total mitochondrial protein in pericardial adipose tissue (mg/g)	7.90 ± 1.01	13.00 ± 1.48	0.021

Pericardial adipose tissue was sampled from 140 day gestation sheep fetuses that consumed either 100% (control, C) or 60% (nutrient-restricted, NR) of total metabolisable energy requirements to maintain metabolism and fetal growth between 28 days and 80 days of gestation. Values are means ± SEM

4.3.2 Presence of UCP1 in pericardial adipose tissue of sheep at 140 d gestation

At 140 days gestation, in pericardial adipose tissue sections, both white and brown adipocytes are clearly visible with large white adipocytes with single lipid droplets interspersed between multilocular, smaller brown adipocytes that strongly stain with UCP1 (Figure 4.2). This pericardial adipose tissue exhibited raised gene expression for UCP1, a difference that was translated into protein (as measured by Western Blotting) (Figure 4.3) and was accompanied with more mitochondrial protein (Table 4.1). Multiple regression analyses incorporating mother's body weight, fetal weight and pericardial adipose tissue weight also identified maternal nutrition group as the only significant predictor of both UCP1 gene expression and relative protein content (Table 4.2). The abundance of the outer mitochondrial protein VDAC (C: 0.94 ± 0.04 ; NR: 0.97 ± 0.04 arbitrary units (a.u.)) and cytochrome c (C: 0.92 ± 0.04 ; NR: 1.02 ± 0.08 a.u.) were both unaffected by maternal diet.

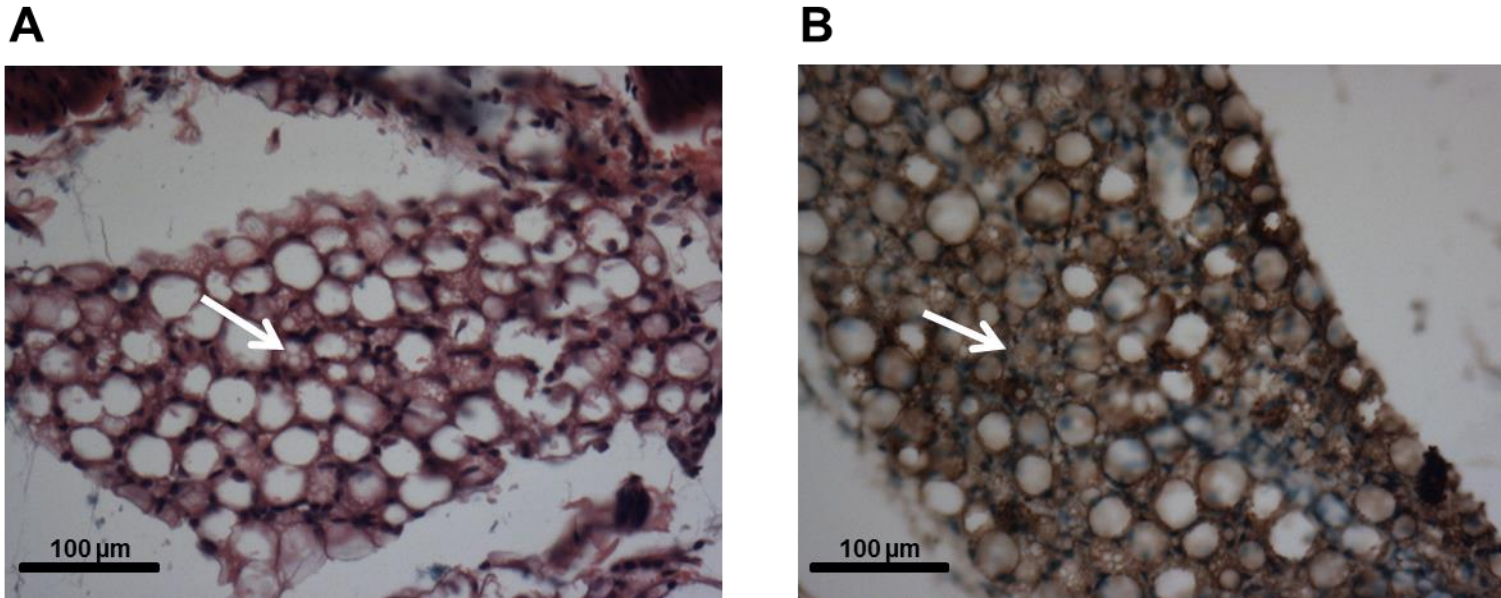


Figure 4.2 Representative images of pericardial adipose tissue structure at 140 day gestation in fetal sheep

Histological sections stained for immunohistochemical detection of uncoupling protein 1 (UCP1): antibody negative (A) and antibody positive (B) showing the presence of small multilocular adipocytes (indicated by white arrows). These multilocular adipocytes stained positive for UCP1 (B) demonstrating that these are brown adipocytes and the depot is brown fat

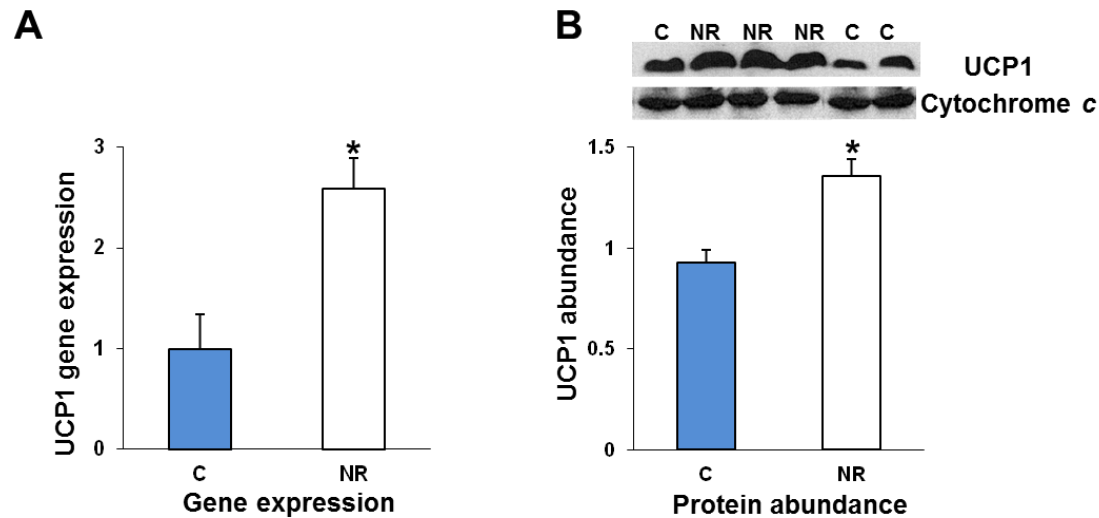


Figure 4.3 Effect of suboptimal maternal nutrition in early-to-mid gestation on (A) uncoupling protein 1 (UCP1) mRNA expression and (B) UCP1 protein abundance in pericardial adipose tissue of 140 day gestation sheep fetus

Pericardial adipose tissue was sampled from 140 day gestation fetuses delivered to sheep that consumed either 100% (control(C)) or 60% (nutrient restricted (NR)) of total metabolisable energy requirements to maintain maternal metabolism and fetal growth between 30 d and 80 d of gestation followed by ad libitum feeding until delivery. Values are means \pm SEM; n = 5-7 per group. *p <0.05.

Table 4.2. Multiple regression analyses for uncoupling protein 1 (UCP1) gene expression and relative protein content as dependent variable and mother's nutrition group, mother's weight, fetal weight and pericardial adipose tissue weight as independent variables (n=12)

UCP1	Gene expression				Relative protein content			
	B	SEM	β	p	B	SEM	β	p
Constant	-8.01	20.33	-	0.70	0.32	1.22	-	0.80
Mother's nutritional group*	1.86	0.70	0.74	0.04	0.46	0.14	0.84	0.01
Mother's weight	-0.14	-0.14	-0.88	0.34	0.03	0.03	0.24	0.35
Fetal weight	-1.88	-2.80	-0.88	0.526	0.07	0.10	0.16	0.52
Pericardial adipose tissue weight	13.69	14.01	2.40	0.37	0.02	0.08	0.07	0.83

Pericardial adipose tissue was sampled from 140 day gestation fetuses of sheep. * The mother's nutritional groups were control group (fed 100% of total metabolisable energy (ME) requirements) or nutrient-restricted group (fed 60% of total ME requirements) between 28 days and 80 days of gestation.

4.3.3 Effect of maternal nutrient restriction on genes involved in adipogenesis

Gene expression for Ki-67, a gene involved in adipocyte proliferation, together with the brown adipogenic gene BMP7 were upregulated in fetal pericardial adipose tissue of mothers nutrient restricted between early-to-mid gestation (Table 4.3), whereas mRNA abundance for PGC1 α and PRDM16 were unaffected. A number of genes that control adipogenesis in white adipocytes exhibited a two to three fold increase in mRNA expression in the fetus delivered to nutritionally manipulated mothers including BMP4, HoxC9, C/EBP α and β , whereas PPAR γ , ADRP and RIP140 were unaffected, as were the adipokines, leptin and adiponectin. Gene expressions for β 1 and β 3, but not β 2ADR, were also raised in pericardial fat, whereas insulin receptor gene expression was reduced without changes in gene expression of the glucocorticoid receptor (Table 4.4).

Table 4.3. Effect of suboptimal maternal nutrition in early-to-mid gestation on genes expression of adipogenic transcription factors in pericardial adipose tissue of fetus at 140 days of gestation

Pathway gene	C (n=5)	NR (n=7)	Effect of suboptimal maternal nutrition (p-value)
Brown adipogenesis			
BMP7	1 ± 0.26	1.87 ± 0.18	0.016
PGC1α	1 ± 0.42	1.95 ± 0.35	0.088
PRDM16	1 ± 0.26	1.30 ± 0.30	0.219
White adipogenesis			
BMP4	1 ± 0.27	2.06 ± 0.43	0.048
HoxC9	1 ± 0.37	3.67 ± 0.30	0.004
C/EBPα	1 ± 0.20	2.02 ± 0.36	0.023
ADRP	1 ± 0.21	0.91 ± 0.34	0.878
Brown and white adipogenesis			
Ki67	1 ± 0.29	1.93 ± 0.29	0.033
C/EBPβ	1 ± 0.20	2.02 ± 0.36	0.024
PPARγ	1 ± 0.21	0.93 ± 0.21	0.811
RIP140	1 ± 0.21	0.87 ± 0.40	0.760

Abbreviations: C, control; NR, Nutrient Restricted; BMP, Bone Morphogenetic Protein; PPAR, peroxisome proliferator-activated receptor; PGC, PPARγ co-activator; PRDM16, PR (PRD1-BF1-RIZ1 homologous)-domain-containing protein; HoX, Homobox; C/EBP, CCAAT-enhancer binding protein; ADRP, Adipose Differentiation Related Protein; ADR, adrenergic receptor; GR, glucocorticoid receptor. Values are means ± SEM.

Table 4.4. Effect of suboptimal maternal nutrition in early-to-mid gestation on genes expression of β -adrenergic receptors, genes involved in adipocyte metabolism and adipokines in pericardial adipose tissue of fetus at 140 days of gestation

Pathway gene	C (n=5)	NR (n=7)	Effect of suboptimal maternal nutrition (p-value)
β-adrenergic receptors			
β 1ADR	1 \pm 0.27	1.86 \pm 0.23	0.035
β 2ADR	1 \pm 0.17	1.2 \pm 0.30	0.089
β 3ADR	1 \pm 0.36	2.56 \pm 0.71	0.036
Adipocyte metabolism			
Insulin receptor	1 \pm 0.34	0.45 \pm 0.15	0.015
GR	1 \pm 0.35	1.03 \pm 0.25	0.944
Adipokines			
Leptin	1 \pm 0.37	0.82 \pm 0.33	0.723
Adiponectin	1 \pm 0.36	1.19 \pm 0.30	0.690

Abbreviations: C, control; NR, Nutrient Restricted; BMP, Bone Morphogenetic Protein; PPAR, peroxisome proliferator-activated receptor; PGC, PPAR γ co-activator; PRDM16, PR (PRD1-BF1-RIZ1 homologous)-domain-containing protein; HoX, Homobox; C/EBP, CCAAT-enhancer binding protein; ADRP, Adipose Differentiation Related Protein; ADR, adrenergic receptor; GR, glucocorticoid receptor. Values are means \pm SEM.

4.4 Discussion

This study demonstrates that suboptimal maternal nutrition between early-to-mid gestation, followed by restoration of feeding to appetite up to term, enhances both adiposity and adipogenic potential in the near-term fetus (Ojha et al. 2013).

4.4.1 Suboptimal maternal nutrition in early-to-mid gestation followed by ad libitum feeding enhances fetal adiposity

Although maternal and fetal total body weights were unaffected at term, fetal adiposity, including pericardial adipose tissue deposition, was raised. Human infants born with growth restriction exhibit increased visceral adiposity (Harrington et al. 2004) and, in ovine models, when suboptimal maternal nutrition during early-to-mid gestation (Bispham et al. 2003) is followed by rearing in an obesogenic environment, ectopic lipid accumulation is enhanced in the liver, kidney and heart (Chan et al. 2009, Hyatt et al. 2011, Fainberg et al. 2013). Increased visceral adiposity is an established risk factor for cardiovascular disease and, in particular, raised pericardial adiposity is closely associated with coronary vascular pathologies (Taguchi et al. 2001). The greater total visceral and pericardial adiposity observed in this study are, therefore, consistent with studies showing that offspring of mothers who were subjected to suboptimal nutrition during embryonic and placental

development have higher blood pressure and compromised cardiovascular physiology in later life even in the absence of changes in birth weight (Gopalakrishnan et al. 2004). These findings further support the view that development of the fetus, particularly of adipose tissue, can be programmed by changes in maternal nutrition even in the absence of alterations in overall fetal growth.

4.4.2 Suboptimal maternal nutrition in early-to-mid gestation followed by ad libitum feeding enhances adipogenic potential in the fetal pericardial depot

Importantly, this study demonstrates that gene expression of several adipogenic transcription factors were upregulated in the pericardial depot of the nutritionally manipulated foetuses (Figure 4.4). BMP7 promotes differentiation of brown preadipocytes and can activate the full programme of brown adipogenesis (Tseng et al. 2008). It induces robust expression of UCP1 mRNA as well as the expression of several brown adipogenic factors including PPAR γ and C/EBP β (Tseng et al. 2008). I also found a significant increase in C/EBP β mRNA expression which could be important as the C/EBP β –PRDM16 complex is essential for the switch of cells from a myogenic to brown adipogenic lineage (Kajimura et al. 2009). C/EBP β also induces the C/EBP α -PPAR γ complex which promotes adipogenesis along the white adipocyte lineage in parallel to increased brown adipogenic transcription factors.

I have also demonstrated enhancement of gene expression of several factors involved in white adipogenesis including CEBP α , BMP4 and HoxC9, which were all upregulated after suboptimal nutrition between early-to-mid gestation followed by ad libitum feeding. BMP4 triggers the commitment of pluripotent cells to the white adipocyte lineage (Tang et al. 2004). Like HoxC9, BMP4 expression is present in ovine adipose tissue from mid-gestation, peaks after birth (Pope et al. 2014) and is highly expressed in white adipose tissue in both mice and humans (Billon and Dani 2012).

Enhanced cell proliferation in the pericardial depot is also suggested by the upregulation of Ki-67 mRNA, a protein associated with cell proliferation and is present in all active phases of the cell cycle (Scholzen and Gerdes 2000). I found that the gene expression of white adipogenic transcription factors was increased more than that of the brown adipogenic genes. For example, gene expression of BMP4 and C/EBP α was increased two fold and expression of HoxC9 increased nearly four times in the offspring of mothers subjected to suboptimal nutrition. Upregulation of all these key transcription factors suggests that both brown and white adipogenesis are enhanced when the fetus is subjected to suboptimal maternal nutrition in early-to-mid gestation followed by the restoration of ad libitum feeding.

4.4.3 Suboptimal maternal nutrition in early-to-mid gestation followed by ad libitum feeding increases thermogenic potential of the fetal pericardial depot

In these near-term fetuses, sampled from nutritionally manipulated mothers, I found that enhanced adipogenesis was accompanied by increases in pericardial adipose tissue UCP1 abundance and gene expression. Moreover, the effect of maternal nutrition on UCP1 gene expression and protein abundance was independent of maternal and fetal weights, and the amount of pericardial adipose tissue present in the near-term fetus.

Along with the increase in UCP1, gene expression for $\beta 1$ and $\beta 3$ ADRs were also enhanced in the fetus of the nutritionally manipulated mothers. Proliferation, differentiation and metabolism of mature brown adipocytes are governed by adrenergic stimulation from the $\beta 3$ ADR and this would, therefore, be predicted to facilitate an enhanced thermogenic potential (Cannon and Nedergaard 2004). Mature brown adipocytes also possess $\beta 1$ ADRs, although they are usually more prominent in preadipocytes where their activation is coupled to cAMP production (Bronnikov et al. 1999). Increased gene expression of $\beta 1$ ADR may, therefore, be due to increased proliferation of preadipocytes.

In contrast, insulin receptor gene expression was downregulated despite the restoration of maternal nutrition from mid gestation. Insulin

signalling is mediated by a series of pathways activated by insulin acting on its cytoplasmic receptor and reduced stimulation of this pathway leads to systemic insulin resistance (Wellen and Hotamisligil 2005). Reduced insulin receptor gene expression could be a precursor of insulin resistance that accompanies obesity and ectopic lipid accumulation (DeFronzo and Ferrannini 1991). Indeed, this maladaptation is found when the offspring are reared in an obesogenic environment and exposed to juvenile onset obesity (Chan et al. 2009).

Enhanced fetal pericardial adiposity, including raised brown and white adipogenesis and greater UCP1 abundance could provide the formerly nutritionally compromised fetus with a survival advantage by increasing its metabolic response to cold exposure at birth. The greater adiposity may further enable the offspring to withstand a period of suboptimal nutrition in later life. However, when this fetus is delivered into an environment of nutrient sufficiency or excess, the enhanced adipogenic potential, particularly in the white adipogenic lineage, is likely to be detrimental to long term metabolic health (Symonds et al. 2012).

Increased pericardial adipose tissue volume is associated with several cardio-metabolic pathologies (Ding et al. 2008) and regulates the presence (Liu et al. 2010) and severity of coronary artery disease in adult humans (Taguchi et al. 2001). The findings of this study suggest that the origins of excess pericardial adiposity may lie in early fetal

development and suboptimal maternal nutrition can programme
increased pericardial adiposity and enhance adipogenesis in this depot.

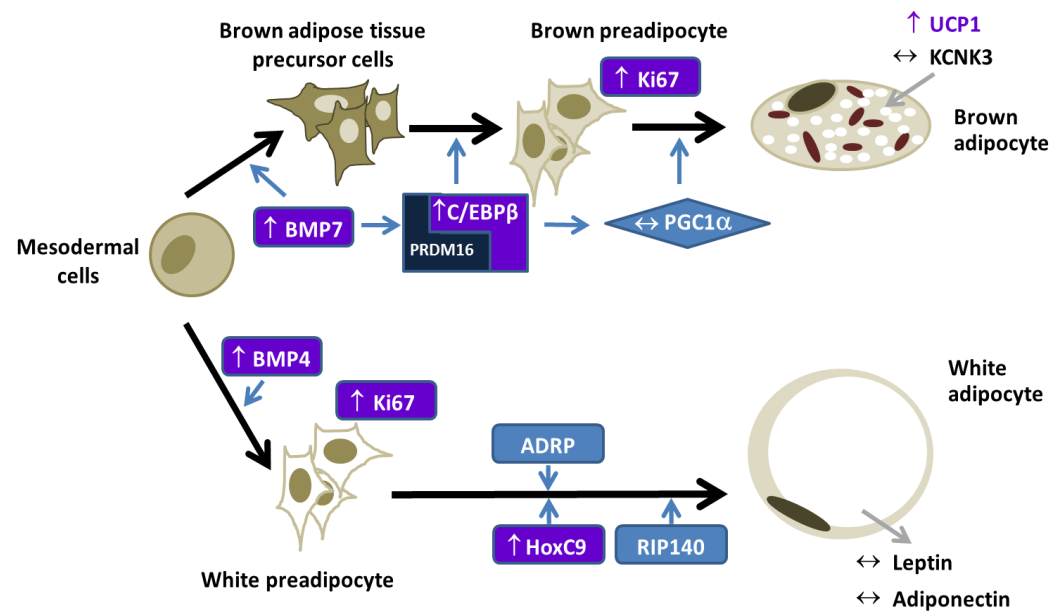


Figure 4.4. Effect of suboptimal maternal nutrition in early-to-mid gestation on adipogenesis

Suboptimal maternal nutrition in early-to-mid gestation increases gene expression of transcription factors involved in both brown and white adipogenesis. UCP: uncoupling protein; BMP: bone morphogenetic protein; ADRP: adipose differentiation related protein; Hox: homobox; RIP: receptor interacting protein; PRDM: PR (PRD1-BF1-Riz1 homologous)-domain-containing protein; C/EBP: CCAAT enhancer binding protein

4.5 Conclusion

The development of adipose tissue in offspring subjected to suboptimal maternal nutrition now needs to be further studied in order to elucidate the precise mechanisms underlying the progression from excess adipogenic potential in the pericardial depot to cardiovascular illness in adulthood. Previously, in the study in Chapter 3, I have shown that pericardial adipose tissue is a primary target of nutritional programming (Ojha et al. 2013) and, in the present study, I have demonstrated further that suboptimal maternal nutrition followed by ad libitum feeding in late gestation produces changes in pericardial adipose tissue, which may be the beginning of excess pericardial adiposity and cardiovascular illness in later life.

5 Epicardial fat is a depot of brown adipose tissue in adult humans

The work described in this chapter has been published (Sacks et al. 2013). The article is included in Appendix 10.4.2.

5.1 Introduction

Epicardial adipose tissue (EAT) is the fat present between the heart and the visceral layer of the pericardium i.e. in direct contact with the myocardium (Figure 1.9). EAT is anatomically and clinically related to cardiac morphology and function and is believed to be a metabolically active organ that generates several bioactive molecules, which may affect cardiac function and the evolution of cardiac pathologies (Iacobellis et al. 2005). Although EAT has the gross appearance of white fat in human adults, it evolves from brown adipose tissue (BAT) and has recently been shown to express high levels of uncoupling protein (UCP) 1 mRNA (Sacks et al. 2009).

In adipose tissue samples collected from 28 patients undergoing coronary artery bypass grafting (CABG) for critical coronary atherosclerosis, Sacks et al. found that UCP1 gene expression was 5-fold higher in EAT when compared to substernal fat. UCP1 gene expression was even lower (barely detectable) in samples taken from subcutaneous adipose tissue from the sternum, abdomen and leg

(Sacks et al. 2009). The gene expression of other BAT related genes, PRDM16 and PGC1 α were also higher in EAT when compared to subcutaneous fat (Sacks et al. 2009). These findings raised the possibility that EAT functions as a depot of BAT. However, gene expression of UCP1 is not definite evidence of the existence of BAT. Presence of the protein is required to conclusively demonstrate that EAT is a depot of brown fat.

5.1.1 Hypothesis and aim

The hypothesis for this study, as mentioned in Chapter 1 (Section 1.12.3), is given that in adult humans, relatively high levels of UCP1 gene expression is present in EAT, I hypothesised that UCP1 is significantly more abundant in EAT when compared to other adipose tissue depots thus confirming that epicardial fat is a depot of BAT in adult humans.

5.2 Methods

5.2.1 Ethical approval

Details of ethical approval and other procedural and legislative declarations are explained in Chapter 2 (Section 2.1.2.1).

5.2.2 Adipose tissue samples

The adipose tissue samples for this study were provided by Professor Harold Sacks and were collected from patients undergoing cardiac

surgery at The Baptist Heart, Baptist Memorial Hospital, Memphis, Tennessee. The details of sample collection, transfer and storage are given in Chapter 2 (Section 2.3.1).

5.2.3 Preparation of mitochondrial extract

Mitochondria were prepared from 7 EAT samples (range, 79-411 mg), 3 paracardial fat samples (196-346 mg), 4 sternal fat samples (196-346 mg), 3 upper abdominal subcutaneous adipose tissue samples (258-568 mg) and 2 lower extremity subcutaneous adipose tissue samples (365-324 mg) as described in Chapter 2 (Section 2.4.1.5).

5.2.3.1 Assessment of protein concentration

Protein concentration of the mitochondrial extract was determined by the Bradford method (Bradford 1976) (Chapter 2 (Section 2.4.3.1.2)).

5.2.3.2 Western Blotting Procedure

Abundance of UCP1 was determined by Western Blotting using the procedure described in Chapter 2 (Section 2.4.3.2). Western Blotting was performed using rabbit polyclonal antibody to human UCP1 (ab 10983; Abcam) at a dilution of 1:1000, together with cytochrome *c* as a reference protein using sc-7159 (Santa Cruz Biotechnology), also at a dilution of 1:1000. Specificity of the detection was confirmed using nonimmune rabbit serum and a range of molecular weight markers was included on all gels. Densitometric analysis was performed on all

membranes after image detection using a Fujifilm LAS-1000 cooled charge-coupled device camera (Fuji Photo Film Co. Ltd) and results were expressed in arbitrary unit. All gels were run in duplicate and reference samples (i.e. from either hepatic or pericardial adipose tissue of the same 6-h-old sheep) were included on each gel.

5.2.4 Statistical analysis

Statistical analysis was performed using IBM SPSS Statistics v.21.0 statistical software for Windows package (IBM Corporation, NT, USA). Kolmogorov-Smirnov normality test was applied to each set of data to test whether the distribution was parametric or non-parametric. As data were not distributed normally, Kruskal-Wallis one-way analysis of variance test with post hoc Dunn's correction was used to determine differences between the groups. GraphPad Prism v 5.00 (GraphPad Software, California, USA) software was used to produce all statistical graphs. All values are expressed as mean \pm SEM.

5.3 Results

There were 2 male and 6 female participants. The details of the participants and the types of samples obtained from them are described in Table 5.1. The mean (\pm SEM) age of the subjects was 65.6 (\pm 1.7) years and body mass index was 29.7 (\pm 1.8) kg/m².

5.3.1.1 Mitochondrial protein in adult human adipose tissue

The mitochondrial protein yield from adult EAT was more than 3-fold less than the yield from pericardial fat from 6 hour old sheep (91.6 ± 3.3 vs. 27.7 ± 3.6 mg/g) however the quantity of protein in adult EAT was higher than that in other adipose depots.

5.3.2 UCP1 in epicardial, visceral paracardial, and subcutaneous fat

UCP1 was highly abundant in each of the EAT samples analysed and the amounts were comparable with the UCP1 content of the positive control (4-fold dilution of mitochondrial extract prepared from pericardial adipose tissue of 6 hour old lamb) (Figure 5.1).

UCP1 was not detected by Western Blotting in sternal, paracardial, and upper abdominal and leg subcutaneous adipose tissue despite similar amounts of the reference protein, cytochrome *c*, being present in all samples (Figure 5.1).

5.3.3 Correlation between relative protein abundance and fold change in gene expression

Gene expression of UCP1 in the EAT samples analysed in this study was measured by Q-PCR by Dr John Fain and Dr Paramjeet Cheema and values were provided for statistical analysis.

There was no correlation between relative protein abundance and fold change of gene expression of UCP1 in the 7 EAT samples analysed in this study (Figure 5.2).

5.3.4 Correlation between relative UCP1 abundance and age and body mass index

There was no significant correlation between age and body mass index and the relative protein abundance of UCP1 in epicardial adipose tissue of the seven subjects included in this study (Figure 5.3).

Table 5.1. Characteristics of patients

	Age (years)	Gender	Weight (kg)	Height (cm)	Body mass index (kg/m²)	Race	Samples
1	74	Female	63.6	160	24.8	Caucasian	Epicardial
2	65	Female	78.0	154.9	32.5	Caucasian	Epicardial, Abdominal, Sternal
3	61	Female	104.5	165.1	38.3	Caucasian	Epicardial
4	69	Female	85.4	177.8	27.0	Caucasian	Epicardial
5	65	Female	75	157.5	30.2	Caucasian	Epicardial, Sternal, Leg, Paracardial
6	66	Female	61.3	160.0	23.9	Asian	Epicardial, Abdominal, Sternal, Leg, Paracardial
7	67	Male	108.9	177.8	34.4	Caucasian	Epicardial, Sternal
8	58	Male	84.8	178.4	26.6	Caucasian	Abdominal, Paracardial

Table 5.2. Total mitochondrial protein content of adipose tissue in different depots

Adipose tissue	Total mitochondrial protein (mg/g)
Epicardial fat	27.7 ± 3.6
Paracardial fat	5.9 ± 0.7
Sternal fat	12.23 ± 3.6
Abdominal fat	9.23 ± 3.07
Leg subcutaneous fat	7.2 ± 3.09

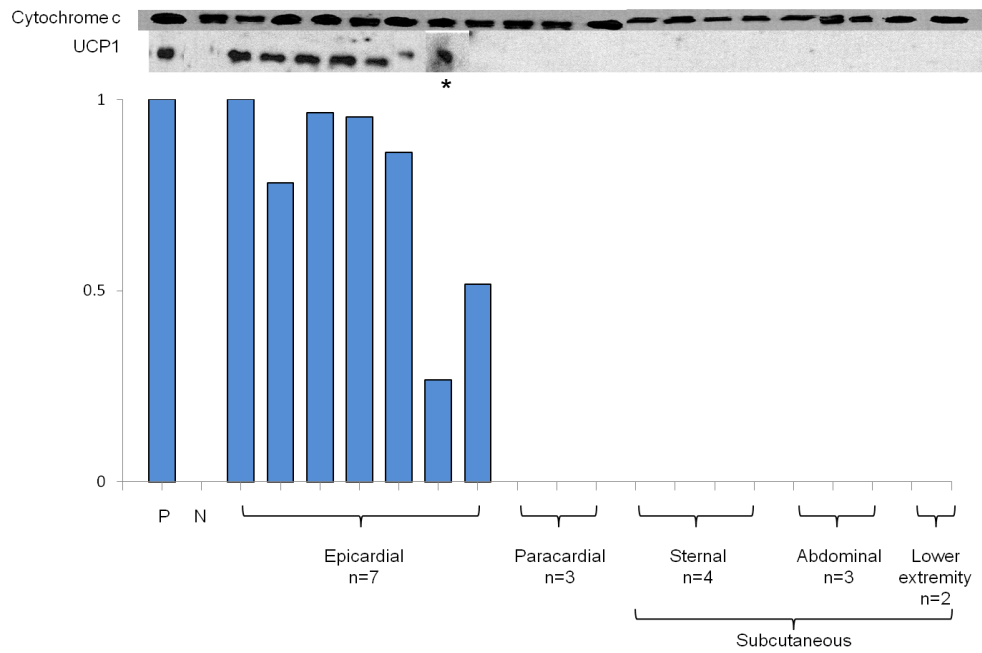


Figure 5.1. Relative protein abundance of UCP1 in fat samples

Optical densities (ordinate) are shown as black bars of Western Blots for uncoupling protein 1 (UCP1) from extracts of epicardial, paracardial, sterna, abdominal, and lower extremity subcutaneous fat. The number of separate patients is shown below each bracket designating the fat depot. Individual bands of UCP1 and their corresponding cytochrome *c* as a loading control are seen above the bars. The end bar with a darker background was from another membrane (marked with *). The figure represents the data from 1 of 5 experiments repeated on different days. P: positive control of brown fat mitochondrial protein; N: negative control of hepatic mitochondrial protein, both prepared from a 6 hour old lamb. No immunoreactive UCP1 was detected in paracardial, sternal and subcutaneous depots.

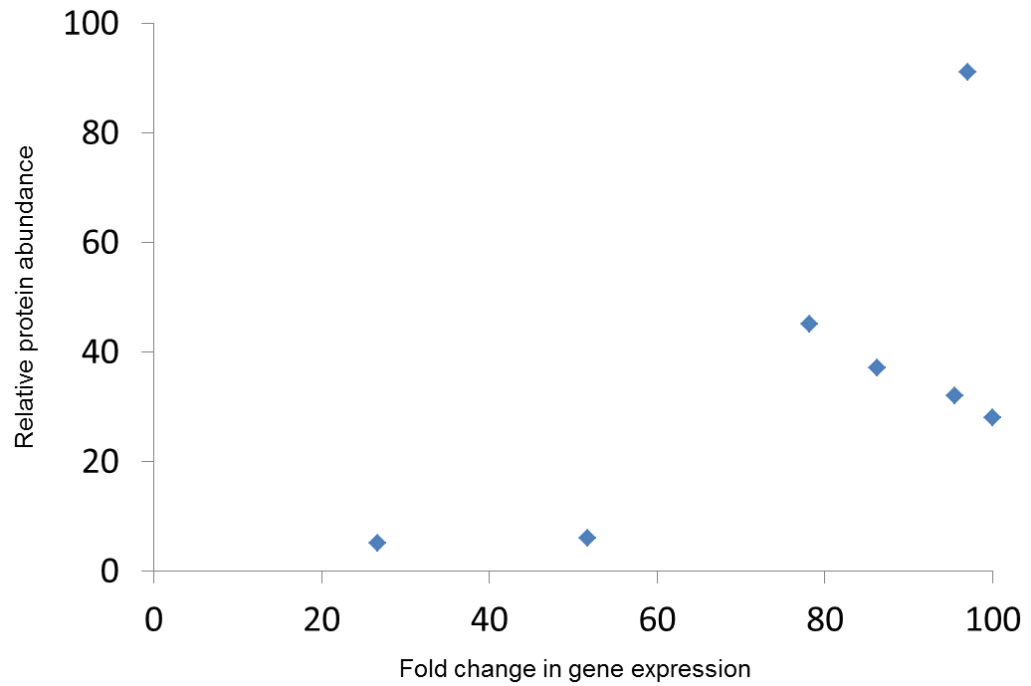


Figure 5.2 Correlation between relative protein abundance and fold change in gene expression of UCP1 in human epicardial adipose tissue

Adipose tissue samples were obtained from 7 adults undergoing cardiac surgery. Protein abundance of uncoupling protein 1 (UCP1) was estimated by Western Bolt and fold change in gene expression was calculated by quantitative polymerase chain reaction.

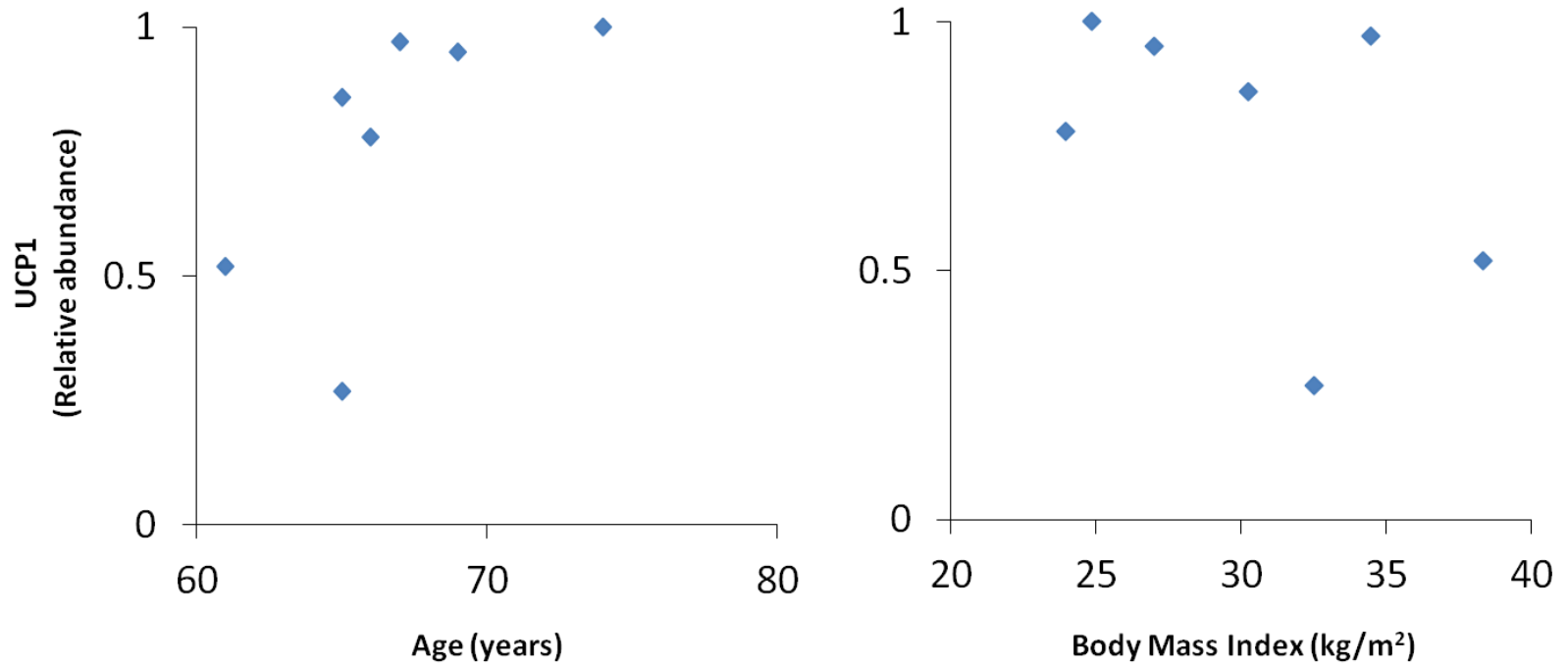


Figure 5.3. Correlation between relative protein abundance of uncoupling protein 1 (UCP1) in epicardial adipose tissue and age and body mass index (BMI) of adult humans

Adipose tissue samples were obtained from 7 adults undergoing cardiac surgery. Protein abundance was estimated by Western Bolt.

5.4 Discussion

The major finding of this study is that UCP1 is present in EAT of adult humans (Sacks et al. 2013). Sack et al. have previously shown that EAT has a significantly higher expression of UCP1 gene when compared to fat from other depots (Sacks et al. 2009). This study demonstrated that the protein itself is present in EAT in quantities that are comparable to the amount of UCP1 in pericardial adipose tissue of newborn lambs in which UCP1 is maximally expressed and activated (Ojha et al. 2013).

Quantitative PCR is a very sensitive technique and measures mRNA expression highly efficiently. It can measure very low levels of gene expression. Quantitative physiological implications cannot be drawn from such measurements of gene expression alone, particularly when the crossing points on the Q-PCR are very high i.e. gene expression is very low. Changes in gene expression of UCP1 may be a marker of tissue response to a stimulus but are not valid parameters for estimating physiological function. The total amount of the protein, i.e. UCP1, in the tissue is a better marker of functional capacity (Cannon et al. 1981). This study has, therefore, confirmed that human EAT is a repository of functional BAT by demonstrating significant levels UCP1 in fat samples obtained from this depot.

The Western Blots did not detect any UCP1 in paracardial or subcutaneous adipose tissue obtained from sternal, upper abdominal, and leg regions although Sacks et al. had demonstrated some degree of gene expression for UCP1 in these samples. This could be because such low levels of gene expression may not translate into protein abundance that are detectable by Western Blot.

5.4.1 UCP1 gene expression does not correlate with protein abundance in human EAT

There was no correlation between gene expression and relative protein abundance of UCP1 in EAT of adult humans. However, as this study was performed on the samples left over from a previous study (Sacks et al. 2009), I had only 8 participants and hence the power is not sufficient to detect a correlation, should there be one.

Despite the lack of statistical power, it should be considered that this lack of correlation between gene expression and protein abundance is in keeping with the findings in newborn lambs (Chapter 3 (Section 3.3.8) and could be due to differences in the half-life of proteins and mRNA and/or due to one of the many steps involved in translation of gene expression into protein abundance and/or several post-translational mechanisms and regulatory processes that affect the turnover of proteins (Greenbaum et al. 2003).

The lack of correlation may be accentuated by the inaccuracies in the quantitative techniques used. Western Blotting is a quasi-quantitative method and there are many potential challenges in obtaining appropriate and reliable quantification when using this procedure. Studies suggest that up to 25% of quantitative data obtained from Western Blotting may be inappropriately interpreted (Taylor et al. 2013). Even with the use of innovative, highly precise technologies such as next-generation sequencing for quantification of RNA abundance and novel proteomics, squared Pearson correlation coefficient achieved between cellular concentrations of proteins with their corresponding mRNA abundance is ~0.4, suggesting that only 40% of variation in protein concentration can be explained by changes in mRNA expression (Vogel and Marcotte 2012).

5.4.2 UCP abundance in human EAT does not correlate with BMI or age of the subjects

There was no correlation between UCP1 abundance and age or body mass index (BMI) of the subjects studied. Other studies, with larger numbers of subjects, have reported that UCP1 positivity correlates with BMI and age. On examination of adipose tissue obtained from the neck of 35 adults, Zingaretti et al. reported that UCP1 positive (as measured by immunohistochemistry) subjects were mainly those who were younger and leaner (Zingaretti et al. 2009). The age range of the subjects studied by Zingaretti et al. was 18 to 82 years and the mean (\pm

SEM) age of the UCP1 positive subjects was 39 (\pm 5) years. The 7 subjects in this study were older (range 58-74 years) and this may be the reason for the lack of correlation between age and UCP1 abundance.

BAT activity as measured by radioactive fluoride (^{18}F) labelled fluorodeoxyglucose (FDG) positron emission tomography/computed tomography (PET-CT) has also been reported to correlate with age and BMI but some aspects of the reports are conflicting. Cypess et al. detected BAT most frequently in patients younger than 50 years and those who were the least obese among their cohort of 3640 subjects who underwent ^{18}F -FDG PET-CT scanning but BMI was a significant predictor of presence of BAT only in the older subjects (Cypess et al. 2009). In contrast, Pfannenbergl et al. reported a significant negative correlation between BAT activity and BMI in younger male subjects while in females the strong negative correlation persisted at all ages (Pfannenbergl et al. 2010). Six of the 7 subjects in this study were females but this study did not demonstrate any relationship between BMI and UCP1 abundance. This may be due to limited number of samples or because ^{18}F -FDG PET-CT studies estimate BAT activity and have classified individuals as BAT positive or BAT negative while in this study, the correlation was measured between the relative quantity of UCP1 and BMI. The amount of protein may not be the same as

presence of concurrently active BAT especially in the absence of stimuli that activate UCP1.

5.4.3 The limitations

The samples analysed in this study were the tissue remaining from a previous study (Sacks et al. 2009) and the number of samples and the amount of tissue available for analysis were limited. Although the original study was prospectively conducted, this analysis was done in retrospect.

The cohort had a mean age of 66 years and BMI of nearly 30 kg/m². Studies investigating the presence of BAT in adult humans have generally shown that active BAT is more prevalent in younger and leaner individuals (Cypess et al. 2009, van Marken Lichtenbelt et al. 2009, Pfannenbergl et al. 2010) hence this cohort was not particularly appropriate group to measure BAT activity. In additions, due to ethical considerations, adipose tissue samples such as supraclavicular fat, which would be more suitable for comparing UCP1 presence, were not acquired. Comparison between depots was dependent on the sites that the surgeon would require to access in the normal course of the open heart surgery.

5.4.4 Significance of UCP1 in human EAT

Until very recently, interest in BAT was restricted to researchers in mitochondrial bioenergetics and hibernation and the only role of BAT in

humans was thought to be the maintenance of body temperature in newborn infants. The rediscovery of BAT in adult humans regenerated interest and recent studies have demonstrated that BAT may have a role in energy homeostasis and intermediary metabolism in human adults. The presence of BAT in EAT i.e. in close proximity and with intimate vascular connections with the myocardium and coronary vasculature raises the possibility that BAT may have a role in cardiac metabolism.

Bartelt et al. demonstrated that activating BAT increases the turnover of triglyceride rich lipoproteins and clears triglycerides from the circulation (Bartelt et al. 2011). In a pathophysiological model of hyperlipidaemia (Apoa5^{-/-} mice), they showed that BAT activation by cold exposure corrected plasma lipid concentrations within hours. In models of obesity, they also found that the clearance of triglyceride rich lipoproteins by brown adipocytes was independent of insulin concentrations and insulin resistance in the animal. This demonstrates that active BAT can improve deleterious effects of obesity and hyperlipidaemia, despite insulin resistance.

In addition to its role in lipid metabolism, BAT is also a major organ of glucose disposal. Presence of active BAT in adult humans was rediscovered due to the highly active uptake of glucose by this tissue (Hany et al. 2002). BAT is highly sensitive to insulin action and insulin-

stimulated glucose uptake by brown adipocytes is close to skeletal muscle uptake (Orava et al. 2011). In addition, stimulation of BAT such as by cold activation, results in rapid uptake of glucose, independent of insulin action.

The above evidence indicates that BAT may have a beneficial effect on metabolic balance, both for lipid and glucose metabolism. Brown adipocytes in EAT may act as lipid and glucose clearing mechanisms prior to the blood reaching the coronary circulation and may have metabolic functions other than, or in addition to, its thermogenic role.

5.5 Conclusion

EAT from adult humans contains UCP1 confirming that EAT is a BAT depot. In view of the potential role of BAT in regulation of lipid and glucose metabolism, this may have therapeutic implications for treatment of cardiovascular complications of obesity.

6 Brown adipose tissue is present in epicardial fat of newborn infants, children and adolescents

6.1 Introduction

A plethora of recent imaging studies using positron emission tomography and computed tomography (PET/CT) (Drubach et al. 2011, Chalfant et al. 2012, Gilsanz et al. 2012) have demonstrated that brown adipose tissue (BAT) persists beyond infancy in children and adolescents and that the major depots of BAT correspond to those found in the early anatomical studies (Aherne and Hull 1966).

Excess fat deposition around the heart has well established links with cardiovascular diseases in adults (Taguchi et al. 2001, Ding et al. 2009) and recent advances in obesity research have demonstrated links between paediatric obesity and metabolic and cardiovascular morbidities suggesting that a similar relationship exists in childhood (Cote et al. 2013). Although some earlier studies in children failed to demonstrate any link between epicardial fat thickness and markers of the metabolic syndrome such as insulin resistance (Mazur et al. 2010), increasing evidence suggests that fat deposition around the heart may be a useful tool in assessing cardiovascular risk in children (Cote et al. 2013).

Among pre-pubertal and early pubertal obese children, those who are insulin resistant have higher volumes of epicardial fat as compared to those who are insulin sensitive (Manco et al. 2013). The process of atherosclerosis can start at an early age and epicardial fat in children and adolescents shows a positive and significant correlation with carotid intima-media thickness (Boyras et al. 2013, Cabrera-Rego et al. 2014), a sensitive marker of atherosclerosis and cardiovascular morbidity and mortality in the adult population (Lorenz et al. 2007).

In view of the potential importance of epicardial fat in the genesis of cardiovascular pathologies and the metabolic syndrome and my previous work demonstrating that BAT is present in the epicardial depot in adults (Chapter 5) (Sacks et al. 2013), I aimed to investigate that presence of BAT in fat depots around the heart in children.

Children with congenital heart disease often require cardiac surgery during which a sample of epicardial adipose tissue may be collected for analysis. With appropriate ethical and regulatory approvals, and informed parental consent, I aimed to collect epicardial fat samples from children undergoing heart surgery at the Glenfield Hospital, Leicester. Due to the nature of their illness, children with congenital cardiac disease may have persistent hypoxia, co-morbidities, and may be on medications. As discussed in Chapter 1 (Section 1.6), hypoxia and medications such as β -adrenergic blockers can affect BAT. Therefore, I

aimed to collect relevant clinical information (Section 6.2.4) about the children who participated in the study. I also collected information about the participant's ethnic origin because volume and activity of BAT may differ in individuals of different racial origins (Bakker et al. 2014, Robinson et al. 2014).

6.1.1 Hypothesis

As in Chapter 1 (Section 1.12.4), I hypothesised that BAT is present in epicardial depot in infants and children and, given that gene expression of the unique BAT protein, uncoupling protein 1 (UCP1), in human adults is inversely proportional to BMI and is higher in women than in men (Cypess et al. 2009), that the gene expression of UCP1 is correlated with age and weight for age and is higher in girls than in boys. I also hypothesised that UCP1 gene expression will be higher in children of Caucasian origin when compared to children of Asian (Indian sub-continent) origin.

Propranolol is a non-selective β -adrenergic antagonist. As discussed in Chapter 1 (Section 1.6.3), development and metabolism of brown fat as well as regulation of the UCP1 gene is under adrenergic control and is thought to be mainly regulated by β -adrenergic receptors (β ADR) (Cannon and Nedergaard 2004). Therefore, I hypothesised that gene expression of UCP1 is downregulated in children receiving regular propranolol therapy.

6.2 Methods

6.2.1 Ethical and Regulatory Approvals

The study was approved by National Research Ethics Service Committee (NRES) East Midlands – Nottingham 2 (REC reference number: 12/EM/0214). Further details of ethical and regulatory approvals obtained for this study are given in Chapter 2 (Section 2.1.2.2).

6.2.2 Adipose tissue samples

Adipose tissue samples for this study were collected with informed parental consent, from children undergoing cardiac surgery at the East Midlands Congenital Heart Centre at the Glenfield Hospital, Leicester by the Paediatric Cardiothoracic Surgery team under the supervision of Mr Attilio Lotto (Paediatric Cardiothoracic Surgeon). All participants had congenital heart disease and the samples were taken at the time of the surgery immediately prior to the child being put onto cardio-pulmonary bypass. This ensured that all participants were normothermic in the hours before, and at the time of sample collection.

Although, due to small volumes, it is difficult to consistently separate the fat present around the heart in infants and children into epicardial adipose tissue (i.e. fat present between the myocardium and visceral pericardium) and paracardial adipose tissue (i.e. fat present between the visceral and parietal layers of the pericardium) at dissection (Greif et

al. 2009, McAuley et al. 2011, Wong et al. 2011), fat for this study was taken from as close to the myocardium as possible and is, therefore, considered to be primarily epicardial adipose tissue.

A sample of epicardial adipose tissue (approximately 5 grams) was collected during the dissection of the pericardium as a part of the standard process undertaken during cardiac surgery. Cardiac surgery is mostly performed through a median sternotomy. The pericardial sac is opened to reach the heart and great vessels and pericardiotomy is performed as an inverted 'T'. This opens the pericardium longitudinally with an extension transversally at the level of the diaphragm. Adipose tissue is present in this area. A small sample from this fat was removed taking care to obtain the sample from as close to the myocardium as possible. Approximately 3 grams of tissue were placed in a collection tube containing 20 ml of Allprotect Tissue Reagent[®] (Qiagen, West Sussex, UK) for RNA extraction and lipid analysis and another 2 grams were placed in a tube containing 3% formalin for immunohistochemistry and stored at room temperature.

With appropriate ethical and regulatory approvals and in keeping with the Human Tissue Act 2004, samples were transferred to the Academic Division of Child Health, University of Nottingham. The samples preserved in Allprotect Tissue Reagent[®] were transferred at room temperature. In the laboratory, the sample was removed from the

solution, snap frozen in liquid nitrogen, and stored at -80°C until further analysis. The formalin-fixed samples were transferred and stored at room temperature until further analysis.

Further details of sample collection, storage and transfer are given in Chapter 2 (Section 2.3.2).

6.2.3 Laboratory analysis

6.2.3.1 Analysis of gene expression

RNA was extracted from the adipose tissue samples as described in Chapter 2 (Section 2.4.1.1). The extracted RNA was tested for purity and integrity by the Nanodrop[®]ND-1000 (Nanodrop Technologies, Wilmington, USA) and the Agilent 2100 Bioanalyzer (Agilent Technologies, USA) as described in Chapter 2 (Section 2.4.1.1.3). RNA was extracted from adipose tissue samples taken from all 63 children who participated in the study. On testing for purity and integrity, 57 out of the 63 RNA samples had RNA integrity number (RIN) >7 and intact 18S and 28S fragments. These 57 samples were selected for further analysis as the quality of RNA extracted from the remaining 6 samples was unsuitable for gene expression analysis.

Gene expression was analysed by microarray analysis. I choose to utilise microarray technology to measure gene expression in these samples rather than analyse individual gene expression by Q-PCR as in the previous studies because microarray technology is capable of

making thousands of gene expression measurements simultaneously and allows the quantification of a large number of transcripts in a single experiment (Stoughton 2005). This technology is ideally suited to the early phases of biological research and high throughput screening studies, where changes in expression of a large number of genes can be examined in relation to key biological characteristics or events (Blohm and Guiseppi-Elie 2001). As the human genome has been successfully sequenced (International Human Genome Sequencing 2004), pre-prepared gene arrays are available to perform large scale microarray analyses on human samples. These gene arrays are DNA probes printed onto glass that are used to detect target complementary DNA in the sample. In addition, this technology is available in only a limited number of laboratories. For this study, the microarray assay was performed by Dr Marcos Castellanos and colleagues at the Nottingham Arabidopsis Stock Centre (University of Nottingham, Sutton Bonington Campus, Plant Science Building, School of Biosciences, Loughborough, UK) using the GeneChip[®] 3' IVT Express kit (Affymetrix, High Wycombe, UK) as described in Chapter 2 (Section 2.4.1.5). As the sheep genome has not been completely sequenced yet, this technology could not be applied to samples in my studies in sheep.

6.2.3.2 Immunohistochemistry

As described in Chapter 2 (Section 2.4.3.3), the formalin fixed tissue samples were rehydrated, loaded into Histosette II (Simport, Quebec,

Canada) cassettes and processed by ethanol dehydration followed by xylene rinse. The samples were then embedded in paraffin wax by the Shandon Excelsior™ tissue wax processor (Thermo Scientific). Five micrometre tissue sections were cut from the samples using a sledge microtome (Anglia Scientific, Cambridge, UK) and mounted on to Superfrost™ Plus slides (Menzel-Gläser Inc, Braunschweig, Germany). Two slides per participant and a negative control were labelled with a random identifier and loaded into the Leica BondMax™ IHC slide processor (Leica Microsystem, Wetzlar, Germany) and run on the automated software programme (Vision Biosystems Bond Version 3.4A) using bond polymer refine detection reagents (Leica Microsystem, Wetzlar, Germany) and 1:500 dilution of pre-optimised primary rabbit polyclonal antibody to UCP1 (ab10983, Abcam, Cambridge, UK) for the antibody positive samples. Full details of the procedure are given in Chapter 2 (Section 2.4.3.3.3).

6.2.4 Data collection

Each participant's date of birth and date of surgery were recorded. The age of the participant at sample collection was calculated from these two dates. In addition, information about gender and ethnic origin was collected. All the participants had some form of congenital heart disease and data about the cardiac and any other co-existing medical conditions, the individual's baseline oxygen saturation level, medications (particularly regular β blocker), weight and height on the

day of admission were also collected. These data were collected using a standardised proforma (Appendix 10.2).

6.2.5 Statistical analysis

The anthropometric assessments of participants was performed using the Emergency Nutrition Assessment Tool (Erhardt and Pollgorn 2011) and the World Health Organisation (WHO) Anthro (version 3.2.2, January 2011). Statistical analysis for initial quality control of labelling and hybridisation, as well as data analysis of the microarray results were conducted using the Partek software (Partek Inc., St. Louis, USA). Multiple gene expression comparisons (Table 6.10 and Table 6.11) were performed using this software. The programme is automated such that it assigns statistical significance to a result only if the p value is <0.05 after correction for multiple testing and only if there is a 1.5 times fold change difference between the two groups (to ensure that the difference has some biological significance).

Other statistical analyses were performed using IBM SPSS Statistics v.21.0 statistical software for Windows package (IBM Corporation, NT, USA).

6.3 Results

With appropriate informed consent, adipose tissue samples were collected from 63 children undergoing cardiac surgery. There were 42 boys and 20 girls. Congenital heart diseases present early in life and most children undergo cardiac surgery in the first two years of life. As a consequence, only 15 out of the 63 participants were over two years of age; the median age was 0.68 years (range 0.1-17.05).

Further characteristics of the participants are given in Table 6.1. The cardiac and other diagnoses of the participants and their regular medications are given in Appendix 10.3 (Table 10.1).

Table 6.1 Basic characteristic of the participants

		Total participants	Gene Analysis participants
		n = 63	n = 57
Gender	Male	42	38
	Female	20	18
	Information missing	1	1
Ethnic origin	Caucasian	51	45
	Asian	10	10
	Other	2	2
	Information missing	0	0
β blocker therapy	Yes	8	7
	No	53	49
	Information missing	2	1
Baseline oxygen saturation	≥ 92%	37	33
	<92%	24	23
	Information missing	2	1

Total participants: all the 0-18 year olds who participated in the study; Gene analysis participants: those 0-18 year olds whose samples had appropriate RNA integrity to be suitable for microarray analysis i.e. 6 participants were excluded from analysis of gene expression as the RNA extracted from their epicardial adipose tissue sample was not suitable for further microarray analysis.

6.3.1 Anthropometric assessment of participants

The anthropometric parameters of all 63 participants are described in Table 6.2. This table also contains information about the anthropometric assessments of the 57 children whose epicardial adipose tissue samples yielded RNA suitable for microarray analysis. The only reason 6 participants were excluded from analysis of gene expression was that the RNA extracted from their epicardial adipose tissue sample was degraded (as indicated by RIN <7) and therefore, not suitable for further analysis. Low quality RNA compromises results derived from microarray analysis. If samples with low RIN are processed the Signal to Noise ratio used to create a background subtraction is too high and results in a variable extent of bias in quantification of different transcripts (Auer et al. 2003). It is recommended that samples with RIN <7 should not be used for analysis (Thompson et al. 2007).

Table 6.2 Anthropometric assessment of all participants and those included in gene analyses

		Total participants	Gene Analysis Participants
		n = 63	n = 57
WAZ	Male	-1.037 ± 0.25	-1.33 ± 0.23
	Female	-1.36 ± 0.36	-1.09 ± 0.47
HAZ	Male	-0.66 ± 0.27	-0.80 ± 0.32
	Female	-0.11 ± 0.38	-0.02 ± 0.44
WHZ	Male	-0.96 ± 0.30	-1.36 ± 0.26
	Female	-1.51 ± 0.41	-1.43 ± 0.51
BMI z-score	Male	-0.63 ± 0.22	-0.66 ± 0.17
	Female	0.76 ± 0.27	-0.33 ± 0.27

The values are mean ± standard error of mean (SEM).

WAZ, weight for age z-score; HAZ, height for age z-score; WHZ, weight for height z-score; BMI, body mass index

Total participants: all the 0-18 year olds who participated in the study; Gene analysis participants: those 0-18 year olds whose samples had appropriate RNA integrity to be suitable for microarray analysis i.e. 6 participants were excluded from analysis of gene expression as the RNA extracted from their epicardial adipose tissue sample was not suitable for further microarray analysis.

6.3.1.1 Anthropometric measures of children 0-2 years of age

As mentioned at the beginning of Section 6.3, most of the participants were ≤ 2 years of age. Among the 57 children whose epicardial adipose tissue samples yielded RNA of suitable integrity, 48 children were ≤ 2 years in age. As I subsequently selected these for further analysis of variations in UCP1 gene expression (Section 6.3.2.2), I analysed their anthropometric measures separately. Of these 48 children in the 0-2 year age group, anthropometric parameters could be computed for 47 as the information about the gender of one participant was missing.

The mean \pm SEM weight for age z-score (WAZ) of children 0-2 years of age was -1.29 ± 0.22 ; the mean \pm SEM height for age z-score (HAZ) was -0.52 ± 0.28 ; the mean \pm SEM weight for height z-score was -1.36 ± 0.25 ; and the mean \pm SEM body mass index z-score (BMI z-score) was -0.53 ± 0.15 . In this cohort, there was no difference in the anthropometric parameters between boys and girls (Table 6.3) but the children of Asian/mixed ethnicity were lighter and shorter than the Caucasian children (Table 6.4). As they were proportionately lighter and shorter, there was no significant difference in the weight for height or BMI z-scores (Table 6.4). Despite the small number of Asian children in this study, it is important to note the significant differences in anthropometry as adipose tissue development in early life can be

affected by both growth and racial origin and the effect of one may be confounded by the other.

Table 6.3. Weight for age, height for age and body mass index z-scores of 0-2 year old children

Anthropometric parameter	Males (n = 33)	Females (n = 14)	p value
WAZ	-1.28 ± 0.24	-1.07 ± 0.51	0.14
HAZ	-0.72 ± 0.33	-0.01 ± 0.48	0.67
BMI z-score	-0.60 ± 0.18	0.21 ± 0.26	0.20

WAZ, weight for age z-score; HAZ, height for age z-score; BMI, body mass index

Table 6.4. Weight for age, height for age and body mass index z-scores of 0-2 year old children classified according to ethnic origin

Anthropometric parameter	Asian/Mixed (n = 11)	Caucasian (n = 36)	p value
WAZ	-2.51 ± 0.40	-0.94 ± 0.23	0.004
HAZ	-1.57 ± 0.41	-0.18 ± 0.34	0.016
BMI z-score	-0.99 ± 0.43	0.45 ± 0.16	0.273

WAZ, weight for age z-score; HAZ, height for age z-score; BMI, body mass index

Infants with congenital heart disease are generally of normal size at birth (Kramer et al. 1990) and suffer faltering growth later in infancy (Salzer et al. 1989). Therefore, to further analyse the growth of the 0-2 year old participants, I performed sub-group analyses of growth in newborn infants (≤ 28 days of age) and those older than 28 days (i.e. 29 days to 2 years of age) and reanalysed their anthropometric measures.

6.3.1.1.1 Newborn infant anthropometric measures were normal but Asian infants were significantly lighter and shorter than Caucasian infants.

There were 15 newborn infants (defined as ≤ 28 days of age) out of the 48 infants in the 0-2 year age group. Mean anthropometric parameters of the newborn infants ($n = 15$) were within 1 SD of the normal (mean \pm SEM WAZ, -0.39 ± 0.35 ; HAZ, -0.12 ± 0.51 ; WHZ, -0.81 ± 0.38 ; BMI z-score, -0.49 ± 0.32) although the newborn infants of Asian origin were significantly lighter and shorter than the Caucasian newborn infants (Table 6.6). There was no difference in WAZ, HAZ or BMI z-score between newborn males and females (Table 6.5).

Table 6.5. Weight for age, height for age and body mass index z-scores of newborn infants classified according to gender

Anthropometric parameter	Males (n = 12)	Females (n = 3)	p value
WAZ	-0.50 ± 0.40	-0.03 ± 1.05	0.56
HAZ	-0.02 ± 0.63	-0.44 ± 0.81	0.75
BMI z-score	-0.69 ± 0.29	0.17 ± 1.06	0.27

WAZ, weight for age z-score; HAZ, height (length) for age z-score; BMI, body mass index

Table 6.6 Weight for age, height for age and body mass index z-scores of newborn infants classified according to ethnic origin

Anthropometric parameter	Asian (n = 4)	Caucasian (n = 11)	p value
WAZ	-1.32 ± 0.29	0.02 ± 0.43	0.026
HAZ	-1.50 ± 0.17	0.50 ± 0.63	0.013
BMI z-score	-0.76 ± 0.68	0.38 ± 0.38	0.646

WAZ, weight for age z-score; HAZ, height for age z-score; WHZ, weight for height z-score; BMI, body mass index

6.3.1.1.2 Wasting was present in one-third of children undergoing cardiac surgery between 29 days and 2 years of age

The group of children between 29 days and 2 years ($n = 33$) of age consisted of 11 females and 21 males (data missing for one child). Seven children were of Asian or mixed ethnic origin, 5 were on regular propranolol therapy and 12 were classified as having low baseline oxygen saturation levels.

Eleven out of the 33 (33%) children between 29 days and 2 years of age had WAZ scores less than -2 SD of that expected for their age and gender. The mean \pm SEM WAZ in this group was -1.66 ± 0.25 . Height was less affected; 8 out of 33 (24%) children were stunted (HAZ < -2 SD) and the mean HAZ \pm SEM was -0.69 ± 0.33 . As a number of children were both wasted and stunted, BMI z-score was less affected (mean \pm SEM, -0.55 ± 0.17).

In this age group also, children of Asian/mixed ethnic origin were significantly lighter than the children of Caucasian origin (mean \pm SEM WAZ Asian/mixed ($n = 7$), -3.02 ± 0.43 ; Caucasian ($n = 26$), 1.28 ± 0.25 ; $p = 0.005$). However, the difference in HAZ was not significant statistically (mean \pm SEM HAZ Asian/mixed, -1.49 ± 0.54 ; Caucasian, 0.45 ± 0.39 ; $p = 0.143$) (Table 6.7).

These subgroup analyses (grouped into newborn infants and those 29 days to 2 years of age) of anthropometric parameters of 0-2 years infants demonstrated that, as expected from the known growth pattern among children with congenital heart disease (Salzer et al. 1989), newborn infants included in this study were of normal size but the older children (29 days to 2 years of age) had poor growth as indicated by lower WAZ and HAZ. However, children of Asian/mixed ethnic origin were significantly lighter than children of Caucasian origin in both age groups suggesting that the smaller size of the Asian children may be due to genetic differences rather than nutritional in nature. Despite the small number of Asian participants in the study, this may be of significance as both genetic factors (determined by racial origin) and growth in early life (possibly due to nutritional factors) could affect the development of adipose tissue.

Table 6.7. Weight for age and height for age z-scores of 29 days to 2 year old children classified according to ethnic origin

Anthropometric parameter	Asian (n = 4)	Caucasian (n = 11)	p value
WAZ	-3.02 ± 0.43	1.28 ± 0.25	0.005
HAZ	-1.49 ± 0.54	0.45 ± 0.39	0.143

WAZ, weight for age z-score; HAZ, height for age z-score; WHZ, weight for height z-score

6.3.2 Analysis of gene expression

After RNA extraction, as explained in Section 6.2.3.1, 6 RNA samples were excluded from further analysis due to low RNA integrity.

Microarray analysis for gene expression was performed on 57 samples.

The description of these participants is given in Table 6.1 and the anthropometric assessment is described in Table 6.2.

6.3.2.1 UCP1 gene is expressed in epicardial fat in children

As hypothesised, UCP1 gene was highly expressed in the epicardial fat of newborn infants. The UCP1 gene was also expressed in epicardial fat of older children and did not appear to change to significantly with age (Figure 6.1).

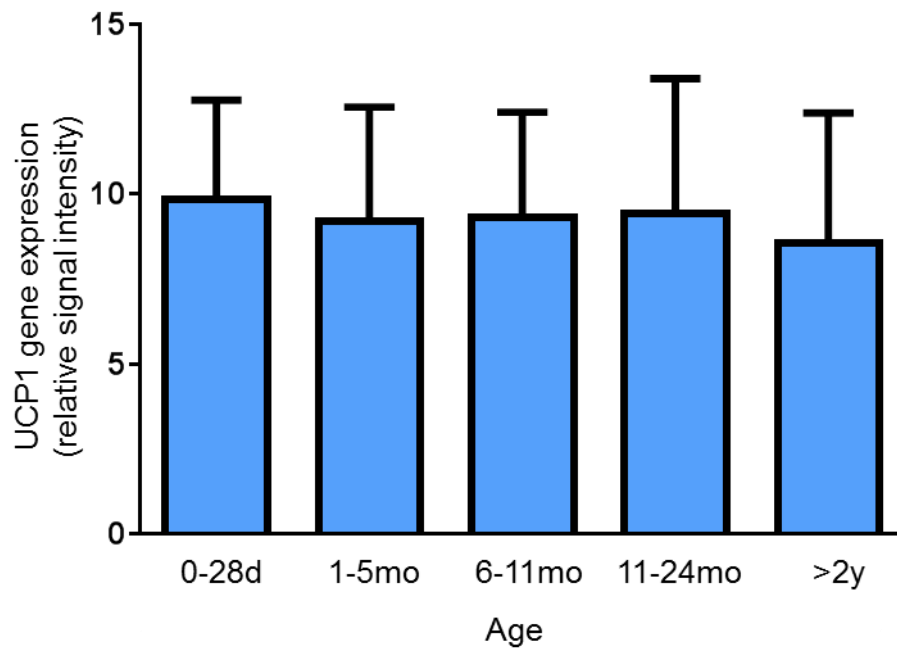


Figure 6.1. Uncoupling protein 1 (UCP1) gene expression in epicardial fat in children

Epicardial adipose tissue was sampled from children undergoing cardiac surgery. Values are means \pm SEM. (n, 0-28d = 15; 1-5mo = 12; 6-11mo = 15; 12-17mo = 3; 18-24mo = 3; >2y = 9).

mRNA expression is measured as a ratio of the signal intensity obtained from the sample relative to the signal intensity obtained from the positive control on the microarray gene chip.

6.3.2.2 UCP1 in children 0-2 years of age

As discussed in Section 6.3, 14 out of the total 63 participants were 0-2 years in age. Among the 57 children whose epicardial adipose tissue samples yielded RNA of suitable integrity, 48 children were 0-2 years in age. As the remaining 9 children were spread over a relatively much wider age range (>2 years to 18 years of age) and data on pubertal development of the older children was not available, I selected those from 0-2 years of age for further analysis of variations in UCP1 gene expression.

This group of forty eight 0-2 year old children consisted of 33 males and 14 females (1 information missing). Thirty seven children were of White British ethnic origin, 9 were of Asian (Indian sub-continent) origin and 2 children of mixed ethnicity (both Asian-Caucasian). Six children were on regular propranolol treatment. The baseline oxygen saturation level in 25 children was $\geq 92\%$, while 22 were relatively hypoxic due to cyanotic congenital heart disease (oxygen saturation levels ranging between 75-91% in air). No participant was on regular home oxygen therapy or any assisted ventilation prior to admission for surgery.

6.3.2.2.1 Effect of gender on expression of UCP1 gene in epicardial adipose tissue of children 0-2 years of age

There were 33 males and 14 females 0-2 year old group. The gene expression for UCP1 did not vary significantly with gender (UCP1 mRNA: males, 9.46 ± 0.57 ; females, 9.37 ± 0.84 relative signal intensity in arbitrary units (mean \pm SEM) $p = 0.93$).

6.3.2.2.2 Effect of use of propranolol on expression of UCP1 gene in epicardial adipose tissue of children 0-2 years of age

Among the children 0-2 years of age, 6 were receiving regular propranolol treatment for their underlying cardiac disease. I found that the gene expression for UCP1 did not differ in children on propranolol when compared to those who were not receiving any β -adrenergic blockers (UCP1 mRNA: no β -blockers, 9.52 ± 0.49 ; on regular propranolol, 9.00 ± 1.38 relative signal intensity in arbitrary units (mean \pm SEM) $p = 0.93$).

6.3.2.2.3 Effect of ethnic origin on expression of UCP1 gene in epicardial adipose tissue of children 0-2 years of age

The expression of UCP1 was significantly higher in children of Caucasian origin as compared to children who were Asian or of mixed ethnicity (UCP1 mRNA: Caucasian, 10.02 ± 0.48 ; Asian/mixed, 7.61 ± 0.99 relative signal intensity in arbitrary units (mean \pm SEM) $p = 0.02$) as demonstrated in (Figure 6.2).

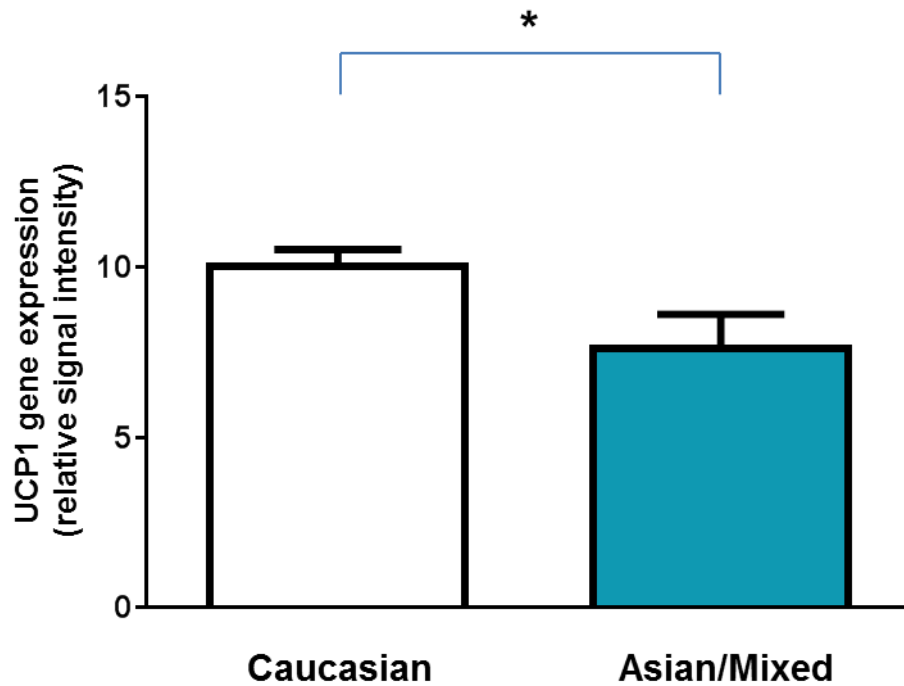


Figure 6.2 Uncoupling protein 1 (UCP1) gene expression in epicardial adipose tissue of children 0-2 years of age

Epicardial adipose tissue was sampled from children undergoing cardiac surgery. Values are means \pm SEM; n= 37 Caucasians; 11 Asian/mixed. *p<0.05

mRNA expression is measured as a ratio of the signal intensity obtained from the sample relative to the signal intensity obtained from the positive control on the microarray gene chip.

6.3.2.2.4 There is no correlation between UCP1 gene expression in epicardial adipose tissue and age in children 0-2 years of age

The gene expression of UCP1 did not correlate with age of the participants (Figure 6.3).

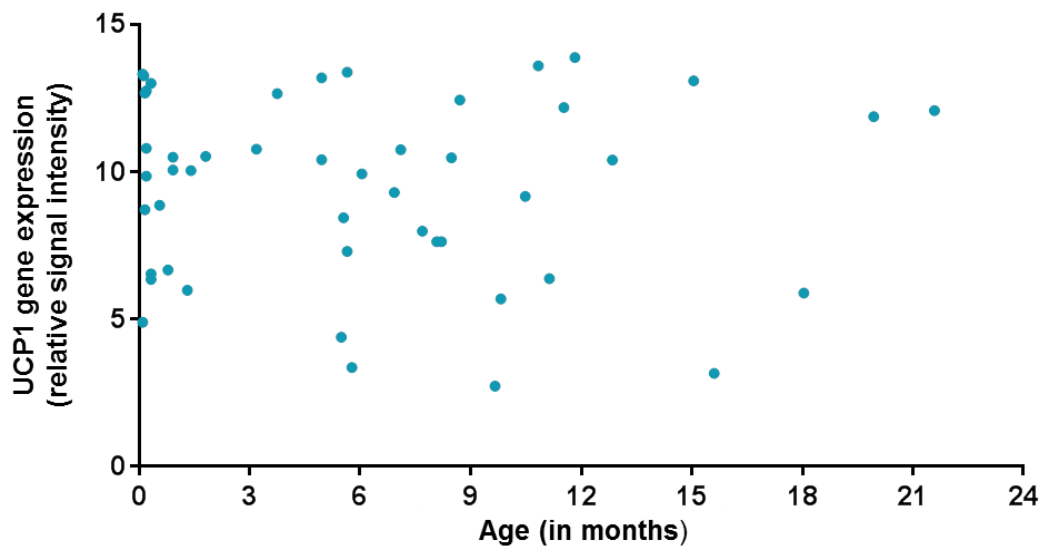


Figure 6.3 Uncoupling protein 1 (UCP1) gene expression in epicardial adipose tissue of children 0-2 years of age does not correlate with age

Epicardial adipose tissue was sampled from children undergoing cardiac surgery. Each point represents a child (n = 48)

mRNA expression of UCP1 is measured as a ratio of the signal intensity obtained from the sample relative to the signal intensity obtained from the positive control on the microarray gene chip.

6.3.2.2.5 UCP1 gene expression in epicardial adipose tissue is associated with weight for age z-score in children 0-2 years of age

A statistically significant correlation was present between UCP1 gene expression in epicardial fat and weight for age z-score of the children (Pearson correlation co-efficient = 0.30; $r^2 = 0.09$ $p < 0.05$) (Figure 6.4).

Whilst this relationship was statistically significant only 9% of the variance in UCP1 gene expression could be explained by WAZ.

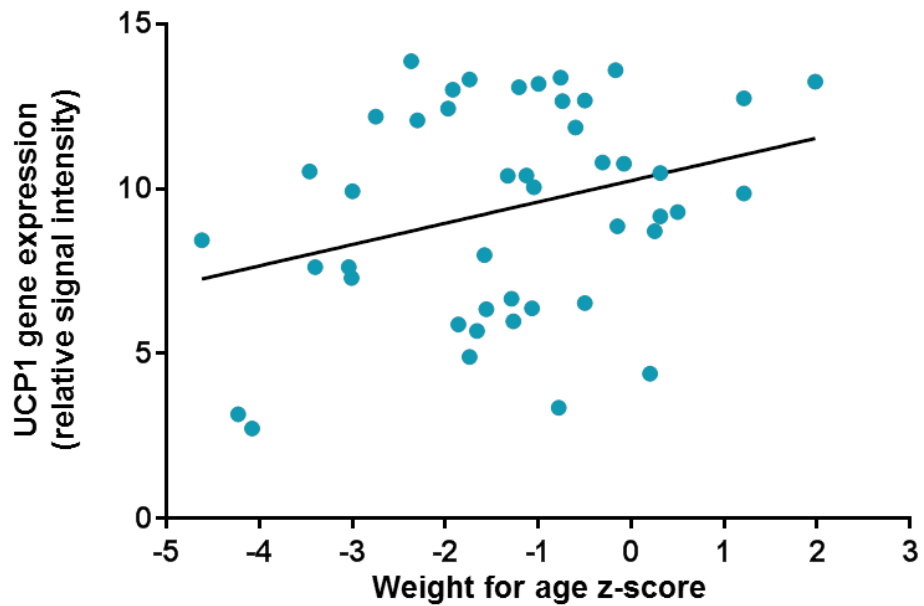


Figure 6.4 Uncoupling protein 1 (UCP1) gene expression in epicardial adipose tissue of children 0-2 years of age correlates with weight for age z-score

Epicardial adipose tissue was sampled from children undergoing cardiac surgery. Each point represents a child ($n = 47$); $r^2 = 0.09$; $p < 0.05$.

mRNA expression of UCP1 is measured as a ratio of the signal intensity obtained from the sample relative to the signal intensity obtained from the positive control on the microarray gene chip.

6.3.2.2.6 The correlation between UCP1 gene expression in epicardial adipose tissue and weight for age z-score is independent of age, gender, baseline oxygen saturations and use of propranolol

On multiple regression analysis, the association between UCP1 gene expression in epicardial adipose tissue and weight for age z-score remained significant despite correcting for age, gender, baseline oxygen saturation levels and use of propranolol in children 0-2 years of age (Table 6.8). However, the relationship was no longer statistically significant when ethnic origin was added to the model (weight for age z-score B = 0.65; SEM = 0.37; β = 0.30; p = 0.08).

Table 6.8 Multiple regression analysis of UCP1 gene expression in epicardial adipose tissue of 0-2 year old children.

UCP1	Gene expression			
	B	SEM	β	p
Constant	9.67	1.15	-	0.00
Age (days)	0.00	0.00	0.05	0.76
Gender	0.26	1.04	0.04	0.80
WAZ	0.79	0.35	0.36	0.03
Baseline SaO ₂	0.92	1.06	0.14	0.39
Use of propranolol	0.91	1.43	0.15	0.47

UCP1, uncoupling protein 1; WAZ, weight for age; SaO₂, oxygen saturation

6.3.2.3 UCP1 in epicardial adipose tissue of newborn infants

There were 15 participants \leq 28 d in age: 12 males and 3 females. Of these, 11 were Caucasian, 3 Asian and 1 of mixed racial origin. Ten had cyanotic congenital heart disease with baseline oxygen saturation levels $<$ 92% while the rest were normoxic. Only one infant was receiving β adrenergic blocker (propranolol). The anthropometric parameters of this group are described in Section 6.3.1.1.1.

6.3.2.3.1 UCP1 gene expression in epicardial adipose tissue of newborn infants (0-28 days) is independent of age, gender, ethnic origin, weight for age z-score or baseline oxygen saturations

The UCP1 gene expression in epicardial fat in this age group was not associated with age, gender, ethnic origin, weight for age z-score, or baseline oxygen saturations (Table 6.9). Only one infant in the 0-28 days age group was on propranolol hence this variable was not included in the analysis.

Table 6.9 Multiple regression analysis of UCP1 gene expression in epicardial adipose tissue of newborn infants.

UCP1	Gene expression			
	B	SEM	β	p
Constant	-12.85	13.72	-	0.31
Age (days)	-0.8	0.14	0.16	0.57
Gender	1.56	2.04	0.26	0.47
Race	-0.28	0.84	-0.10	0.75
WAZ	0.66	0.67	0.28	0.36
Baseline SaO ₂	0.26	0.15	0.50	0.12

UCP1, uncoupling protein 1; WAZ, weight for age; SaO₂, oxygen saturation

6.3.2.4 Epicardial fat mRNA expression of other genes involved in brown and white adipose tissue development and metabolism

6.3.2.4.1 Effect of gender on gene expression

The gene expression of leptin receptor and BMP4 was higher in females compared to males. There was no difference in the gene expression of the other genes between males and females (Table 6.10).

6.3.2.4.2 Effect of ethnic origin on gene expression in epicardial fat

On comparing the gene expression between children of Caucasian and Asian origin, I found that the leptin receptor gene was significantly less expressed in Asian children as compared to children of Caucasian origin but there was no difference in the expression of any of the other genes studied (Table 6.11).

Table 6.10 Comparison between gene expression in males vs. females in epicardial adipose tissue of 0-2 year old children.

Pathway gene	Male (n = 32)	Female (n = 14)	p-value
Leptin	8.84 ± 0.26	8.80 ± 0.42	0.94
Leptin receptor	5.01 ± 0.19	5.56 ± 0.18	0.04
DIO2	3.26 ± 0.07	3.30 ± 0.17	0.85
PPAR α	5.84 ± 0.16	6.07 ± 0.26	0.45
BMP7	4.86 ± 0.06	4.87 ± 0.06	0.92
BMP4	5.08 ± 0.13	5.70 ± 0.16	0.01
Insulin receptor	5.45 ± 0.10	5.30 ± 0.17	0.40
IGF1	9.55 ± 0.12	9.27 ± 0.12	0.10
IGFBP1	5.14 ± 0.13	5.20 ± 0.21	0.82
IGFBP2	5.64 ± 0.09	5.63 ± 0.08	0.98
IGFBP3	4.10 ± 0.08	4.40 ± 0.13	0.06
Ki67	5.49 ± 0.11	5.38 ± 0.19	0.64
β 1ADR	5.76 ± 0.19	5.94 ± 0.14	0.45
β 2ADR	5.32 ± 0.11	5.33 ± 0.15	0.97
β 3ADR	5.45 ± 0.15	5.26 ± 0.43	0.68
GR	8.83 ± 0.12	8.89 ± 0.13	0.74

Abbreviations: DIO2, type 2 iodothyronine deiodinase; PPAR, peroxisome proliferator-activated receptor; BMP, Bone Morphogenetic Protein; IGF, insulin-like growth factor; IGFBP, insulin-like growth factor binding protein; ADR, adrenergic receptor; GR, glucocorticoid receptor. Values are means \pm SEM.

Table 6.11 Comparison between gene expression in Caucasian vs. Asians subjects in epicardial adipose tissue of 0-2 year old children.

Pathway gene	Caucasian (n = 36)	Asian (n = 9)	p-value
Leptin	9.04 ± 0.22	8.44 ± 0.60	0.37
Leptin receptor	5.30 ± 0.16	4.51 ± 0.32	0.04
DIO2	3.32 ± 0.08	3.14 ± 0.07	0.12
PPAR α	6.07 ± 0.14	5.55 ± 0.37	0.22
BMP7	4.90 ± 0.05	4.72 ± 0.08	0.09
BMP4	5.33 ± 0.13	5.05 ± 0.24	0.32
Insulin receptor	5.34 ± 0.10	5.61 ± 0.21	0.62
IGF1	9.48 ± 0.10	9.50 ± 0.30	0.95
IGFBP1	5.28 ± 0.12	4.92 ± 0.23	0.18
IGFBP2	5.65 ± 0.07	5.58 ± 0.16	0.71
IGFBP3	4.26 ± 0.08	3.92 ± 0.13	0.04
Ki67	5.35 ± 0.07	5.55 ± 0.26	0.48
β 1ADR	5.76 ± 0.12	6.07 ± 0.42	0.50
β 2ADR	5.39 ± 0.10	5.16 ± 0.17	0.27
β 3ADR	5.65 ± 0.12	5.12 ± 0.36	0.16
GR	8.77 ± 0.10	9.08 ± 0.23	0.52

Abbreviations: DIO2, type 2 iodothyronine deiodinase; PPAR, peroxisome proliferator-activated receptor; BMP, Bone Morphogenetic Protein; IGF, insulin-like growth factor; IGFBP, insulin-like growth factor binding protein; ADR, adrenergic receptor; GR, glucocorticoid receptor. Values are means ± SEM.

6.3.2.5 Expression of leptin gene in epicardial fat is associated with weight for age z-score in 0-2 year old children

As leptin is thought to be related to white fat mass, I further analysed the relationship between the child's nutritional status (as measured by weight for age z-score) and gene expression of leptin in the epicardial adipose tissue and found there was a significant correlation between the gene expression of leptin and weight for age z-score ($r^2 = 0.13$; $p = 0.02$). Gene expression of leptin was upregulated with increase in weight for age z-score (Figure 6.5).

6.3.2.6 Expression of leptin gene in epicardial fat is not associated with age in children 0-2 years of age

There was no significant correlation between age and leptin gene expression in children ($R^2 = 0.01$; $p = 0.41$).

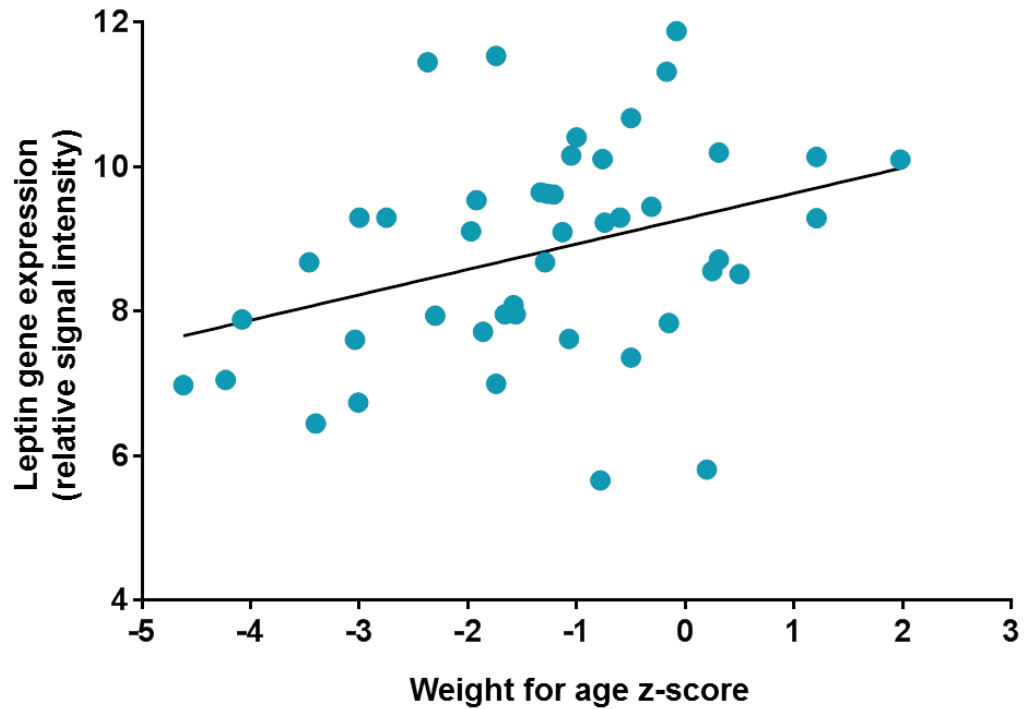


Figure 6.5 Leptin gene expression in epicardial adipose tissue of children 0-2 year old correlates with weight for age z-score

Epicardial adipose tissue was sampled from children undergoing cardiac surgery. Each point represents a child ($n = 47$); $r^2 = 0.13$; $p < 0.05$

mRNA expression of leptin is measured as a ratio of the signal intensity obtained from the sample relative to the signal intensity obtained from the positive control on the microarray gene chip.

6.3.3 Gene expression in children with high vs. low UCP1 gene expression

UCP1 gene expression is a marker of presence of BAT (Nedergaard and Cannon 2013). The mean \pm SEM relative expression of UCP1 mRNA for the 15 newborn infants included in this study was 9.84 ± 0.78 . As it is well known, and accepted, that newborn infants have significant amounts of brown fat (Aherne and Hull 1966), I assumed that participants who have UCP1 gene expression comparable to that in newborn infants, are likely to have significant amounts of BAT.

Therefore, to analyse the expression of other genes related to brown and white fat development and metabolism, I divided the 42 participants (out of 57 total participants (0-18 years old)) whose samples were analysed by microarray into those whose UCP1 relative gene expression was equal to, or higher than, the UCP1 gene expression in the newborn infants (high UCP1) and those whose relative UCP1 gene expression was lower than the mean of the newborn infants (low UCP1).

The gene expression of glucocorticoid receptor (GR) was significantly downregulated and the expression of leptin, type 2 iodothyronine deiodinase (DIO2), peroxisome proliferator-activated receptor (PPAR) α , insulin-like growth factor binding protein (IGFBP) 1, IGFBP2, β 2 adrenergic receptor (ADR), and β 3ADR were significantly upregulated

in children with high UCP1 gene expression when compared to those who had low UCP1 gene expression (Table 6.12).

In addition, in children with high UCP1 gene expression, UCP1 expression had a positive correlation with expression of the leptin gene ($R^2 = 0.53$; $p < 0.001$) and negative correlation with mRNA expression of the gene for glucocorticoid receptor ($R^2 = 0.51$; $p < 0.001$).

Furthermore, in these children, gene expression of UCP1 also had a significant positive correlation with mRNA expression of BAT related genes: DIO2 ($R^2 = 0.26$; $p < 0.001$) and $\beta 3$ ADR ($R^2 = 0.16$; $p = 0.005$).

Table 6.12 Comparison between gene expression in children with high vs. low UCP1 gene expression.

Pathway gene	High UCP1 (n = 22)	Low UCP1 (n = 20)	p-value
Leptin	9.52 ± 0.22	7.56 ± 0.31	<0.001
Leptin receptor	5.04 ± 0.91	5.47 ± 1.05	0.161
DIO2	3.38 ± 0.11	3.08 ± 0.05	0.019
PPAR α	6.38 ± 0.15	5.31 ± 0.21	<0.001
BMP7	4.98 ± 0.08	4.79 ± 0.07	0.090
BMP4	5.31 ± 0.13	5.47 ± 0.14	0.431
Insulin receptor	5.35 ± 0.11	5.55 ± 0.11	0.209
IGF1	9.36 ± 0.15	9.70 ± 0.18	0.140
IGFBP1	5.58 ± 0.12	4.77 ± 0.19	0.001
IGFBP2	5.77 ± 0.08	5.44 ± 0.13	0.031
IGFBP3	4.40 ± 0.12	4.08 ± 0.12	0.073
Ki67	5.23 ± 0.11	5.50 ± 0.66	0.145
β 1ADR	5.94 ± 0.14	5.99 ± 0.25	0.869
β 2ADR	5.60 ± 0.09	5.07 ± 0.14	0.002
β 3ADR	5.93 ± 0.10	4.83 ± 0.31	0.001
GR	8.59 ± 0.12	9.41 ± 0.09	<0.001

Abbreviations: DIO2, type 2 iodothyronine deiodinase; PPAR, peroxisome proliferator-activated receptor; BMP, Bone Morphogenetic Protein; IGF, insulin-like growth factor; IGFBP, insulin-like growth factor binding protein; ADR, adrenergic receptor; GR, glucocorticoid receptor. Values are means \pm SEM.

6.3.4 Uncoupling Protein 1 is present in epicardial adipose tissue

6.3.4.1 Epicardial adipose tissue of newborn infants is predominantly brown fat

Immuno-histochemical analysis of sections of epicardial adipose tissue from all 15 newborn infants included in the study demonstrated the presence of UCP1 in multilocular adipocytes with only occasional interspersed large unilocular adipocytes that did not stain for UCP1. An example of the images obtained from these participants is shown in Figure 6.6.

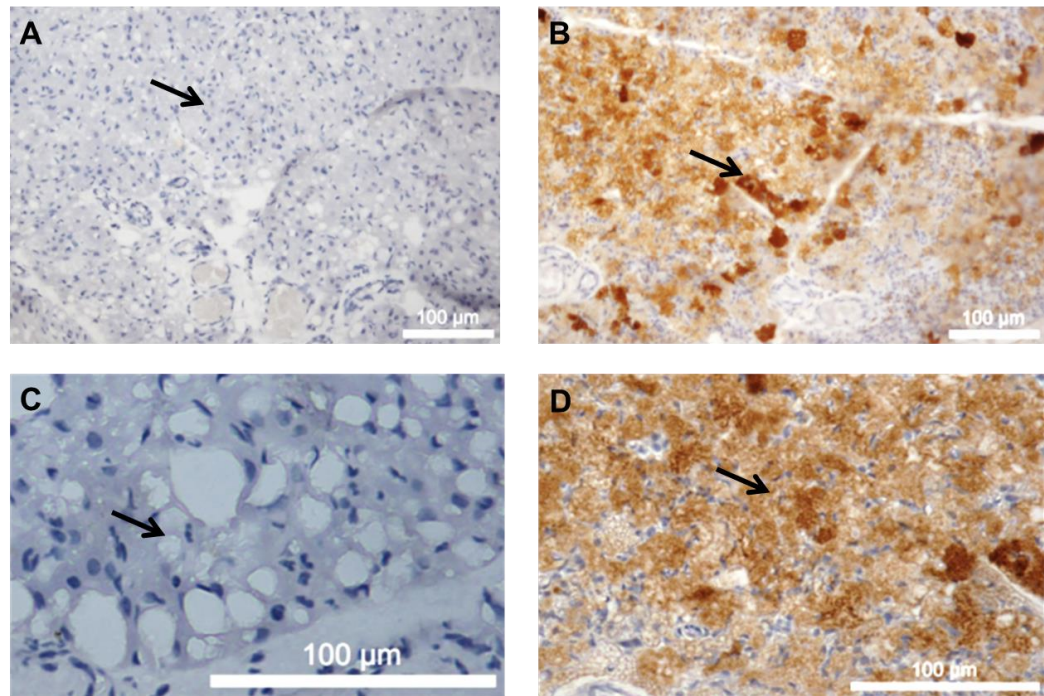


Figure 6.6 Representative images of epicardial adipose tissue from a 6 day old male infant

Immunohistochemical detection of uncoupling protein 1 (UCP1): antibody negative (A and C) and antibody positive (B and D) showing the presence of small multilocular adipocytes (indicated by black arrows). These multilocular adipocytes stained positive for UCP1 (B and D) demonstrating that these are brown adipocytes and the depot is brown fat.

6.3.4.2 Islands of brown adipose tissue are present in epicardial fat of older infants and adolescents.

Epicardial adipose tissue samples obtained from older infants (>28 days of age) were predominantly white. A representative sample from these participants showing large unilocular white adipocytes that did not stain with UCP1 is given in Figure 6.7. However, randomly selected histological sections taken from 9 out of 40 (22.5%) participants over 28 days of age contained interspersed islands of small, multilocular adipocytes that stained positive with UCP1 antibody as demonstrated in the representative images in Figure 6.8.

In addition, UCP1 positive multilocular adipocytes were also present in samples from all the three adolescents who participated in this study as shown in the representative images shown in Figure 6.9.

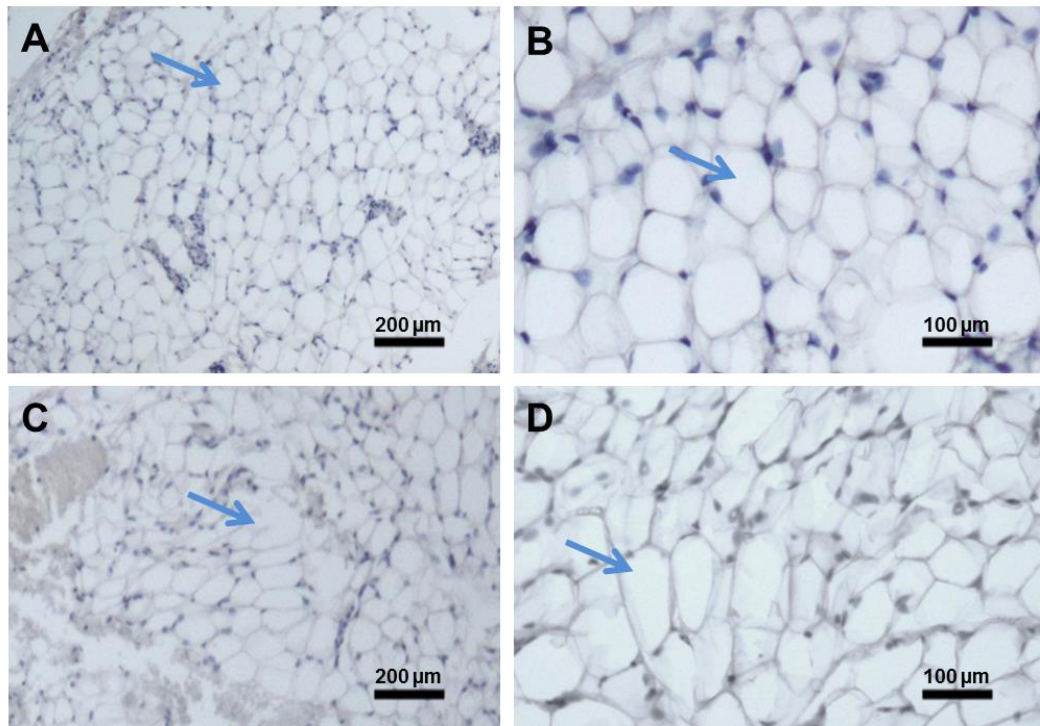


Figure 6.7 Representative images of epicardial adipose tissue from an 18 month old male child

Immunohistochemical detection of uncoupling protein 1 (UCP1): antibody negative (A and C) and antibody positive (B and D) showing the presence of large unilocular adipocytes(indicated by blue arrows) that did not stain positive with UCP1 antibody demonstrating that these are white adipocytes and the depot is white fat

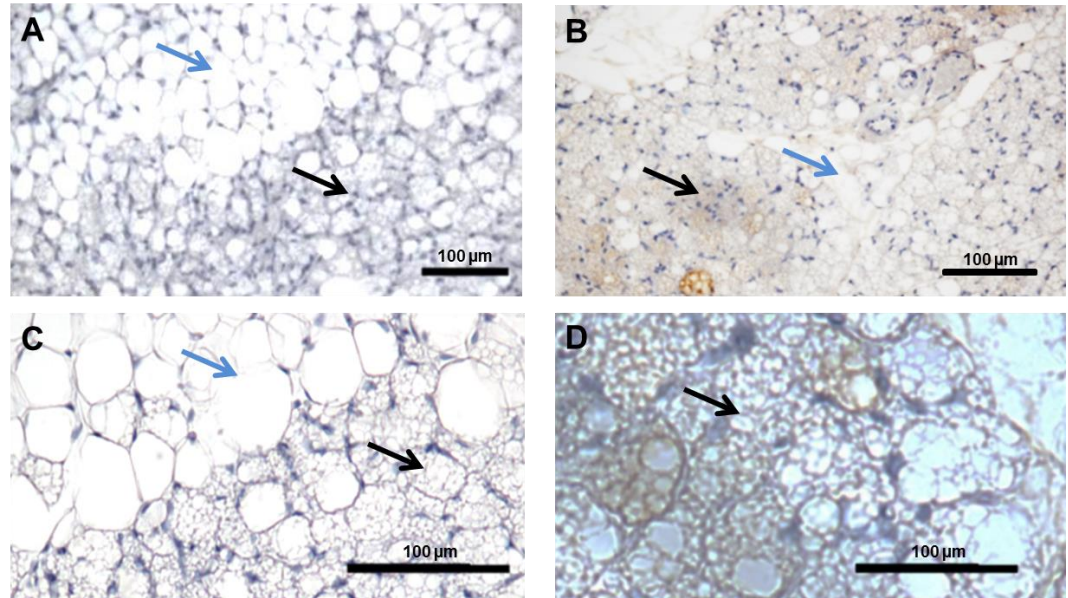


Figure 6.8 Representative images of epicardial adipose tissue from a 3 year old male child

Immunohistochemical detection of uncoupling protein 1 (UCP1): antibody negative (A and C) and antibody positive (B and D) showing the presence of large unilocular adipocytes (indicated by blue arrows) with adjoining areas with small multilocular adipocytes (indicated by black arrows). The multilocular adipocytes stained positive for UCP1 (B and D) demonstrating that these are brown adipocytes and the depot a mixture of brown and white fat.

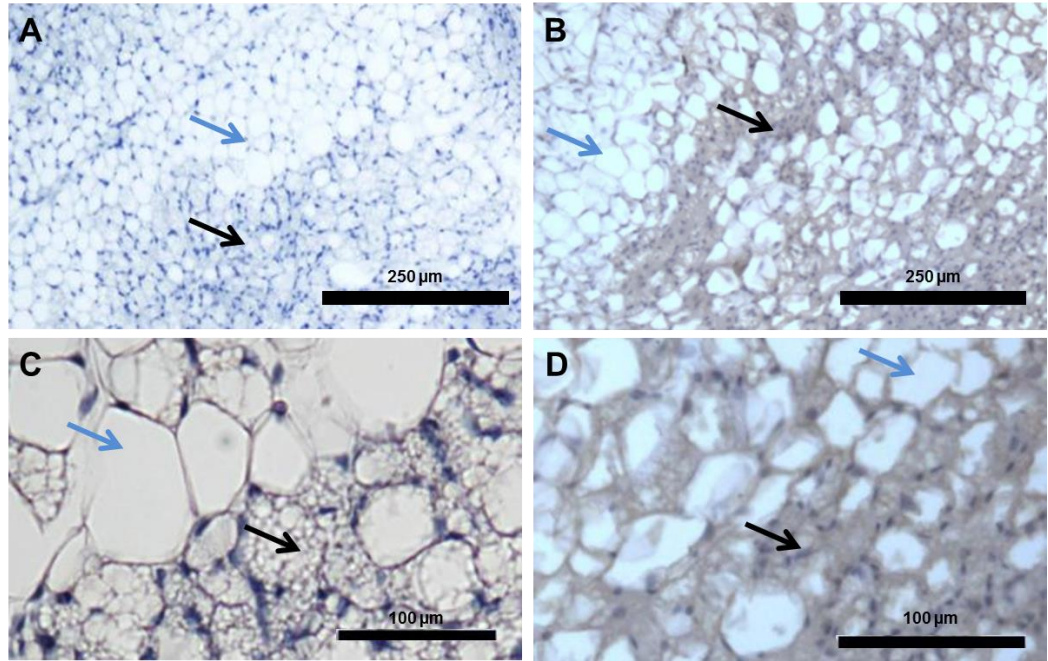


Figure 6.9 Representative images of epicardial adipose tissue from a 17 year old male

Immunohistochemical detection of uncoupling protein 1 (UCP1): antibody negative (A and C) and antibody positive (B and D) showing the presence of large unilocular adipocytes (indicated by blue arrows) with adjoining areas with small multilocular adipocytes (indicated by black arrows). The multilocular adipocytes stained positive for UCP1 (B and D) demonstrating that these are brown adipocytes and the depot a mixture of brown and white fat.

6.4 Discussion

6.4.1 Human epicardial adipose tissue is a depot of brown fat in newborn infants and children

The most significant finding of this study is that epicardial adipose tissue is a depot of brown fat in newborn infants and older children. Sack *et al.* reported UCP1 gene expression in epicardial fat of adults and I have confirmed the presence of brown fat in the depot by demonstrating the presence of UCP1 by Western Blotting (Chapter 5). In this study, I found that UCP1 gene is expressed in epicardial fat throughout early childhood and in adolescence. Furthermore, it appears that the gene expression of UCP1 does not decline with age, at least up to 2 years of age, as there was no difference between gene expression in newborn infants and older children. Whilst this study had relatively few children older than 2 years of age, the 13 samples obtained from older children demonstrate that UCP1 gene expression is present in later childhood and adolescence.

The presence of brown fat in the epicardial depot was confirmed by histology and immunohistochemistry. The histological sections taken from newborn infants were replete with multilocular, small adipocytes that stained strongly for UCP1, demonstrating that epicardial fat is brown at this age. In older children, the depot appears to be predominantly white, with large, unilocular adipocytes that do not stain

with UCP1 with islands of small, multilocular adipocytes that stained positive for UCP1. Samples taken from all the three adolescents included in this study demonstrated the presence of islands of UCP1 positive, multilocular, smaller adipocytes interspersed between white adipocytes. These findings establish that, although epicardial fat is predominantly white after the newborn period, the depot contains clusters of brown or “brown-like” adipocytes throughout childhood and adolescence.

My finding that many children have high levels of UCP1 gene expression and demonstrable UCP1 on immunohistochemistry is in keeping with ¹⁸F-FDG PET-CT scan studies demonstrating that BAT is detected more frequently in children than in adults (Gelfand et al. 2005, Bar-Sever et al. 2007, Zukotynski et al. 2009, Drubach et al. 2011, Gilsanz et al. 2013). Detection of “hot spots” using infrared thermography also suggests that BAT is present in all healthy children (Robinson et al. 2014).

This study confirms that BAT is present in children and that epicardial fat is a depot of BAT in humans. The findings presented here demonstrate, for the first time, that the epicardial fat depot is BAT in newborn infants and UCP1 gene expression is present throughout childhood. Furthermore, the results reveal that, at least in some individuals, particularly in adolescence, pockets of brown or “brown-like”

adipocytes persist within the predominantly white adipose tissue that makes up the epicardial fat mass.

6.4.2 Caucasian children have a higher expression of UCP1 gene when compared to children of South Asian and mixed ethnicity

Further analysis of UCP1 gene expression in 0-2 year old children showed that children of Caucasian origin had a significantly higher expression of the UCP1 gene when compared to Asian/mixed ethnic children. Although mRNA expression of UCP1 gene is a good marker of presence of BAT, caution should be exercised when interpreting the results as UCP1 gene expression is not a measure of BAT function and such differences in mRNA expression may not signify differences in metabolic or other functional capacities of BAT in the individual.

Asians originating from the Indian sub-continent are known to have a greater risk of cardiovascular and metabolic illnesses. In the UK, this sub-group of the population has a 3-4 times higher risk of developing Type 2 diabetes as compared to the general population, in parallel to a similar scale of increased risk for coronary heart disease and metabolic syndrome even at the same body mass index (HSE 2006). The underlying cause of this risk is not completely understood but might involve genetic differences in metabolism and energy homeostasis (Hall et al. 2010).

It has been suggested that a reduced amount of BAT may be one of the factors contributing to the disadvantaged metabolic profile seen among Asians from the Indian sub-continent (Bakker et al. 2014).

Bakker and colleagues demonstrated that healthy lean young men of South Asian descent had lower resting energy expenditure, lower BAT volumes and were more dependent on shivering thermogenesis to maintain body temperature during cold exposure when compared to white Caucasians of similar age and BMI (Bakker et al. 2014). In a similar study, Admiraal *et al.* could not find an ethnic difference in metabolic activity in BAT when comparing South Asians with Caucasians (Admiraal et al. 2013). The differences, however, may not have been apparent in the study of Admiraal *et al.* as the authors used a room with a fixed cool temperature (16-18°C) to activate BAT in the participants. There are inter-individual differences in the onset temperature of shivering and less intense cooling may have underestimated BAT volume and activity in some study participants. Indeed, Bakker *et al.* found that, despite an increased fat mass percentage, the temperature at which shivering started was higher in South Asians than in Caucasians (Bakker et al. 2014). In a previous smaller, retrospective review of PET-CT images, no difference in BAT volume was detected between African and Caucasian cancer patients but BAT was detectable in only a small number of Asian patients (Perkins et al. 2013).

Conversely, a study of assessment of BAT function by infrared thermography in 6-11 year old children indicated that those who were non-Caucasians (but born in the UK) had more active BAT than the Caucasian children (Robinson et al. 2014). The children included in the latter study were healthy and older and had a higher BMI (BMI centile 58.8 ± 28.0 (mean \pm SD)) than the cohort included in my study. The non-Caucasian children included in Robinson et al. study were of several different ethnic origins while the non-Caucasian children in my current study were all of South Asian (Indian subcontinent) origin. The two mixed ethnic origin children had one parent who was Asian.

In the present study, I found that ethnic differences in molecular characteristics of BAT are present from early childhood. Given its high capacity to dissipate excess energy and its role in lipid and glucose metabolism, such differences in BAT may be a contributing factor to the disadvantageous metabolic phenotype that makes South Asians more susceptible to obesity and its adverse cardio-metabolic complications.

6.4.3 There was no difference in UCP1 gene expression between boys and girls in early childhood

I did not find any difference in UCP1 gene expression between boys and girls either in the newborn period (0-28 days of life) or up to 2 years of age. Due to limited number of participants over two years of age, I

was unable to analyse the relationship between gender and UCP1 gene expression in older children and adolescents.

In adults, it is unclear whether there is a clear gender dimorphism in BAT deposition (Bloor and Symonds 2014). Men and women have a similar distribution of BAT although some studies have reported greater mass of BAT and higher ^{18}F -FDG uptake in women as compared to men (Cypess et al. 2009), while others did not demonstrate any gender differences in ^{18}F -FDG uptake (Saito et al. 2009). The difference in ^{18}F -FDG intake may be explained by greater cold sensitivity in females (Quevedo et al. 1998) although it does not explain the finding by Pfannenber *et al.* that age related reduction in BAT activity and volume occurs more rapidly in men than in women (Pfannenber *et al.* 2010).

Studies in children have not reported differences in BAT detection rate between boys and girls (Drubach et al. 2011, Gilsanz et al. 2012).

Some gender differences in BAT prevalence may depend on stage of pubertal development. Gilsanz *et al.* found no significant differences in the prevalence of PET-CT studies depicting BAT (20 of 35 girls and 23 of 38 boys; $p = 0.769$) but as BAT volume increased with puberty, the volume became significantly greater in boys than in girls during Tanner stages 4 and 5 of pubertal development (Gilsanz et al. 2012). This supports my finding that, among children under 2 years of age, there is no difference in UCP1 gene expression. Differences in BAT volume and

characteristics may arise later in adolescence. Indeed, in the male adolescents included in this study, I found islands of UCP1 positive, multilocular adipocytes within the epicardial adipose sections studied. However, due to limitation of sample size and absence of female adolescent participants, no definite conclusions on post-pubertal gender dimorphism can be derived.

6.4.4 UCP1 gene expression was not affected by treatment with propranolol

The children who participated in this study had congenital heart disease and six participants were receiving regular treatment with propranolol, a β -ADR blocker. I did not find any difference in UCP1 gene expression between children who were on regular propranolol when compared to children who were not receiving any β -adrenergic blockers. This is contrary to my hypothesis as β adrenergic stimulation is the major stimulant for UCP1 gene expression and BAT development and activity, at least in rodents (Cannon and Nedergaard 2004).

Brown adipose depots are richly innervated by sympathetic nerves and β adrenergic stimulation is the major drive for proliferation, differentiation and metabolism in brown adipocytes including the expression and function of the UCP1 gene (Cannon and Nedergaard 2004). In adults, there is some evidence that brown fat activation can be inhibited by a single dose of propranolol (Parysow et al. 2007, Agrawal

et al. 2009). Söderlund and colleagues studied eleven adults with strong brown fat uptake on ^{18}F -FDG PET-CT scans; BAT activity almost completely disappeared on the repeat scan performed two hours after oral administration of 80 mg propranolol (Soderlund et al. 2007). Similarly, Parysow *et al.* found a significant reduction in BAT activity with a smaller dose (20 mg) (Parysow et al. 2007). The usual therapeutic dose of propranolol is 80-240 mg in a day in adults and 2-5mg/kg/day in children.

However, despite the above mentioned studies, there is contradictory evidence and it is unclear whether propranolol and other β -adrenergic blockers affect BAT activity in humans. Wijers *et al.* conducted an elaborate experiment with ten lean male subjects in a respiration chamber and studied the effect of propranolol intake on energy expenditure and mitochondrial uncoupling in muscle biopsy samples after cold exposure (Wijers et al. 2011). They found that cold exposure increased energy expenditure and this response was decreased by intake of propranolol. However, despite efficient inhibition of the sympathetic nervous system (as indicated by significantly reduced heart rate and decrease in energy expenditure), cold-induced thermogenesis was not affected. This is supported by the finding that pharmacological stimulation of the β -adrenergic sympathetic nervous system activity increases energy expenditure similar to that in response to cold exposure but, although BAT activity is increased in response to cold,

adrenergic stimulants such as ephedrine and isoprenaline do not increase BAT activity in humans (Cypess et al. 2012, Vosselman et al. 2012). These findings suggest that additional mechanisms may be involved in regulation of BAT thermogenesis in humans.

In this study, I have analysed the gene expression of UCP1 and found no effect of propranolol therapy. Epicardial adipose tissue sections taken from children on propranolol also stained positive for UCP1. It is possible that although there is no difference in gene expression and some UCP1 positive cells persist, children on regular propranolol may have reduced activation of brown fat in response to cold or other stimulation. This requires further investigation.

Another explanation for the lack of an effect of propranolol on BAT may be that sympathetic stimulation of BAT is mainly governed by β_3 adrenergic receptors, at least in rodents (Cannon and Nedergaard 2004). Propranolol is more selective for β_2 and β_1 adrenergic receptors and this may also explain why UCP1 gene expression was not downregulated by intake of propranolol. Although clinical trials of selective β_3 receptor agonists did not demonstrate any effect on energy metabolism or weight loss (Larsen et al. 2002, Redman et al. 2007), novel selective β_3 receptor agonists have recently been shown stimulate BAT thermogenesis in humans (Cypess et al. 2015) and as a

consequence are being investigated as a potential pharmacological strategy against obesity.

6.4.5 In early childhood (0-2 years), gene expression of UCP1 in epicardial fat is downregulated in children with lower weight for age z-scores

The participants of this study were all patients with congenital heart disease, a group particularly vulnerable to poor nutrition and growth (Steltzer et al. 2005). The newborn infants included in the study were of normal weight and length but, beyond the newborn period (> 28 days of age), one third of children had WAZ less than – 2 SD below the mean for their age and gender and one quarter had HAZ less than – 2 SD below the mean. This is in keeping with the existing records of growth in children with congenital heart disease; most infants with these conditions have normal weight for gestational age at birth but develop nutritional and growth problems in early infancy (Bayer and Robinson 1969, Salzer et al. 1989, Cameron et al. 1995, Daymont et al. 2013). Although growth deficits are global (Daymont et al. 2013), weight can be more affected than height (Thommessen et al. 1992). Energy imbalance as a consequence of reduced intake due to feeding problems and increased energy requirements due to hypermetabolic state are believed to be causes of faltering growth (Nydegger and Bines 2006, Medoff-Cooper and Ravishankar 2013). Detailed data on nutritional intake and energy expenditure in the participants was not

available and I was unable to analyse the exact aetiology of the lower than expected weights and heights.

WAZ reflects body mass relative to chronological age and is a marker of nutritional status of the child (WHO 1986). Changes in weight can be precipitated by inter-current illnesses and short periods of poor nutrition and, therefore, it may not be a good marker of long term nutrition (Gorstein et al. 1994). However, as weight increases more rapidly in infancy than height, WAZ can be a sensitive marker of nutrition in early life (WHO 1986).

In this cohort, gene expression of UCP1 was downregulated with poor nutrition as indicated by a low WAZ. Rockstroh and colleagues recently published an analysis of UCP1 gene expression in adipose tissue samples from children and adults and did not find any correlation between anthropometric markers and UCP1 gene expression in subcutaneous adipose tissue (Rockstroh et al. 2015). Subcutaneous adipose tissue is not a typical depot of BAT and Rockstroh found that only 3 out of 80 subcutaneous adipose tissue samples were positive for UCP1 on immunohistochemistry. In the epicardial adipose tissue samples that I have analysed, UCP1 was present in a much higher proportion (23%) of children and adolescents. An association between anthropometry and gene expression of UCP1 may therefore be more demonstrable in this richer depot of BAT.

UCP1 gene expression in fetus and newborn is known to be nutritionally regulated, at least in sheep (Symonds et al. 2003, Budge et al. 2004, Mostyn et al. 2004). In the adipose depot present around the heart, I have previously shown that, in sheep, UCP1 gene expression is upregulated with suboptimal maternal nutrition in early-to-mid gestation followed by ad libitum feeding in later pregnancy (Chapter 4 (Ojha et al. 2014)) while it is down regulated by reduced maternal nutrition in late gestation (Chapter 3 (Ojha et al. 2013)). The results of the current study indicate that UCP1 gene expression in humans is also nutritionally regulated in the early years of postnatal life; children with poorer nutritional states as indicated by low WAZ have less UCP1 gene expression. This relationship was independent of the child's gender, postnatal age, base line oxygen saturation levels and whether the child was taking regular β -blockers or not. However, the finding was confounded by the child's ethnic origin. As the children of Asian origin had a significantly lower WAZ as compared to children of Caucasian origin, it is difficult to ascertain whether the downregulation in the UCP1 gene is due to poor nutrition or genetic/phenotypic ethnic differences.

In older children, it is unclear whether BAT volume and activity, as measured by ^{18}F -FDG uptake on PET-CT scans, correlates with anthropometric measures. Gilsanz and colleagues did not find any difference in weight, BMI or measures of adiposity in children with or without BAT although muscle volume was greater in BAT positive

children (Gilsanz et al. 2011). Conversely, Durbach et al. found an inverse relation between BMI centile and BAT activity in a cohort of children; the patients in this study were older with age of 14.2 ± 3.7 (mean \pm SD) years and had higher BMI centiles (62.9 ± 31.5 (mean \pm SD)) (Drubach et al. 2011) than the younger children with lower weights and BMI included in the current study. Similarly, measuring BAT activity by infrared thermography, Robinson *et al.* also found a negative relationship between BMI percentile and baseline supraclavicular region temperature, which may be a marker of baseline BAT activity (Robinson et al. 2014).

All previous studies assessing BAT activity and BMI in children include older children who are relatively better nourished (including a proportion of overweight and obese children) (Drubach et al. 2011, Gilsanz et al. 2011, Robinson et al. 2014) than those included in my study. The nutritional regulation of UCP1 may be age dependent and poor nutrition in early life may reduce BAT development to enable the rapidly growing child to conserve energy for growth.

6.4.6 In early childhood (0-2 years), gene expression of leptin in epicardial fat is downregulated in children with lower weight for age z-scores

In parallel to the positive linear relationship between WAZ and UCP1 in the 0-2 year old children, I also found a positive correlation between WAZ score and leptin gene expression. Leptin is a marker of white

adipose tissue and high serum leptin concentrations are associated with increasing fat mass in children (Johnson et al. 2001). Leptin mRNA expression increases with obesity in adults (Lonnqvist et al. 1995, Maffei et al. 1995) and in children (Hassink et al. 1996) and is higher in adipose tissue obtained from obese children when compared to samples from non-obese children (Lindgren et al. 1997). This is in keeping with my finding that leptin mRNA expression is downregulated with reduction in WAZ in children.

There are depot specific differences in leptin gene expression and children with congenital heart disease have higher leptin gene expression in subcutaneous fat compared with intra-thoracic fat (Schoof et al. 2004). Some studies have reported increasing leptin mRNA expression with age at specific sites such as subcutaneous (Lindgren et al. 1997, Schoof et al. 2004), intrathoracic and omental fat but not in mesenteric fat (Schoof et al. 2004). I did not find a relationship between leptin gene expression and age in this cohort. This may be due to depot specific differences between fat in the epicardial and other sites.

6.4.7 Children with high UCP1 gene expression have a different mRNA expression pattern as compared to children with low UCP1 gene expression

It is now well recognised that BAT is present beyond the newborn period, at least in some individuals (Cypess et al. 2009, Gilsanz et al. 2013, Rockstroh et al. 2015). In the cohort of children included in the

current study, 23% of those over 28 days of age had UCP1 present on immunohistochemical examination of their epicardial adipose tissue samples. More than half of the children over 28 days of age had UCP1 gene expression equal to, or more than, the mean of the UCP1 gene expression found in newborn infants. Comparison between children with high vs. low UCP1 gene expression revealed differences in expression of other genes related to brown and white adipose tissue development and metabolism.

Children with low UCP1 gene expression had low leptin mRNA expression and there was a positive correlation between the expressions of these two adipose tissue markers. Leptin is a marker of white adipose tissue (Margetic et al. 2002) and Rockstroh *et al.* found a reduction in leptin gene expression in the UCP1 positive adipose tissue samples (Rockstroh et al. 2015). The opposite finding in my study could be due to the relatively poor nutritional status of the participants. Both UCP1 and leptin gene expression correlated with WAZ and it is possible that the poor nutrition in these children suppressed both brown and white fat development as reflected by the concomitant reduction in UCP1 and leptin gene expression, respectively. This is supported by the finding that gene expression of peroxisome proliferator-activated receptor alpha (PPAR α), a ligand activated transcription factor that is a regulator of adipocyte differentiation and lipid metabolism (Ferre 2004), was also downregulated in children with low UCP1 gene expression.

Genes related to BAT were upregulated in those who had high UCP1 gene expression and the mRNA concentrations of BAT related genes such as DIO2 and β 3ADR had a positive correlation with gene expression of UCP1. DIO2 is an enzyme that catalyses the conversion of thyroxine (T4) into triiodothyronine (T3). It is highly expressed in BAT (Silva and Larsen 1983), is an inducer of UCP1 gene expression and protein synthesis in brown adipocytes (Bianco and Silva 1987) and is essential for optimum thermogenesis (de Jesus et al. 2001).

Sympathetic control of BAT development, activity and metabolism are believed to be regulated mainly via β 3ADRs (Rohlf's et al. 1995) and the thermogenic response of brown adipocytes is predominantly mediated via these receptors (Zhao et al. 1994). Reduction of gene expression of DIO2 and β 3ADR suggest that BAT function may also be compromised in these children.

The gene expression of GR was increased in children with low UCP1 gene expression while genes for insulin like growth factor binding proteins 1 and 2 were reduced signifying that adipose tissue metabolism may have been affected in these children. Glucocorticoid action is dependent on the density of the intracellular receptors and the level of pre-receptor metabolism. Cortisol binds to GR within the cytoplasm and the cortisol-GR complex translocates to the nucleus where it regulates the transcription of target genes (Campbell et al. 2011). Glucocorticoid action induces differentiation in preadipocytes,

thereby enhancing adipogenesis, whereas cortisol increases lipolysis in mature adipocytes. Normally the adipogenic action of glucocorticoids is more prominent than the lipolytic effect such that excessive glucocorticoids increase adipose tissue mass through hyperplasia rather than hypertrophy. In addition, glucocorticoids also modulate adipose tissue via effect on inflammation and low GR abundance can attenuate the immunomodulatory and other effects of glucocorticoids. Increased tissue cortisol concentration and increased tissue-specific glucocorticoid sensitivity have been implicated in the pathophysiology of the metabolic syndrome (Anagnostis et al. 2009). Glucocorticoid sensitivity is influenced by and directly related to the amount GR mRNA (Melo et al. 2004, Sousa e Silva et al. 2010) and elevated local increase in GR gene expression in visceral adipose tissue can increase the predisposition to metabolic abnormalities including insulin resistance (Vegiopoulos and Herzig 2007).

6.4.8 Epicardial fat in children

Epicardial fat, the fat deposited within the pericardial sac, is a metabolically active adipose tissue (Sacks and Fain 2007). Deposits of fat within the pericardium are present in the fetus and the newborn human (Fletcher et al. 1987) and other species (Marchington et al. 1989). Primary epicardial cells grown from human embryonic heart tissue explants demonstrate prominent adipocyte differentiation both spontaneously and in response to exposure to adipogenesis-inducing

mixtures, a process that is driven by the expression of PPAR γ in several cell types (Yamaguchi et al. 2015). This behaviour, when occurring in vivo, results in the presence of epicardial fat over the heart in newborn infants and thereafter throughout childhood and later life.

Several studies in adults have demonstrated the relationship between epicardial fat accumulation and cardiovascular pathologies (as discussed in Chapter 1 (Section 1.10.3.1)). Although most studies have been performed in adults, emerging evidence suggests that epicardial fat could be equally important in children and accumulation of fat in this depot may be an early marker of adverse cardiovascular and metabolic outcomes.

In a study of 46 obese subjects (10.2 ± 2.5 years of age, 25 boys) and 30 age- and gender matched lean subjects (10.8 ± 3.1 years of age, 13 boys), Abaci *et al.* demonstrated that accumulation of fat in the epicardial depot is correlated with BMI and, above a cut off value of 4.1mm, thickness predicts insulin resistance in obese children (Abaci et al. 2009). This finding was reproduced in another study of peri-pubertal children (Manco et al. 2013). However, Mazur *et al.* found that although thickness of epicardial fat was a good indicator of visceral adiposity, it was not an independent predictor of metabolic syndrome or insulin resistance in children (Mazur et al. 2010). Schusterova *et al.* also found that epicardial fat thickness in children is associated with an

unfavourable cardio-metabolic risk profile but that body mass index was a stronger indicator (Schusterova et al. 2014).

In addition, similar to the associations found in adults, epicardial fat thickness in children is significantly correlated with left atrial and left ventricular mass and has a significant and independent association with increased carotid intima-media thickness, a subclinical form of carotid atherosclerosis (Cabrera-Rego et al. 2014). In children with a family history of Type 2 diabetes, Mahfouz *et al.* found increased epicardial fat thickness with increased diastolic dysfunction as compared to age and BMI matched controls who did not have family history of type 2 diabetes (Mahfouz et al. 2015).

Emerging evidence suggests that the epicardial depot in children, as in adults, may be an important repository of visceral fat and, due to its proximity to the heart, it is postulated that it could play a vital role in the evolution of cardio-metabolic pathologies. BAT has a vital role in energy homeostasis and particularly in lipid (Bartelt et al. 2011) and glucose (Orava et al. 2011) metabolism. The novel finding here that epicardial fat is a depot of BAT in newborn infants and retains brown or brown-like adipocytes throughout childhood and adolescence raises the possibility that BAT could play a role in evolution of cardiovascular physiology and pathogenesis from early life and the potential of using

BAT activation as a therapeutic target for prevention and treatment of cardiovascular illnesses.

6.4.9 Strengths of the study

This is the first study looking at the presence of BAT in epicardial fat in children. The large number of participants included in the study enabled a detailed analysis of gene expression in early childhood. Availability of clinical data made it possible to further analyse gene expression in relation to age and anthropometric parameters. The population from which the patients were derived (in and around Leicester, U.K.) is such that the cohort contains adequate number of Asian patients from a similar ethnic background allowing analysis of UCP1 gene expression in relation to ethnic origin. As the participants were patients with congenital heart disease, effects of the use of β -adrenergic blocker medication and of low oxygen saturation levels, both factors that may have affected UCP1 gene expression, these could be analysed without any additional intervention in the children.

UCP1 gene expression, especially when measured by highly sensitive technologies such as microarray assay, does not prove the presence of BAT. The additional strength of this work is that the presence of BAT was confirmed by immunohistochemical demonstration of UCP1 in epicardial fat.

6.4.10 Limitations of the study

The children who contributed to this study were not healthy volunteers. Their illness and poor nutritional status may have confounded the findings of the gene analysis. However, this was unavoidable as epicardial tissue samples can only be collected from individuals undergoing cardiac surgery, a population that is, by definition, unwell and is known to have poor nutrition (Salzer et al. 1989, Daymont et al. 2013). Nevertheless, this is the first study to demonstrate the presence of BAT in epicardial fat in children and access to these numbers of epicardial tissue samples from living subjects could only be obtained from children undergoing cardiac surgery.

Another limitation of this study is the skewed age distribution of the participants. Whilst 48 out of 57 adipose tissue samples suitable for gene analysis were from children less than or equal to two years of age making the study findings very strong in children in the 0-2 year age group, gene analysis results were available for only 12 children between 2 and 18 years of age. This is because most children with congenital heart disease require surgery in the first few years of life and the samples could only be collected at the time of the surgery. It is, therefore, difficult to make any firm conclusions about the gene expression results in later childhood and adolescence. However, children >2 years old had detectable levels of UCP1 gene expression that were comparable to the expression in the younger children.

Nevertheless, larger numbers of samples are required to study the changes in UCP1 and other gene expression over the childhood years and adolescence.

Pubertal development may have a major impact on BAT development in children (Gilsanz et al. 2012); adipose tissue samples collected from a larger number of older pre- and post- pubertal children would allow a better analysis of changes in BAT during a childhood and puberty. Further details of pubertal development and data on nutritional intake and body composition of the participants would enable more sophisticated analyses.

The results were affected by the finding that children of Asian ethnic origin had significantly lower WAZ at all ages; this makes it difficult to ascertain whether the differences in UCP1 gene expression are due to ethnic differences in BAT development or an effect of lower weight gain in early life.

In the current work, I have presented gene expression measured by microarray analysis. Further confirmation of gene expression using Q-PCR may be required, although gene expression levels obtained using microarray technology are highly correlated with results obtained from Q-PCR when identical transcripts are targeted by the two methods (Dallas et al. 2005, Allanach et al. 2008). It is also important to point out that gene expression levels are not a measure of function and detection

of UCP1 gene expression does not prove the presence of BAT. In addition, high or low UCP1 gene expression do not necessarily indicate more or less BAT activity (Nedergaard and Cannon 2013).

However, in this study, demonstration of UCP1, the BAT specific protein, by immunohistochemistry confirms that BAT is present in epicardial fat in children but even this cannot quantify the functional capabilities of the tissue. To utilise physiological techniques designed to measure the thermogenic and other metabolic function of BAT can be measured by physiological techniques which may be logistically unfeasible to perform in epicardial fat in humans, especially in children where small volumes of epicardial fat are present.

6.5 Conclusion

Epicardial fat from newborn infants, children and adolescents contains UCP1 confirming that it is a BAT depot in humans. UCP1 gene expression in early years of life in humans is downregulated with poor nutrition. In view of the potential role of BAT in regulation of lipid and glucose metabolism, this may have therapeutic implications for prevention and treatment of cardiovascular complications of obesity.

7 Summary and conclusions

7.1 Pericardial fat is a depot of brown adipose tissue

The studies in this thesis categorically demonstrate, for the first time, that adipose tissue depots present around the heart are a repository of brown fat, at least in humans and sheep.

Adipose tissue present around the heart, particularly epicardial fat, has unique anatomical and functional characteristics. Apart from forming a protective layer around the heart and great vessels, fat in this depot has unique metabolic and endocrine/paracrine properties (Iacobellis and Bianco 2011). Under physiological conditions, epicardial fat, due to high rates of FFA uptake and incorporation, acts as a buffering system against toxic levels of fatty acids between the myocardium and blood in the coronary circulation (Iacobellis and Bianco 2011). Presence of BAT in this location could further enhance this protective effect as brown adipocytes are particularly efficient in clearing lipoproteins and glucose, even in the presence of obesity and insulin resistance (Bartelt et al. 2011, Orava et al. 2011).

In sheep, I have demonstrated that UCP1 gene expression and protein are present in pericardial adipose tissue samples taken from late gestation fetus and newborn lambs. Sacks and colleagues demonstrated gene expression of UCP1 in epicardial fat from adult

humans and suggested that epicardial adipose tissue might function as brown fat (Sacks et al. 2009). UCP1 gene expression, however, is not definite evidence of presence of functional BAT (Nedergaard and Cannon 2013). In my thesis, I have presented results that, for the first time, confirm the suggestion made by Sacks et al. by demonstrating the presence of the unique BAT protein, UCP1, by Western Blot, in this location thus providing definite evidence that epicardial fat in adult humans is a depot of BAT.

I have further demonstrated the novel finding that, in humans, BAT is present in epicardial fat throughout childhood and adolescence. The epicardial fat of newborn infants is almost entirely brown as evident by immunohistological staining with UCP1 antibody. Beyond the newborn period, histologically, epicardial fat appears to be predominantly white. However, islands of small, multilocular adipocytes that are positive for UCP1 are present in more than 20% of children and all the adolescents in my study, and UCP1 gene expression is present in epicardial fat throughout childhood establishing, for the first time, that epicardial fat contains at least some BAT throughout childhood and adolescence.

7.2 Pericardial fat is a nutritionally regulated depot of brown adipose tissue

Adipose tissue first appears in early to mid-gestation (Poissonnet et al. 1984) and total adipose tissue mass increases through late gestation

and early childhood (Griffin and Cooke 2012). Experimental evidence from animal models and observational studies in humans suggest that early life experiences are important in setting later adiposity such as the effects of early life nutrition on adipose tissue mass, adipocyte numbers and relative distribution of brown and white fat in later life (Symonds et al. 2011). In my studies, I found that development of brown adipose tissue in the pericardial depot is affected by nutritional experiences in early life.

In sheep, suboptimal maternal nutrition in early to mid-gestation followed by ad libitum feeding until term, enhances UCP1 gene expression and protein abundance along with increased pericardial and total body adiposity and augments the gene expression of key adipogenic genes involved in both brown and white adipogenic pathways. Such enhanced fetal fat stores and increased adipogenic potential may be beneficial in the short term but could subsequently result in excess fat deposition leading to obesity in later life. Excess adiposity in the pericardial depot may be particularly detrimental as increased pericardial fat deposition is associated with cardiovascular illness (Iacobellis and Bianco 2011). In contrast, restricting maternal nutrition in late gestation reduces UCP1 gene expression and protein abundance and downregulates the expression of genes controlling non-shivering thermogenesis suggesting compromised BAT development in the newborn animal. In children, I found that UCP1 gene expression

was downregulated in children with poorer nutrition as indicated by low weight for age z-scores (WAZ) suggesting that, even in postnatal life, BAT development continues to be affected by nutrition. These findings suggest that suboptimal nutrition in late gestation and early years of postnatal life can suppress BAT development.

Suboptimal nutrition in utero and during early life compromises fetal and childhood development. Physiological and metabolic adaptations, including changes in adiposity, made by the individual to an inadequate, or excess nutritional environment, may promote immediate survival but are lasting, conferring significantly increased risks of ill health in childhood and adulthood. It is now accepted that BAT persists beyond the neonatal period into adult life and, therefore, presents a potential target for long-lasting nutritional manipulations (Ojha et al. 2013). How these changes in composition of adipose tissue affect long-term adipose tissue function and propensity towards obesity remains to be elucidated. However, a reduction in thermogenesis presents a plausible mechanism for the increased metabolic efficiency associated with nutritional deprivation in early life.

8 Future research

The pandemic of obesity and related non-communicable diseases continues unabated despite attempts at preventing and managing obesity via interventions ranging from community and family based approaches (Wang et al. 2013) to marketing strategies that may change food purchasing behaviours (Glanz et al. 2012). Approaches to weight loss by diet, exercise, behavioural modification, with or without pharmacological support, can be successful in the short term but the benefits do not last beyond a few years (Nguyen et al. 2012). This lack of success in finding the remedy for prevention or cure of obesity highlights the need to further investigate the avenues which make obesity and metabolic illness such difficult problems.

Growing evidence suggests that maternal health and the offspring's early childhood nutritional experience influence long term health outcomes. Both under and over nutrition in mothers and young children are linked to subsequent obesity and adult diseases. Although the mechanisms behind these associations remain controversial and the developmental origins hypothesis faces several challenges (Horton 2013), there is little doubt that whether it is via in utero programming or genetic, epigenetic and/or life style factors, the early years of life are key determinants of health.

8.1 Implications for future research

The role of nutrition and environmental exposures in early life in the etiology of obesity and related metabolic diseases is supported by human observational and animal experimental studies, such as those described here, but there is a lack of randomised trials of interventions that may ameliorate the effects of, or prevent developmental programming. While animal studies provide proof of principle and suggest mechanisms, and epidemiological observational studies on human cohorts demonstrate associations and can provide some evidence to support the case for interventions, only randomised control trials will provide definite evidence to support any potential therapeutic intervention.

However, in addition to the ethical difficulties of performing experimental trials in pregnant women and young children, the numerous confounders which cannot be controlled in human populations and the temporal dissociation between the occurrence of the etiological insults and the ultimate emergence of the diseases pose challenges to the design of such trials. Despite these challenges, there have been some attempts at randomised control trials in this field. These have demonstrated that interventions such as dietary counselling, physical activity and supplementary weight monitoring can control gestational weight gain (Streuling et al. 2010) and treatment of mild gestational diabetes can reduce risk of fetal overgrowth (Landon et al. 2009).

Follow up of health outcomes in offspring of participants of such trials (Gillman et al. 2010) and other large human cohorts can provide direct evidence to support or refute the role of such interventions in reducing the risks of obesity and other illness in later life.

Developmental origins of health is an interdisciplinary field involving a multi-directional interplay of basic sciences, genetics, epidemiology, behavioural sciences and various clinical disciplines ranging from obstetrics and child health to adolescent health and, adult cardiology, endocrinology and psychiatry (Ojha et al. 2015). A concerted approach to design and execution of research that test randomly assigned interventions in mothers and young children and study the long term effects may produce the vital evidence that could be instrumental in controlling the currently uncontrollable intergeneration amplification of the global obesity crisis. If conducted properly, these ought to be multi-centred and multi-disciplinary efforts which bring together the expertise and resources from all the above mentioned domains of science.

8.2 Implications for public health

The public health importance of this approach was highlighted in the Chief Medical Officer's report (2012) which included a key message that "the primary prevention of obesity should begin in infancy with the delivery of interventions aimed at improving the eating and activity patterns of young children" (CMO 2012).

Integrating interventions that improve maternal nutrition with other public health programmes aimed at young children should therefore be the priority of public health. Evidence to support this has been demonstrated in some regions such as in an undernourished population in India, where children whose mothers took nutritional supplements during pregnancy as part of an integrated child development programme had lower insulin resistance in adolescence (Kinra et al. 2008).

The evidence base clearly identifies that events that occur in early life affect health and wellbeing in later life. Optimal nutritional intake alongside the development of healthy eating and activity patterns have been identified as key to building resilience and protecting against later chronic diseases (CMO 2012). Public health interventions that target maternal and child health and wellbeing and those that support mothers during significant periods of child development such as before and during pregnancy, while breast feeding, and in managing nutrition in infancy will produce benefits with a positive impact on the health of the future adult population.

9 References

- Abaci, A., M. E. Tascilar, T. Saritas, Y. Yozgat, E. Yesilkaya, A. Kilic, V. Okutan and M. K. Lenk (2009). Threshold value of subepicardial adipose tissue to detect insulin resistance in obese children. *Int J Obes (Lond)* **33**(4): 440-446.
- Admiraal, W. M., H. J. Verberne, F. A. Karamat, M. R. Soeters, J. B. Hoekstra and F. Holleman (2013). Cold-induced activity of brown adipose tissue in young lean men of South-Asian and European origin. *Diabetologia* **56**(10): 2231-2237.
- Agrawal, A., N. Nair and N. S. Baghel (2009). A novel approach for reduction of brown fat uptake on FDG PET. *Br J Radiol* **82**(980): 626-631.
- Aherne, W. and D. Hull (1964). The Site of Heat Production in the Newborn Infant. *Proc R Soc Med* **57**: 1172-1173.
- Aherne, W. and D. Hull (1966). Brown adipose tissue and heat production in the newborn infant. *J Pathol Bacteriol* **91**(1): 223-234.
- Alberti, K. G., R. H. Eckel, S. M. Grundy, P. Z. Zimmet, J. I. Cleeman, K. A. Donato, J. C. Fruchart, W. P. James, C. M. Loria and S. C. Smith, Jr. (2009). Harmonizing the metabolic syndrome: a joint interim statement of the International Diabetes Federation Task Force on Epidemiology and Prevention; National Heart, Lung, and Blood Institute; American Heart Association; World Heart Federation; International Atherosclerosis Society; and International Association for the Study of Obesity. *Circulation* **120**(16): 1640-1645.
- Allanach, K., M. Mengel, G. Einecke, B. Sis, L. G. Hidalgo, T. Mueller and P. F. Halloran (2008). Comparing microarray versus RT-PCR assessment of renal allograft biopsies: similar performance despite different dynamic ranges. *Am J Transplant* **8**(5): 1006-1015.
- Almind, K., M. Manieri, W. I. Sivitz, S. Cinti and C. R. Kahn (2007). Ectopic brown adipose tissue in muscle provides a mechanism for differences in risk of metabolic syndrome in mice. *Proc Natl Acad Sci U S A* **104**(7): 2366-2371.
- Anagnostis, P., V. G. Athyros, K. Tziomalos, A. Karagiannis and D. P. Mikhailidis (2009). Clinical review: The pathogenetic role of cortisol in the metabolic syndrome: a hypothesis. *J Clin Endocrinol Metab* **94**(8): 2692-2701.

Aquila, H., T. A. Link and M. Klingenberg (1985). The uncoupling protein from brown fat mitochondria is related to the mitochondrial ADP/ATP carrier. Analysis of sequence homologies and of folding of the protein in the membrane. *EMBO J* **4**(9): 2369-2376.

Arita, Y., S. Kihara, N. Ouchi, M. Takahashi, K. Maeda, J. Miyagawa, K. Hotta, I. Shimomura, T. Nakamura, K. Miyaoka, H. Kuriyama, M. Nishida, S. Yamashita, K. Okubo, K. Matsubara, M. Muraguchi, Y. Ohmoto, T. Funahashi and Y. Matsuzawa (2012). Paradoxical decrease of an adipose-specific protein, adiponectin, in obesity. 1999. *Biochem Biophys Res Commun* **425**(3): 560-564.

Armitage, J. A., L. Poston and P. D. Taylor (2008). Developmental origins of obesity and the metabolic syndrome: the role of maternal obesity. *Front Horm Res* **36**: 73-84.

Arya, M., I. S. Shergill, M. Williamson, L. Gommersall, N. Arya and H. R. Patel (2005). Basic principles of real-time quantitative PCR. *Expert Rev Mol Diagn* **5**(2): 209-219.

Atit, R., S. K. Sgaier, O. A. Mohamed, M. M. Taketo, D. Dufort, A. L. Joyner, L. Niswander and R. A. Conlon (2006). Beta-catenin activation is necessary and sufficient to specify the dorsal dermal fate in the mouse. *Dev Biol* **296**(1): 164-176.

Auer, H., S. Lyianarachchi, D. Newsom, M. I. Klisovic, G. Marcucci and K. Kornacker (2003). Chipping away at the chip bias: RNA degradation in microarray analysis. *Nat Genet* **35**(4): 292-293.

Bakker, L. E., M. R. Boon, R. A. van der Linden, L. P. Arias-Bouda, J. B. van Klinken, F. Smit, H. J. Verberne, J. W. Jukema, J. T. Tamsma, L. M. Havekes, W. D. van Marken Lichtenbelt, I. M. Jazet and P. C. Rensen (2014). Brown adipose tissue volume in healthy lean south Asian adults compared with white Caucasians: a prospective, case-controlled observational study. *Lancet Diabetes Endocrinol* **2**(3): 210-217.

Bar-Sever, Z., Z. Keidar, A. Ben-Barak, R. Bar-Shalom, S. Postovsky, L. Guralnik, M. W. Ben Arush and O. Israel (2007). The incremental value of 18F-FDG PET/CT in paediatric malignancies. *Eur J Nucl Med Mol Imaging* **34**(5): 630-637.

Barker, D. J. (1995). Fetal origins of coronary heart disease. *BMJ* **311**(6998): 171-174.

Barker, D. J., P. D. Gluckman, K. M. Godfrey, J. E. Harding, J. A. Owens and J. S. Robinson (1993). Fetal nutrition and cardiovascular disease in adult life. *Lancet* **341**(8850): 938-941.

Barker, D. J. and C. Osmond (1986). Infant mortality, childhood nutrition, and ischaemic heart disease in England and Wales. *Lancet* **1**(8489): 1077-1081.

Bartelt, A., O. T. Bruns, R. Reimer, H. Hohenberg, H. Ittrich, K. Peldschus, M. G. Kaul, U. I. Tromsdorf, H. Weller, C. Waurisch, A. Eychmuller, P. L. Gordts, F. Rinninger, K. Bruegelmann, B. Freund, P. Nielsen, M. Merkel and J. Heeren (2011). Brown adipose tissue activity controls triglyceride clearance. *Nat Med* **17**(2): 200-205.

Bartelt, A. and J. Heeren (2014). Adipose tissue browning and metabolic health. *Nat Rev Endocrinol* **10**(1): 24-36.

Bayer, L. M. and S. J. Robinson (1969). Growth history of children with congenital heart defects. Size according to sex, age decade, surgical status, and diagnostic category. *Am J Dis Child* **117**(5): 564-572.

Bedford, E. (1972). The story of fatty heart. A disease of Victorian times. *Br Heart J* **34**(1): 23-28.

Bianco, A. C. and J. E. Silva (1987). Intracellular conversion of thyroxine to triiodothyronine is required for the optimal thermogenic function of brown adipose tissue. *J Clin Invest* **79**(1): 295-300.

Billon, N. and C. Dani (2012). Developmental origins of the adipocyte lineage: new insights from genetics and genomics studies. *Stem Cell Rev* **8**(1): 55-66.

Bispham, J., G. S. Gopalakrishnan, J. Dandrea, V. Wilson, H. Budge, D. H. Keisler, F. Broughton Pipkin, T. Stephenson and M. E. Symonds (2003). Maternal endocrine adaptation throughout pregnancy to nutritional manipulation: consequences for maternal plasma leptin and cortisol and the programming of fetal adipose tissue development. *Endocrinology* **144**(8): 3575-3585.

Blohm, D. H. and A. Guiseppi-Elie (2001). New developments in microarray technology. *Curr Opin Biotechnol* **12**(1): 41-47.

Bloor, I. D. and M. E. Symonds (2014). Sexual dimorphism in white and brown adipose tissue with obesity and inflammation. *Horm Behav* **66**(1): 95-103.

Bonora, E., G. Targher, G. Formentini, F. Calcaterra, S. Lombardi, F. Marini, L. Zenari, F. Saggiani, M. Poli, S. Perbellini, A. Raffaelli, L.

Gemma, L. Santi, R. C. Bonadonna and M. Muggeo (2004). The Metabolic Syndrome is an independent predictor of cardiovascular disease in Type 2 diabetic subjects. Prospective data from the Verona Diabetes Complications Study. *Diabet Med* **21**(1): 52-58.

Bordicchia, M., D. Liu, E. Z. Amri, G. Ailhaud, P. Dessi-Fulgheri, C. Zhang, N. Takahashi, R. Sarzani and S. Collins (2012). Cardiac natriuretic peptides act via p38 MAPK to induce the brown fat thermogenic program in mouse and human adipocytes. *J Clin Invest* **122**(3): 1022-1036.

Bouret, S. G., S. J. Draper and R. B. Simerly (2004). Trophic action of leptin on hypothalamic neurons that regulate feeding. *Science* **304**(5667): 108-110.

Boyras, M., O. Pirgon, B. Akyol, B. Dundar, F. Cekmez and N. Eren (2013). Importance of epicardial adipose tissue thickness measurement in obese adolescents, its relationship with carotid intima-media thickness, and echocardiographic findings. *Eur Rev Med Pharmacol Sci* **17**(24): 3309-3317.

Bradford, M. M. (1976). A rapid and sensitive method for the quantitation of microgram quantities of protein utilizing the principle of protein-dye binding. *Anal Biochem* **72**: 248-254.

Bronnikov, G., T. Bengtsson, L. Kramarova, V. Golozoubova, B. Cannon and J. Nedergaard (1999). beta1 to beta3 switch in control of cyclic adenosine monophosphate during brown adipocyte development explains distinct beta-adrenoceptor subtype mediation of proliferation and differentiation. *Endocrinology* **140**(9): 4185-4197.

Bruck, K. (1967). [Importance of brown adipose tissue for temperature regulation in the newborn and cold-adapted mammal]. *Naturwissenschaften* **54**(7): 156-162.

Budge, H., J. Dandrea, A. Mostyn, Y. Evens, R. Watkins, C. Sullivan, P. Ingleton, T. Stephenson and M. E. Symonds (2003). Differential effects of fetal number and maternal nutrition in late gestation on prolactin receptor abundance and adipose tissue development in the neonatal lamb. *Pediatr Res* **53**(2): 302-308.

Budge, H., L. J. Edwards, I. C. McMillen, A. Bryce, K. Warnes, S. Pearce, T. Stephenson and M. E. Symonds (2004). Nutritional manipulation of fetal adipose tissue deposition and uncoupling protein 1 messenger RNA abundance in the sheep: differential effects of timing and duration. *Biol Reprod* **71**(1): 359-365.

- Budge, H., M. G. Gnanalingham, D. S. Gardner, A. Mostyn, T. Stephenson and M. E. Symonds (2005). Maternal nutritional programming of fetal adipose tissue development: long-term consequences for later obesity. *Birth Defects Res C Embryo Today* **75**(3): 193-199.
- Burnette, W. N. (1981). "Western blotting": electrophoretic transfer of proteins from sodium dodecyl sulfate--polyacrylamide gels to unmodified nitrocellulose and radiographic detection with antibody and radioiodinated protein A. *Anal Biochem* **112**(2): 195-203.
- Cabrera-Rego, J. O., G. Iacobellis, J. A. Castillo-Herrera, J. Valiente-Mustelier, J. C. Gandarilla-Sarmientos, S. M. Marin-Julia and J. Navarrete-Cabrera (2014). Epicardial fat thickness correlates with carotid intima-media thickness, arterial stiffness, and cardiac geometry in children and adolescents. *Pediatr Cardiol* **35**(3): 450-456.
- Cameron, J. W., A. Rosenthal and A. D. Olson (1995). Malnutrition in hospitalized children with congenital heart disease. *Arch Pediatr Adolesc Med* **149**(10): 1098-1102.
- Campbell, J. E., A. J. Peckett, M. D'Souza A, T. J. Hawke and M. C. Riddell (2011). Adipogenic and lipolytic effects of chronic glucocorticoid exposure. *Am J Physiol Cell Physiol* **300**(1): C198-209.
- Cannon, B. and J. Nedergaard (2004). Brown adipose tissue: function and physiological significance. *Physiol Rev* **84**(1): 277-359.
- Cannon, B., J. Nedergaard and U. Sundin (1981). Thermogenesis, Brown Fat and Thermogenin. *Survival in the Cold: Hibernation and other Adaptations*. X. J. Musacchia and L. Jansky. Amsterdam, Elsevier-North: 99-120.
- Cantile, M., A. Procino, M. D'Armiento, L. Cindolo and C. Cillo (2003). HOX gene network is involved in the transcriptional regulation of in vivo human adipogenesis. *J Cell Physiol* **194**(2): 225-236.
- Carneheim, C., J. Nedergaard and B. Cannon (1984). Beta-adrenergic stimulation of lipoprotein lipase in rat brown adipose tissue during acclimation to cold. *Am J Physiol* **246**(4 Pt 1): E327-333.
- Cassard, A. M., F. Bouillaud, M. G. Mattei, E. Hentz, S. Raimbault, M. Thomas and D. Ricquier (1990). Human uncoupling protein gene: structure, comparison with rat gene, and assignment to the long arm of chromosome 4. *J Cell Biochem* **43**(3): 255-264.
- Chalfant, J. S., M. L. Smith, H. H. Hu, F. J. Dorey, F. Goodarzian, C. H. Fu and V. Gilsanz (2012). Inverse association between brown adipose

tissue activation and white adipose tissue accumulation in successfully treated pediatric malignancy. *Am J Clin Nutr* **95**(5): 1144-1149.

Chan, L. L., S. P. Sebert, M. A. Hyatt, T. Stephenson, H. Budge, M. E. Symonds and D. S. Gardner (2009). Effect of maternal nutrient restriction from early to midgestation on cardiac function and metabolism after adolescent-onset obesity. *Am J Physiol Regul Integr Comp Physiol* **296**(5): R1455-1463.

Chernogubova, E., B. Cannon and T. Bengtsson (2004). Norepinephrine increases glucose transport in brown adipocytes via beta3-adrenoceptors through a cAMP, PKA, and PI3-kinase-dependent pathway stimulating conventional and novel PKCs. *Endocrinology* **145**(1): 269-280.

Cinti, S., R. C. Frederich, M. C. Zingaretti, R. De Matteis, J. S. Flier and B. B. Lowell (1997). Immunohistochemical localization of leptin and uncoupling protein in white and brown adipose tissue. *Endocrinology* **138**(2): 797-804.

Clarke, L., M. J. Bryant, M. A. Lomax and M. E. Symonds (1997). Maternal manipulation of brown adipose tissue and liver development in the ovine fetus during late gestation. *Br J Nutr* **77**(6): 871-883.

Clement, K., A. Basdevant and A. Dutour (2009). Weight of pericardial fat on coronaropathy. *Arterioscler Thromb Vasc Biol* **29**(5): 615-616.

CMO. (2012). Chief Medical Officer's annual report 2012: Our Children Deserve Better: Prevention Pays. Retrieved 26/03/2014, 2014, from <https://www.gov.uk/government/publications/chief-medical-officers-annual-report-2012-our-children-deserve-better-prevention-pays>.

Collins, S. (2011). beta-Adrenoceptor Signaling Networks in Adipocytes for Recruiting Stored Fat and Energy Expenditure. *Front Endocrinol (Lausanne)* **2**: 102.

Collins, S., E. Yehuda-Shnaidman and H. Wang (2010). Positive and negative control of Ucp1 gene transcription and the role of beta-adrenergic signaling networks. *Int J Obes (Lond)* **34 Suppl 1**: S28-33.

Cote, A. T., K. C. Harris, C. Panagiotopoulos, G. G. Sandor and A. M. Devlin (2013). Childhood obesity and cardiovascular dysfunction. *J Am Coll Cardiol* **62**(15): 1309-1319.

Cox, R. A. and H. R. Arnstein (1963). The Isolation, Characterization and Acid-Base Properties of Ribonucleic Acid from Rabbit-Reticulocyte Ribosomes. *Biochem J* **89**: 574-584.

- Curhan, G. C., G. M. Chertow, W. C. Willett, D. Spiegelman, G. A. Colditz, J. E. Manson, F. E. Speizer and M. J. Stampfer (1996). Birth weight and adult hypertension and obesity in women. *Circulation* **94**(6): 1310-1315.
- Cypess, A. M., Y. C. Chen, C. Sze, K. Wang, J. English, O. Chan, A. R. Holman, I. Tal, M. R. Palmer, G. M. Kolodny and C. R. Kahn (2012). Cold but not sympathomimetics activates human brown adipose tissue in vivo. *Proc Natl Acad Sci U S A* **109**(25): 10001-10005.
- Cypess, A. M., S. Lehman, G. Williams, I. Tal, D. Rodman, A. B. Goldfine, F. C. Kuo, E. L. Palmer, Y. H. Tseng, A. Doria, G. M. Kolodny and C. R. Kahn (2009). Identification and importance of brown adipose tissue in adult humans. *N Engl J Med* **360**(15): 1509-1517.
- Cypess, A. M., L. S. Weiner, C. Roberts-Toler, E. F. Elia, S. H. Kessler, P. A. Kahn, J. English, K. Chatman, S. A. Trauger, A. Doria and G. M. Kolodny (2015). Activation of Human Brown Adipose Tissue by a beta3-Adrenergic Receptor Agonist. *Cell Metab* **21**(1): 33-38.
- Cypess, A. M., A. P. White, C. Vernochet, T. J. Schulz, R. Xue, C. A. Sass, T. L. Huang, C. Roberts-Toler, L. S. Weiner, C. Sze, A. T. Chacko, L. N. Deschamps, L. M. Herder, N. Truchan, A. L. Glasgow, A. R. Holman, A. Gavrilu, P. O. Hasselgren, M. A. Mori, M. Molla and Y. H. Tseng (2013). Anatomical localization, gene expression profiling and functional characterization of adult human neck brown fat. *Nat Med*.
- Dallas, P. B., N. G. Gottardo, M. J. Firth, A. H. Beesley, K. Hoffmann, P. A. Terry, J. R. Freitas, J. M. Boag, A. J. Cummings and U. R. Kees (2005). Gene expression levels assessed by oligonucleotide microarray analysis and quantitative real-time RT-PCR -- how well do they correlate? *BMC Genomics* **6**: 59.
- Dallner, O. S., E. Chernogubova, K. A. Brolinson and T. Bengtsson (2006). Beta3-adrenergic receptors stimulate glucose uptake in brown adipocytes by two mechanisms independently of glucose transporter 4 translocation. *Endocrinology* **147**(12): 5730-5739.
- Davis, T. R. (1961). Chamber cold acclimatization in man. *J Appl Physiol* **16**: 1011-1015.
- Daymont, C., A. Neal, A. Prosnitz and M. S. Cohen (2013). Growth in children with congenital heart disease. *Pediatrics* **131**(1): e236-242.
- de Jesus, L. A., S. D. Carvalho, M. O. Ribeiro, M. Schneider, S. W. Kim, J. W. Harney, P. R. Larsen and A. C. Bianco (2001). The type 2

iodothyronine deiodinase is essential for adaptive thermogenesis in brown adipose tissue. *J Clin Invest* **108**(9): 1379-1385.

de Onis, M., M. Blossner and E. Borghi (2010). Global prevalence and trends of overweight and obesity among preschool children. *Am J Clin Nutr* **92**(5): 1257-1264.

DeFronzo, R. A. and E. Ferrannini (1991). Insulin resistance. A multifaceted syndrome responsible for NIDDM, obesity, hypertension, dyslipidemia, and atherosclerotic cardiovascular disease. *Diabetes Care* **14**(3): 173-194.

Del Mar Gonzalez-Barroso, M., D. Ricquier and A. M. Cassard-Doulcier (2000). The human uncoupling protein-1 gene (UCP1): present status and perspectives in obesity research. *Obes Rev* **1**(2): 61-72.

Denman, S. E. and C. S. McSweeney (2005). Quantitative (real-time) PCR. *Methods in Gut Microbial Ecology for Ruminants*. H. P. S. Makkar and C. S. McSweeney, Springer Netherlands: 105-115.

Diez, J. J. and P. Iglesias (2003). The role of the novel adipocyte-derived hormone adiponectin in human disease. *Eur J Endocrinol* **148**(3): 293-300.

Ding, J., F. C. Hsu, T. B. Harris, Y. Liu, S. B. Kritchevsky, M. Szklo, P. Ouyang, M. A. Espeland, K. K. Lohman, M. H. Criqui, M. Allison, D. A. Bluemke and J. J. Carr (2009). The association of pericardial fat with incident coronary heart disease: the Multi-Ethnic Study of Atherosclerosis (MESA). *Am J Clin Nutr* **90**(3): 499-504.

Ding, J., S. B. Kritchevsky, T. B. Harris, G. L. Burke, R. C. Detrano, M. Szklo and J. Jeffrey Carr (2008). The association of pericardial fat with calcified coronary plaque. *Obesity (Silver Spring)* **16**(8): 1914-1919.

Ding, J., S. B. Kritchevsky, T. B. Harris, G. L. Burke, R. C. Detrano, M. Szklo, J. Jeffrey Carr and A. Multi-Ethnic Study of (2008). The association of pericardial fat with calcified coronary plaque. *Obesity (Silver Spring)* **16**(8): 1914-1919.

Drubach, L. A., E. L. Palmer, 3rd, L. P. Connolly, A. Baker, D. Zurakowski and A. M. Cypess (2011). Pediatric brown adipose tissue: detection, epidemiology, and differences from adults. *J Pediatr* **159**(6): 939-944.

Edwards, L. J., J. R. McFarlane, K. G. Kauter and I. C. McMillen (2005). Impact of periconceptual nutrition on maternal and fetal leptin and fetal adiposity in singleton and twin pregnancies. *Am J Physiol Regul Integr Comp Physiol* **288**(1): R39-45.

- Edwards, L. J. and I. C. McMillen (2001). Maternal undernutrition increases arterial blood pressure in the sheep fetus during late gestation. *J Physiol* **533**(Pt 2): 561-570.
- Enerback, S., A. Jacobsson, E. M. Simpson, C. Guerra, H. Yamashita, M. E. Harper and L. P. Kozak (1997). Mice lacking mitochondrial uncoupling protein are cold-sensitive but not obese. *Nature* **387**(6628): 90-94.
- Erhardt, J. and M. Pollgorn (2011). ENA for Smart- Software for Emergency Nutrition Assessment.
- Eriksson, P., S. Reynisdottir, F. Lonnqvist, V. Stemme, A. Hamsten and P. Arner (1998). Adipose tissue secretion of plasminogen activator inhibitor-1 in non-obese and obese individuals. *Diabetologia* **41**(1): 65-71.
- Fain, J. N., H. S. Sacks, S. W. Bahouth, D. S. Tichansky, A. K. Madan and P. S. Cheema (2010). Human epicardial adipokine messenger RNAs: comparisons of their expression in substernal, subcutaneous, and omental fat. *Metabolism* **59**(9): 1379-1386.
- Fainberg, H. P., D. Sharkey, S. Sebert, V. Wilson, M. Pope, H. Budge and M. E. Symonds (2013). Suboptimal maternal nutrition during early fetal kidney development specifically promotes renal lipid accumulation following juvenile obesity in the offspring. *Reprod Fertil Dev* **25**(5): 728-736.
- Feldmann, H. M., V. Golozoubova, B. Cannon and J. Nedergaard (2009). UCP1 ablation induces obesity and abolishes diet-induced thermogenesis in mice exempt from thermal stress by living at thermoneutrality. *Cell Metab* **9**(2): 203-209.
- Ferre, P. (2004). The biology of peroxisome proliferator-activated receptors: relationship with lipid metabolism and insulin sensitivity. *Diabetes* **53 Suppl 1**: S43-50.
- Festing, M. F. (2006). Design and statistical methods in studies using animal models of development. *ILAR J* **47**(1): 5-14.
- Festuccia, W. T., P. G. Blanchard and Y. Deshaies (2011). Control of Brown Adipose Tissue Glucose and Lipid Metabolism by PPARgamma. *Front Endocrinol (Lausanne)* **2**: 84.
- Festuccia, W. T., P. G. Blanchard, V. Turcotte, M. Laplante, M. Sariahmetoglu, D. N. Brindley, D. Richard and Y. Deshaies (2009). The PPARgamma agonist rosiglitazone enhances rat brown adipose tissue

lipogenesis from glucose without altering glucose uptake. *Am J Physiol Regul Integr Comp Physiol* **296**(5): R1327-1335.

Finn, D., M. A. Lomax and P. Trayhurn (1998). An immunohistochemical and in situ hybridisation study of the postnatal development of uncoupling protein-1 and uncoupling protein-1 mRNA in lamb perirenal adipose tissue. *Cell Tissue Res* **294**(3): 461-466.

Finucane, M. M., G. A. Stevens, M. J. Cowan, G. Danaei, J. K. Lin, C. J. Paciorek, G. M. Singh, H. R. Gutierrez, Y. Lu, A. N. Bahalim, F. Farzadfar, L. M. Riley, M. Ezzati and G. Global Burden of Metabolic Risk Factors of Chronic Diseases Collaborating (2011). National, regional, and global trends in body-mass index since 1980: systematic analysis of health examination surveys and epidemiological studies with 960 country-years and 9.1 million participants. *Lancet* **377**(9765): 557-567.

Fitzgibbons, T. P. and M. P. Czech (2014). Epicardial and perivascular adipose tissues and their influence on cardiovascular disease: basic mechanisms and clinical associations. *J Am Heart Assoc* **3**(2): e000582.

Fletcher, B. D., M. D. Jacobstein, C. R. Abramowsky and R. H. Anderson (1987). Right atrioventricular valve atresia: anatomic evaluation with MR imaging. *AJR Am J Roentgenol* **148**(4): 671-674.

Forner, F., C. Kumar, C. A. Lubber, T. Fromme, M. Klingenspor and M. Mann (2009). Proteome differences between brown and white fat mitochondria reveal specialized metabolic functions. *Cell Metab* **10**(4): 324-335.

Forsdahl, A. (1977). Are poor living conditions in childhood and adolescence an important risk factor for arteriosclerotic heart disease? *Br J Prev Soc Med* **31**(2): 91-95.

Fowden, A. L., J. Li and A. J. Forhead (1998). Glucocorticoids and the preparation for life after birth: are there long-term consequences of the life insurance? *Proc Nutr Soc* **57**(1): 113-122.

Fried, S. K., C. D. Russell, N. L. Grauso and R. E. Brolin (1993). Lipoprotein lipase regulation by insulin and glucocorticoid in subcutaneous and omental adipose tissues of obese women and men. *J Clin Invest* **92**(5): 2191-2198.

Friedlander, S. L., E. K. Larkin, C. L. Rosen, T. M. Palermo and S. Redline (2003). Decreased quality of life associated with obesity in school-aged children. *Arch Pediatr Adolesc Med* **157**(12): 1206-1211.

- Fruhbeck, G., S. Becerril, N. Sainz, P. Garrastachu and M. J. Garcia-Velloso (2009). BAT: a new target for human obesity? *Trends Pharmacol Sci* **30**(8): 387-396.
- Fruhbeck, G., P. Sesma and M. A. Burrell (2009). PRDM16: the interconvertible adipo-myocyte switch. *Trends Cell Biol* **19**(4): 141-146.
- Gardner, D. S., K. Tingey, B. W. Van Bon, S. E. Ozanne, V. Wilson, J. Dandrea, D. H. Keisler, T. Stephenson and M. E. Symonds (2005). Programming of glucose-insulin metabolism in adult sheep after maternal undernutrition. *Am J Physiol Regul Integr Comp Physiol* **289**(4): R947-954.
- Garipey, G., D. Nitka and N. Schmitz (2010). The association between obesity and anxiety disorders in the population: a systematic review and meta-analysis. *Int J Obes (Lond)* **34**(3): 407-419.
- Gelfand, M. J., M. O'Hara S, L. A. Curtwright and J. R. Maclean (2005). Pre-medication to block [(18)F]FDG uptake in the brown adipose tissue of pediatric and adolescent patients. *Pediatr Radiol* **35**(10): 984-990.
- Gessner, K. (1551). *Conradi Gesneri medici Tigurine Historiae Animalium: Lib. I De Quadrupedibus viviparis*.
- Gesta, S. and C. Ronald Kahn (2012). *White Adipose Tissue. Adipose Tissue Biology*. M. E. Symonds, Springer: 71-121.
- Gillman, M. W. (2005). Developmental origins of health and disease. *N Engl J Med* **353**(17): 1848-1850.
- Gillman, M. W., H. Oakey, P. A. Baghurst, R. E. Volkmer, J. S. Robinson and C. A. Crowther (2010). Effect of treatment of gestational diabetes mellitus on obesity in the next generation. *Diabetes Care* **33**(5): 964-968.
- Gilsanz, V., S. A. Chung, H. Jackson, F. J. Dorey and H. H. Hu (2011). Functional brown adipose tissue is related to muscle volume in children and adolescents. *J Pediatr* **158**(5): 722-726.
- Gilsanz, V., H. H. Hu and S. Kajimura (2013). Relevance of brown adipose tissue in infancy and adolescence. *Pediatr Res* **73**(1): 3-9.
- Gilsanz, V., M. L. Smith, F. Goodarzian, M. Kim, T. A. Wren and H. H. Hu (2012). Changes in brown adipose tissue in boys and girls during childhood and puberty. *J Pediatr* **160**(4): 604-609 e601.

Glanz, K., M. D. Bader and S. Iyer (2012). Retail grocery store marketing strategies and obesity: an integrative review. *Am J Prev Med* **42**(5): 503-512.

Glick, Z., S. Y. Wu, J. Lupien, R. Reggio, G. A. Bray and D. A. Fisher (1985). Meal-induced brown fat thermogenesis and thyroid hormone metabolism in rats. *Am J Physiol* **249**(5 Pt 1): E519-524.

Gopalakrishnan, G. S., D. S. Gardner, S. M. Rhind, M. T. Rae, C. E. Kyle, A. N. Brooks, R. M. Walker, M. M. Ramsay, D. H. Keisler, T. Stephenson and M. E. Symonds (2004). Programming of adult cardiovascular function after early maternal undernutrition in sheep. *Am J Physiol Regul Integr Comp Physiol* **287**(1): R12-20.

Gorstein, J., K. Sullivan, R. Yip, M. de Onis, F. Trowbridge, P. Fajans and G. Clugston (1994). Issues in the assessment of nutritional status using anthropometry. *Bull World Health Organ* **72**(2): 273-283.

Greco-Perotto, R., D. Zaninetti, F. Assimacopoulos-Jeannet, E. Bobbioni and B. Jeanrenaud (1987). Stimulatory effect of cold adaptation on glucose utilization by brown adipose tissue. Relationship with changes in the glucose transporter system. *J Biol Chem* **262**(16): 7732-7736.

Greenbaum, D., C. Colangelo, K. Williams and M. Gerstein (2003). Comparing protein abundance and mRNA expression levels on a genomic scale. *Genome Biol* **4**(9): 117.

Greif, M., A. Becker, F. von Ziegler, C. Lebherz, M. Lehrke, U. C. Broedl, J. Tittus, K. Parhofer, C. Becker, M. Reiser, A. Knez and A. W. Leber (2009). Pericardial adipose tissue determined by dual source CT is a risk factor for coronary atherosclerosis. *Arterioscler Thromb Vasc Biol* **29**(5): 781-786.

Griffin, I. J. and R. J. Cooke (2012). Development of whole body adiposity in preterm infants. *Early Hum Dev* **88** Suppl 1: S19-24.

Hadi, M., C. C. Chen, M. Whatley, K. Pacak and J. A. Carrasquillo (2007). Brown fat imaging with (18)F-6-fluorodopamine PET/CT, (18)F-FDG PET/CT, and (123)I-MIBG SPECT: a study of patients being evaluated for pheochromocytoma. *J Nucl Med* **48**(7): 1077-1083.

Hales, C. N. and D. J. Barker (2001). The thrifty phenotype hypothesis. *Br Med Bull* **60**: 5-20.

Hall, L. M., C. N. Moran, G. R. Milne, J. Wilson, N. G. MacFarlane, N. G. Forouhi, N. Hariharan, I. P. Salt, N. Sattar and J. M. Gill (2010). Fat oxidation, fitness and skeletal muscle expression of oxidative/lipid

metabolism genes in South Asians: implications for insulin resistance? PLoS One **5**(12): e14197.

Hany, T. F., E. Gharehpapagh, E. M. Kamel, A. Buck, J. Himms-Hagen and G. K. von Schulthess (2002). Brown adipose tissue: a factor to consider in symmetrical tracer uptake in the neck and upper chest region. Eur J Nucl Med Mol Imaging **29**(10): 1393-1398.

Harrington, T. A., E. L. Thomas, G. Frost, N. Modi and J. D. Bell (2004). Distribution of adipose tissue in the newborn. Pediatr Res **55**(3): 437-441.

Hassink, S. G., D. V. Sheslow, E. de Lancey, I. Opentanova, R. V. Considine and J. F. Caro (1996). Serum leptin in children with obesity: relationship to gender and development. Pediatrics **98**(2 Pt 1): 201-203.

Hellmer, J., C. Marcus, T. Sonnenfeld and P. Arner (1992). Mechanisms for differences in lipolysis between human subcutaneous and omental fat cells. J Clin Endocrinol Metab **75**(1): 15-20.

Higuchi, R., C. Fockler, G. Dollinger and R. Watson (1993). Kinetic PCR analysis: real-time monitoring of DNA amplification reactions. Biotechnology (N Y) **11**(9): 1026-1030.

Hilton, C., M. J. Neville and F. Karpe (2013). MicroRNAs in adipose tissue: their role in adipogenesis and obesity. Int J Obes (Lond) **37**(3): 325-332.

Ho, E. and Y. Shimada (1978). Formation of the epicardium studied with the scanning electron microscope. Dev Biol **66**(2): 579-585.

Horton, R. (2013). Offline: DOHaD—coming out, with questions. Lancet **382**(9907): 1768.

Hossain, P., B. Kavar and M. El Nahas (2007). Obesity and diabetes in the developing world--a growing challenge. N Engl J Med **356**(3): 213-215.

Hotta, K., T. Funahashi, N. L. Bodkin, H. K. Ortmeyer, Y. Arita, B. C. Hansen and Y. Matsuzawa (2001). Circulating concentrations of the adipocyte protein adiponectin are decreased in parallel with reduced insulin sensitivity during the progression to type 2 diabetes in rhesus monkeys. Diabetes **50**(5): 1126-1133.

HSE (2006). Health Survey for England 2004: Volume 1: Health of minority ethnic groups., London: The Information Centre, 2006.

Hubert, H. B. (1986). The importance of obesity in the development of coronary risk factors and disease: the epidemiologic evidence. *Annu Rev Public Health* **7**: 493-502.

Hutley, L., W. Shurety, F. Newell, R. McGeary, N. Pelton, J. Grant, A. Herington, D. Cameron, J. Whitehead and J. Prins (2004). Fibroblast growth factor 1: a key regulator of human adipogenesis. *Diabetes* **53**(12): 3097-3106.

Huttunen, P., J. Hirvonen and V. Kinnula (1981). The occurrence of brown adipose tissue in outdoor workers. *Eur J Appl Physiol Occup Physiol* **46**(4): 339-345.

Hyatt, M. A., D. S. Gardner, S. Sebert, V. Wilson, N. Davidson, Y. Nigmatullina, L. L. Chan, H. Budge and M. E. Symonds (2011). Suboptimal maternal nutrition, during early fetal liver development, promotes lipid accumulation in the liver of obese offspring. *Reproduction* **141**(1): 119-126.

Iacobellis, G. (2009). Epicardial and pericardial fat: close, but very different. *Obesity (Silver Spring)* **17**(4): 625; author reply 626-627.

Iacobellis, G. and A. C. Bianco (2011). Epicardial adipose tissue: emerging physiological, pathophysiological and clinical features. *Trends Endocrinol Metab* **22**(11): 450-457.

Iacobellis, G., D. Corradi and A. M. Sharma (2005). Epicardial adipose tissue: anatomic, biomolecular and clinical relationships with the heart. *Nat Clin Pract Cardiovasc Med* **2**(10): 536-543.

International Human Genome Sequencing, C. (2004). Finishing the euchromatic sequence of the human genome. *Nature* **431**(7011): 931-945.

Iozzo, P. (2011). Myocardial, perivascular, and epicardial fat. *Diabetes Care* **34 Suppl 2**: S371-379.

Ishii, T., N. Asuwa, S. Masuda and Y. Ishikawa (1998). The effects of a myocardial bridge on coronary atherosclerosis and ischaemia. *J Pathol* **185**(1): 4-9.

Isomaa, B., P. Almgren, T. Tuomi, B. Forsen, K. Lahti, M. Nissen, M. R. Taskinen and L. Groop (2001). Cardiovascular morbidity and mortality associated with the metabolic syndrome. *Diabetes Care* **24**(4): 683-689.

Jia, H. and E. I. Lubetkin (2005). The impact of obesity on health-related quality-of-life in the general adult US population. *J Public Health (Oxf)* **27**(2): 156-164.

- Joel, C. D. and E. G. Ball (1962). The electron transmitter system of brown adipose tissue. *Biochemistry* **1**: 281-287.
- Johnson, M. S., T. T. Huang, R. Figueroa-Colon, J. H. Dwyer and M. I. Goran (2001). Influence of leptin on changes in body fat during growth in African American and white children. *Obes Res* **9**(10): 593-598.
- Kajimura, S., P. Seale, K. Kubota, E. Lunsford, J. V. Frangioni, S. P. Gygi and B. M. Spiegelman (2009). Initiation of myoblast to brown fat switch by a PRDM16-C/EBP-beta transcriptional complex. *Nature* **460**(7259): 1154-1158.
- Kajimura, S., P. Seale and B. M. Spiegelman (2010). Transcriptional control of brown fat development. *Cell Metab* **11**(4): 257-262.
- Karnehed, N., F. Rasmussen and M. Kark (2007). Obesity in young adulthood and later disability pension: a population-based cohort study of 366,929 Swedish men. *Scand J Public Health* **35**(1): 48-54.
- Kaushik, M. and Y. M. Reddy (2011). Distinction of "fat around the heart". *J Am Coll Cardiol* **58**(15): 1640; author reply 1640-1641.
- Keegan, J., P. D. Gatehouse, G. Z. Yang and D. N. Firmin (2004). Spiral phase velocity mapping of left and right coronary artery blood flow: Correction for through-plane motion using selective fat-only excitation. *Journal of Magnetic Resonance Imaging* **20**(6): 953-960.
- Kershaw, E. E. and J. S. Flier (2004). Adipose tissue as an endocrine organ. *J Clin Endocrinol Metab* **89**(6): 2548-2556.
- Kim, B. (2008). Thyroid hormone as a determinant of energy expenditure and the basal metabolic rate. *Thyroid* **18**(2): 141-144.
- Kind, K. L., C. T. Roberts, A. I. Sohlstrom, A. Katsman, P. M. Clifton, J. S. Robinson and J. A. Owens (2005). Chronic maternal feed restriction impairs growth but increases adiposity of the fetal guinea pig. *Am J Physiol Regul Integr Comp Physiol* **288**(1): R119-126.
- Kinra, S., K. V. Rameshwar Sarma, Ghafoorunissa, V. V. Mendu, R. Ravikumar, V. Mohan, I. B. Wilkinson, J. R. Cockcroft, G. Davey Smith and Y. Ben-Shlomo (2008). Effect of integration of supplemental nutrition with public health programmes in pregnancy and early childhood on cardiovascular risk in rural Indian adolescents: long term follow-up of Hyderabad nutrition trial. *BMJ* **337**: a605.
- Klemm, D. J., J. W. Leitner, P. Watson, A. Nesterova, J. E. Reusch, M. L. Goalstone and B. Draznin (2001). Insulin-induced adipocyte

differentiation. Activation of CREB rescues adipogenesis from the arrest caused by inhibition of prenylation. *J Biol Chem* **276**(30): 28430-28435.

Klingenspor, M., S. Herzig and A. Pfeifer (2012). Brown fat develops a brite future. *Obes Facts* **5**(6): 890-896.

Klingenspor, M., M. Ivemeyer, H. Wiesinger, K. Haas, G. Heldmaier and R. J. Wiesner (1996). Biogenesis of thermogenic mitochondria in brown adipose tissue of Djungarian hamsters during cold adaptation. *Biochem J* **316** (Pt 2): 607-613.

Kochanowski, B. and W. Jilg (1999). Competitive PCR quantitation utilizing a microtiter plate based format for the detection of PCR products. *Methods Mol Med* **26**: 171-182.

Kopecky, J., G. Clarke, S. Enerback, B. Spiegelman and L. P. Kozak (1995). Expression of the mitochondrial uncoupling protein gene from the aP2 gene promoter prevents genetic obesity. *J Clin Invest* **96**(6): 2914-2923.

Kopelman, P. G. (2000). Obesity as a medical problem. *Nature* **404**(6778): 635-643.

Kozak, L. P. (2010). Brown fat and the myth of diet-induced thermogenesis. *Cell Metab* **11**(4): 263-267.

Kozak, U. C., J. Kopecky, J. Teisinger, S. Enerback, B. Boyer and L. P. Kozak (1994). An upstream enhancer regulating brown-fat-specific expression of the mitochondrial uncoupling protein gene. *Mol Cell Biol* **14**(1): 59-67.

Kramer, H. H., H. J. Trampisch, S. Rammos and A. Giese (1990). Birth weight of children with congenital heart disease. *Eur J Pediatr* **149**(11): 752-757.

Landon, M. B., C. Y. Spong, E. Thom, M. W. Carpenter, S. M. Ramin, B. Casey, R. J. Wapner, M. W. Varner, D. J. Rouse, J. M. Thorp, Jr., A. Sciscione, P. Catalano, M. Harper, G. Saade, K. Y. Lain, Y. Sorokin, A. M. Peaceman, J. E. Tolosa and G. B. Anderson (2009). A multicenter, randomized trial of treatment for mild gestational diabetes. *N Engl J Med* **361**(14): 1339-1348.

Larsen, T. M., S. Toubro, M. A. van Baak, K. M. Gottesdiener, P. Larson, W. H. Saris and A. Astrup (2002). Effect of a 28-d treatment with L-796568, a novel beta(3)-adrenergic receptor agonist, on energy expenditure and body composition in obese men. *Am J Clin Nutr* **76**(4): 780-788.

- Lean (1989). Brown adipose tissue in man.
- Lee, P., M. M. Swarbrick, J. T. Zhao and K. K. Ho (2011). Inducible brown adipogenesis of supraclavicular fat in adult humans. *Endocrinology* **152**(10): 3597-3602.
- Lee, Y. H., A. P. Petkova, E. P. Mottillo and J. G. Granneman (2012). In vivo identification of bipotential adipocyte progenitors recruited by beta3-adrenoceptor activation and high-fat feeding. *Cell Metab* **15**(4): 480-491.
- Lefebvre, A. M., M. Laville, N. Vega, J. P. Riou, L. van Gaal, J. Auwerx and H. Vidal (1998). Depot-specific differences in adipose tissue gene expression in lean and obese subjects. *Diabetes* **47**(1): 98-103.
- Leibel, R. L., M. Rosenbaum and J. Hirsch (1995). Changes in energy expenditure resulting from altered body weight. *N Engl J Med* **332**(10): 621-628.
- Lindgren, A. C., C. Marcus, C. Skwirut, A. Elimam, L. Hagenas, M. Schalling, M. Anvret and F. Lonnqvist (1997). Increased leptin messenger RNA and serum leptin levels in children with Prader-Willi syndrome and nonsyndromal obesity. *Pediatr Res* **42**(5): 593-596.
- Liu, J., C. S. Fox, D. Hickson, D. Sarpong, L. Ekunwe, W. D. May, G. W. Hundley, J. J. Carr and H. A. Taylor (2010). Pericardial adipose tissue, atherosclerosis, and cardiovascular disease risk factors: the Jackson heart study. *Diabetes Care* **33**(7): 1635-1639.
- Livak, K. J. and T. D. Schmittgen (2001). Analysis of relative gene expression data using real-time quantitative PCR and the 2^{(-Delta Delta C(T))} Method. *Methods* **25**(4): 402-408.
- Lonnqvist, F., P. Arner, L. Nordfors and M. Schalling (1995). Overexpression of the obese (ob) gene in adipose tissue of human obese subjects. *Nat Med* **1**(9): 950-953.
- Lopez, M., L. Varela, M. J. Vazquez, S. Rodriguez-Cuenca, C. R. Gonzalez, V. R. Velagapudi, D. A. Morgan, E. Schoenmakers, K. Agassandian, R. Lage, P. B. Martinez de Morentin, S. Tovar, R. Nogueiras, D. Carling, C. Lelliott, R. Gallego, M. Oresic, K. Chatterjee, A. K. Saha, K. Rahmouni, C. Dieguez and A. Vidal-Puig (2010). Hypothalamic AMPK and fatty acid metabolism mediate thyroid regulation of energy balance. *Nat Med* **16**(9): 1001-1008.
- Lord, G. M., G. Matarese, J. K. Howard, R. J. Baker, S. R. Bloom and R. I. Lechler (1998). Leptin modulates the T-cell immune response and

reverses starvation-induced immunosuppression. *Nature* **394**(6696): 897-901.

Lorenz, M. W., H. S. Markus, M. L. Bots, M. Rosvall and M. Sitzer (2007). Prediction of clinical cardiovascular events with carotid intima-media thickness: a systematic review and meta-analysis. *Circulation* **115**(4): 459-467.

Lucas, A. (1991). Programming by early nutrition in man. *Ciba Found Symp* **156**: 38-50; discussion 50-35.

Luppino, F. S., L. M. de Wit, P. F. Bouvy, T. Stijnen, P. Cuijpers, B. W. Penninx and F. G. Zitman (2010). Overweight, obesity, and depression: a systematic review and meta-analysis of longitudinal studies. *Arch Gen Psychiatry* **67**(3): 220-229.

Maffei, M., J. Halaas, E. Ravussin, R. E. Pratley, G. H. Lee, Y. Zhang, H. Fei, S. Kim, R. Lallone, S. Ranganathan and et al. (1995). Leptin levels in human and rodent: measurement of plasma leptin and ob RNA in obese and weight-reduced subjects. *Nat Med* **1**(11): 1155-1161.

Mahabadi, A. A., J. M. Massaro, G. A. Rosito, D. Levy, J. M. Murabito, P. A. Wolf, C. J. O'Donnell, C. S. Fox and U. Hoffmann (2009). Association of pericardial fat, intrathoracic fat, and visceral abdominal fat with cardiovascular disease burden: the Framingham Heart Study. *Eur Heart J* **30**(7): 850-856.

Mahfouz, R. A., A. Alzaiat and A. Yousry (2015). Relationship of epicardial fat thickness with endothelial and cardiac functions in children with family history of type 2 diabetes mellitus. *Echocardiography* **32**(1): 28-33.

Manchester, K. L. (1996). Use of UV methods for measurement of protein and nucleic acid concentrations. *Biotechniques* **20**(6): 968-&.

Manco, M., A. Morandi, M. Marigliano, F. Rigotti, R. Manfredi and C. Maffei (2013). Epicardial fat, abdominal adiposity and insulin resistance in obese pre-pubertal and early pubertal children. *Atherosclerosis* **226**(2): 490-495.

Marchington, J. M., C. A. Mattacks and C. M. Pond (1989). Adipose-Tissue in the Mammalian Heart and Pericardium - Structure, Fetal Development and Biochemical-Properties. *Comparative Biochemistry and Physiology B-Biochemistry & Molecular Biology* **94**(2): 225-232.

Marchington, J. M., C. A. Mattacks and C. M. Pond (1989). Adipose tissue in the mammalian heart and pericardium: structure, foetal

development and biochemical properties. *Comp Biochem Physiol B* **94**(2): 225-232.

Margetic, S., C. Gazzola, G. G. Pegg and R. A. Hill (2002). Leptin: a review of its peripheral actions and interactions. *Int J Obes Relat Metab Disord* **26**(11): 1407-1433.

Mazur, A., M. Ostanski, G. Telega and E. Malecka-Tendera (2010). Is epicardial fat tissue a marker of metabolic syndrome in obese children? *Atherosclerosis* **211**(2): 596-600.

Mazurek, T., L. Zhang, A. Zalewski, J. D. Mannion, J. T. Diehl, H. Arafat, L. Sarov-Blat, S. O'Brien, E. A. Keiper, A. G. Johnson, J. Martin, B. J. Goldstein and Y. Shi (2003). Human epicardial adipose tissue is a source of inflammatory mediators. *Circulation* **108**(20): 2460-2466.

McAuley, P. A., F. C. Hsu, K. K. Loman, J. J. Carr, M. J. Budoff, M. Szklo, A. R. Sharrett and J. Ding (2011). Liver attenuation, pericardial adipose tissue, obesity, and insulin resistance: the Multi-Ethnic Study of Atherosclerosis (MESA). *Obesity (Silver Spring)* **19**(9): 1855-1860.

Medoff-Cooper, B. and C. Ravishankar (2013). Nutrition and growth in congenital heart disease: a challenge in children. *Curr Opin Cardiol* **28**(2): 122-129.

Melo, M. R., C. D. Faria, K. C. Melo, N. A. Reboucas and C. A. Longui (2004). Real-time PCR quantitation of glucocorticoid receptor alpha isoform. *BMC Mol Biol* **5**(1): 19.

Merklin, R. J. (1974). Growth and distribution of human fetal brown fat. *Anat Rec* **178**(3): 637-645.

Mitchell, P. (1961). Coupling of phosphorylation to electron and hydrogen transfer by a chemi-osmotic type of mechanism. *Nature* **191**: 144-148.

Montague, C. T. and S. O'Rahilly (2000). The perils of portliness: causes and consequences of visceral adiposity. *Diabetes* **49**(6): 883-888.

Moore, K. L. and T. V. N. Persaud (2003). *The developing human. Clinically oriented embryology.* , Saunders.

Moreno-Navarrete, J. M. and J. M. Fernandez-Real (2012). Adipocyte differentiation. *Adipose Tissue Biology*. M. E. Symonds. New York, Springer Science+Business Media. **1**: 17-38.

Mostyn, A., S. Pearce, T. Stephenson and M. E. Symonds (2004). Hormonal and nutritional regulation of adipose tissue mitochondrial development and function in the newborn. *Exp Clin Endocrinol Diabetes* **112**(1): 2-9.

Mostyn, A., V. Wilson, J. Dandrea, D. P. Yakubu, H. Budge, M. C. Alves-Guerra, C. Pecqueur, B. Miroux, M. E. Symonds and T. Stephenson (2003). Ontogeny and nutritional manipulation of mitochondrial protein abundance in adipose tissue and the lungs of postnatal sheep. *Br J Nutr* **90**(2): 323-328.

Muhlhausler, B. S., I. C. McMillen, G. Rouzaud, P. A. Findlay, E. M. Marrocco, S. M. Rhind and C. L. Adam (2004). Appetite regulatory neuropeptides are expressed in the sheep hypothalamus before birth. *J Neuroendocrinol* **16**(6): 502-507.

Nedergaard, J. and B. Cannon (2013). UCP1 mRNA does not produce heat. *Biochim Biophys Acta* **1831**(5): 943-949.

Nedergaard, J., V. Golozoubova, A. Matthias, A. Asadi, A. Jacobsson and B. Cannon (2001). UCP1: the only protein able to mediate adaptive non-shivering thermogenesis and metabolic inefficiency. *Biochim Biophys Acta* **1504**(1): 82-106.

Neovius, M., M. Kark and F. Rasmussen (2008). Association between obesity status in young adulthood and disability pension. *Int J Obes (Lond)* **32**(8): 1319-1326.

Nguyen, N., J. K. Champion, J. Ponce, B. Quebbemann, E. Patterson, B. Pham, W. Raum, J. N. Buchwald, G. Segato and F. Favretti (2012). A review of unmet needs in obesity management. *Obes Surg* **22**(6): 956-966.

NHSIC, T. N. I. C. (2012) Statistics on obesity, physical activity and diet: England, 2012.

Nicholls, D. G. and V. S. Bernson (1977). Inter-relationships between proton electrochemical gradient, adenine-nucleotide phosphorylation potential and respiration, during substrate-level and oxidative phosphorylation by mitochondria from brown adipose tissue of cold-adapted guinea-pigs. *Eur J Biochem* **75**(2): 601-612.

NOO, N. O. O. (2010) The economic burden of obesity.

Nydegger, A. and J. E. Bines (2006). Energy metabolism in infants with congenital heart disease. *Nutrition* **22**(7-8): 697-704.

Ojha, S., H. P. Fainberg, S. Sebert, H. Budge and M. E. Symonds (2015). Maternal health and eating habits: metabolic consequences and impact on child health. *Trends Mol Med* **21**(2): 126-133.

Ojha, S., L. Robinson, M. E. Symonds and H. Budge (2013). Suboptimal maternal nutrition affects offspring health in adult life. *Early Hum Dev* **89**(11): 909-913.

Ojha, S., L. Robinson, M. Yazdani, M. E. Symonds and H. Budge (2013). Brown adipose tissue genes in pericardial adipose tissue of newborn sheep are downregulated by maternal nutrient restriction in late gestation. *Pediatr Res* **74**(3): 246-251.

Ojha, S., M. E. Symonds and H. Budge (2014). Suboptimal maternal nutrition during early-to-mid gestation in the sheep enhances pericardial adiposity in the near-term fetus. *Reprod Fertil Dev*.

Orava, J., P. Nuutila, M. E. Lidell, V. Oikonen, T. Noponen, T. Viljanen, M. Scheinin, M. Taittonen, T. Niemi, S. Enerback and K. A. Virtanen (2011). Different metabolic responses of human brown adipose tissue to activation by cold and insulin. *Cell Metab* **14**(2): 272-279.

Ortega, F. J., J. M. Moreno-Navarrete, V. Ribas, E. Esteve, J. I. Rodriguez-Hermosa, B. Ruiz, B. Peral, W. Ricart, A. Zorzano and J. M. Fernandez-Real (2009). Subcutaneous fat shows higher thyroid hormone receptor-alpha1 gene expression than omental fat. *Obesity (Silver Spring)* **17**(12): 2134-2141.

Ouellet, V., S. M. Labbe, D. P. Blondin, S. Phoenix, B. Guerin, F. Haman, E. E. Turcotte, D. Richard and A. C. Carpentier (2012). Brown adipose tissue oxidative metabolism contributes to energy expenditure during acute cold exposure in humans. *J Clin Invest* **122**(2): 545-552.

Parysow, O., A. M. Mollerach, V. Jager, S. Racioppi, J. San Roman and V. H. Gerbaudo (2007). Low-dose oral propranolol could reduce brown adipose tissue F-18 FDG uptake in patients undergoing PET scans. *Clin Nucl Med* **32**(5): 351-357.

Perkins, A. C., D. S. Mshelia, M. E. Symonds and M. Sathekge (2013). Prevalence and pattern of brown adipose tissue distribution of 18F-FDG in patients undergoing PET-CT in a subtropical climatic zone. *Nucl Med Commun* **34**(2): 168-174.

Petrovic, N., T. B. Walden, I. G. Shabalina, J. A. Timmons, B. Cannon and J. Nedergaard (2010). Chronic peroxisome proliferator-activated receptor gamma (PPARgamma) activation of epididymally derived white adipocyte cultures reveals a population of thermogenically competent,

UCP1-containing adipocytes molecularly distinct from classic brown adipocytes. *J Biol Chem* **285**(10): 7153-7164.

Pfannenberger, C., M. K. Werner, S. Ripkens, I. Stef, A. Deckert, M. Schmadl, M. Reimold, H. U. Haring, C. D. Claussen and N. Stefan (2010). Impact of age on the relationships of brown adipose tissue with sex and adiposity in humans. *Diabetes* **59**(7): 1789-1793.

Pierdomenico, S. D., A. M. Pierdomenico, F. Cuccurullo and G. Iacobellis (2013). Meta-analysis of the relation of echocardiographic epicardial adipose tissue thickness and the metabolic syndrome. *Am J Cardiol* **111**(1): 73-78.

Pisani, D. F., M. Djedaini, G. E. Beranger, C. Elabd, M. Scheideler, G. Ailhaud and E. Z. Amri (2011). Differentiation of Human Adipose-Derived Stem Cells into "Brite" (Brown-in-White) Adipocytes. *Front Endocrinol (Lausanne)* **2**: 87.

Poissonnet, C. M., A. R. Burdi and S. M. Garn (1984). The chronology of adipose tissue appearance and distribution in the human fetus. *Early Hum Dev* **10**(1-2): 1-11.

Pope, M., H. Budge and M. E. Symonds (2013). The developmental transition of ovine adipose tissue through early life. *Acta Physiol (Oxf)*.

Pope, M., H. Budge and M. E. Symonds (2014). The developmental transition of ovine adipose tissue through early life. *Acta Physiol (Oxf)* **210**(1): 20-30.

Poppitt, S. D., F. E. Leahy, G. F. Keogh, Y. Wang, T. B. Mulvey, M. Stojkovic, Y. K. Chan, Y. S. Choong, B. H. McArdle and G. J. Cooper (2006). Effect of high-fat meals and fatty acid saturation on postprandial levels of the hormones ghrelin and leptin in healthy men. *Eur J Clin Nutr* **60**(1): 77-84.

Power, G. G., T. R. Gunn, B. M. Johnston, G. Nichols and P. D. Gluckman (1989). Umbilical cord occlusion but not increased plasma T3 or norepinephrine stimulate brown adipose tissue thermogenesis in the fetal sheep. *J Dev Physiol* **11**(3): 171-177.

Puigserver, P., D. Herron, M. Gianotti, A. Palou, B. Cannon and J. Nedergaard (1992). Induction and degradation of the uncoupling protein thermogenin in brown adipocytes in vitro and in vivo. Evidence for a rapidly degradable pool. *Biochem J* **284** (Pt 2): 393-398.

Puigserver, P., Z. Wu, C. W. Park, R. Graves, M. Wright and B. M. Spiegelman (1998). A cold-inducible coactivator of nuclear receptors linked to adaptive thermogenesis. *Cell* **92**(6): 829-839.

Quevedo, S., P. Roca, C. Pico and A. Palou (1998). Sex-associated differences in cold-induced UCP1 synthesis in rodent brown adipose tissue. *Pflugers Arch* **436**(5): 689-695.

Rabkin, S. W. (2007). Epicardial fat: properties, function and relationship to obesity. *Obes Rev* **8**(3): 253-261.

Ravelli, A. C., J. H. van Der Meulen, C. Osmond, D. J. Barker and O. P. Bleker (1999). Obesity at the age of 50 y in men and women exposed to famine prenatally. *Am J Clin Nutr* **70**(5): 811-816.

Redman, L. M., L. de Jonge, X. Fang, B. Gamlin, D. Recker, F. L. Greenway, S. R. Smith and E. Ravussin (2007). Lack of an effect of a novel beta3-adrenoceptor agonist, TAK-677, on energy metabolism in obese individuals: a double-blind, placebo-controlled randomized study. *J Clin Endocrinol Metab* **92**(2): 527-531.

Reilly, J. J. and J. Kelly (2011). Long-term impact of overweight and obesity in childhood and adolescence on morbidity and premature mortality in adulthood: systematic review. *Int J Obes (Lond)* **35**(7): 891-898.

Ricquier, D., G. Mory, F. Bouillaud, J. Thibault and J. Weissenbach (1984). Rapid increase of mitochondrial uncoupling protein and its mRNA in stimulated brown adipose tissue. Use of a cDNA probe. *FEBS Lett* **178**(2): 240-244.

Robinson, L., S. Ojha, M. E. Symonds and H. Budge (2014). Body mass index as a determinant of brown adipose tissue function in healthy children. *J Pediatr* **164**(2): 318-322 e311.

Rockstroh, D., K. Landgraf, I. V. Wagner, J. Gesing, R. Tauscher, N. Lakowa, W. Kiess, U. Buhligen, M. Wojan, H. Till, M. Bluher and A. Korner (2015). Direct evidence of brown adipocytes in different fat depots in children. *PLoS One* **10**(2): e0117841.

Rohlf, E. M., K. W. Daniel, R. T. Premont, L. P. Kozak and S. Collins (1995). Regulation of the uncoupling protein gene (*Ucp*) by beta 1, beta 2, and beta 3-adrenergic receptor subtypes in immortalized brown adipose cell lines. *J Biol Chem* **270**(18): 10723-10732.

Roseboom, T. J., J. H. van der Meulen, C. Osmond, D. J. Barker, A. C. Ravelli and O. P. Bleker (2001). Adult survival after prenatal exposure to the Dutch famine 1944--45. *Paediatr Perinat Epidemiol* **15**(3): 220-225.

Roseboom, T. J., J. H. van der Meulen, C. Osmond, D. J. Barker, A. C. Ravelli, J. M. Schroeder-Tanka, G. A. van Montfrans, R. P. Michels and

O. P. Bleker (2000). Coronary heart disease after prenatal exposure to the Dutch famine, 1944-45. *Heart* **84**(6): 595-598.

Roseboom, T. J., J. H. van der Meulen, A. C. Ravelli, C. Osmond, D. J. Barker and O. P. Bleker (2001). Effects of prenatal exposure to the Dutch famine on adult disease in later life: an overview. *Mol Cell Endocrinol* **185**(1-2): 93-98.

Rosell, M., M. C. Jones and M. G. Parker (2011). Role of nuclear receptor corepressor RIP140 in metabolic syndrome. *Biochim Biophys Acta* **1812**(8): 919-928.

Rosen, E. D. and B. M. Spiegelman (2000). Molecular regulation of adipogenesis. *Annu Rev Cell Dev Biol* **16**: 145-171.

Rosenbaum, M. and R. L. Leibel (2010). Adaptive thermogenesis in humans. *Int J Obes (Lond)* **34 Suppl 1**: S47-55.

Rosito, G. A., J. M. Massaro, U. Hoffmann, F. L. Ruberg, A. A. Mahabadi, R. S. Vasan, C. J. O'Donnell and C. S. Fox (2008). Pericardial fat, visceral abdominal fat, cardiovascular disease risk factors, and vascular calcification in a community-based sample: the Framingham Heart Study. *Circulation* **117**(5): 605-613.

Rothwell, N. J. and M. J. Stock (1979). A role for brown adipose tissue in diet-induced thermogenesis. *Nature* **281**(5726): 31-35.

Rothwell, N. J. and M. J. Stock (1983). Luxuskonsumtion, diet-induced thermogenesis and brown fat: the case in favour. *Clin Sci (Lond)* **64**(1): 19-23.

Ruberg, F. L., Z. Chen, N. Hua, S. Bigornia, Z. Guo, K. Hallock, H. Jara, M. LaValley, A. Phinikaridou, Y. Qiao, J. Viereck, C. M. Apovian and J. A. Hamilton (2010). The relationship of ectopic lipid accumulation to cardiac and vascular function in obesity and metabolic syndrome. *Obesity (Silver Spring)* **18**(6): 1116-1121.

Sacks, H. S. and J. N. Fain (2007). Human epicardial adipose tissue: a review. *Am Heart J* **153**(6): 907-917.

Sacks, H. S., J. N. Fain, S. W. Bahouth, S. Ojha, A. Frontini, H. Budge, S. Cinti and M. E. Symonds (2013). Adult epicardial fat exhibits beige features. *J Clin Endocrinol Metab* **98**(9): E1448-1455.

Sacks, H. S., J. N. Fain, P. Cheema, S. W. Bahouth, E. Garrett, R. Y. Wolf, D. Wolford and J. Samaha (2011). Inflammatory genes in epicardial fat contiguous with coronary atherosclerosis in the metabolic

syndrome and type 2 diabetes: changes associated with pioglitazone. *Diabetes Care* **34**(3): 730-733.

Sacks, H. S., J. N. Fain, B. Holman, P. Cheema, A. Chary, F. Parks, J. Karas, R. Optican, S. W. Bahouth, E. Garrett, R. Y. Wolf, R. A. Carter, T. Robbins, D. Wolford and J. Samaha (2009). Uncoupling protein-1 and related messenger ribonucleic acids in human epicardial and other adipose tissues: epicardial fat functioning as brown fat. *J Clin Endocrinol Metab* **94**(9): 3611-3615.

Saito, M., Y. Okamatsu-Ogura, M. Matsushita, K. Watanabe, T. Yoneshiro, J. Nio-Kobayashi, T. Iwanaga, M. Miyagawa, T. Kameya, K. Nakada, Y. Kawai and M. Tsujisaki (2009). High incidence of metabolically active brown adipose tissue in healthy adult humans: effects of cold exposure and adiposity. *Diabetes* **58**(7): 1526-1531.

Salzer, H. R., F. Haschke, M. Wimmer, M. Heil and R. Schilling (1989). Growth and nutritional intake of infants with congenital heart disease. *Pediatr Cardiol* **10**(1): 17-23.

Schmittgen, T. D. and K. J. Livak (2008). Analyzing real-time PCR data by the comparative C(T) method. *Nat Protoc* **3**(6): 1101-1108.

Scholzen, T. and J. Gerdes (2000). The Ki-67 protein: from the known and the unknown. *J Cell Physiol* **182**(3): 311-322.

Schoof, E., A. Stuppy, F. Harig, R. Carbon, T. Horbach, W. Stohr, W. Rascher and J. Dotsch (2004). Comparison of leptin gene expression in different adipose tissues in children and adults. *Eur J Endocrinol* **150**(4): 579-584.

Schulz, T. J. and Y. H. Tseng (2009). Emerging role of bone morphogenetic proteins in adipogenesis and energy metabolism. *Cytokine Growth Factor Rev* **20**(5-6): 523-531.

Schusterova, I., F. H. Leenen, A. Jurko, F. Sabol and J. Takacova (2014). Epicardial adipose tissue and cardiometabolic risk factors in overweight and obese children and adolescents. *Pediatr Obes* **9**(1): 63-70.

Scott, K. M., R. Bruffaerts, G. E. Simon, J. Alonso, M. Angermeyer, G. de Girolamo, K. Demyttenaere, I. Gasquet, J. M. Haro, E. Karam, R. C. Kessler, D. Levinson, M. E. Medina Mora, M. A. Oakley Browne, J. Ormel, J. P. Villa, H. Uda and M. Von Korff (2008). Obesity and mental disorders in the general population: results from the world mental health surveys. *Int J Obes (Lond)* **32**(1): 192-200.

Seale, P., B. Bjork, W. Yang, S. Kajimura, S. Chin, S. Kuang, A. Scime, S. Devarakonda, H. M. Conroe, H. Erdjument-Bromage, P. Tempst, M. A. Rudnicki, D. R. Beier and B. M. Spiegelman (2008). PRDM16 controls a brown fat/skeletal muscle switch. *Nature* **454**(7207): 961-967.

Seale, P., S. Kajimura, W. Yang, S. Chin, L. M. Rohas, M. Uldry, G. Tavernier, D. Langin and B. M. Spiegelman (2007). Transcriptional control of brown fat determination by PRDM16. *Cell Metab* **6**(1): 38-54.

Shabalina, I. G., M. Ost, N. Petrovic, M. Vrbacky, J. Nedergaard and B. Cannon (2010). Uncoupling protein-1 is not leaky. *Biochim Biophys Acta* **1797**(6-7): 773-784.

Shimabukuro, M. (2009). Cardiac adiposity and global cardiometabolic risk: new concept and clinical implication. *Circ J* **73**(1): 27-34.

Silva, J. E. and P. R. Larsen (1983). Adrenergic activation of triiodothyronine production in brown adipose tissue. *Nature* **305**(5936): 712-713.

Singh, A. S., C. Mulder, J. W. Twisk, W. van Mechelen and M. J. Chinapaw (2008). Tracking of childhood overweight into adulthood: a systematic review of the literature. *Obes Rev* **9**(5): 474-488.

Soderlund, V., S. A. Larsson and H. Jacobsson (2007). Reduction of FDG uptake in brown adipose tissue in clinical patients by a single dose of propranolol. *Eur J Nucl Med Mol Imaging* **34**(7): 1018-1022.

Sousa e Silva, T., C. A. Longui, M. N. Rocha, C. D. Faria, M. R. Melo, T. G. Faria, J. A. de Souza and L. V. Rizzo (2010). Prolonged physical training decreases mRNA levels of glucocorticoid receptor and inflammatory genes. *Horm Res Paediatr* **74**(1): 6-14.

Souza, T. L. V., C. T. Coelho, P. B. Guimaraes, E. M. Goto, S. M. A. Silva, J. A. Silva, M. T. Nunes, S. S. M. Ihara and J. Luz (2012). Intrauterine food restriction alters the expression of uncoupling proteins in brown adipose tissue of rat newborns. *Journal of Thermal Biology* **37**(2): 138-143.

Steltzer, M., N. Rudd and B. Pick (2005). Nutrition care for newborns with congenital heart disease. *Clin Perinatol* **32**(4): 1017-1030, xi.

Stoughton, R. B. (2005). Applications of DNA microarrays in biology. *Annu Rev Biochem* **74**: 53-82.

Streuling, I., A. Beyerlein and R. von Kries (2010). Can gestational weight gain be modified by increasing physical activity and diet

- counseling? A meta-analysis of interventional trials. *Am J Clin Nutr* **92**(4): 678-687.
- Sugden, M. C. and M. J. Holness (1993). Physiological modulation of the uptake and fate of glucose in brown adipose tissue. *Biochem J* **295** (Pt 1): 171-176.
- Svensson, P. A., M. Jernas, K. Sjöholm, J. M. Hoffmann, B. E. Nilsson, M. Hansson and L. M. Carlsson (2011). Gene expression in human brown adipose tissue. *Int J Mol Med* **27**(2): 227-232.
- Symonds, M. E., M. J. Bryant, L. Clarke, C. J. Darby and M. A. Lomax (1992). Effect of maternal cold exposure on brown adipose tissue and thermogenesis in the neonatal lamb. *J Physiol* **455**: 487-502.
- Symonds, M. E., H. Budge, A. C. Perkins and M. A. Lomax (2011). Adipose tissue development--impact of the early life environment. *Prog Biophys Mol Biol* **106**(1): 300-306.
- Symonds, M. E., H. Budge and T. Stephenson (2000). Limitations of models used to examine the influence of nutrition during pregnancy and adult disease. *Arch Dis Child* **83**(3): 215-219.
- Symonds, M. E., A. Mostyn, S. Pearce, H. Budge and T. Stephenson (2003). Endocrine and nutritional regulation of fetal adipose tissue development. *J Endocrinol* **179**(3): 293-299.
- Symonds, M. E., M. Pope, D. Sharkey and H. Budge (2012). Adipose tissue and fetal programming. *Diabetologia* **55**(6): 1597-1606.
- Symonds, M. E., T. Stephenson, D. S. Gardner and H. Budge (2007). Long-term effects of nutritional programming of the embryo and fetus: mechanisms and critical windows. *Reprod Fertil Dev* **19**(1): 53-63.
- Taguchi, R., J. Takasu, Y. Itani, R. Yamamoto, K. Yokoyama, S. Watanabe and Y. Masuda (2001). Pericardial fat accumulation in men as a risk factor for coronary artery disease. *Atherosclerosis* **157**(1): 203-209.
- Tang, Q. Q., M. Gronborg, H. Huang, J. W. Kim, T. C. Otto, A. Pandey and M. D. Lane (2005). Sequential phosphorylation of CCAAT enhancer-binding protein beta by MAPK and glycogen synthase kinase 3beta is required for adipogenesis. *Proc Natl Acad Sci U S A* **102**(28): 9766-9771.
- Tang, Q. Q. and M. D. Lane (2012). Adipogenesis: from stem cell to adipocyte. *Annu Rev Biochem* **81**: 715-736.

Tang, Q. Q., T. C. Otto and M. D. Lane (2004). Commitment of C3H10T1/2 pluripotent stem cells to the adipocyte lineage. *Proc Natl Acad Sci U S A* **101**(26): 9607-9611.

Taylor, P. D. and L. Poston (2007). Developmental programming of obesity in mammals. *Exp Physiol* **92**(2): 287-298.

Taylor, S. C., T. Berkelman, G. Yadav and M. Hammond (2013). A defined methodology for reliable quantification of Western blot data. *Mol Biotechnol* **55**(3): 217-226.

Teruel, T., A. M. Valverde, M. Benito and M. Lorenzo (1996). Insulin-like growth factor I and insulin induce adipogenic-related gene expression in fetal brown adipocyte primary cultures. *Biochem J* **319** (Pt 2): 627-632.

Thanassoulis, G., J. M. Massaro, U. Hoffmann, A. A. Mahabadi, R. S. Vasan, C. J. O'Donnell and C. S. Fox (2010). Prevalence, distribution, and risk factor correlates of high pericardial and intrathoracic fat depots in the Framingham heart study. *Circ Cardiovasc Imaging* **3**(5): 559-566.

Thommessen, M., A. Heiberg and B. F. Kase (1992). Feeding problems in children with congenital heart disease: the impact on energy intake and growth outcome. *Eur J Clin Nutr* **46**(7): 457-464.

Thompson, K. L., P. S. Pine, B. A. Rosenzweig, Y. Turpaz and J. Retief (2007). Characterization of the effect of sample quality on high density oligonucleotide microarray data using progressively degraded rat liver RNA. *BMC Biotechnol* **7**: 57.

Timmons, J. A., K. Wennmalm, O. Larsson, T. B. Walden, T. Lassmann, N. Petrovic, D. L. Hamilton, R. E. Gimeno, C. Wahlestedt, K. Baar, J. Nedergaard and B. Cannon (2007). Myogenic gene expression signature establishes that brown and white adipocytes originate from distinct cell lineages. *Proc Natl Acad Sci U S A* **104**(11): 4401-4406.

Tseng, Y. H., E. Kokkotou, T. J. Schulz, T. L. Huang, J. N. Winnay, C. M. Taniguchi, T. T. Tran, R. Suzuki, D. O. Espinoza, Y. Yamamoto, M. J. Ahrens, A. T. Dudley, A. W. Norris, R. N. Kulkarni and C. R. Kahn (2008). New role of bone morphogenetic protein 7 in brown adipogenesis and energy expenditure. *Nature* **454**(7207): 1000-1004.

Uldry, M., W. Yang, J. St-Pierre, J. Lin, P. Seale and B. M. Spiegelman (2006). Complementary action of the PGC-1 coactivators in mitochondrial biogenesis and brown fat differentiation. *Cell Metab* **3**(5): 333-341.

Vague, J. (1947). La differenciation sexuelle; facteur determinant des formes de l'obesite. *Presse Med* **55**(30): 339.

van Baak, M. A. (2008). Meal-induced activation of the sympathetic nervous system and its cardiovascular and thermogenic effects in man. *Physiol Behav* **94**(2): 178-186.

van der Lans, A. A., J. Hoeks, B. Brans, G. H. Vijgen, M. G. Visser, M. J. Vosselman, J. Hansen, J. A. Jorgensen, J. Wu, F. M. Mottaghy, P. Schrauwen and W. D. van Marken Lichtenbelt (2013). Cold acclimation recruits human brown fat and increases nonshivering thermogenesis. *J Clin Invest* **123**(8): 3395-3403.

Van Harmelen, V., S. Reynisdottir, P. Eriksson, A. Thorne, J. Hoffstedt, F. Lonnqvist and P. Arner (1998). Leptin secretion from subcutaneous and visceral adipose tissue in women. *Diabetes* **47**(6): 913-917.

van Marken Lichtenbelt, W. D. and P. Schrauwen (2011). Implications of nonshivering thermogenesis for energy balance regulation in humans. *Am J Physiol Regul Integr Comp Physiol* **301**(2): R285-296.

van Marken Lichtenbelt, W. D., J. W. Vanhommerig, N. M. Smulders, J. M. Drossaerts, G. J. Kemerink, N. D. Bouvy, P. Schrauwen and G. J. Teule (2009). Cold-activated brown adipose tissue in healthy men. *N Engl J Med* **360**(15): 1500-1508.

Vandesompele, J., K. De Preter, F. Pattyn, B. Poppe, N. Van Roy, A. De Paepe and F. Speleman (2002). Accurate normalization of real-time quantitative RT-PCR data by geometric averaging of multiple internal control genes. *Genome Biol* **3**(7): RESEARCH0034.

Vegiopoulos, A. and S. Herzig (2007). Glucocorticoids, metabolism and metabolic diseases. *Mol Cell Endocrinol* **275**(1-2): 43-61.

Vieau, D., N. Sebaai, M. Leonhardt, I. Dutriez-Casteloot, O. Molendi-Coste, C. Laborie, C. Breton, S. Deloof and J. Lesage (2007). HPA axis programming by maternal undernutrition in the male rat offspring. *Psychoneuroendocrinology* **32 Suppl 1**: S16-20.

Virtanen, K. A., M. E. Lidell, J. Orava, M. Heglind, R. Westergren, T. Niemi, M. Taittonen, J. Laine, N. J. Savisto, S. Enerback and P. Nuutila (2009). Functional brown adipose tissue in healthy adults. *N Engl J Med* **360**(15): 1518-1525.

Visscher, T. L. and J. C. Seidell (2001). The public health impact of obesity. *Annu Rev Public Health* **22**: 355-375.

Vogel, C. and E. M. Marcotte (2012). Insights into the regulation of protein abundance from proteomic and transcriptomic analyses. *Nat Rev Genet* **13**(4): 227-232.

Vosselman, M. J., B. Brans, A. A. van der Lans, R. Wierds, M. A. van Baak, F. M. Mottaghy, P. Schrauwen and W. D. van Marken Lichtenbelt (2013). Brown adipose tissue activity after a high-calorie meal in humans. *Am J Clin Nutr* **98**(1): 57-64.

Vosselman, M. J., A. A. van der Lans, B. Brans, R. Wierds, M. A. van Baak, P. Schrauwen and W. D. van Marken Lichtenbelt (2012). Systemic beta-adrenergic stimulation of thermogenesis is not accompanied by brown adipose tissue activity in humans. *Diabetes* **61**(12): 3106-3113.

Vrieze, A., J. E. Schopman, W. M. Admiraal, M. R. Soeters, M. Nieuwdorp, H. J. Verberne and F. Holleman (2012). Fasting and postprandial activity of brown adipose tissue in healthy men. *J Nucl Med* **53**(9): 1407-1410.

Wajchenberg, B. L. (2000). Subcutaneous and visceral adipose tissue: their relation to the metabolic syndrome. *Endocr Rev* **21**(6): 697-738.

Walden, T. B., I. R. Hansen, J. A. Timmons, B. Cannon and J. Nedergaard (2012). Recruited vs. nonrecruited molecular signatures of brown, "brite," and white adipose tissues. *Am J Physiol Endocrinol Metab* **302**(1): E19-31.

Wang, Q., M. Zhang, G. Ning, W. Gu, T. Su, M. Xu, B. Li and W. Wang (2011). Brown adipose tissue in humans is activated by elevated plasma catecholamines levels and is inversely related to central obesity. *PLoS One* **6**(6): e21006.

Wang, Y., Y. Wu, R. F. Wilson, S. Bleich, L. Cheskin, C. Weston, N. Showell, O. Fawole, B. Lau and J. Segal (2013). Childhood Obesity Prevention Programs: Comparative Effectiveness Review and Meta-Analysis. *Effective health care programme* **Review No. 115**.

Wellen, K. E. and G. S. Hotamisligil (2005). Inflammation, stress, and diabetes. *J Clin Invest* **115**(5): 1111-1119.

Werner, M., A. Chott, A. Fabiano and H. Battifora (2000). Effect of formalin tissue fixation and processing on immunohistochemistry. *Am J Surg Pathol* **24**(7): 1016-1019.

WHO (1986). Use and interpretation of anthropometric indicators of nutritional status. *Bulletin of the World Health Organization* **64**(6): 929-941.

WHO (2006) European Charter on counteracting obesity.

- WHO, W. H. O. E. C. (1995). Physical Status: The Use and Interpretation of Anthropometry, . WHO Technical Report **854**.
- Widdowson, E. M. and R. A. McCance (1963). The Effect of Finite Periods of Undernutrition at Different Ages on the Composition and Subsequent Development of the Rat. *Proc R Soc Lond B Biol Sci* **158**: 329-342.
- Wijers, S. L., W. H. Saris and W. D. van Marken Lichtenbelt (2007). Individual thermogenic responses to mild cold and overfeeding are closely related. *J Clin Endocrinol Metab* **92**(11): 4299-4305.
- Wijers, S. L., P. Schrauwen, M. A. van Baak, W. H. Saris and W. D. van Marken Lichtenbelt (2011). Beta-adrenergic receptor blockade does not inhibit cold-induced thermogenesis in humans: possible involvement of brown adipose tissue. *J Clin Endocrinol Metab* **96**(4): E598-605.
- Williams, G. and G. M. Kolodny (2008). Method for decreasing uptake of ¹⁸F-FDG by hypermetabolic brown adipose tissue on PET. *AJR Am J Roentgenol* **190**(5): 1406-1409.
- Wong, C. X., H. S. Abed, P. Molaee, A. J. Nelson, A. G. Brooks, G. Sharma, D. P. Leong, D. H. Lau, M. E. Middeldorp, K. C. Roberts-Thomson, G. A. Wittert, W. P. Abhayaratna, S. G. Worthley and P. Sanders (2011). Pericardial fat is associated with atrial fibrillation severity and ablation outcome. *J Am Coll Cardiol* **57**(17): 1745-1751.
- Xu, Y., X. Cheng, K. Hong, C. Huang and L. Wan (2012). How to interpret epicardial adipose tissue as a cause of coronary artery disease: a meta-analysis. *Coron Artery Dis* **23**(4): 227-233.
- Yamaguchi, Y., S. Cavallero, M. Patterson, H. Shen, J. Xu, S. R. Kumar and H. M. Sucov (2015). Adipogenesis and epicardial adipose tissue: A novel fate of the epicardium induced by mesenchymal transformation and PPARgamma activation. *Proc Natl Acad Sci U S A* **112**(7): 2070-2075.
- Yubero, P., C. Manchado, A. M. Cassard-Doulcier, T. Mampel, O. Vinas, R. Iglesias, M. Giral and F. Villarroya (1994). CCAAT/enhancer binding proteins alpha and beta are transcriptional activators of the brown fat uncoupling protein gene promoter. *Biochem Biophys Res Commun* **198**(2): 653-659.
- Zhao, J., L. Unelius, T. Bengtsson, B. Cannon and J. Nedergaard (1994). Coexisting beta-adrenoceptor subtypes: significance for thermogenic process in brown fat cells. *Am J Physiol* **267**(4 Pt 1): C969-979.

Zingaretti, M. C., F. Crosta, A. Vitali, M. Guerrieri, A. Frontini, B. Cannon, J. Nedergaard and S. Cinti (2009). The presence of UCP1 demonstrates that metabolically active adipose tissue in the neck of adult humans truly represents brown adipose tissue. *FASEB J* **23**(9): 3113-3120.

Zukotynski, K. A., F. H. Fahey, S. Laffin, R. Davis, S. T. Treves, F. D. Grant and L. A. Drubach (2009). Constant ambient temperature of 24 degrees C significantly reduces FDG uptake by brown adipose tissue in children scanned during the winter. *Eur J Nucl Med Mol Imaging* **36**(4): 602-606.

10 Appendices

10.1 Ethical approvals for human studies

10.1.1 Study of brown adipose tissue in epicardial fat of adult humans

The samples for the study of brown adipose tissue in epicardial fat of human adults were obtained from the participants of the Human Epicardial Fat Adipokines and Coronary Atherosclerosis study. Ethical approval for this study was obtained from the Baptist Memorial Health Care Corporation Institutional Review Board.

**BAPTIST MEMORIAL HEALTH CARE CORPORATION
INSTITUTIONAL REVIEW BOARD**

6025 Walnut Grove Road, Suite 404
MEMPHIS, TENNESSEE 38120

J. CAMERON HALL, M.D., CHAIRMAN

October 19, 2010

Harold S. Sacks, M.D.
6027 Walnut Grove Road, Suite 307
Memphis, TN 38120

BMH-IRB 05-48

Protocol Amendment dated September 27, 2010 approved 10/14/10

Dear Dr. Sacks:

On October 19, 2010, the Baptist Memorial Health Care Corporation Institutional Review Board reviewed the amendment to your study entitled **"Human Epicardial Fat Adipokines and Coronary Atherosclerosis"**. The IRB has approved the amendment to your protocol. The amendment is now in effect.

The approval/reapproval of your study expires on December 24, 2010, and must be renewed prior to this date, if the study is ongoing, or the study will be terminated.

The Baptist Memorial Health Care Corporation Institutional Review Board approval of this protocol does not imply granting of practice privileges or credentialing for clinical activities described or included in this protocol. The Baptist Memorial Health Care Corporation Institutional Review Board assumes that the responsible physicians or professionals already have active privileges in this institution pertinent to the application of the protocol.

The Baptist Memorial Health Care Corporation Institutional Review Board expects that patients enrolled in this study who have identified adverse events will have these events reported. The PI is responsible for reporting adverse events to the FDA, the Sponsor and the Baptist Memorial Health Care Corporation Institutional Review Board.

Both the FDA and the IRB require periodic reports, at least annually, concerning this research project. Annual reports must include a completed application for renewal or termination wherein the following items are summarized:

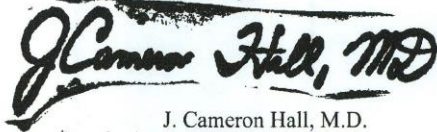
1. the number of new BMH patients entered into the study during the preceding year;
2. the total number of BMH patients entered, the number dropped from the study, and the reasons for patient non-compliance;

3. the results to date, including patient response (favorable or unfavorable response, no response). If results from the sponsor or collaborating group are not available, a brief description of the responses of your BMH patients should be supplied.
4. any complications or toxic effects not previously submitted to the IRB.

The Baptist Memorial Health Care Corporation Institutional Review Board must be notified at once if any of the following events occur:

1. a change in the protocol (amendments, updates, revisions);
2. a change in the investigators listed in the application;
3. serious toxic effects, adverse reactions, or unexpected deaths.

Sincerely,

A handwritten signature in black ink that reads "J. Cameron Hall, M.D." in a cursive style.

J. Cameron Hall, M.D.
Chairman

JCH:sms

10.1.2 Study of brown adipose tissue in pericardial fat of newborns, infants and children

The sample collection for the study of pericardial adipose tissue in children was conducted with ethical approval from National Research Ethics Service Committee (NRES) East Midlands – Nottingham 2 (REC reference number: 12/EM/0214).

NRES Committee East Midlands - Nottingham 2

The Old Chapel
Royal Standard Place
Nottingham
NG1 6FS

Telephone: 0115 8839428
Facsimile: 0115 9123300

29 November 2012

Dr Helen Budge
Reader in Neonatology University
Nottingham Academic Child Health
Queen's Medical Centre
Nottingham
NG7 2UH

Dear Dr Budge

Study title: A Study of Presence of Brown Adipose Tissue in Abdominal Visceral Adipose Tissue in Newborn Infants and Children
REC reference: 12/EM/0428
Protocol number: 12111
IRAS Project ID: 112195

The Research Ethics Committee reviewed the above application at the meeting held on 26 November 2012. Thank you for attending to discuss the application.

We plan to publish your research summary wording for the above study on the NRES website, together with your contact details, unless you expressly withhold permission to do so. Publication will be no earlier than three months from the date of this favourable opinion letter. Should you wish to provide a substitute contact point, require further information, or wish to withhold permission to publish, please contact the Co-ordinator Miss Heather Harrison, heather.harrison@nottspct.nhs.uk.

Ethical opinion

- The committee stated that there are a number of unexplained acronyms within the IRAS application form. You explained that the acronyms are explained within the protocol, they are genes which help differentiate brown fat.
- The committee queried whether long term storage may be a possibility for the DNA extracted in the study. You stated that 5 grams would be collected for the study which would be divided between slides and gene assessment. There will be inadequate tissue for long term storage.
- The committee mentioned that the insurance for this study does not cover under 5 year olds. You stated that the University insurance provides a disclaimer that if no interventions are involved for the participants under 5 they will be covered.

The members of the Committee present gave a favourable ethical opinion of the above research on the basis described in the application form, protocol and supporting documentation, subject to the conditions specified below.

Ethical review of research sites

NHS Sites

The favourable opinion applies to all NHS sites taking part in the study, subject to management permission being obtained from the NHS/HSC R&D office prior to the start of the study (see "Conditions of the favourable opinion" below).

Conditions of the favourable opinion

The favourable opinion is subject to the following conditions being met prior to the start of the study.

Management permission or approval must be obtained from each host organisation prior to the start of the study at the site concerned.

Management permission ("R&D approval") should be sought from all NHS organisations involved in the study in accordance with NHS research governance arrangements.

Guidance on applying for NHS permission for research is available in the Integrated Research Application System or at <http://www.rdforum.nhs.uk>.

Where a NHS organisation's role in the study is limited to identifying and referring potential participants to research sites ("participant identification centre"), guidance should be sought from the R&D office on the information it requires to give permission for this activity.

For non-NHS sites, site management permission should be obtained in accordance with the procedures of the relevant host organisation.

Sponsors are not required to notify the Committee of approvals from host organisations

1. It should be taken into consideration that 16-17 year old participants are able to give consent if it is deemed that they fully comprehend the study.

It is responsibility of the sponsor to ensure that all the conditions are complied with before the start of the study or its initiation at a particular site (as applicable).

You should notify the REC in writing once all conditions have been met (except for site approvals from host organisations) and provide copies of any revised documentation with updated version numbers. The REC will acknowledge receipt and provide a final list of the approved documentation for the study, which can be made available to host organisations to facilitate their permission for the study. Failure to provide the final versions to the REC may cause delay in obtaining permissions.

Approved documents

The documents reviewed and approved at the meeting were:

<i>Document</i>	<i>Version</i>	<i>Date</i>
Covering Letter	Letter from Shalini Ojha	29 October 2012
Evidence of insurance or indemnity	Henderson Corporate	08 August 2012
Investigator CV	Dr Helen Budge	29 October 2012
Letter from Sponsor	Signed by Paul Cartledge	25 October 2012

Other: CV	Dr Shalini Ojha	25 October 2012
Participant Consent Form: Parent Consent Form	1.0	12 October 2012
Participant Information Sheet: AITC Study Leaflet for Parents	1.0	12 October 2012
Participant Information Sheet: AITC Study Leaflet for Parents (Antenatal)	1.0	12 October 2012
Participant Information Sheet: AITC Study Leaflet for Young Persons 11-15 Years Old	1.0	12 October 2012
Participant Information Sheet: AITC Study Leaflet for Young Persons 16-17 Years Old	1.0	12 October 2012
Protocol	1.0	12 October 2012
REC application	112195/377008/1/109	25 October 2012

Membership of the Committee

The members of the Ethics Committee who were present at the meeting are listed on the attached sheet.

A committee member declared that they know the Chief Investigator Helen Budge and researcher Shalini Ojha however has no involvement in the study and will partake in the discussion.

Statement of compliance

The Committee is constituted in accordance with the Governance Arrangements for Research Ethics Committees and complies fully with the Standard Operating Procedures for Research Ethics Committees in the UK.

After ethical review

Reporting requirements

The attached document "After ethical review – guidance for researchers" gives detailed guidance on reporting requirements for studies with a favourable opinion, including:

- Notifying substantial amendments
- Adding new sites and investigators
- Notification of serious breaches of the protocol
- Progress and safety reports
- Notifying the end of the study

The NRES website also provides guidance on these topics, which is updated in the light of changes in reporting requirements or procedures.

Feedback

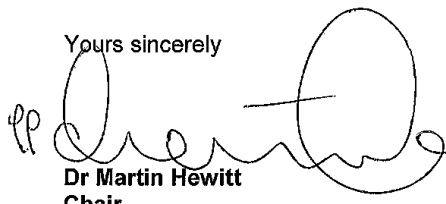
You are invited to give your view of the service that you have received from the National Research Ethics Service and the application procedure. If you wish to make your views known please use the feedback form available on the website.

Further information is available at National Research Ethics Service website > After Review

12/EM/0428	Please quote this number on all correspondence
-------------------	---

With the Committee's best wishes for the success of this project

Yours sincerely

A handwritten signature in black ink, appearing to read 'Dr Martin Hewitt'. The signature is fluid and cursive, with a large loop at the end. To the left of the signature, there are small initials 'ep'.

Dr Martin Hewitt
Chair

Email: heather.harrison@nottspct.nhs.uk

*Enclosures: List of names and professions of members who were present at the meeting and those who submitted written comments
"After ethical review – guidance for researchers"*

Copy to: Sponsor - Mr Paul Cartledge

Care organisation - Maria Koufali, Nottingham University Hospitals NHS Trust

10.2 Data collection proforma for the Study of brown adipose tissue in pericardial fat of newborns, infants and children

For this study, each participant's date of birth and date of surgery were recorded. In addition, information about gender and ethnic origin, type of congenital heart disease and data about the cardiac and any other co-existing medical conditions, the individual's baseline oxygen saturation level, medications (particularly regular beta blocker), weight and height on the day of admission were also collected using a standardised proforma given in the next page.

Study Number:

Patient Identification Number for this trial:

Study of Presence of Brown Adipose Tissue in Pericardial Adipose Tissue in Newborn Infants and Children

(A Study of Fat around the Heart of Newborn Infants and Children)

(Analysis of Pericardial Adipose Tissue in Children (a-PAC) Study)

Data Collection Proforma

(Draft version 1.0: 03/07/2012)

Date of Birth (dd/mm/yyyy):	___/___/_____
Sex:	Male/Female
Weight (kg):	_____
Height (cm):	_____
Racial origin:	_____

Primary cardiac diagnosis:

Baseline oxygen saturations (%) _____

Other medical conditions

Medications *(in the period before and during surgery)*

Name of the drug	Dose

10.3 Clinical characteristics of participants

Table 10.1 Characteristics of participants: diagnosis and medications

Study number	Age (in years)	Gender	Primary Cardiac diagnosis	Other medical conditions	Regular medications
1	0.46	Male	Ventricular septal defect Right ventricular outflow tract obstruction	none	frusemide, spironolactone
2	16.48	Male	Atrial septal defect	none	atomoxetine prostaglandin E2
3	0.02	Male	Hypoplastic left heart syndrome	none	dobutamine

4	0.08	Male	Hypoplastic left heart syndrome	none	none
5	0.15	Male	Ventricular septal defect Aortopulmonary valve dysplasia	Tracheo-oesophageal fistula	frusemide captopril ranitidine domperidone
6	0.01	Female	Hypoplastic left heart syndrome	none	prostaglandin E2 dobutamine
7	0.67	Female	Ventricular septal defect	none	frusemide captopril
8	0.68	Male	Ventricular septal defect	Trisomy 21 Intrauterine growth restriction Infant of diabetic mother	frusemide spironolactone
9	0.31	Male	Tetralogy of Fallot	Prematurity (36 weeks gestation)	propranolol
10	0.12	Male	Ventricular septal	none	frusemide

			defect		spironolactone
11	17.05	Male	Partial anomalous pulmonary venous drainage ostium primum atrial septal defect	none	none
12	3.46	Male	Atrial septal defect	none	none
13	0.93	Male	Pulmonary stenosis	Noonan's syndrome	none
14	2.61	Male	Ventricular septal defect Co-arctation of aorta Hypoplastic aortic arch	none	frusemide spironolactone
15	0.47	Female	Ventricular septal defect Atrial septal defect	none	frusemide spironolactone
16	3.11	Female	Ventricular septal defect	none	frusemide

			Atrial septal defect		spironolactone
17	1.30	Male	Absent pulmonary valve	Prematurity (26 week gestation) Post-NEC ileostomy	fentanyl midazolam spironolactone enoxaparin
18	0.87	Male	Tetralogy of Fallot	none	aspirin
19	0.59		Pulmonary atresia Ventricular septal defect Major aorto-pulmonary collateral arteries	22q deletion	none
20	6.38	Male	Mixed aortic valve disease	none	amoxicillin
21	0.58	Female	Tetralogy of Fallot Left pulmonary artery stenosis	none	none

22	14.84	Male	Mixed aortic valve disease	none	none
23	0.64	Female	Ventricular septal defect	none	frusemide captopril
24	0.80	Female	Ventricular septal defect	22q deletion	frusemide captopril
25	0.99	Male	Pulmonary stenosis	none	none
26	3.40	Female	Atrial septal defect	none	none
27	1.51	Female	Atrio-ventricular septal defect	none	none
28	6.69	Male	Hypertrophic cardiomyopathy	none	propranolol
29	0.96	Female	Mild right pulmonary artery stenosis	none	none

30	0.50	Female	Atrial septal defect	none	none
31	3.36	Female	Tumour extension into IVC	Wilm's tumor	none
32	0.90	Female	ventricular septal defect	none	frusemide captopril
33	7.15	Female	severe RVOTO	none	none
34	0.11	Male	TA + VSD	none	none
35	1.50	Male	AS + AR	Bronchial asthma	frusemide, spironolactone inhaled steroids
36	0.34	Male	TOF	none	none
37	4.47	Male	ventricular septal defect	none	enalapril
38	0.41	Male	ventricular septal defect	none	none

39	0.01	Male	TA + PA	none	prostaglandin
40	0.01	Male	TGA	none	
41	0.02	Male	TGA	none	frusemide spironolactone prostaglandin
42	0.48	Male	TOF	none	propranolol
43	0.46	Male	TOF	none	frusemide spironolactone
44	3.61	Female	Atrial septal defect	none	none
45	0.82	Male	Ventricular septal defect	none	frusemide captopril
46	1.25	Female	Ventricular septal defect	none	frusemide captopril
47	0.03	Female	Transposition of great arteries	none	frusemide spironolactone

					prostaglandin
48	0.71	Female	Tetralogy of Fallot	none	propranolol
49	1.66	Male	Tetralogy of Fallot	Prematurity	none
50	0.07	Male	Truncus arteriosus	Inversion of chromosome 8	frusemide propranolol
51	2.18	Male	Atrial septal defect	Prematurity	frusemide spironolactone salbutamol betamethasone
52	0.27	Female	Corrected transposition of great arteries	Atrio-ventricular block	frusemide spironolactone
53	0.05	Male	Transposition of great arteries Ventricular septal defect Atrial septal defect	Prematurity	frusemide spironolactone

54	0.99	Male	Ventricular septal defect Right ventricular outflow tract obstruction	none	frusemide propranolol
55	0.25	Male	Total anomalous pulmonary venous connections	none	frusemide propranolol
56	0.02	Male	Transposition of great arteries	none	prostaglandin
57	0.41	Male	Tetralogy of Fallot	none	propranolol
58	1.80	Male	Atrial septal defect Pulmonary stenosis	none	none

59	1.07	Male	Tetralogy of Fallot	none	propranolol
60	0.47	Male	Atrioventricular septal defect	Trisomy 21	frusemide digoxin captopril domperidone
61	0.03	Male	Transposition of great arteries	none	prostaglandin
62	0.03	Female	Hypoplastic aortic arch	none	prostaglandin frusemide digoxin
63	0.73	Male	Ventricular septal defect Persistent foramen ovale	Trisomy 21	movicol [®]

10.4 Abstracts of original peer reviewed publications and papers

10.4.1 Brown adipose tissue genes in pericardial adipose tissue of newborn sheep are downregulated by maternal nutrient restriction in late gestation.

Ojha, S., Robinson, L., Yazdani, M., Symonds, M. E. and Budge, H. (2013). *Pediatr Res* 74, 246-251.

Background: Brown adipose tissue (BAT) thermogenesis is essential for newborn survival. Pericardial adipose tissue is a visceral depot that promotes metabolic and cardiovascular adaptations. We determined whether BAT is present in pericardial adipose tissue in newborns and whether maternal nutrition during late gestation compromises BAT in the postnatal period.

Methods: We measured uncoupling protein 1 (UCP1) and other BAT-specific genes (e.g., β 3-adrenergic receptor (β 3ADR) and deiodinase type 2 (DIO2)), together with markers of white adipose tissue (WAT) in sheep on either the first or 30th day after birth. These were twin offspring born to mothers fed with either 100% or nutrient restricted (NR) to 60% of their total metabolizable requirements from 110 d gestation to term.

Results: Gene expression of UCP1 and other BAT-related genes decreased significantly with age. In newborns, maternal nutrient

restriction downregulated gene expression of DIO2 and the β 3-adrenergic receptor with reduced UCP1 but had no effect on genes predominantly expressed in WAT.

Conclusion: BAT is present around the heart in newborns. Exposure to a suboptimal maternal diet in late gestation specifically compromises BAT development and has the potential to place these offspring at increased risk of hypothermia afterbirth without effects on the subsequent appearance of WAT.

10.4.2 Adult Epicardial Fat Exhibits Beige Features

Sacks, H.S., Fain, J.N., Bahouth, S.W., Ojha, S. Frontini, A., Budge, H., Cinti, S., and Symonds, M.E. (2013). J Clin Endocrinol Metab. 98, E1448-E1455

Context: Human epicardial fat has been designated previously as brown-like fat. The supraclavicular fat depot in man has been defined as beige coexistent with classical brown based on its gene expression profile.

Objective: The aim of the study was to establish the gene expression profile and morphology of human epicardial and visceral paracardial fat compared with sc fat.

Setting: The study was conducted at a tertiary care hospital cardiac center.

Patients: Epicardial, visceral paracardial, and sc fat samples had been taken from middle-aged patients with severe coronary atherosclerosis or valvular heart disease.

Interventions: Gene expression was determined by reverse transcription- quantitative PCR and relative abundance of the mitochondrial uncoupling protein-1 (UCP-1) by Western blotting. Epicardial tissue sections from patients were examined by light microscopy, UCP-1 immunohistochemistry, and cell morphometry.

Main Outcome measures: We hypothesized that epicardial fat has a mixed phenotype with a gene expression profile similar to that described for beige cell lineage.

Results: Immunoreactive UCP-1 was clearly measurable in each epicardial sample analyzed but was undetectable in each of the 4 other visceral and sc depots. Epicardial fat exhibited high expression of genes for UCP-1, PRDM16, PGC-1 α , PPAR γ , and the beige adipocyte-specific marker CD137, which were also expressed in visceral paracardial fat but only weakly in sternal, upper abdominal, and lower extremity sc fat. Histology of epicardial fat showed small unilocular adipocytes without UCP-1 immunostaining.

Conclusion: UCP-1 is relatively abundant in epicardial fat, and this depot possesses molecular features characteristic of those found in vitro in beige lineage adipocytes.

10.4.3 Suboptimal maternal nutrition during early-to-mid gestation in the sheep enhances pericardial adiposity in the near-term fetus

Ojha, S., Symonds, M.E. and Budge, H. (2014) *Reproduction, Fertility and Development*

Manipulation of the maternal diet at defined stages of gestation influences long-term health by inducing changes in fetal adipose tissue development, characterised as possessing brown and white adipocytes. We determined whether suboptimal maternal nutrition in early-to-mid gestation, followed by *ad libitum* feeding until term, increases adiposity in the pericardial depot of the sheep fetus. Pericardial adipose tissue was sampled from near-term (140 days) fetuses delivered to mothers fed either 100% (C) or 60% (i.e. nutrient restricted (NR)) of their total metabolisable requirements from 28 to 80 days gestation and then fed *ad libitum*. Adipose tissue mass, uncoupling protein (UCP) 1 and gene expression of brown and white adipogenic genes was measured. Total visceral and pericardial adiposity was increased in offspring born to NR mothers. The abundance of UCP1 was increased, together with those genes involved in brown (e.g. *BMP7* and *C/EBPβ*) and white (e.g. *BMP4* and *C/EBPα*) adipogenesis, whereas insulin receptor gene expression was downregulated. In conclusion, suboptimal maternal nutrition between early-to-mid gestation followed by *ad libitum* feeding enhances pericardial adiposity near to term. A combination of raised

UCP1 and adipose tissue mass could improve survival following cold exposure at birth. In the longer term, this enhanced adipogenic potential could predispose to greater pericardial adiposity.

10.5 Details of suppliers

Abcam®, 330 Cambridge Science Park, Cambridge, CB4 0FL, UK;
www.abcam.com

Abgene Ltd, Abgene House, Blenheim Road, Epsom, KT19 9AP, UK;
www.abgene.com

Actigraph™, 15 W Mainstreet, Pensacola, Florida (FL), 32502, USA;
www.theactigraph.com

Affymetrix UK Limited, Voyager, Mercury Park, Wycombe Lane,
Wooburn Green, High Wycombe, HP10 0HH, United Kingdom;
<http://www.affymetrix.com>

Alpha Laboratories Ltd, 40 Parnham Drive, Eastleigh, Hampshire,
SO50 4NU, UK; www.alphalabs.co.uk

Anglia Scientific Ltd, 94 Fordham Road, Soham, Ely, Cambridgeshire,
CB7 5AJ, UK; <http://www.angliainst.co.uk/>

Antec International Ltd, Windham Road, Chilton Industrial Estate,
Sudbury, Suffolk, CO10 2XD, UK; www.ahs.dupont.com

Applied Biosystems, 5791 Van Allen Way, PO Box 6482, Carlsbad,
California (CA), USA; www.appliedbiosystems.com

Bibby Scientific Ltd, Beacon Road, Stone, Staffordshire, ST15 0SA,
UK; www.techne.com

Biotek UK, 6 Bull Street, Potton, Bedfordshire, SG19 2NR, UK;
www.biotek.com

Bio-Rad Laboratories Ltd, Bio-Rad House, Maxted Road, Hemel
Hempstead, Hertfordshire, HP2 7DX, UK; www.bio-rad.com

Bioron, Rheingoenheimer Str. 36, D-67065, Ludwigshafen, Germany;
www.bioron.net

Cell Biolabs Inc., 7758 Arjons Drive, San Diego, California (CA),
92126, USA; www.cellbiolabs.com

Diagnostic Products Corporation, Llanberis, Glyn Rhonwy,
Caernarfon, Gwynedd, LL55 4EL, UK; www.pharmaceutical-int.com

Ecolabs®, 370 Wabasha St N, Saint Paul, Minnesota (MN), 55102,
USA; www.ecolab.com

Fisher Scientific UK Ltd, Bishop Meadow Road, Loughborough,
Leicestershire, LE11 5RG, UK; www.fisher.co.uk

GE Healthcare Ltd, Amersham Place, Little Chalfont,
Buckinghamshire, HP7 9NA, UK; www.gehealthcare.com

Genetex Inc., 2456 Alton Parkway, Irvine, California (CA), 92606, USA;
www.genetex.com

GraphPad Software Inc., 2236 Avenida de la Playa, La Jolla,
California (CA), 92037, USA; www.graphpad.com

Grenier Bio-One Ltd, Brunel Way, Stroudwater Business Park,
Stonehouse, GL10 3SX, UK; www.greinerbioone.com

Hoefer® Inc., 84 October Hill Road, Holliston, Massachusetts (MA),
01746, USA; www.hoeferinc.com

IBM UK Ltd, PO Box 41, North Harbour, Portsmouth, Hampshire, PO6
3AU, UK; www.spss.com

Invitrogen Ltd, 3 Fountain Drive, Inchinnan Business Park, Paisley,
PA4 9RF, UK; www.invitrogen.com

Leica Microsystems (UK) Ltd, Davy Avenue Knowlhill, Milton Keynes,
Buckinghamshire, MK5 8LB, UK; www.leica-microsystems.com

Linton Instrumentation, 1 Forge Business Centre, Upper Rose Lane,
Palgrave, Diss, Norfolk, IP22 1AP, UK; www.lintoninst.co.uk

Manor Farm Feeds Ltd, Owston, Oakham, Rutland, LE15 8DH, UK;
www.manorfarmfeeds.co.uk

Mercodia, Sylveniusgatan, 8A, SE-754 50, Uppsala, Sweden;
www.mercodia.se

Menzel-Gläser Inc., Glasbearbeitungswerk GmbH & Co.,
Saarbrückener Str. 248, D-38116, Braunschweig, Germany;
www.menzel.de

Microsoft Corporation, One Microsoft Way, Redmond, Washington
(WA), 98052, USA; www.microsoft.com

Millipore, 290 Concord Road, Billerica, Massachusetts (MA), 01821,
USA; www.millipore.com

Minitab Ltd, Brandon Court, Unit E1-E2, Progress Way, Coventry, CV3
2TE, UK; www.minitab.com

Partek Incorporated, 624 Trade Center Boulevard, St. Louis, Missouri
63005 U.S.A; <http://www.partek.com/>

PerkinElmer, Saxon Way Bar Hill, Cambridge, Cambridgeshire, CB23
8SL, UK; www.perkinelmer.co.uk

Premier Biosoft International, 3786 Corina Way, Palo Alto, California
(CA), 94303, USA; www.premierbiosoft.com

Primer Design Ltd, Millbrook Technology Campus, Second Avenue,
Southampton, Hampshire, SO15 0DJ, UK; www.primerdesign.co.uk

Qiagen UK Ltd, Qiagen House, Fleming Way, Crawley, West Sussex, RH10 9NQ, UK; www.qiagen.com

Randox Laboratories Ltd, 55 Diamond Road, Crumlin, County Antrim, BT29 4QY, UK; www.randox.com

Raytek Corporation, 1201 Shaffer Road, Santa Cruz, California (CA), 95061, USA; www.raytek.com

Roche Diagnostics Ltd, Applied Science, Charles Avenue, Burgess Hill, West Sussex, RH15 9RY, UK; www.rocheuk.com

Scientific Laboratory Supplies (SLS) Ltd, Orchard House, The Square, Hessle, East Riding of Yorkshire, HU13 0AE, UK; www.scientificlabs.co.uk

Severn Biotech Ltd, Unit 2, Park Lane, Kidderminster, Worcestershire, DY11 6TJ, UK; www.severnbiotech.com

Sigma-Aldrich Company Ltd, Fancy Road, Poole, Dorset, BH12 4QH, UK; www.sigmaaldrich.com

Simport Ltd, 2588 Bernard-Pilon, Beloeil, Quebec (QC) J3G 4S5, Canada; www.simport.com

VWR International, Hunter Boulevard, Magna Park, Lutterworth, Leicestershire, LE17 4XN, UK; www.vwr.com

Wolf Laboratories Ltd, Colenso House, 1 Deans Lane, Pocklington, York, YO42 2PX, UK; www.wolflabs.co.uk

